

Durham E-Theses

New Synthetic Routes for Natural and Synthetic Fragrance Ingredients

GAMBACORTA, GUIDO

How to cite:

GAMBACORTA, GUIDO (2022) *New Synthetic Routes for Natural and Synthetic Fragrance Ingredients*, Durham theses, Durham University. Available at Durham E-Theses Online:
<http://etheses.dur.ac.uk/14734/>

Use policy

The full-text may be used and/or reproduced, and given to third parties in any format or medium, without prior permission or charge, for personal research or study, educational, or not-for-profit purposes provided that:

- a full bibliographic reference is made to the original source
- a [link](#) is made to the metadata record in Durham E-Theses
- the full-text is not changed in any way

The full-text must not be sold in any format or medium without the formal permission of the copyright holders.

Please consult the [full Durham E-Theses policy](#) for further details.

New Synthetic Routes for Natural and Synthetic Fragrance Ingredients

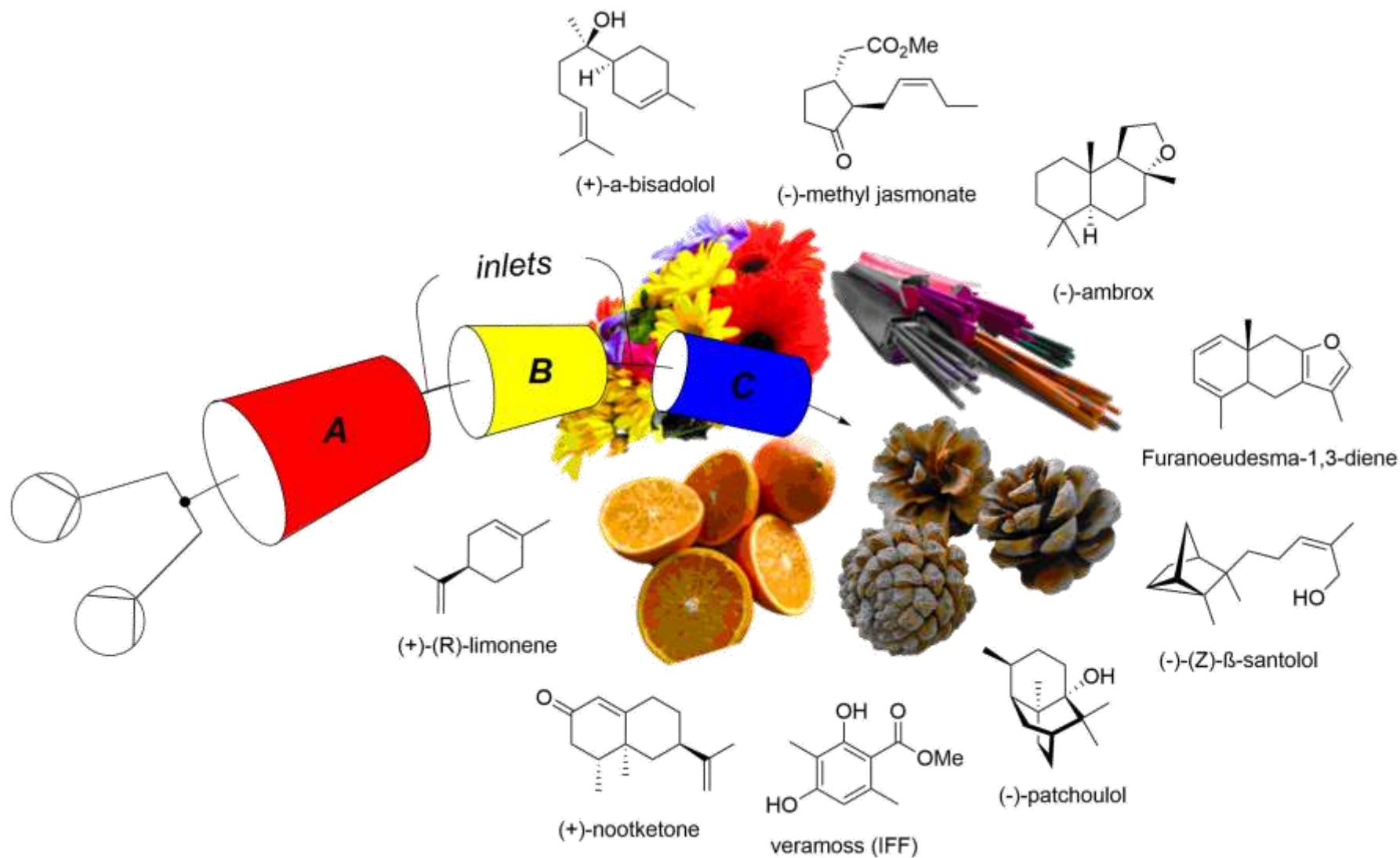
*A thesis submitted for the degree of
Doctor of Philosophy*



*By
Guido Gambacorta*

*Under the supervision of
Prof. Ian R. Baxendale*

06/08/2022



Declaration

The work described in this thesis was carried out in the Department of Chemistry at Durham University between January 2018 and July 2021, under the supervision of Prof. Ian R. Baxendale. In 2020, due to the Covid-19 pandemic, the PhD candidate was prevented from entering the Chemistry building for 4 months (20th of March 2020 until 18th of July 2020), access when the department reopened but was still limited (part time working, including restricted access to equipment and facilities). For these reasons the candidate was granted an extension until 31st of July 2021. The material contained has not been previously submitted for a degree at this or any other university. The research reported within this thesis has been conducted by the author unless indicated otherwise.

The PhD candidate also declares to have participated in other research projects unrelated with the scope of this thesis and have published the following articles:

- Gambacorta, G.; Apperley, D.C.; Baxendale, I.R. A One-Pot Divergent Sequence to Pyrazole and Quinoline Derivatives. *Molecules* **2020**, *25* (9), 2160. <https://doi.org/10.3390/molecules25092160>;
- Gambacorta, G.; Sharley, J.S.; Baxendale, I.R. A comprehensive review of flow chemistry techniques tailored to the flavours and fragrances industries *Beilstein J. Org. Chem.* **2021**, *17*, 1181–1312. <https://doi.org/10.3762/bjoc.17.90>;
- Murie, V.E.; Nicolino, P.V.; Dos Santos, T.; Gambacorta, G.; Nishimura, R.H.V.; Perovani, I.S.; Furtado, L.C.; Costa-Lotufo, L.V.; de Oliveira, A.M.; Vessecchi, R.; Baxendale, I.R.; Clososki, G.C. Synthesis of 7-Chloroquinoline Derivatives Using Mixed Lithium-Magnesium Reagents *J. Org. Chem.* **2021**, *86* (19), 13402–13419. <https://doi.org/10.1021/acs.joc.1c01521>;
- Gambacorta, G.; Baxendale, I.R. Continuous-Flow Hofmann Rearrangement Using Trichloroisocyanuric Acid for the Preparation of 2-Benzoxazolinone *Organic Process Research & Development* **2022**, *26* (2), 422–430. <https://doi.org/10.1021/acs.oprd.1c00440>;
- Tinivella, A.; Pinzi, L.; Gambacorta, G.; Baxendale, I.R.; Rastelli, G. Identification of potential biological targets of oxindole scaffolds via *in silico* repositioning strategies

[version 2; peer review: 2 approved]. *F1000Research* **2022**, 11(Chem Inf Sci):217.
<https://doi.org/10.12688/f1000research.109017.2>.

Abstract

Research & development of alternative routes for fragrance ingredients currently produced by International Flavours & Fragrances Inc. (IFF) in Benicarlò, Spain is reported herein. Past and current industrial syntheses of these ingredients are initially summarised as well as their primary role in the industry. The research disclosed has focused on designing and developing sustainable and safe methods for their industrial preparation and, where possible, evaluation to/of continuous flow approaches.

The first target was the musky, earthy natural ingredient known as Veramoss. For this molecule, three alternative synthetic pathways were explored starting with cheap and widely available raw materials such as butanone, dimethyl malonate, methyl acetoacetate, methyl crotonate, and acetaldehyde. Despite being unable to achieve the final compound, the study enabled the development of a continuous-flow Knoevenagel reaction employing polymer-supported dimethylamine catalyst to obtain dimethyl ethylidene malonate in moderate yields (38%) as well as an interesting one-pot methodology for the preparation of 4-chlorohex-4-en-3-one from dimethyl oxalate and butanone in good yields (76%). These developed methodologies could become interesting starting points for future works. Along with route scouting, the main goal of the project was to propose an improved “green” alternative to the currently employed toxic elemental chlorine. To this aim, four main alternative chlorination processes were investigated, one of which proved to be the candidate of choice: trichloroisocyanuric acid (TCCA). An optimisation based on utilizing TCCA was carried out by employing one-factor-at-the-time (OFAT) and design of experiment (DoE) approaches. The optimised one-pot procedure was scaled up to multi-grams quantities allowing the isolation of Veramoss whose quality was validated for commercial purposes. Furthermore, the study also proposed a *de novo* procedure for the purification of discoloured Veramoss obtained from mischarge and side reactions during chlorination. The methodology based upon selective phenol-amine H-bonded complex formation allowed the recovery of purified white material in 60% overall yield, reducing waste and the need to dispose of discoloured batches.

The second target molecule was the newly established IFF compound Ambertonic™, a synthetic tricyclic musk odorant featuring a pyrimidine scaffold. The investigation focused on finding valuable alternative routes starting from a readily available intermediate: Cashmeran. Five

viable methods were explored, however, only one allowed the ultimate cyclisation to occur. The effective strategy was then optimised for the preparation of the material. Hence, a two steps one-pot synthesis was developed to yield Ambertonic™ in good yield (53%). The methodology consists in the formylation of the dihydro-cashmeran material with subsequent pyrimidine formation inspired by a publication by Brederick *et al.* The optimisation of both stages were initially found to be challenging presenting low yields, solid precipitation, and formation of impurities. Scouting different reaction conditions and parameters, the issues were tackled and eventually solved. Additionally, the first SCXRD structure and racemic resolution of the *trans*-isomer was carried out allowing us to gain a deeper understanding of the absolute configuration of the active odorant species.

The final target investigated was dehydroherbac, a key intermediate for the preparation of the fresh, green odorant known as Galbascone. Three synthetic routes were envisioned starting from different raw materials such as acrylonitrile, 4,4-dimethylcyclohexanone, 5-methylhexan-2-one, and 3-carene. Two of the proposed strategies aimed at preparing an enaminone intermediate which undergoes de-amination through selective enamine reduction and elimination. The latter procedure ultimately proved to be impracticable on the desired scaffold. Regardless of the outcomes, a continuous-flow photo-catalysed method for the preparation of a cyano-ketone was optimised to yield 630 mg h⁻¹ of material in 63% isolated yield as a proof-of-concept study. Employing 3-carene as a precursor was also considered through catalytic hydrogenolysis and CH activation of a tertiary carbon. Such a strategy allowed access to three possible oxidative hydroxylation methods as described in the literature utilising dioxiranes, and peracids. Due to the lack of time, the investigation was not completed, however it has established a solid foundation for future work. The project also involved the optimisation of a previously designed route to Galbascone via a Henry-Nef reaction. Kinetic studies performed on the amine-catalysed Henry reaction enabled establishment of a better understanding of the latter and reduced the amount of nitroethane employed for the reaction.

In summary, potential preparative routes to the three fragrance ingredients were developed and optimised. The process utilised known chemistry which employs safe and cheap raw materials. Both the developed methodologies for Veramoss and Galbascone have also been considered for scale up at IFF in Benicarlò, achieving interesting manufacturing results.

Acknowledgements

Firstly, I would like to thank Prof. Ian R. Baxendale for this opportunity and the enormous help and assistance given throughout my entire doctoral studies. My gratitude also goes to our industrial collaborators (IFF & Co.) as well as the research group, its group members, and all those people that briefly visited the laboratory, many of whom become good friends. Particularly, I would like to thank Valter E. Murie, Michele Ruggeri, Alex Nicholls, Camilla Rodrigues De Souza Bertallo, Eilish Bonner, Zhang Yinfeng, Anna Maria Lozza, Wenjuan Xue, Antoine Legato, and Marcus Baumann for their support and help as well as for allowing me to learn so many new cultures, ways of thinking, and languages throughout my studies. I would finally like to express my thanks to my family, my friends, and my partner for encouraging me to experience one of the most exciting periods of my life.

Abbreviations

Ac	Acetyl
AcOH	Acetic acid
ASAP	Atmospheric solids analysis probe
b.p.	Boiling point
<i>n</i> -Bu	<i>n</i> -Butyl
°C	Degrees centigrade
CD	Circular dichroism
COPC	Cobaloxime pyridine chloride
COSY	Correlation spectroscopy
CSTR	Continuous stirrer tank reactor
CPP	Critical process parameter
Da	Dalton
DABCO	1,4-Diazabicyclo[2.2.2]octane
DBU	1,8-Diazabicyclo[5.4.0]undec-7-ene
DCM	Dichloromethane
DEPT	Distortionless enhancement by polarization transfer
DMAc	<i>N,N</i> -dimethylacetamide
DMDO	Dimethyldioxirane
DME	1,2-Dimethoxyethane
DMF	<i>N,N</i> -Dimethylformamide
DMFDMA	<i>N,N</i> -Dimethylformamide dimethyl acetal
DMSO	Dimethylsulfoxide
DoE	Design of experiment
DOSY	Diffusion-ordered NMR spectroscopy
DSD	Definitive screening design
EI	Electron impact ionization
EMA	European medicines agency
Et	Ethyl
EtOH	Ethanol
ESI	Electrospray ionization
FDA	Food and drug administration
F&F	Flavour & fragrance
g	Gram

kg	Kilogram
h	Hours
GC-MS	Gas chromatography – mass spectrometry
GSK	GlaxoSmithKline
HAT	Hydrogen atom transfer
HClO	Hypochlorous acid
HIV	Human immunodeficiency virus
HMBC	Heteronuclear multiple bond correlation
HMDS	Hexamethyldisilazane
HMTA	Hexamethylenetetramine
HRMS	High-resolution mass spectrometry
HSQC	Heteronuclear single quantum coherence
Hz	Hertz
ICM	Integrated continuous manufacturing
IFRA	International Fragrance Association
IFF	International Flavours & Fragrances
<i>i</i> Pr	<i>iso</i> -Propyl
IR	Infrared
Iso. yield	Isolated yield
<i>J</i>	coupling constant
L	Litre
mL	Millilitre
LC-MS	Liquid chromatography – mass spectrometry
LDA	Lithium diisopropylamide
LED	Light-emitting diode
M	Molarity
MeCN	Acetonitrile
MeOH	Methanol
MeONa	Sodium methoxide
Me	Methyl
min	Minutes
MIT	Massachusetts Institute of Technology
mol	Moles
mmol	Millimoles

MS	Molecular sieves
MtBE	Methyl <i>tert</i> -butyl ether
MW	Microwave
NMR	Nuclear magnetic resonance
NOESY	Nuclear Overhauser effect spectroscopy
OFAT	One factor at the time
ON	Overnight
PAT	Process analytical technology
PC	Photocatalyst
PFA	Polyfluoroalkoxy alkane
Ph	Phenyl
PMDA	Pharmaceuticals and medicinal devices agency
PPA	Polyphosphoric acid
ppm	parts per million
PS-BZA	Polystyrene-supported benzylamine
PS-DMA	Polystyrene-supported dimethylamine
PS-TsOH	Polystyrene sulfonic acid resin
PSYCHE	Pure shift yielded by chirp excitation
PTFE	Polytetrafluoroethylene
QC	Quality check
RAP	Relative percentage area
R&D	Research & Development
Re	Reynold's number
RMSE	Root mean square estimate
Rt	Retention time
r.t.	Room temperature
SAR	Structure-activity relationship
SCXRD	Single crystal X-ray diffractometry
SET	Single electron transfer
SFC	Solvent free conditions
T	Temperature
t	Time
TBADT	Tetrabutylammonium decatungstate
TBPB	<i>tert</i> -Butyl peroxybenzoate

TCCA	Trichloroisocyanuric acid
TEMPO	2,2,6,6-Tetramethylpiperidine-1-oxyl
TFDO	Trifluoromethyldioxirane
TFA	Trifluoroacetic acid
THF	Tetrahydrofuran
4-Me-THP	4-Methyl-tetrahydropyran
TLC	Thin-layer chromatography
TMEDA	Tetramethylethylenediamine
TMOF	Trimethyl orthoformate
Tpa	Tonnes per annum
Triglyme	<i>Bis</i> (2-methoxyethyl)ether
Ts	4-Methylbenzenesulfonyl
<i>p</i> -TSA	<i>para</i> -toluenesulfonic acid
UPLC	Ultra-performance liquid chromatography
UV	Ultraviolet

Contents

Declaration.....	3
Abstract.....	5
Acknowledgements.....	7
Abbreviations.....	8
1. Introduction.....	14
1.1. Chemistry in the Flavour and Fragrance Industry.....	14
1.2. Flow Chemistry.....	19
1.3. Molecules of Synthetic Interest.....	24
1.3.1. Veramoss.....	24
1.3.2. Ambertonic.....	28
1.3.3. Galbascone.....	30
1.4. Summary aims and objectives – Bullet points.....	37
2. Results and discussion.....	38
2.1. Veramoss.....	38
2.1.1. Alternative strategy starting from ethyl 1,6-dihydro-orsellinate.....	38
2.1.2. Synthetic strategy from 2-butanone: Route A.....	44
2.1.3. Synthetic strategy from 2-butanone: Route B.....	50
2.1.4. Alternative chlorinating agents to elemental chlorine.....	54
2.1.5. Optimising the preparation method for compound 23.....	81
2.1.6. Final Optimisation of the one-pot preparation to Veramoss.....	84
2.1.7. An alternative purification method for the final material.....	86
2.1.8. Summary and Conclusions.....	94
2.2. Ambertonic.....	96
2.2.1. Ambertonic via formyl-dihydro-cashmeran: Route C.....	96
2.2.2. Alternative strategies to the pyrimidine scaffold: Route D.....	120
2.2.3. X-Ray structure of Ambertonic™ and the nature of its “selective” configuration.....	129
2.2.4. Resolution and characterisation of the enantiomers.....	131
2.2.5. Summary and Conclusions.....	133
2.3. Galbascone.....	134

2.3.1.	Galbascone from 4,4-dimethylcyclohexanone (183): Route E.....	136
2.3.2.	Galbascone from 5-methyl-hexan-2-one and acrylonitrile: Route F.....	141
2.3.3.	Galbascone starting from 3-cerene: Route G.....	148
2.3.4.	Galbascone from 3,3-dimethylcyclohexanone: Route H.....	151
2.3.5.	Summary and Conclusions	163
3.	Conclusions and outlooks	164
4.	Experimental Procedures	170
4.1.	Veramoss.....	172
4.2.	Ambertonic.....	195
4.3.	Galbascone	214
5.	References.....	230

1. Introduction

1.1. Chemistry in the Flavour and Fragrance Industry

Fragrances, with their glamour, have always been celebrated as powerful psychosomatic stimulants enhancing subconscious emotions and revealing hidden desires. The quest for novel scents has led to the development of many different methods for acquiring fragrances. Distillation, perfected by Persians and exported to Europe in the 9th century, is one of the preferred techniques, along with extraction, which facilitates isolation of a mixture of fragrance compounds comprising the scented part of the natural material. The coexistence of these developed techniques permitted the eventual industrialization of the so-obtained essential oils 10 centuries later. Despite their success, the often-limited chemical stability of the key components enabled collection of only a limited selection of oils, thus narrowing down the available choice of scent for perfumers. Furthermore, apart from some specific oils (e.g. lavender and eucalyptus oils), whose bulk prices (55 to 65 £/Kg)^{1,2} are widely accessible due to their ease of cultivation and extraction, others such as Jasmine oils are much more expensive (its price ranges around £2,900/Kg)^{3,4} restricting their usage to niche applications. Consequently, the utility of Synthetic Chemistry was leveraged as a means of reducing the economic burden of such aromatic chemicals and uncovering novel molecules to enrich the perfumers' palette.

With the appearance of many naturally occurring materials as coumarin (**1**, 1866),⁵ vanillin (**2**, 1876),⁶ and β -ionone (**3**, 1893),⁷ and novel synthetic odorants, for instance musk xylol (**4**, 1891),⁸ methyl ionone (**6**, 1893),⁹ and ethyl vanillin (**5**, 1894),¹⁰ the 19th century was a revolution of fragrance chemistry for usage in several areas; from the rapidly expanding perfumery businesses to the newly developing household cleaning market (*Figure 1*). Between 1759 and 1998, around 2,500 active fragrance ingredients were made available for perfumers. It is worth noting, in the early days of this new chemistry, the discovery of novel synthetic ingredients was either serendipitous (see discovery of musk xylene and cyclamen aldehyde)^{8,11} or rationalised by preparing a range of analogues based on known odorants.^{12,13} In the past 20 years, the number of available ingredients has risen to almost 4,000 (International Fragrance Association (IFRA) published a list of active F&F chemicals),^{14,15} as a consequence of scientific and technological advances in theory and computational chemistry and in odorant chemoreception (2004 Nobel prize),¹⁶⁻¹⁸ allowing to establish new more effective methods of

discovering potent and novel odorants (Ligand-olfactory receptor design, Conformational analysis, and SAR).^{19–21} Along with these new strategies, toxicological and bio-accumulative tests have been implemented in the early stage of development to allow the design of safer and more environmental-friendly synthetic odorants.^{22–24}

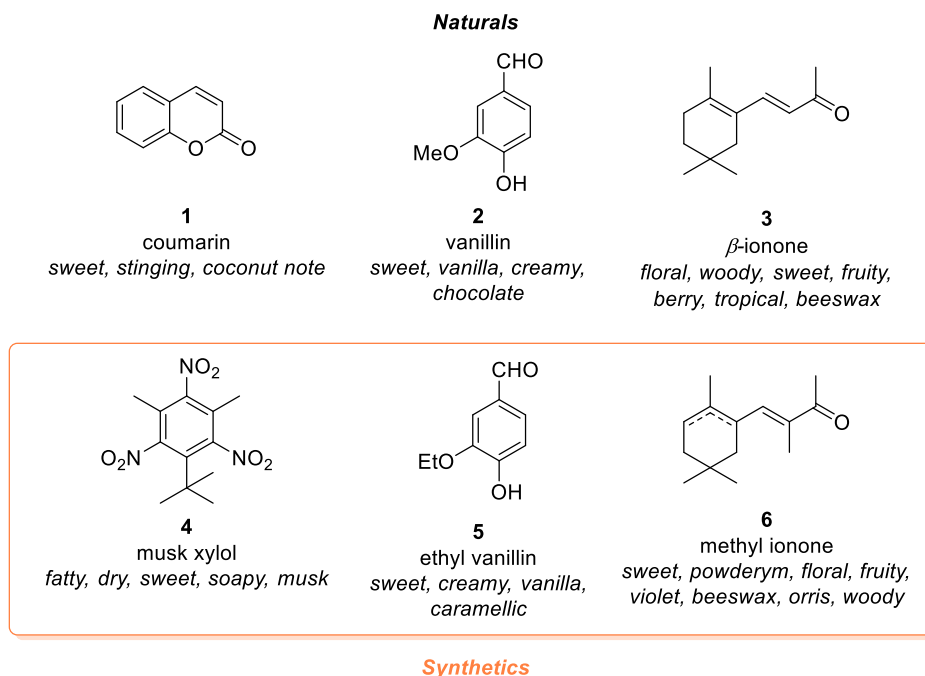


Figure 1. Examples of early synthetic and natural fragrance ingredients prepared/isolated by the evolving Fragrance industry.

With the increase of odorants, a better classification was required to install order and allow comparison between different fragrance materials. In 1983, Michael Edwards reported a full spectrum of fragrance in his book “fragrance wheel”,²⁵ and this is currently used as the standard system for categorisation of fragrances (*Figure 2*). The *Wheel* subdivides a scent into one of four families: Floral, Oriental, Fresh, and Woody. The system, built upon the experience of a single perfumer, was found to be highly consistent with other approaches.²⁵ The principal notes are sub-divided into related sub-classes which more thoroughly describes them. *Figure 3* represents examples of fragrances whose notes would be associated with the corresponding family.

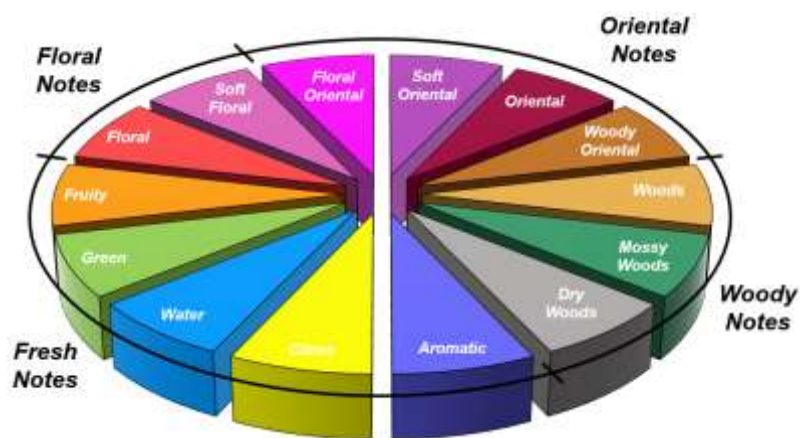


Figure 2. The Michael Edwards fragrance Wheel.²⁵

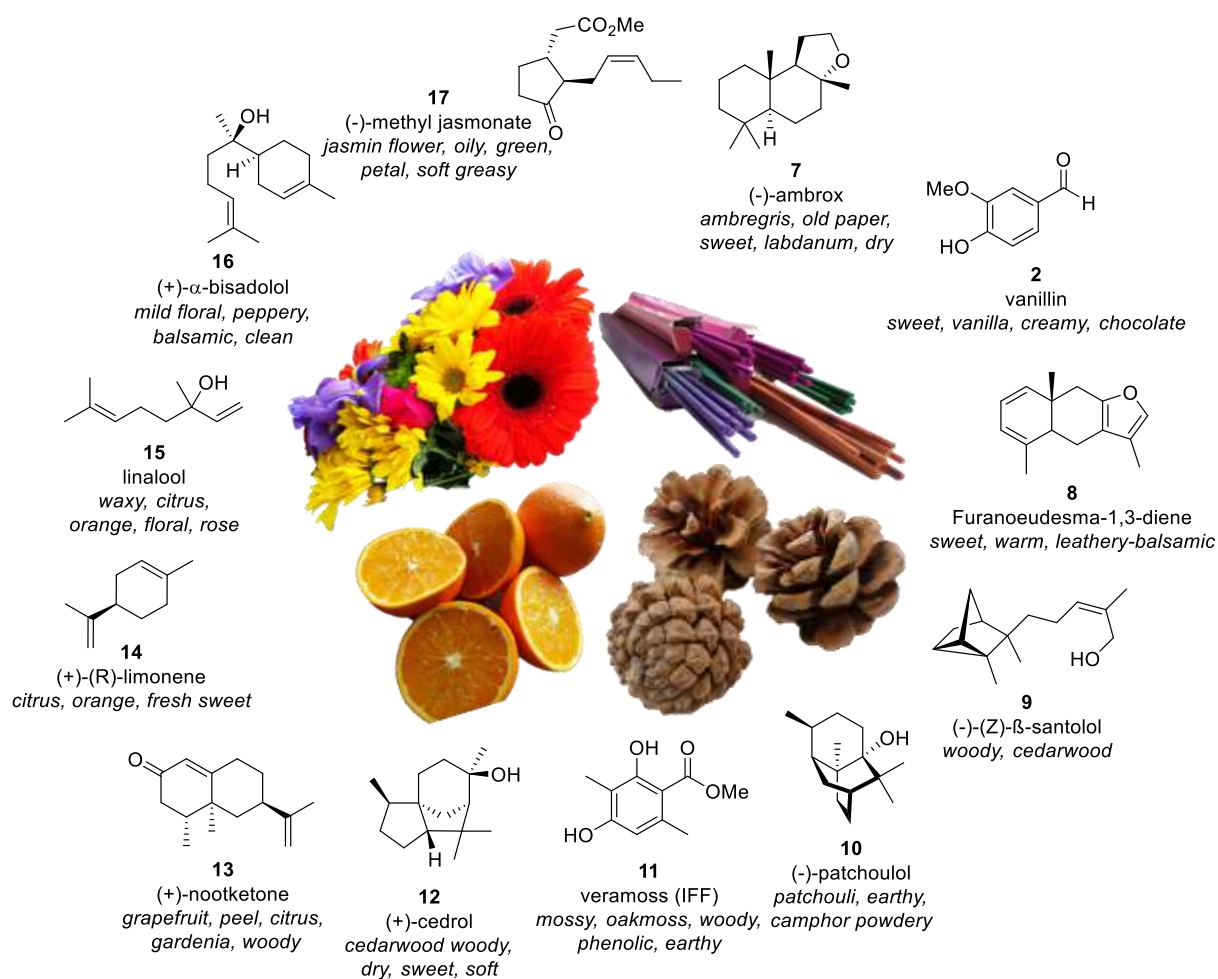


Figure 3. Examples of molecules representing the oriental (2,7-8), woody (9-12), fresh (13-15), and floral (16-17) notes.²⁶

Nowadays, Flavour & Fragrance (F&F) manufacturers provide a wide range of aromas which are blended and utilised in final formulations of many everyday products (*Figure 4*). Fragrance ingredients are involved in preparations of fine fragrances, cosmetics, toiletries, soaps, detergents and air fresheners, whereas flavours affect the beverages industry, dairy, confectionary, bakery and savoury/convenience foods. Synthetic fragrances predominate against the natural products (ca. 560 synthetics vs ca. 50 naturals produced at IFF's (International Flavours & Fragrances) manufacturing plant in Benicarló, Spain), nonetheless the latter remain an important contributing class of F&F ingredients.

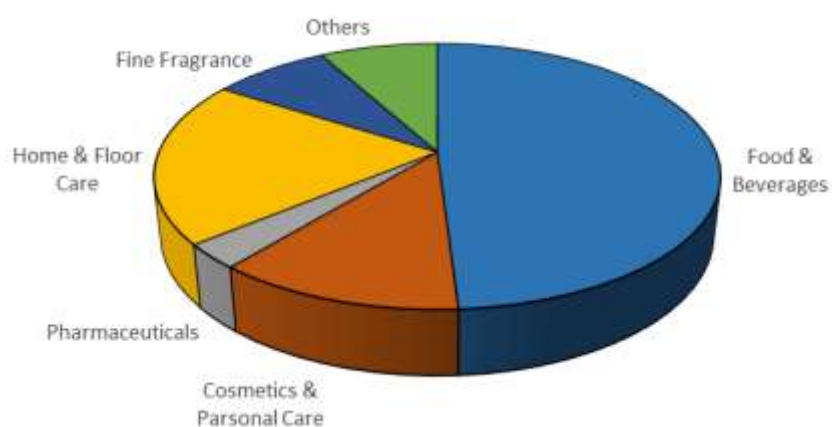


Figure 4. Representative shares of the global market for F&F in 2018.²⁷

In 2021, the F&F industry had estimated sales of more than \$25 billion with a decline of over 9% from the previous year due to the Covid-19 Global pandemic. However, the market value is expected to rebound and to grow by over 5% yearly with an annual value of more than \$36 billion by 2028.²⁷ It is apparent, the F&F industry is smaller than other chemistry-based industries such as pharma and agrochemical (2020 global sales; Pharma ~ \$1,200 bn, Agrochemicals ~ \$209 bn, F&F ~ \$25 bn).^{28,29} This is mainly due to the fact that flavour & fragrance companies principally act as intermediates between raw material suppliers and high value consumers goods manufacturers. *Table 1* represents some of the most important synthetic fragrances along with their approximate annual tonnage and prices. Some listed chemicals are commonly used as intermediates for the manufacturing of other ingredients; for instance,

myrcene is used to prepare linalool, geraniol, nerol, and 4-(4-hydroxy-4-methylpentyl)cyclohex-3-ene-1-carbaldehyde (Lyal, IFF). As can be seen, F&F products prices can be comparable to feedstock's, yet with volumes akin to pharmaceutical ingredients. As a result, costs are highly-dependant on the methods of production and great competition transpires between companies, whose R&D strategies are mainly aimed at cost-reduction.

Table 1. Some of the most important synthetic fragrance materials.³⁰⁻³²

Name	Tonnes per year	£/Kg^a	Odour type
Myrcene	30,000 ^b	1	Balsamic
Pine oil/Terpineol	30,000	1	Pine
Menthol	12,000	10	Mint/coolant
Linalool	10,000	4	Floral/wood
Citral	5,000	5	Lemon ^c
Dihydromyrcene	5,000 ^b	1	-
Geraniol	5,000	4	Rose
(Methyl)ionones	5,000	15	Violet
Dihydromyrcenol	4,000	4	Citrus/floral
Limonene	3,500	1	Orange ^{d,e}
Citronellol	3,000	7	Rose
Isobornyl acetate	2,000	1	Pine
Linalyl acetate	2,000	4	Fruity/floral
Tetrahydrolinalool	2,000	4	Floral
Carvone	1,500	10	Spearmint
Hydroxycitronellal	1,000	8	Muguet
Lyal (IFF)	1,000	12-23 ^f	Floral
Terpenylcyclohexanols	1,000	4-38 ^f	Sandalwood
Zenolide & analogues	1,300-4,300	60-250 ^f	Musk
Civetone & analogues	50-500	8-80 ^f	Musk
Cedrene derivatives	500	20	Cedarwood
Amberlyn [®] /Ambrox [®] /Ambroxan [®]	50	500-	Ambergris
Bangalol & analogues	30	30	Sandalwood

^aThese prices and volumes are estimated;^bA substantial proportion of the total consumption is used for manufactured of other ingredients;^c Citral has little use in the direct fragrance market. The tonnage is used for manufacturing ionones and methylionones;^dThe material used is actually orange terpenes, which is about 80% limonene but the odour comes from minor components;^e This figure relates to the use of orange oil in perfumery. About 1,500 tonnes per annum (tpa) are used in the manufacture of carvone. The total production exceeds 50,000 tpa;^fPrices are approximate value acquired from Alibaba.com (accessed November 13, 2021).

Although it could be implied that the F&F industry mostly utilises old and well-established chemistry, a wave of changes has affected the sector. In the last few years, F&F companies have been investing in the development of new synthetic strategies aiming at reducing the environmental impact from manufacturing. In fact, F&F companies have developed different programs to highlight these efforts, such as “EcoScent Compass™” (Firmenich),³³ “Towards a Circular Future” (IFF),³⁴ “Green Motion” (Mane),³⁵ “Responsible Care” (Symrise),³⁶ and “FiveCarbon Path” (Givaudian).³⁷ For such instances, the adoption of biotechnological processes have allowed them to establish synthesis of complex ingredients from renewable feedstocks. In fact, development of enzymatic processes have been reported for the preparation of Clearwood™ (Patchoulol, **12**),^{38,39} Ambrox (**7**),⁴⁰ and other musky analogues of **7**.^{41,42}

Flow chemistry (flow manufacturing) is regarded as a potential innovative and cost-reducing technology for process production. Over the last few decades, different pharmaceutical companies such as Novartis, Vertex, GSK, and Johnson & Johnson have been investing tens of millions dollars in this area.^{43–46} Although less emphasised, other chemical manufacturing as well as F&F industries have also been actively evaluating and developing their own approaches based upon the general principles of continuous flow manufacturing.²⁶ Flow chemistry could certainly provide an interesting addition for targeting cost and waste reduction in F&F manufacturing.

1.2. Flow Chemistry

Being sustainable is becoming a crucial part of human life. As a result, industries have been putting into place innovation projects (Industry 4.0, Smart manufacturing, Internet of things) aimed at reducing their environmental impact through the application of automation and enabling technologies.^{47–49} In particular, chemical industry has been gradually innovating over the last 20 years following the principles of “Green Chemistry” (*Table 2*) and “Green engineering” (*Table 3*).^{50,51} These principles, defined in 2000 and 2003 by respectively Warner and Anastas, offer guidance for the design of environmental-friendly chemistry processes, and they can be summarised in terms of process efficiency, waste reduction, and safety improvements.

One of the enabling technologies which goes hand-in-hand with these principles and facilitates easy automation is Flow Chemistry (*Table 2 & Table 3*), or more generally integrated continuous manufacturing (ICM). Continuous operation systems have been implementing for many years in the manufacturing of bulk chemicals,⁵² nonetheless the variety of chemical reactions involved for fine chemicals manufacturing and their small production volume had always favoured the more flexible and versatile multi-purpose batch approach. With the advances in microreactor technology and the increasing availability of lab-scale flow equipment, applications of flow chemistry have become gradually more appealing from both academic and industrial perspectives, and the benefits of employing this technology are now well-documented in the literature.⁵³⁻⁵⁷

Table 2. The 12 principles of green chemistry.

	Principle	Flow
1	Prevent Waste	↑
2	Atom Economy	↑
3	Less Hazardous Chemical Syntheses	↑
4	Design Benign Chemicals	↓
5	Benign Solvents and Auxiliaries	↑
6	Design for Energy Efficiency	↑
7	Use of Renewable Feed Stocks	↔
8	Reduce Derivatives	↔
9	Catalysis (vs. Stoichiometric)	↑
10	Design for Degradation	↔
11	Real-Time Analysis for Pollution Prevention	↑
12	Inherently Benign Chemistry for Accident Prevention	↑

Table 3. The 12 principles of green engineering.

	Principle	Flow Adherence
1	Inherent Rather Than Circumstantial	↑
2	Prevention Instead of Treatment	↑
3	Design for Separation	↑
4	Maximize Efficiency	↑
5	Output-Pulled Versus Input-Pushed	↑
6	Conserve Complexity	↔
7	Durability Rather Than Immortality	↔
8	Meet Need, Minimize Excess	↑
9	Minimize Material Diversity	↔
10	Integrate Material and Energy Flows	↑
11	Design for Commercial "Afterlife"	↔
12	Renewable Rather Than Depleting	↔

Essentially, flow chemistry is built upon the premise of unifying two or more streams of reagents to react in a confined space, which can be a chip or a coil (inlet), and then collecting the products at the reactor exit (outlet). The small architectures of the reactor channels result in higher surface-to-volume ratios than classic batch vessels ($30,000 - 40 \text{ m}^2\text{m}^{-3}$ vs $100 - 1 \text{ m}^2\text{m}^{-3}$) enabling improved heat and mass transfer rates which provides a better control over highly exothermic reactions and thermally-unstable intermediates.^{58,59} Additionally, flow streams in micropipes (lateral dimensions $< 1 \text{ mm}$) will intrinsically have shorter diffusion pathways than large batch reactors (lateral dimensions = 1 m) allowing a far more efficient mixing regime than batch set-ups, and therefore linear scalability of the systems from lab scale to production plant.⁶⁰⁻⁶⁴ In the event of laminar flow profiles ($\text{Re} < 2,000$), mixing issues can be solved by employing active (stirrers,⁶⁵ acoustic waves,⁶⁶ pulsations⁶⁷) or passive (static mixers⁶⁸) mixing techniques.^{69,70} Furthermore, the small dimensions of the flow reactors facilitate to employ higher pressures by applying back pressure regulators. Coupled with high temperatures, easily obtainable through microwave irradiations,⁷¹ heating ovens,⁷² oil baths,⁷³ or electric current,⁷⁴ flow chemistry enables one to explore reaction conditions which are largely outside the operation range of most stirrer tanks (up to $600 \text{ }^\circ\text{C}$ vs $200 \text{ }^\circ\text{C}$). Such conditions can be exploited to exert the Arrhenius rate law and efficiently enhance the reactivity of slow reactions reducing risks.⁷⁵ Flow chemistry has also become an excellent tool for applying heterogeneous catalysis, thanks to the high surface area and easily recovery/reusability of the catalyst which increase the catalyst productivity and reduces waste.⁷⁶⁻⁷⁸ For hazardous gas-solid catalysed reactions such as hydrogenations, flow conditions allows safe handling of pyrophoric catalysts with highly flammable materials.⁷⁹ Alternative energy sources such as electrochemistry, microwave irradiation, and photochemistry have been gathering an increasing amount of interest in the last decade and this could be mainly attributed to the application of flow apparatus which allows a possible industrial scale-up.⁸⁰⁻⁸² Moreover, in multi-step synthesis, this concept of inlet and outlet enables the integration of in-line purification systems,⁸³⁻⁸⁹ reducing discontinuous time-consuming work-ups, for “telescoping” a number of steps in a sequence creating a continuous inlet-to-outlet connected process which reduces the footprint in large scale manufacturing plant (*Figure 5*).^{63,64,90}

Besides offering the economic advantages for around the clock unmanned operation, developing fully automated production and manufacturing systems can provide numerous

additional advantages in terms of safety and process reliability. Flow chemistry can facilitate the step to automated systems as process parameters can be easily controlled through a digital software. In addition, in combination with in-line monitoring tools (ReactIR, NMR, UV, MS, Raman) this allows real-time assessments of process changeovers and product quality.⁹¹⁻⁹⁶ Apart from a production point of view, automated systems could also potentially reduce the time of process development and optimisation in laboratories speeding up the scale-up sequence.⁹⁷

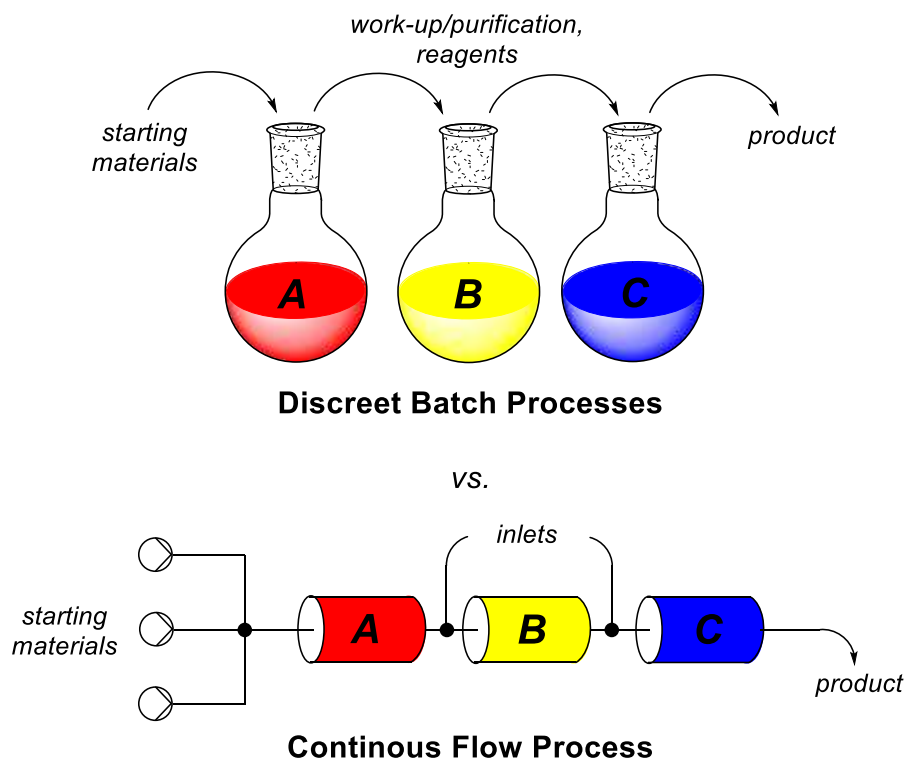


Figure 5. Batch vs Flow synthesis approaches.

These are the main reasons that justify the adoption of flow chemistry and *Table 4* bullet-points the above cited arguments. Alongside its advantages, it should also be acknowledged that several drawbacks have been identified in utilising flow chemistry, and it is therefore in these cases more convenient to adopt a batch set-up (e.g., cascade Continuous stirred tank reactors, CSTRs). Nonetheless, current research is mainly directed towards solving these issues and thus improving the scope of flow chemistry.^{83-86,98,99} Continuous processing of slurries, for

examples, is now routinely performed despite this having been previously identified as a flow process critical issue to avoid.^{98–102}

Table 4. Flow chemistry advantages and disadvantages.

Advantages		Disadvantages	
✓	Enabling automation systems to be implemented	✗	Quenching/work-up issues
✓	High heat and mass transfer rates	✗	Dilution effects of additional downstream flow streams
✓	Potential for in-line purification and telescoping	✗	Solvent limitations for multi-step procedures
✓	Compatibility with “forbidden chemistries”	✗	Inability to compensate for reaction kinetics
✓	Efficient mixing	✗	Start-up and shut-down procedures
✓	Linear scalability and high throughput	✗	Issues with heterogeneity
✓	Health and safety implications	✗	Higher training and implementation requirements
✓	Facile access to high temperatures and pressures		
✓	Reduced footprint space requirements		

The efficiency of flow chemistry as well as its possibility to continuously monitor critical process parameters (CPPs) has in fact been noticed by most fine chemical industries which have been directing investment towards implementing flow chemistry and automation. Taking into consideration the pharmaceutical industry, regulatory agencies such as Food and Drugs Administration (FDA), European medicines agency (EMA), and Japan’s Pharmaceuticals and Medical Devices Agency (PMDA) have been exhorting greater implementation of process analytical technologies (PATs) and simultaneous diagnostic data monitoring and analysis (identification of process issues and automation) enabled by ICM (Integrated Continuous Manufacturing) and in fact are actively supporting their development.^{103–105} For these reasons, pharmaceutical companies have been devoting large amounts of resources into automation and ICM facilities.^{43,44,106–108} The first example of FDA-approved continuous manufacturing came in 2016 with Janssen (J&J) establishing an ICM facility in Porto Rico for the preparation of Darunavir, an antiretroviral used to treat and prevent HIV.¹⁰⁹ This “hybrid” system (part ICM and part batch) was reported to reduce waste by 33% and cut manufacturing and testing cycle times by over 80%. “Hybrid” ICM facilities have also been implemented by GSK for Dolutegravir, Vertex for Elexacaftor, Eli Lilly for Abemaciclib, and Pfizer for Glasdegib.¹¹⁰ A

further step forward was implemented by the Novartis-MIT centre, which proposed in 2013 an end-to-end ICM plant for the preparation of Aliskiren hemifumarate.¹¹¹ This system was projected to continuously manufacture final dosage forms (tablets) of the drug from the direct commercially available raw materials (3 synthetic stages). This work was reported to cut the operational units required by 33% (14 vs 21) and by 84% the process cycle time (47 h vs 300 h) allowing the preparation of 2.7 million tablets per year. However, the system was never used in full production instead it represents a proof-of-concept and learning experience. As such other end-to-end ICM routes have been developing in the last few years confirming this trend.^{112,113}

Although these are promising results for the chemical industry, much has still to be done and many companies still have to embrace the acquisition of cultural knowledge and equipment for this new technology. Particularly, in the F&F area products and intermediates are typically liquids and therefore inherently well suited to processing in flow set-ups. In addition, contrary to other purification methods, distillation in continuous manner can be considered a well-established unit operation in industry. Although it is taking longer for the adoption to occur²⁶ in the F&F industry it is only a matter of time before ICM facilities will also be adopted in this area due to the advantages these offer.

1.3. Molecules of Synthetic Interest

The aim of this thesis is to explore the use of flow chemistry where applicable and devise new routes to a range of Fragrance and Flavours molecules of general interest to the sponsor, International Flavors & Fragrances Inc. (IFF).¹¹⁴

1.3.1. Veramoss

The compound methyl 2,4-dihydroxy-3,6-dimethylbenzoate (**11**; CAS: 4707-47-5), trade named Veramoss (IFF), Evernyl (Givaudian) or methyl atrarate (more generically) has as many names as it does uses. Compound **11** was first isolated from Oakmoss extract in 1924 and was reported to form “prismatic needles with a melting point of 142 °C”.¹¹⁵ Its odour, which

constitutes the main character of oakmoss extract, is described as mossy, woody and earthy (*Figure 6*).

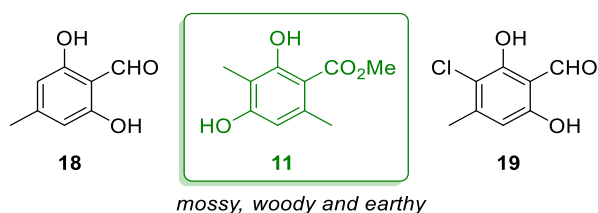
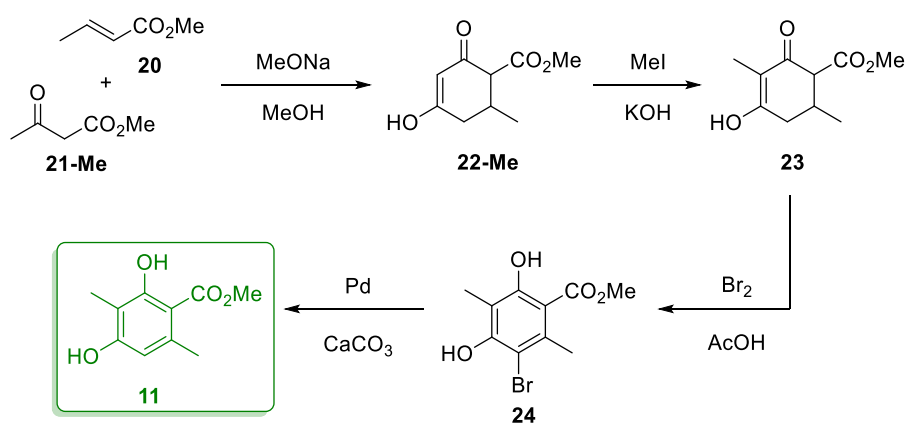


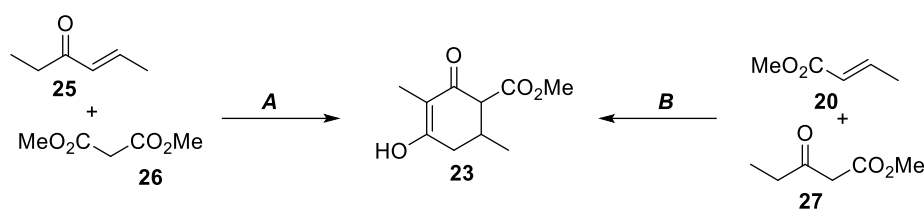
Figure 6. Structures of Veramoss (**11**) and two of the allergens atranol (**18**) and chloroatranol (**19**).

Initially, Oakmoss essential oil, obtained from the lichen *Evernia prunastri* (*L.*) *Arch*, was an essential ingredient in perfumes such as *chypre* and *fougère*.^{116,117} However, the 43rd IFRA amendment of 2009 restricted its usages because of the presence of some skin sensitizers such as atranol (**18**) and chloroatranol (**19**), *Figure 6*.¹¹⁸ To avoid the latter metabolites, the extract was replaced by synthetic Veramoss material, which reproduces oakmoss characteristics with high fidelity. It became available to the perfumists in the late 1960s and immediately became a central constituent of notes in common scents like “Chanel N°19” (Chanel, 1971) and “Polo” (Ralph Lauren, 1978).¹¹⁹



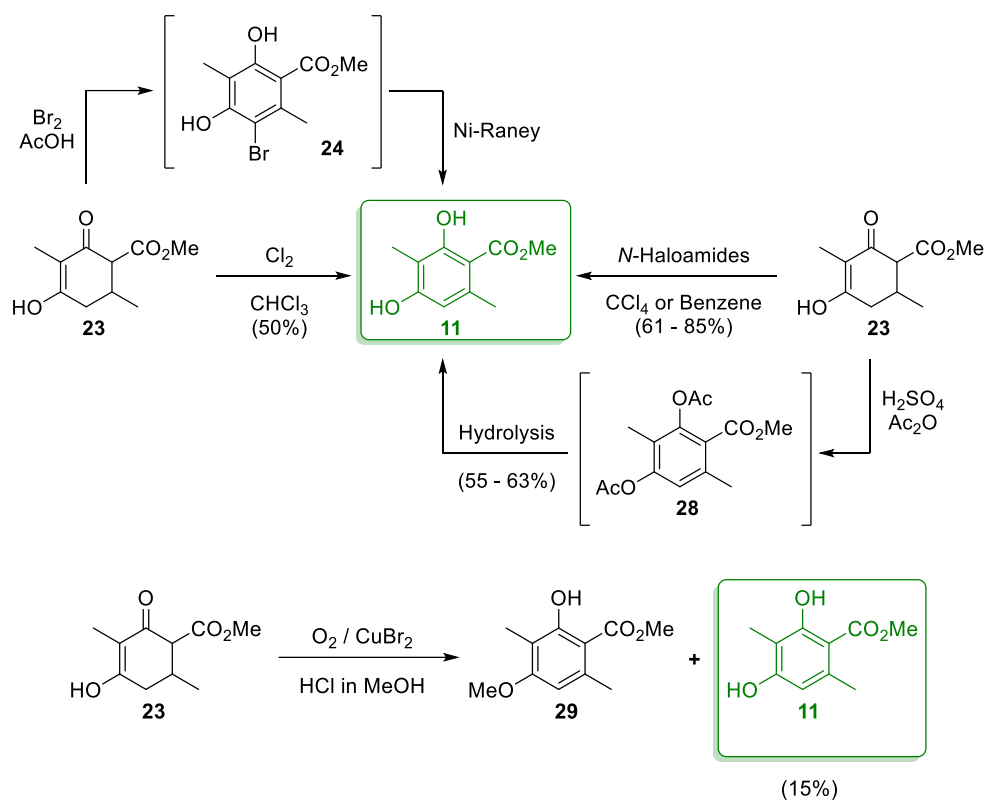
Scheme 1: Sonn’s method for the synthesis of Evernyl (**11**) from methyl crotonate (**20**) and methyl acetoacetate (**21-Me**), yields not provided.

Evernyl was first synthesized in 1929 by Sonn *et al.* from methyl crotonate (**20**) and methyl acetoacetate (**21-Me**).¹²⁰ The Michael addition and subsequent Claisen condensation yielded the methyl β -dihydroresorcyate (**22-Me**) which was methylated with methyl iodide and oxidized with molecular bromine.¹²⁰ Finally, the intermediate methyl 5-bromo-3,6-dimethyl β -resorcyate (**24**) was debrominated to gain the target compound **11** (*Scheme 1*).¹²¹ As outlined in *Scheme 2*, there are two possible condensations that can be used to prepare the key cyclic species **23**: one is the above α,β -unsaturated carboxylate **20** with the β -ketoester **27** (Route B),¹²⁰ and the other is the condensation between malonate **26** and the α,β -unsaturated ketone **25** (Route A).¹²² The latter compound **25**, can be prepared from propyl chloride and propionyl easily at industrial scale.¹²³



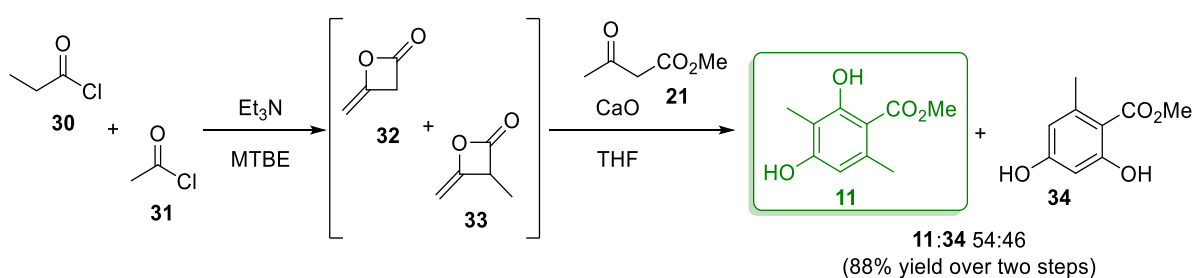
Scheme 2: General ways to obtain **7** via condensation of either **25** with **26** (A) or **20** with **27** (B).

To obtain Veramoss (**11**), the methyl β -dihydroresorcyate (**23**) still has to be oxidised (aromatized). However, this transformation has become one of the most challenging steps of its synthesis. In 1970, a chlorine-mediated oxidation was employed, but still required the same number of synthetic steps compared to the original 1929 preparative method.¹²⁴ In an attempt to replace the toxic chlorine gas the usage of *N*-haloamides was demonstrated in 1976.¹²⁵ One year earlier, a new version of Sonn's synthesis was described using bromine in acetic acid and Raney nickel for the reduction instead of the more expensive palladium, however, a toxic metal catalyst and an additional step were still required.¹²⁶ Symrise patented a two-step method which oxidizes **23** with sulfuric acid and acetic anhydride to gain the diacetylated compound **28**.¹²⁷ The latter was then hydrolysed, either under acid or basic conditions, to yield methyl atrarate (**11**) (*Scheme 3*). A Cu-catalysed aerobic oxidation was also reported in 1984 by BASF, although the main product obtained was actually the mono methyl ether **29**, Veramoss was isolated only in small amounts (max. 15% yield).¹²⁸



Scheme 3. Synthetic pathways to Veramoss (**11**) starting from precursor **23**.

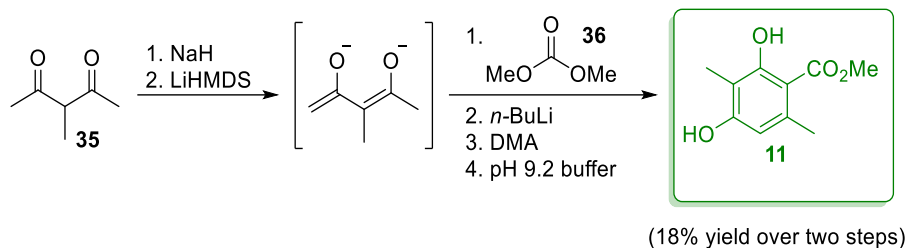
Other synthetic routes have also been considered for instance through the intermediary of ketenes, but this only enabled a 1:1 mixture of **11** and the derivative methyl β -resorcyate **34** to be obtained (*Scheme 4*).¹²⁹



Scheme 4. Synthesis of Veramoss (**11**) via the β -lactones **32** and **33**.

An approach taking inspiration from nature utilised a 1,3-dicarbonyl compound for the preparation of **11**.^{130,131} The synthetic pathway started with a carbonylation of the methyl

acetoacetone (**35**) dianion, which was formed *in situ*, and subsequently acetylated with *N,N*-dimethylacetamide (DMAc). The DMAc as acetylating agent was found to be the best out of a series of 11 different agents that were explored. The non-isolated intermediate was then cyclized at pH 9.2, yielding Veramoss (**11**) although in only 18% (*Scheme 5*).



Scheme 5. Biosynthesis inspired preparation of polyketide metabolites such as **11**.

Apart from these syntheses performed at relatively small scale, the industrial scale preparation of Veramoss is mostly based on the oxidation of the methyl β -dihydroresorcylate (**23**). As described above, miscellaneous conditions have been investigated, although the oxidations with elemental chlorine and bromine remains the most effective and consistent even if they do not represent the most atom economic or safest process to run at scale. Thus, a more efficient and environmental-friendly approach is highly sought after. A principle aim of this investigation was therefore to identify alternative methods for the synthesis of Veramoss (**11**) and if possible to develop a continuous flow process from either the raw materials or the intermediate **23**.

1.3.2. *Ambertonic*

Ambertonic™ (**37**) is a current commercial branded product developed by IFF, first patented in 2012, as a property molecule with characteristic amber, woody and musky notes.¹³² The mixture has been found to be composed by the main two isomers depicted in *Figure 7* where the *trans* configured ring product is the main component (*trans*-**37**).

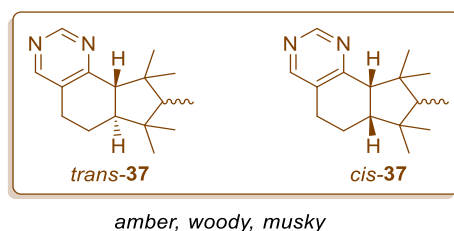
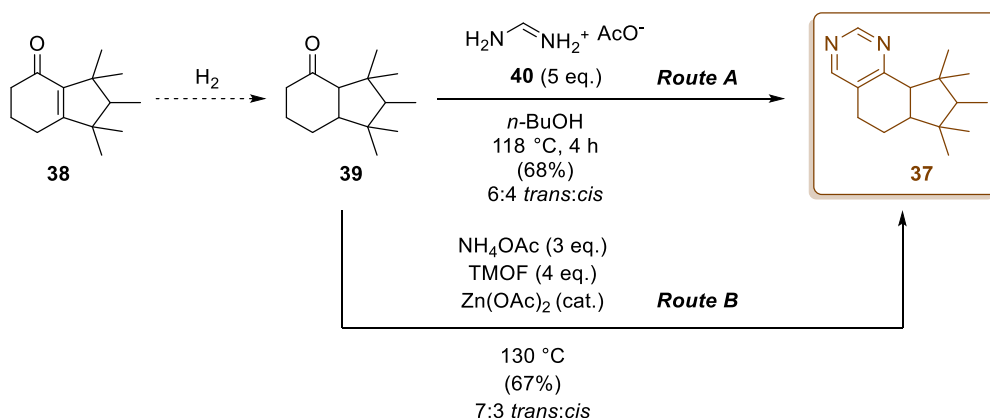


Figure 7. Structure of Ambertonic™ (**37**), a synthetic fragrance sold by IFF.

The only reported synthetic preparation of **37** starts from an IFF commercially available compound namely, Cashmeran™ (**38**). The route involves first hydrogenation and then reaction with formamidine acetate (**40**) in butanol to yield Ambertonic™ (*Route A in Scheme 6*). The pyrimidine ring is therefore formed following a known method described by Baran *et al.* in 2006 and in this way the compound **37** is obtained in 68% yield.¹³³ An alternative preparation described in a more recent publication by Bathula *et al.* was also attempted, gaining the final material **37** with similar yields (*Route B in Scheme 6*).¹³⁴ In this example, the pyrimidine ring formation employs zinc acetate as a catalyst and trimethyl orthoformate (TMOF) and ammonium acetate as replacement to the formamidine acetate **40**.



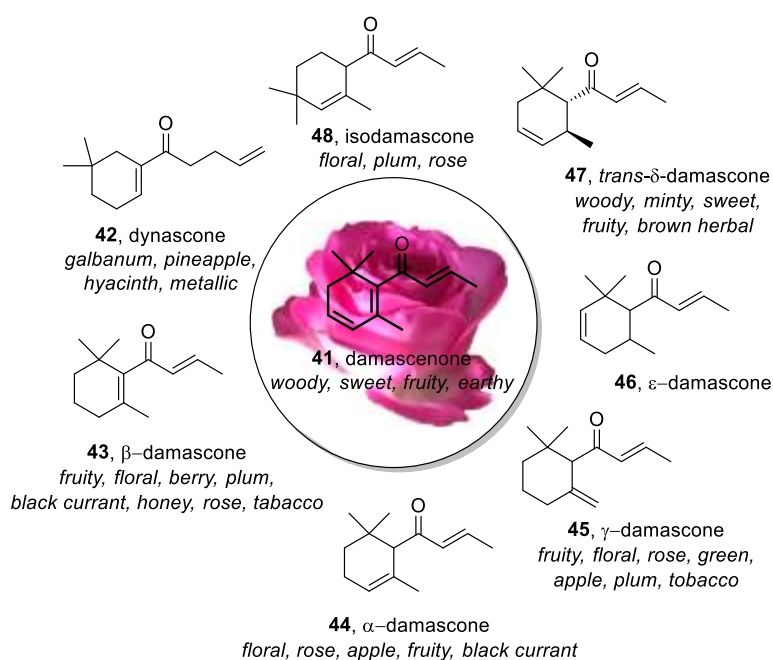
Scheme 6. Synthetic route to Ambertonic™ starting from Cashmeran™ (**2**).

The weakness of the latter preparations (*Route A&B*), other than the moderate yields (67 – 68%), is the quantity of reagents required (equivalent excesses). This makes the current synthetic processes poorly efficient and difficult to apply at an industrial scale. A principle aim of this investigation was therefore to identify alternative methods for the synthesis of Ambertonic™ and develop a continuous flow process where possible. Furthermore, the

industrial collaborator was also interested in characterising the main isomer of the mixture by revealing possible absolute configurations.

1.3.3. Galbascone

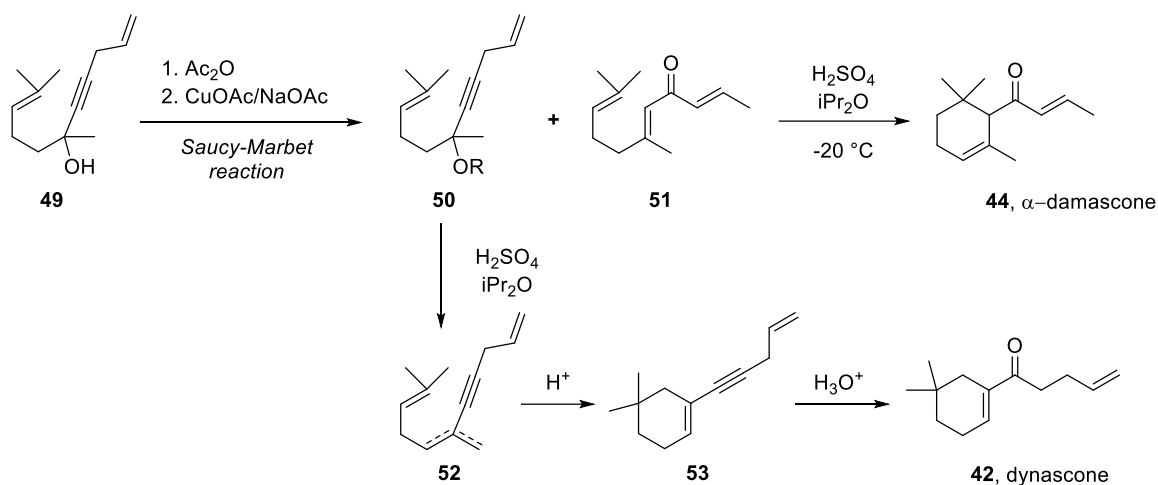
First discovered in 1973 by Firmenich, and later commercialised as Galbascone (IFF) or Dynascone (Firmenich), 1-(5,5-dimethylcyclohex-1-en-1-yl)pent-4-en-1-one (**42**), immediately found great interest with perfumers for its characteristic galbanum, pineapple, hyacinth odour profile, and it became the most frequently used odorant of Firmenich in the period between 1970 and 1980. In 1967, after the full characterisation of α -damascenone (**41**), the natural key component of Bulgarian rose oil, 6 more analogues of **41** were prepared and these group of molecules constitute the Rose ketone family (*Scheme 7*).¹³⁵



Scheme 7. Representation of the rose ketones family based upon the parent structure of damascenone **41**.

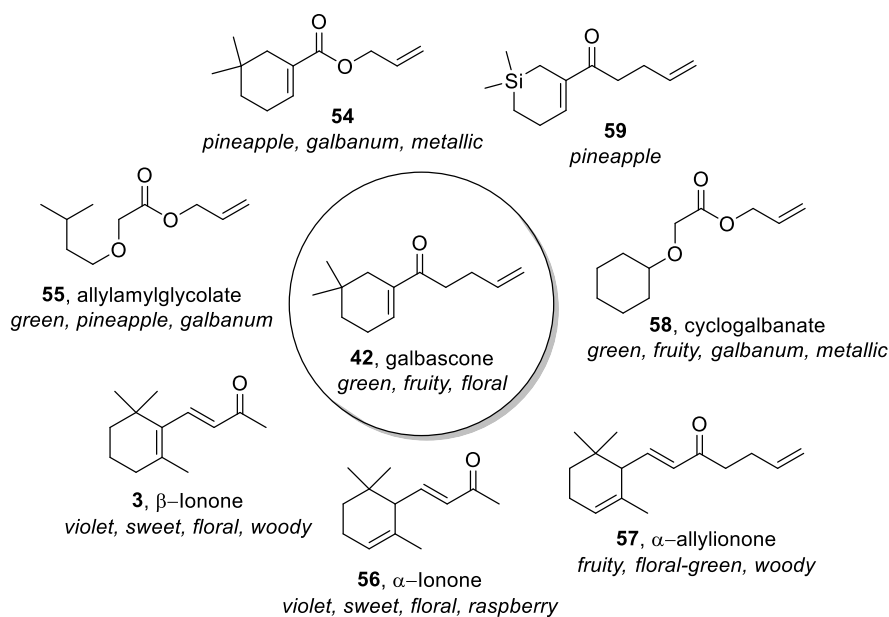
During an attempt to prepare the rose analogue α -damascone (**44**) starting from pseudo-damascone (**49**), an attractive galbanum off-note was found accompanying the composition of the final mixture (*Scheme 8*). The note was eventually isolated and characterised via gas

chromatography-sniffing method as Dynascone **42**. Dynascone's formation was attributed to a cyclisation of the triene intermediate **52** formed through initial loss of water.¹³⁶



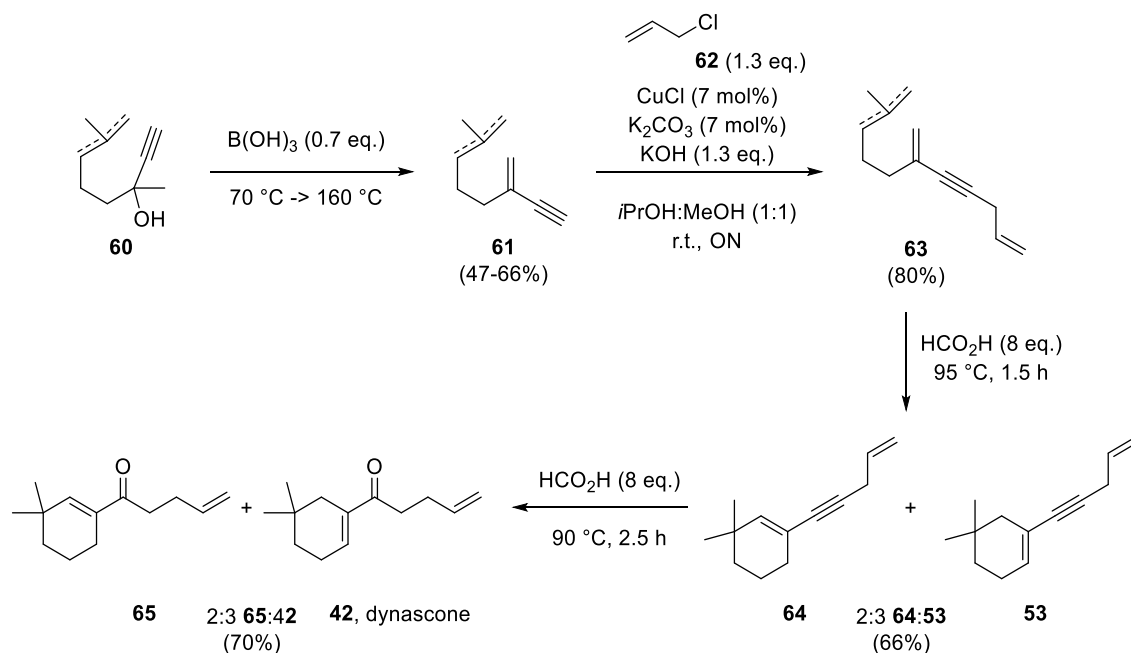
Scheme 8. Proposed reaction sequence for the formation of dynascone **42** from pseudo-damascone **49**.

The “Firmenich’s ultimate captive” odorant,¹³⁷ as it was described by Morris and co-workers at Firmenich, had outstanding tenacity and diffusive properties as well as exceptional stability which allowed it to gain a dominant role in the fragrance industry. Subsequent odour-structure relationship studies revealed that by replacing a methylene group with an oxygen atom the structure still retains its odour characteristics (**54**, *Scheme 9*). As such, a new family of glyoxylates such as allylamylglycolate (**55**), and cyclogalbanate (**58**) were evolved to have similar galbanum characteristics and high odour strength; however, these new molecules possessed much lower stability than Galbascone. The dimethylcyclohexenyl group equivalent to the characteristic part of the ionone family (**3** and **56**), may be attributed to the floral note of the molecule, however, the rose analogue α -damascone has more similarities with this family than Galbascone. The allylic groups may be attributing the fruity note of the molecule as it can be noticed α -ionone (**56**) also acquires this characteristic scent in α -allylionone (**57**). Recently, analogues of dynascone where the quaternary carbon atom was replaced with a silicon atom (**59**) has also been investigated and found to have a much higher odour strength with a different odour spectra, thus revealing the key role of the cyclohexene.¹³⁸



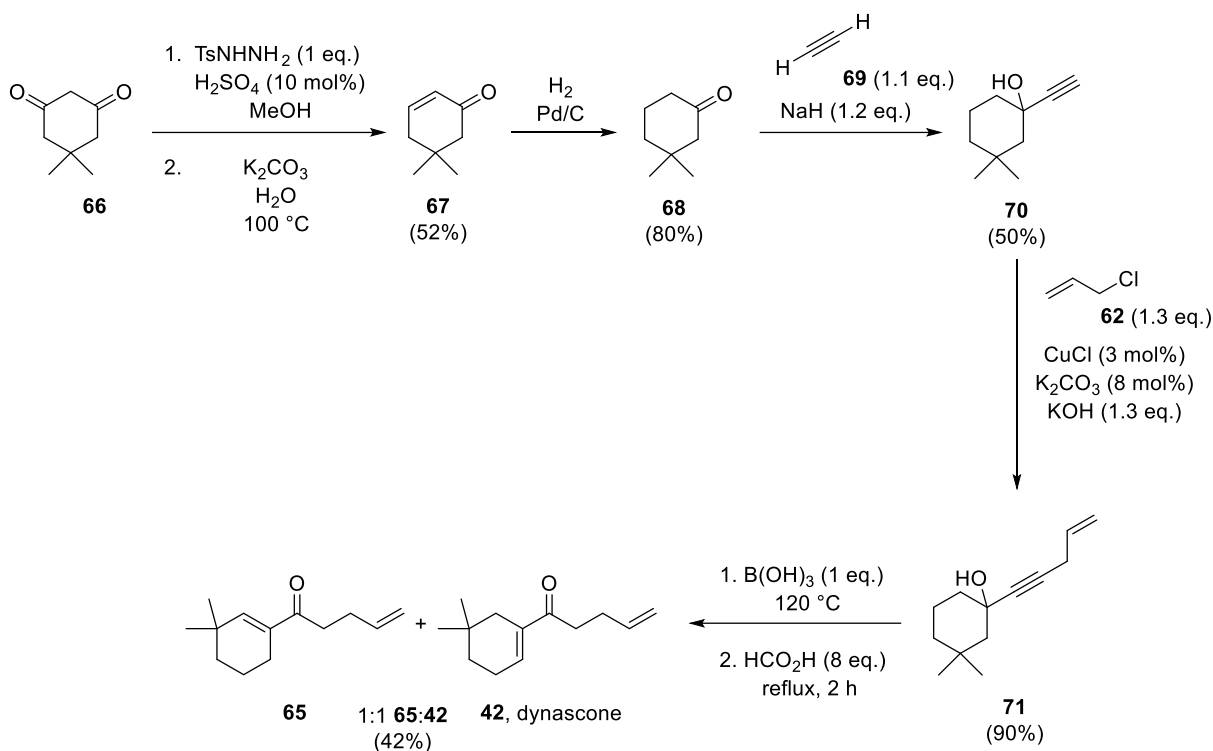
Scheme 9. Odour-structure relationship with the analogues of Dynascone **42**.

Many syntheses of Galbascone (**42**) have already been described in the literature.^{136,137,139–142} In 1979, Fimernich patented four possible synthetic pathways deriving from diverse raw materials such as 3-carene, dehydrolinalool, isobutyraldehyde, and methyl vinyl ketone.¹³⁶ Starting from α/β -dehydrolinalool (**60**), the compound was dehydrated employing boric acid and then alkylated with allyl chloride in potassium hydroxide, copper chloride, and potassium carbonate (*Scheme 10*). The intermediate **63** then undergoes an acid-catalysed cyclisation as described above (*Scheme 8*). A final distillation purification yields a 3:2 mixture of the desired molecules **42** and the product from double bond isomerisation **65**. Ultimately, this 4-step route gains Dynascone (**42**) in 24% overall yield.



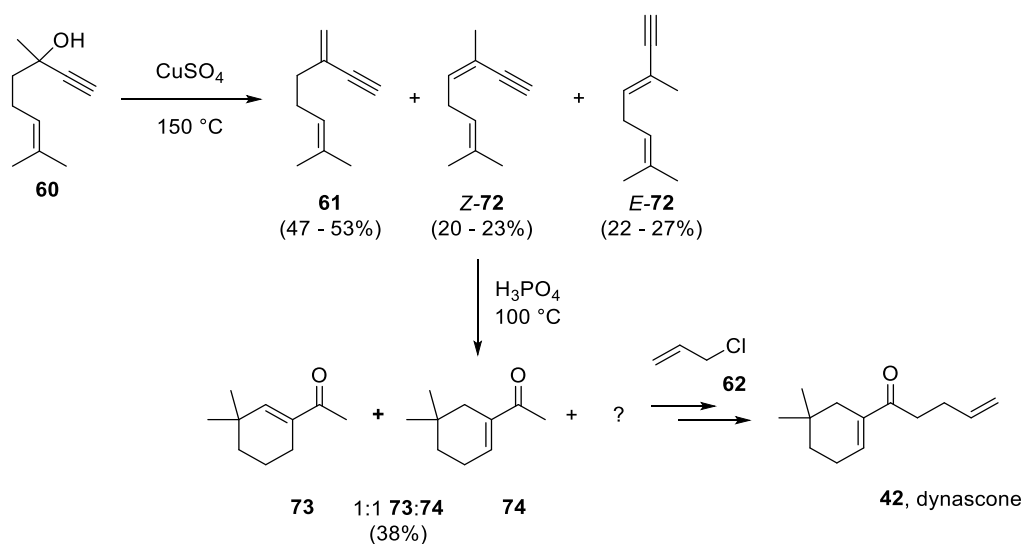
Scheme 10. First industrial route to dynascone (**42**) from dehydrolinalool (**60**) as patented by the fragrance company Firmenich.

In an alternative approach the semi-hydrogenation of dimedone (**66**) efficiently forms the intermediate 3,3-dimethylcyclohexanone (**68**), which can be alkylated with acetylene and then allylated to form the tertiary alcohol intermediate **70** (*Scheme 11*). This alcohol then undergoes dehydrogenation and hydration of the alkyne group to furnish a 1:1 mixture of isomers **42** and **65**. Since the compounds have very similar properties, an isolation of the pure desired material becomes difficult. Many of the synthetic preparations reported also suffer from this issue and therefore the development of a stereoselective route to Galbascone is still an on-going challenge.



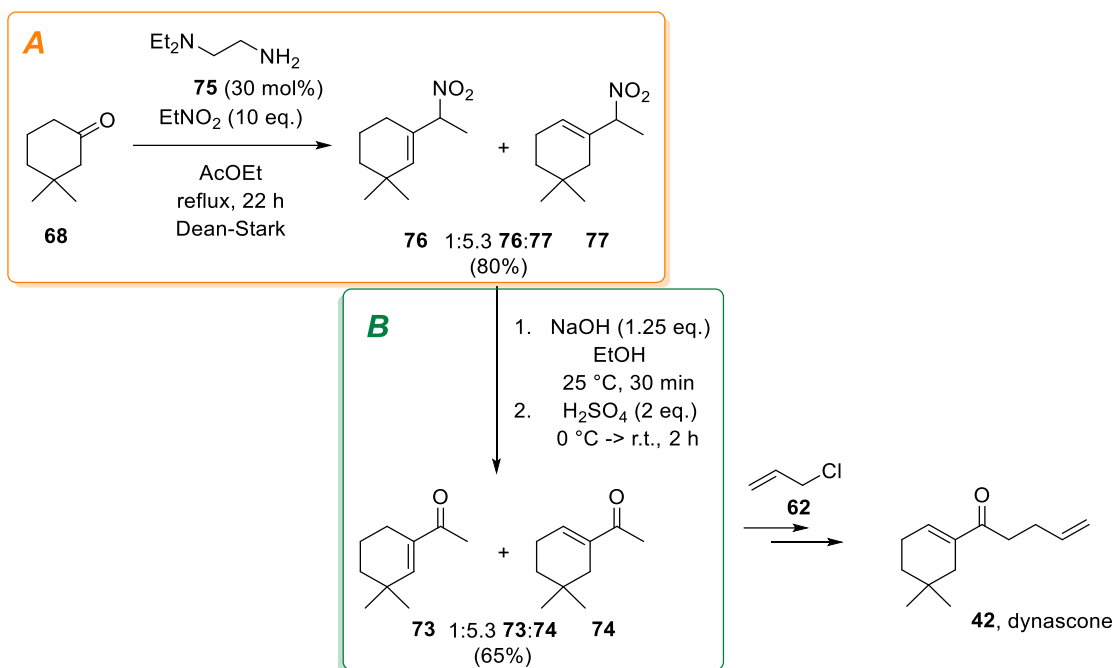
Scheme 11. Route to Dynascone (**42**) from dimedone (**66**) as patented by the company Firmenich.

The current industrial manufacturing route for Galbascone (**42**) as employed by IFF mirrors the one Firmenich first described, however the alkylation with allyl chloride (**62**) occurs only at the last step after the cyclisation (*Scheme 12*). The Rupe rearrangement on dehydrolinalool (**60**) is reported to form mainly the undesired product β -dehydroherbac (**73**) along with several pyran structures,¹⁴³ however, this is not the case when the reaction is performed on the dehydrated analogues **61** and **72** (*Scheme 12*). Thus, a copper sulfate dehydration of dehydrolinalool (**60**) is carried out before the acid-catalysed Rupe rearrangement to gain an enriched mixture (40%) of the α -dehydroherbac (**74**). The process takes over 12 hours and has a low efficiency (overall 19% yield, isomer purity: 50%), however the low price of the raw starting material allows economic viability keeping the final material's production price down. This route is carried out on a multi-tonne scale per batch (>9,000 kg of raw material) at the IFF site in Benicarló (Spain).



Scheme 12. Outlined industrial route to Galbascone (**42**) as developed and employed by IFF on a multi-tonnes scale.

In 2018, a collaboration between the Baxendale research group and IFF Benicarló established a new and highly efficient methodology for the synthesis of the α -dehydroherbac (**74**) exploiting an Henry-Nef two-steps reaction (*Scheme 13*).¹⁴¹ The sequence starts from 3,3-dimethylcyclohexanone (**68**) progressing through; (A) nitro condensation Henry reaction to the nitro compound **77**, and (B) hydrolysis of the latter through sequential base and acid treatment.



Scheme 13. Preparation of β -dehydroherbac via Henry-Nef reaction as patented by IFF.

The first step, A, of the synthesis was a base-catalysed nitro aldol reaction between the ketone **68** and nitroethane. The reaction process was initially exploited by Zard and co-workers in 1982 for the preparation of new 20-oxo-corticosteroids derivatives.¹⁴⁴ In this example, *N,N*-dimethylethylenediamine (**75**) was employed as the catalyst and the nitro derivatives were isolated. Four years later, Tamura *et al.* efficiently employed a similar methodology starting from miscellaneous ketones and nitroalkanes and the authors isolated 23 homoallylic nitro compounds in low-to-high yields (24 – 80%).¹⁴⁵ The authors claimed the reaction was highly susceptible to steric hindrance and that high equivalents of the nitroalkane help to increase the rate of the reaction and the overall yields.

Due to the asymmetry of the starting material, two possible homoallylic nitro isomers can be formed from ketone **68** (i.e., **76** & **77**) under the current reaction conditions, the selectivity toward the desired material **77** was achieved by controlling the alkyl substituents on the tertiary nitrogen of the ethylenediamine catalyst. Despite the relatively high efficiency (80%) and selectivity (1:5.3, **76:77**), the procedure still requires long reaction times which was noted to be affecting the isomer content in the final material. In fact, an enriched mixture of the nitro

compound **77** with **76** was shown to lead to decomposition over time under the applied reaction conditions.

The aim of this investigation was to expand the reaction understanding of the previously developed route with a more detailed investigation of the different parameters (concentration, solvent, catalyst) and reaction time as well as scouting alternative synthetic routes to evaluate new raw materials. In addition, it was also thought valuable to evaluate different continuous setup that employs heterogenous catalyst, which would simplify the catalyst recovery and reusage.

1.4. Summary aims and objectives – Bullet points

The aims for this thesis are various and extensive. For these reasons, to allow a clear reading of the thesis, a summary of the key points are hereby described.

Veramoss

- Design new route to Veramoss and derivatives
- Develop greener conditions of the current industrial procedure
- Evaluate potential applications of continuous flow process

Ambertonic

- Evaluate the difference in olfactory properties between the two enantiomers of the major *trans* isomer material
- Design new routes for the preparation of Ambertonic™ starting either from Cashmeran (**38**) or other raw materials
- Optimise the designed routes for a possible industrial application
- Evaluate a potential application of a continuous flow process

Galbascone

- Design new selective routes to Galbascone starting from cheap raw materials
- Optimise previous designed procedures

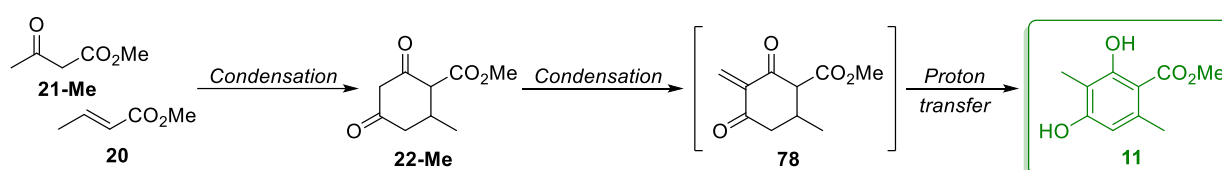
- Develop continuous flow systems for the synthesis of the Galbascone key intermediate (**74**)

2. Results and discussion

2.1. Veramoss

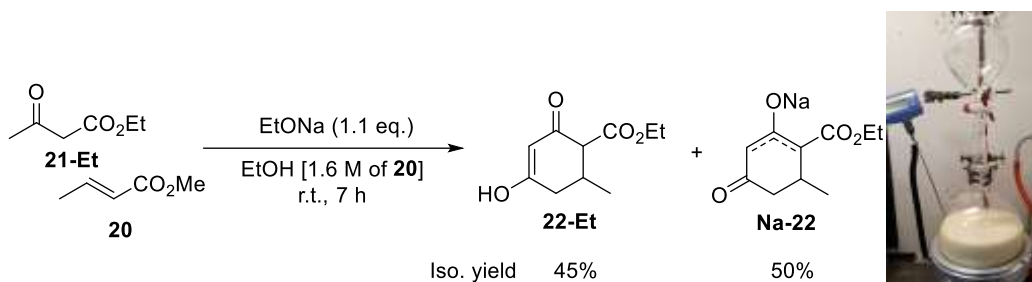
2.1.1. Alternative strategy starting from ethyl 1,6-dihydro-orsellinate

The first strategy was to explore the usage of 1,6-dihydro-orsellinate (**22-Me**) as intermediate for the synthesis of Veramoss (**11**). This intermediate can be easily obtained from cheap and widely available raw materials such as methyl acetoacetate (**21-Me**) and methyl crotonate (**20**). As depicted in *Scheme 14*, this route involves first the generation of the methyl 1,6-dihydro-orsellinate (**22-Me**) and a successive introduction of an *exo*-olefin. The intermediate **78** has the required methyl and the same oxidation state as Veramoss (**11**), enabling in theory the aromatization to take place by internal proton transfer and hence avoiding the requirements for any additional oxidation process.



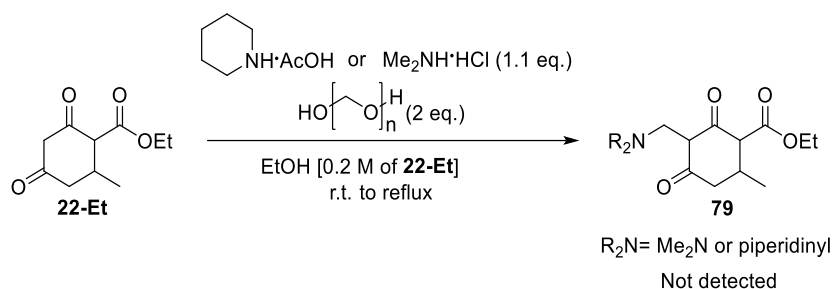
Scheme 14. Proposed synthetic pathway to Veramoss (**11**).

Bearing this hypothesis in mind, the synthesis started from the preparation at gram-scale of the intermediate **22-Et**, which was obtained in excellent yield partially isolated as the neutral form and also as its sodium enolate salt (*Scheme 15*).¹⁴⁶ Due to the laboratory availability of the ethyl acetoacetate (**21-Et**), compound **22-Et** was synthesised instead of its methyl analogue, which was not expected to affect the subsequent chemistry. The position of the enol double bond in compound **22-Et** has not been confirmed since no proper single crystals were obtained during the investigation.



Scheme 15. Preparation at 1 mol-scale of the intermediate **22-Et** and picture of the equipment used along with the precipitate formation.

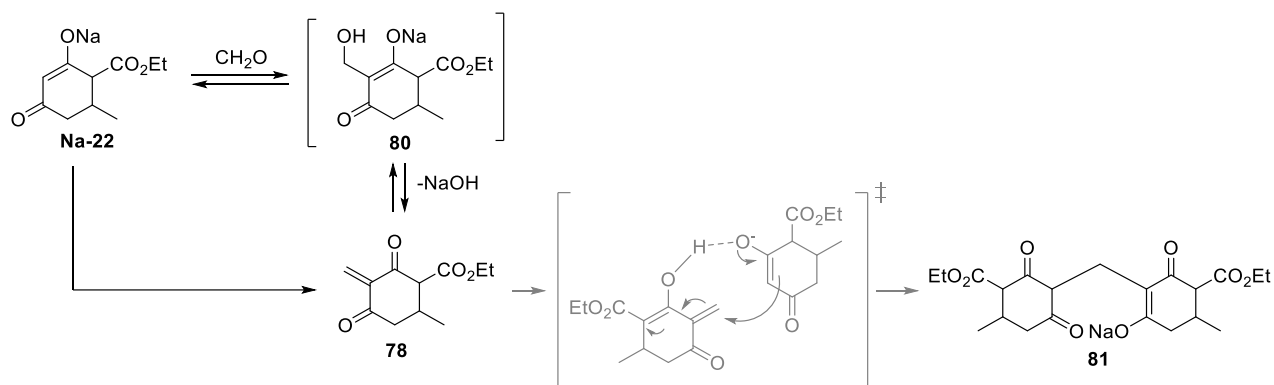
Having access to quantities of compound **22-Et**, a Mannich reaction was deemed to be the most suitable route to the desired olefination. An example of the later reaction on a similar scaffold with successive palladium-catalysed reduction was found in literature, which gave good yields.¹⁴⁷ As it was in our interest to synthesis the *exo*-olefin **78**, a Mannich reaction was performed without any reduction step and using paraformaldehyde instead of a solution of the monomer.^{148–151} The reaction was performed in two different ways, either using stoichiometric or catalytic amounts of hydrochloride and acetate amine salts (*Scheme 16*). Unfortunately, none of the desired product was detected even after several hours in the crude mixture as analysed by liquid chromatography – mass spectrometry (LC-MS, ESI).



Scheme 16. Attempted reaction conditions investigated to synthesise **79** with a Mannich reaction.

It was then considered to attempt the formaldehyde addition to **Na-22** since the formation of a less basic base such as sodium hydroxide could provide the necessary driving force for the reaction (black area, *Scheme 17*). However, it is noteworthy that the electrophilic compound

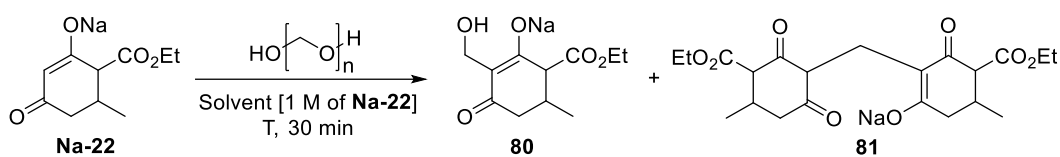
78 could react with the remaining starting material to form the dimer **81** (grey area, *Scheme 17*) as also reported during a similar study by Wang *et al.*¹⁵²



Scheme 17. Proposed mechanism for the formation of **78** (in the black area) and the possible by-product **81** (in the grey area).

Different parameters could affect this side reaction, such as the nature of the solvent, concentration and the molar ratio between **Na-22** and paraformaldehyde. Hence, different conditions have been screened as shown in *Table 5*. As ¹H-NMR spectra and thin-layer chromatography (TLC) were hard to interpret, the crude reaction mixtures were only assessed initially for speciation using LC-MS (ESI).

Table 5. Screening of different reactions conditions for the formation of **81**.

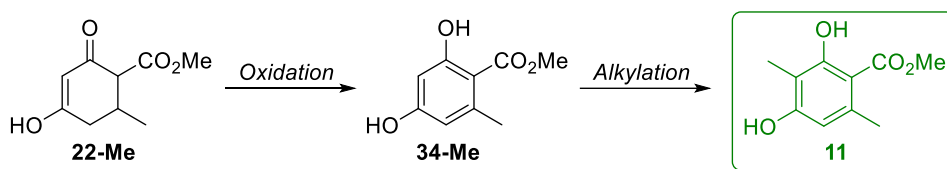


Entry ^a	Solvent	Eq. formaldehyde	T (°C)	Results ^b
1	EtOH	1	reflux	81
2	EtOH	1	36	81
3	EtOH	6	36	81
4	EtOH	30	36	81
5	MeOH	1	36	81/80^c
6	THF	1	45	81
7	H ₂ O [0.1 M of Na-22]	10	36	81/80^c

^aAll reaction were carried out on a 10 mmol scale; ^b Results based on the LC-MS (ESI) following the *m/z* of **80** (229) and **81** (409); ^c The presence of **80** in the mixture was not confirmed by any other analyses.

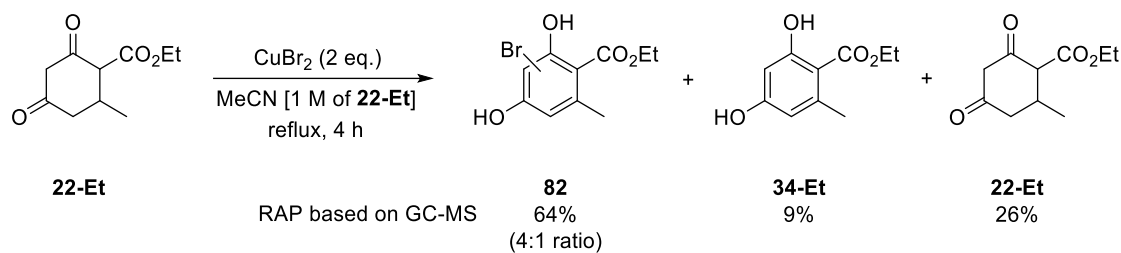
As seen in *Table 5*, in all the reactions carried out the chromatograms obtained showed the presence of several different species along with the main compound which was indicated as the dimer **81**. Only under two sets of conditions (*Table 5, Entries 5&7*), were peaks found where the m/z matched that of the mass of **80**, however, further analyses ($^1\text{H-NMR}$ spectra) failed to confirm this result. The effect of the order of addition was also found to have negligible impact on the reaction selectivity.

Unable to achieve a reproducible and meaningful outcome from the paraformaldehyde addition due to the extreme reactivity of the *in situ*-derived substrate **80**, it was decided to first perform the oxidation step prior to the formaldehyde addition/reduction (*Scheme 18*). An example of aldehyde addition on methyl 2,4-dihydroxybenzoate (**34-Me**) has been described in the literature.¹⁵³



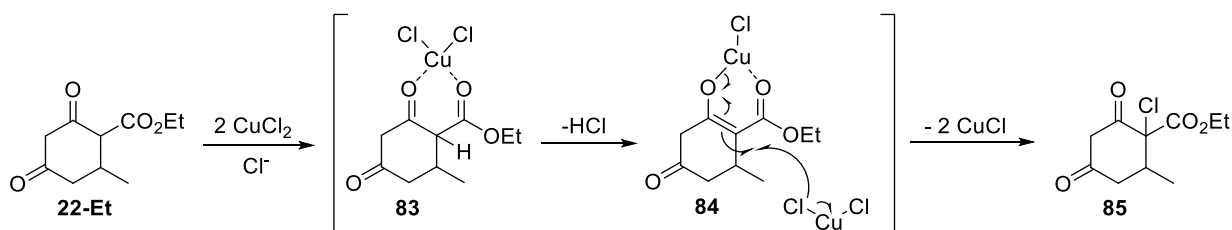
Scheme 18. Proposed alternative strategy to Veramoss **11** via oxidation and alkylation steps.

Different oxidative conditions were screened, starting from a process which had been evaluated for the synthesis of Hedione[®] using CuBr_2 .¹⁵⁴ After 4 hours in acetonitrile at reflux, the mixture was analysed via GC-MS (EI) and found to be formed mainly by the bromo-substituted compounds **82** (the intermediates were not isolated and therefore the nature of the two isomers could not be assessed), whereas the desired compound **34-Et** was found only in trace amounts (*Scheme 19*). A catalytic version (10 mol%) of the described reaction was then tested, although without producing any oxidised compounds.



Scheme 19. Oxidation with CuBr_2 which formed mainly the bromo-substituted compounds **82**. RAP = relative percentage area. The ratio was obtained by dividing the GC integral of the major isomer **82** ($R_t = 5.26$ min) with the GC integral of the minor isomer **82** ($R_t = 5.28$ min).

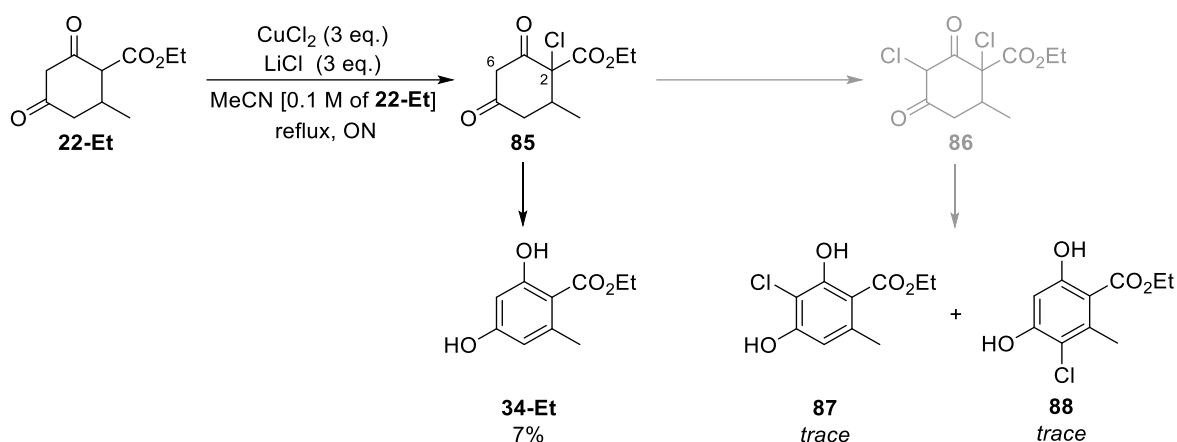
In the literature, a procedure has been described for the formation of phenol using CuCl_2 as the oxidizing agent along with LiCl as an additional chloride source in *N,N*-dimethylformamide (DMF).¹⁵⁵ The mechanism of the chlorination is not understood at present, although a study based on the chlorination of acetone seems to support the formation of an initial coordination of the ketone to form the π -complex **83** and subsequent deprotonation to the σ -complex **84** which disproportionates with a second molecule of copper(II) chloride to form the chlorinated intermediate **85** and two molecules of copper(I) chloride (*Scheme 20*).^{156–159} The authors of the article suggest an increase in the reaction rate when additional chloride was added to the reaction mixture. The chloro-intermediate would then eliminate a molecule of HCl to form the phenolic material.



Scheme 20. Proposed mechanism for the copper(II) chloride chlorination of ketones based on literature.¹⁵⁵

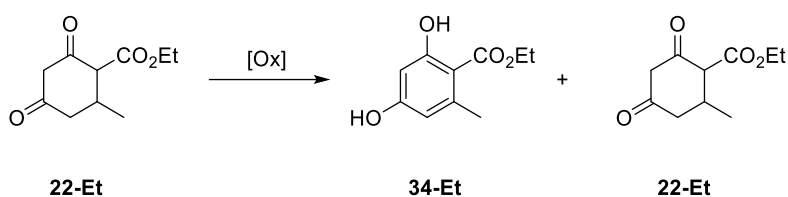
However, to avoid the use of DMF and the large excesses of inorganic reagents, it was decided to attempt a modification of the conditions. Therefore, acetonitrile (MeCN) was used as the

solvent and a 1:1 ratio of copper(II) chloride and lithium chloride (*Scheme 21*). The reaction was followed by LC-MS (ESI). During the first 3 hours, mono-chlorinated phenols such as **87** and **88** were identified. In the following 3 hours there was no change in the composition of the mixture, and, after refluxing the reaction overnight, the crude mixture was found to be composed mainly of unreacted starting material **22-Et** and traces of chlorinated phenols. The desired material **34-Et** was only isolated in a low 7% yield. The same results were obtained when methanol was used as the reaction solvent. This result implies that the chlorination is sluggish (hence why large excess copper loading {10-15 eq.} is potentially used in previous literature oxidation example), and as a consequence no further investigations were performed.



Scheme 21. Proposed reaction sequence for the oxidation of **22-Et** using CuCl_2 . The compound **87** and **88** were obtained as a mixed fraction and characterised by $^1\text{H-NMR}$ spectra.

A brief investigation of alternative oxidative conditions was also performed and is herein reported (*Table 6*). CuCl/TEMPO ,¹⁶⁰ $\text{TEMPO}/\text{ammonium cerium nitrate}$,¹⁶¹ MnO_2 ,¹⁶² and charcoal¹⁶³ were screened, although without gaining the desirable outcomes. In most of cases only starting material **22-Et** was recovered and no further work was pursued due to the decision of the sponsoring company.

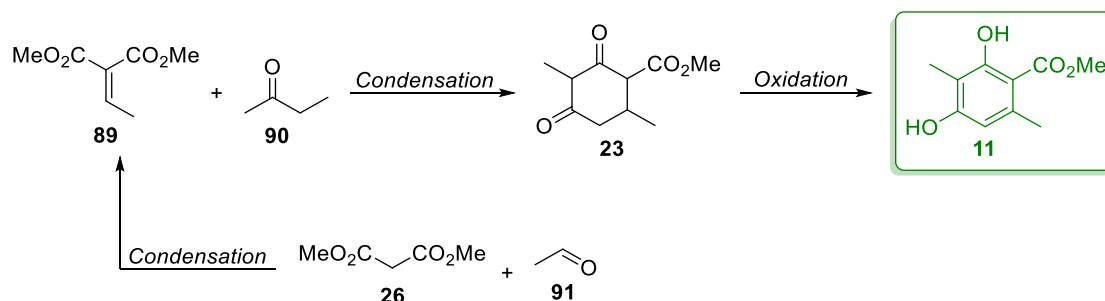
Table 6. Additional reaction conditions attempted for the oxidation of **22-Et** to **34-Et**.

Entry ^a	Reaction conditions	Conv. 34-Et (%) ^b	Experimental Notes
1	CuCl (5 mol%), MeOH:MeCN (1:1) [0.1 M of 22-Et], r.t., 3 h	-	- Mainly 22-Et - Some <i>O</i> -methylation observed
2	CuCl (15 mol%), TEMPO (30 mol%), Et ₃ N (1 eq.), toluene [0.5 M of 22-Et], r.t., 16 h	-	Traces of chlorinated compounds
3	TEMPO (20 mol%), Ammonium Cerium Nitrate (20 mol%), O ₂ , MeCN [0.1 M of 22-Et], reflux, 12 h	-	Only 22-Et
4	MnO ₂ (0.5 mol%), O ₂ , MeCN [1 M of 22-Et], r.t., 24 h	-	Only 22-Et
5	MnO ₂ (2 eq.), MeCN [1 M of 22-Et], r.t., 24 h	-	Only 22-Et
6	O ₂ , Charcoal (50 %wt), AcOH [0.25 M of 22-Et], reflux, 18 h	-	Only 22-Et

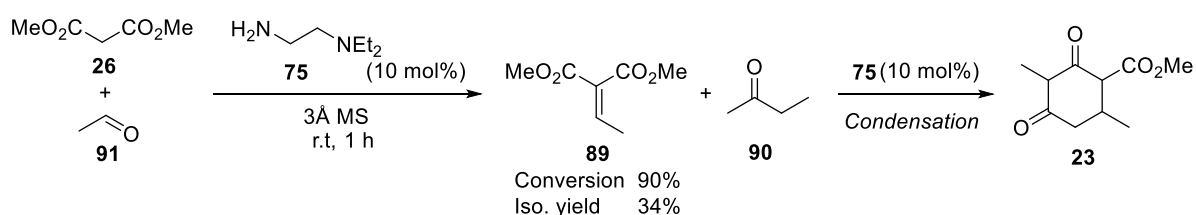
^aThe experiments were carried out on a 10 mmol scale: ^bBased on LC-MS (ESI) and ¹H-NMR spectra.

2.1.2. Synthetic strategy from 2-butanone: Route A

The second evaluated route to Veramoss consisted of synthesising dimethyl ethylenemalonate (**89**) which is subsequently condensed with butanone (**90**) (*Scheme 22*). In order to obtain the intermediate **89** and to start from cheaper and more commercially available materials, a condensation between dimethyl malonate (**26**) and acetaldehyde (**91**) was investigated.

**Scheme 22.** Proposed synthetic strategy for an alternative synthesis of Veramoss (**11**).

The initial studies were focused on the Knoevenagel condensation between compounds **26** and **91**. Only limited examples of this reaction were found in the literature, however, they all indicated low isolated yields and difficult purification strategies.^{164–167} Consequently, we decided to attempt an alternative route to precursor **89**. Since the condensation was expected to occur more efficiently under basic conditions, it was initially considered to use a catalyst which could be feasible also for the subsequent condensation step. Hence, an aminocatalyst such as *N,N*-diethylethylenediamine (**75**) was tested and the desired compound **89** was isolated via vacuum distillation, although only in 34% yield (*Scheme 23*). To avoid the usage of molecular sieves, a Dean-Stark apparatus using refluxing toluene was utilized, however, no desired compound was obtained.



Scheme 23. Condensation of dimethyl malonate (**26**) and acetaldehyde (**91**) using amine **75** as a catalyst. The conversion was determined by ¹H-NMR spectra using dimethyl fumarate as internal standard.

The main by-products of the Knoevenagel condensation were the compounds **92** and **93** (*Table 7*). These compounds are formed by the conjugate addition to the olefine **89** of either the unreacted dimethyl malonate **26** (**93**) or methanol/water (**92**), which are present in the reaction mixture. To evaluate this reaction, we screened a selection of different base and acid catalysts under different reaction conditions as depicted in *Table 7*.

Table 7. Screening catalysts and reaction conditions for Knoevenagel condensation.

Entry ^a	Catalyst	Loading (mol%)	Solvent	time(h)	Additive	Conv. (%) ^b	Conv. 89 (%) ^b
1	PS-DMA ^c	3	SFC ^c	48	-	66	45
2	PS-DMA	3	SFC	48	Na ₂ SO ₄	82	40

3	PS-BZA ^c	3	SFC	48		12	10
4	PS-BZA	3	SFC	48	Na ₂ SO ₄	65	54
5	-	-	MeOH (2M) ^e	72	-	64	43
6	PS-DMA	3	MeOH (2M) ^e	48	-	82	46
7	PS-DMA	3	MeOH (0.5M) ^e	48	-	66	40
8	Montmorillonite	3	MeOH (0.5M) ^e	48	-	0	-
9	Ba(OH) ₂	10	MeOH (0.5M) ^e	48	-	30	20
10	PS-DMA	3	MeOH (2M) ^e	24	TMOF (0.1%mol) ^c	67	43
11	PS-DMA	3	MeOH (2M) ^e	24	TMOF (0.5%mol) ^c	68	41
12	PS-DMA	50	MeOH (2M) ^e	1	-	76	39
13	H ₂ SO ₄	50	MeOH (2M) ^e	7	-	0	- ^d
14	PS-TsOH ^c	50	MeOH (2M) ^e	7	-	5	-

^a All reactions were carried out in a 100 mmol-scale;^b All conversions were determined by ¹H-NMR spectra using dimethyl fumarate as internal standard;^c PS-DMA: polystyrene-supported dimethylamine, PS-BZA: polystyrene-supported benzylamine, SFC: solvent-free conditions, TMOF: trimethylorthoformate, PS-TsOH: polystyrene sulfonic acid resin;^d The reaction was worked up with saturated NaHCO₃ aqueous solution, water and washed with brine to obtain a yellow solution which was then concentrated under vacuum;^e The molarity of the solvent is in respect with the moles of compound **26**.

We first considered the use of a heterogeneous catalyst with no solvent since it would be easier to purify the product via distillation or allow dilution and use of the crude material in the subsequent reaction. As can be seen in *Table 7*, polystyrene-supported dimethylamine (PS-DMA) was found to be the best heterogeneous catalyst for the condensation under these solvent free conditions (*Table 7, Entries 1&3*). The addition of sodium sulfate increased the conversion; however, its use at scale would not be feasible as it is required as a stoichiometric agent (*Table 7, Entries 2&4*). For these reasons, methanol was tested and found to be a good dehydrating agent, increasing the conversions, and reducing the quantities of **92** formed (*Table 7, Entries 5 – 7*). Furthermore, trimethylorthoformate (TMOF) was also found to be a good dehydrating agent (*Table 7, Entries 10&11*). The absence of any catalyst slows down the reaction rates and decreases the selectivities (*Table 7, Entry 5*). Other catalysts such as montmorillonite and barium hydroxide were examined, although lower or no conversions were observed (*Table 7, Entries 8&9*). To reduce the reaction times, an increase of the loading of the catalyst to 50 mol% was investigated which reduced the reaction time to 1 hour, yet this also diminished the selectivity for **89** (*Table 7, Entry 12*). The usage of acid catalysts such as sulfuric acid and a sulfonic acid resin was also exploited, although no conversion occurred even after 7 hours (*Table 7, Entries 13&14*).

Having found some promising conditions, we decided to investigate a continuous-flow system approach similar to the one previously reported by Kobayashi *et al.*^{168,169} Therefore, a repeat experiment using the PS-DMA catalyst was carried out in flow but varying the reaction times and conditions as depicted in *Table 8*. The reaction times decreased to 15 minutes, although the selectivity also decreased yielding only the dimer **92** after 30 minutes (*Table 8, Entries 1 – 4*). The addition of TMOF as a dehydrating agent increased the selectivity towards **89**, allowing yields 38% of desired material after 60 minutes of residence time, however less selectivity was obtained using these longer reaction times (*Table 8, Entries 5 – 7*).

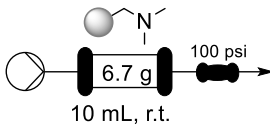
Table 8. Optimization in flow and reactions conditions for the formation of **89**.

COC(=O)CC(=O)OC
26
 in MeOH

+

C=O
91

→



COC(=O)C=C(C)C(=O)OC
89

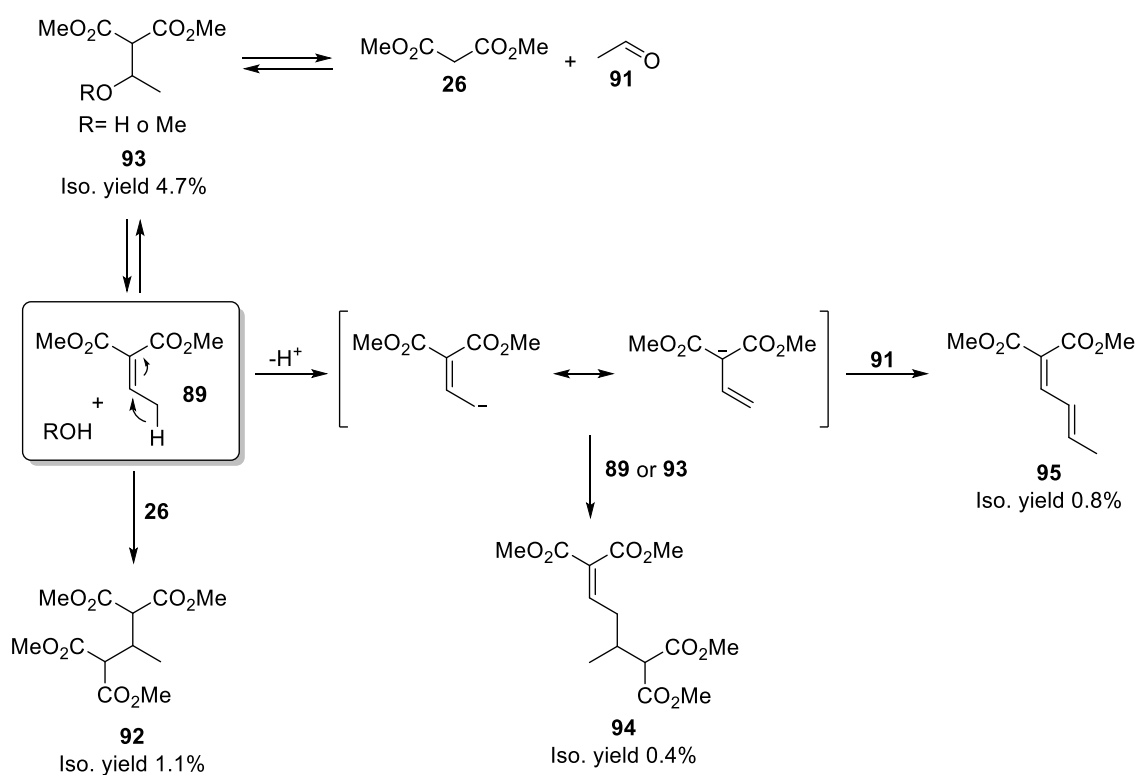


Entry	time(min) ^a	Conv. (%) ^b	Conv. to 89 (%) ^b	Additive
1	12.5	23	15	-
2	15	26	16	-
3	30	50	10	-
4	45	80	- ^c	-
5	30	40	26	TMOF (0.1mol%)
6	60	50	38	TMOF (0.1mol%)
7	90	64	34	TMOF (0.1mol%)

^a All the experiments were carried out pumping a solution of **26** (100 mmol) and **91** (100 mmol) in MeOH (50 mL) through a column Omnifit 15 mm x 100 mm filled with 6.7 g of PS-DMA and the flow rate was set to change the reaction times;^b Conversions were determined via ¹H NMR spectra using dimethyl fumarate as internal standard;^c No compound **89** was detected, the compound **92** was instead detected in 31% conversion.

During this screening all the crude reaction mixtures were collected for isolation of compound **89** via a vacuum distillation. Firstly, starting from a 27%_{w/w} mixture of **89**, the first obtained distillate was a mixture of 47%_{w/w} enriched in **89** with some dimethyl malonate (**26**) impurity. The residue was a dark, cherry red oil, in which ¹H-NMR spectroscopy did not identify any remaining enone **89**. In an attempt to obtain a purer product, the distillate was purified via a second distillation, this time using a Vigreux column. The isolated material was 70%_{w/w}

enriched in **89** with remaining material being the starting material (**26**). During this procedure, considering the initial crude, roughly 29%_{w/w} of the product was lost. To look into this weight loss, it was decided to attempt purification via flash chromatography of the crude mixture from the experiment relating to *Entry 12 (Table 7)* which had been left stirring for a further 48 h gaining a comparable cherry red oil as the product. The isolated by-products such as **92**, **94** and **95** revealed an interesting reactivity of the product **89** (*Scheme 24*). In fact, a vinylogous aldol reaction as well as a conjugate addition takes place under the distillation conditions, forming higher boiling point molecules such as **94** and highly conjugate materials as **95**. With these outcomes in mind, it was realised further treatment of the reaction mixture was needed to obtain the isolation of **89** (catalyst removal).

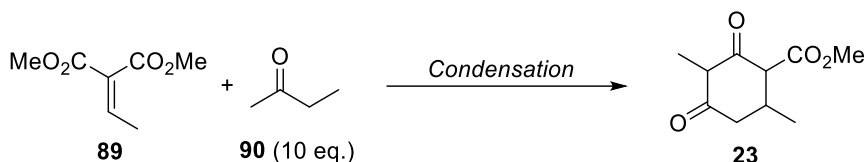


Scheme 24. Proposed mechanism for the formation of the by-products **92**, **94** and **95**.

In the meantime, to evaluate the feasibility of the chosen route, the subsequent condensation step between a purified intermediate **89** and butanone (**90**) was carried out. As initially considered, an amino-catalysed condensation was exploited, employing the ethylenediamine catalyst **75**. Similar conjugate additions have been reported previously in the literature

employing diamines.¹⁷⁰ Unfortunately, the reaction did not occur even after 1 week at room temperature or after 3 hours heating under reflux (*Table 9, Entry 2*). It was therefore decided to screen additional amino catalysts and reaction conditions (*Table 9, Entries 1 – 7*), however none of the tested ones gave the desired condensation.

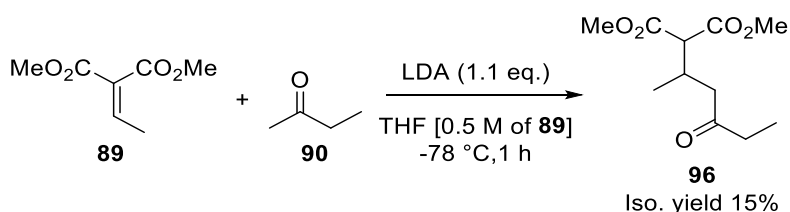
Table 9. Reaction condition attempter for the condensation of dimethyl ethylidenemalonate (**89**) and butanone (**90**).



Entry ^a	Reaction conditions	Conv. 23 (%) ^b	Experimental Notes
1	Cu(OTf) ₂ (17 mol%), Et ₃ N (1 eq.), MeOH [1 M of 89], r.t., 18 h	-	Only recovered compound 89
2	75 (10 mol%), MeOH [1 M of 89], r.t., 1 w → reflux, 3 h	-	Only recovered compound 89
3	Diisopropylamine (10 mol%), MeOH [1 M of 89], r.t., 1 w	-	Only recovered compound 89
4	PS-DMA (21 mol%), MeOH [2 M of 89], r.t., 1 w	-	Only recovered compound 89
5	PS-DMA (21 mol%), MeOH [2 M of 89], r.t., 1 w	-	Only recovered compound 89
6	Proline (10 mol%), MeOH [2 M of 89], r.t., 1 w	-	Only recovered compound 89
7	Morpholine (1 eq.), MeOH [2 M of 89], r.t., 1 w	-	Only recovered compound 89

^aThe experiments were carried out on a 10 mmol scale; ^bBased on GC-MS (EI) and ¹H-NMR spectra.

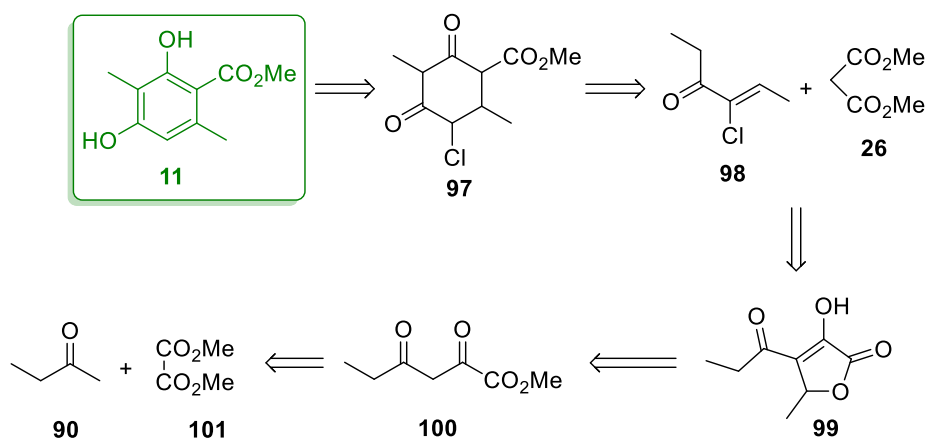
It was decided to attempt a conjugate addition using lithium diisopropylamide (LDA) to fully deprotonate the butanone (**90**) (*Scheme 25*).¹⁷¹ Unfortunately, the desired final product **96** was only isolated in a low 15% isolated yield.



Scheme 25. Conjugate addition of **90** with **89** using LDA obtaining the desired material **96**.

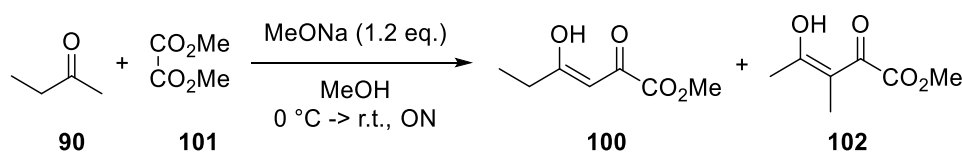
2.1.3. Synthetic strategy from 2-butanone: Route B

Despite the results obtained from the previous synthetic approach, butanone (**90**) remains a valuable alternative building block for the preparation of Veramoss (**11**) as it is cheaper than the currently employed methyl propionylacetate (**27**) and hex-4-en-3-one (**25**). The synthetic route B starts from the formation of the intermediate **100**,¹⁷²⁻¹⁷⁴ which can be prepared from 2-butanone (**90**) and methyl oxalate (**101**) (Scheme 26). The addition of acetaldehyde (**91**) forms the 4-acyl-3-hydroxyl-2,5-dihydrofuran-2-one (**99**),^{175,176} which is described to rearrange to the 3-chloro-hex-4-en-3-one (**98**) after chlorination.¹⁷⁷ The latter could then be used to prepare the chloro-intermediate **97**, which may eliminate HCl to form the desired material.



Scheme 26. Proposed retrosynthesis for the preparation of Veramoss (**11**) from butanone (**90**).

For the preparation of the key intermediate **100**, we first adopted the strategy described by Burnouf *et al.* where sodium methoxide was slowly added to an ice-cooled solution of the two reactants in MeOH (Table 10).¹⁷² Once evaporation of the solvent had occurred, the mixture was composed of the two main products sodium salts of **100** and **102**, respectively 37% w/w, and 25% w/w (Table 10, Entry 1). We managed to isolate the two materials; however, we did not manage to isolate any of the accompanying side products formed. Poor results were obtained when the reaction was carried out under more diluted conditions, probably due to an increased amount of water content in the mixture, however it appears slightly less of the thermodynamic product **102** was formed (Table 10, Entry 2).

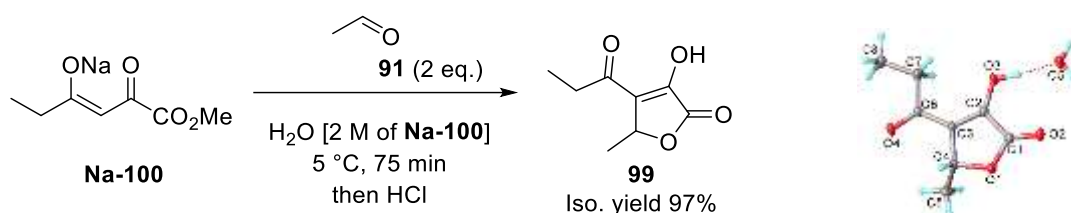
Table 10. Reaction conditions for the synthesis of the intermediate **100** from butanone (**90**).

Entry ^a	Solvent	Conc (M of 90)	Conv. 100&102 (%) ^b	Quenching ^c	Ratio 100:102
1	MeOH	1.6	40	no	6:4
2	MeOH	0.5	28	no	64:36
3	Et ₂ O	0.75	41	no	67:33
4	Et ₂ O	0.75	65 ^d	yes	6:4

^a The experiments were carried out on 100 mmol scale; ^b Based on ¹H-NMR spectra employing 1,2-dimethoxybenzene as internal standard; ^c The reaction mixture was either concentrated under vacuum (no), or quenched with conc. HCl and extracted (yes); ^d Isolated yield.

Changing the solvent to diethyl ether, and working in diluted conditions, improved the **100:102** ratio (67:33), however the conversion (of starting materials) still remained at around 40% and the final product was still only a small fraction of the all crude (*Table 10, Entry 3*). As the mass is conserved from the start to the end of the experiment, we assumed decomposition due to self-condensation was probably the main issue. Also the observed deepening of the colour during solvent evaporation suggests some form of additional side reaction may be occurring. To our delight, high overall yield (65%) was obtained when the mixture was quenched with concentrated HCl and immediately extracted (*Table 10, Entry 4*).

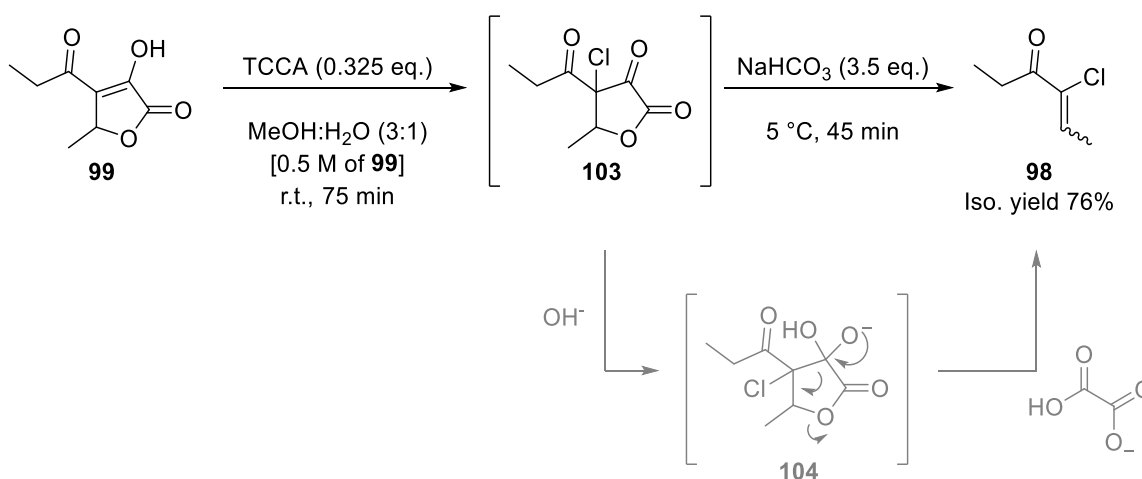
With some of the desired material **Na-100** in hand, we attempted the second step. The sodium salt was solubilised in water and acetaldehyde was added to the ice-cooled solution. The mixture was then quenched after 75 minutes and an orange suspension was formed. Filtering the solid and crystallising it from MeOH:H₂O 1:1, the furanone **99** was isolated in 97% yield (*Scheme 27*).



Scheme 27. Preparation of the intermediate **99** starting from **Na-100**.

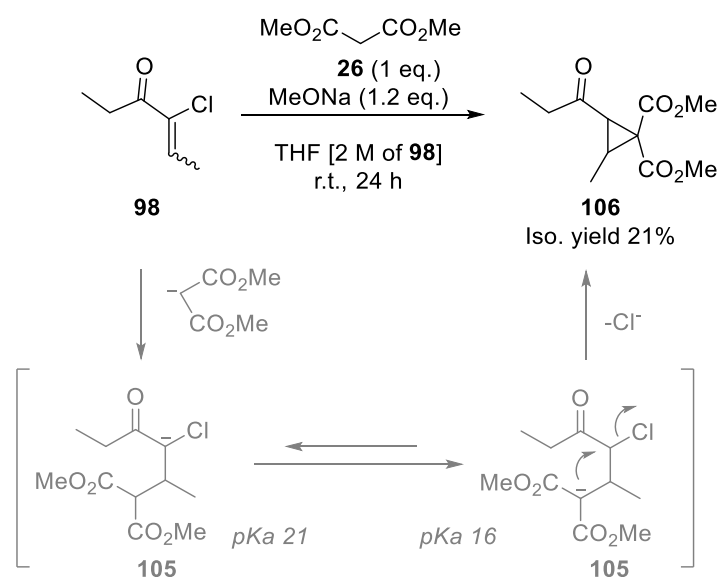
To avoid quenching the desired sodium salt **Na-100** and for an optimal preparation of the intermediate **99**, the reaction mixture from the first step was quenched through an aqueous extraction to collect the formed salts. The aqueous phase was then directly treated with acetaldehyde and, once quenched, the desired material **99** was isolated through filtration in 53% yield. To our delight, no sign of the by-product **102** was found in the final product **99**.

Having determined a more efficient preparation of **99**, the latter was chlorinated using trichloroisocyanuric acid (TCCA) and directly hydrolysed to the 2-chloro-ene **98** via addition of NaHCO_3 (*Scheme 28*). The chlorination was performed at room temperature adding the chlorinating agent solid portion wise. The hydrolysis of **103** through NaHCO_3 triggers a base catalysed rearrangement which realises sodium oxalate forming the desired compound **98** in good yields (76%).



Scheme 28. Reaction conditions for the preparation of the chloroene **98** from **99**.

The chloroene **98** was then exploited for the synthesis of the compound **97**, which it was hoped would then de-hydrochlorinate to Veramoss (**11**) (*Scheme 29*). Addition of malonates to bromo/chloroene materials had previously been described by Arai, Shioiri and co-workers to furnish cyclopropane scaffolds using phase-transfer catalyst (PTC).¹⁷⁸ To avoid the cyclopropane formation, kinetic conditions were adopted. Therefore, ideally aprotic solvent and low temperatures should be exploited, however, due to a low solubility of the sodium salt of dimethyl malonate, the mixture had to be kept at room temperature. After quenching, the cyclopropane **106** was isolated in 21% yield, but none of the desired product was detected. The reaction was also carried out at -78 °C employing a 5.4 M methanolic solution of MeONa. Even under these conditions the cyclopropane **106** was the sole product in 62% conversion based on ¹H-NMR analysis. Unfortunately, we were unable to prevent the intramolecular prototropic tautomerism from happening.

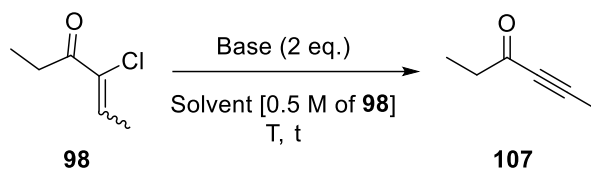


Scheme 29. Reaction conditions for the desired synthesis of Veramoss (**11**), but showing the encountered cyclopropane **106** formation.

Having the chloroene-ene **98** in quantities, it was considered worthwhile to investigate the formation of its alkyne derivative **107** through dehydro-chlorination of the former. Alkynes have already been employed for the preparation of resorcinol's derivatives via conjugate addition-Dieckman cyclisation.^{179,180} Beside the presented literature, de-hydrochlorinations have never been performed on similar ketone-chloro-ene substrates such as **98**. The reason may

be attributed to a competition between the α -deprotonation of the carbonyl with the dehydrochlorination reaction. Nevertheless, in our group unreported dehydro-chlorination on a similar derivative was successfully attained, therefore an attempt was carried out exploiting several reaction conditions (*Table 11*). Unfortunately, all the efforts resulted in complex mixtures and unstable compounds which were not able to be isolated.

Table 11. Attempted reaction conditions for the preparation of alkyne **107** from **98**.

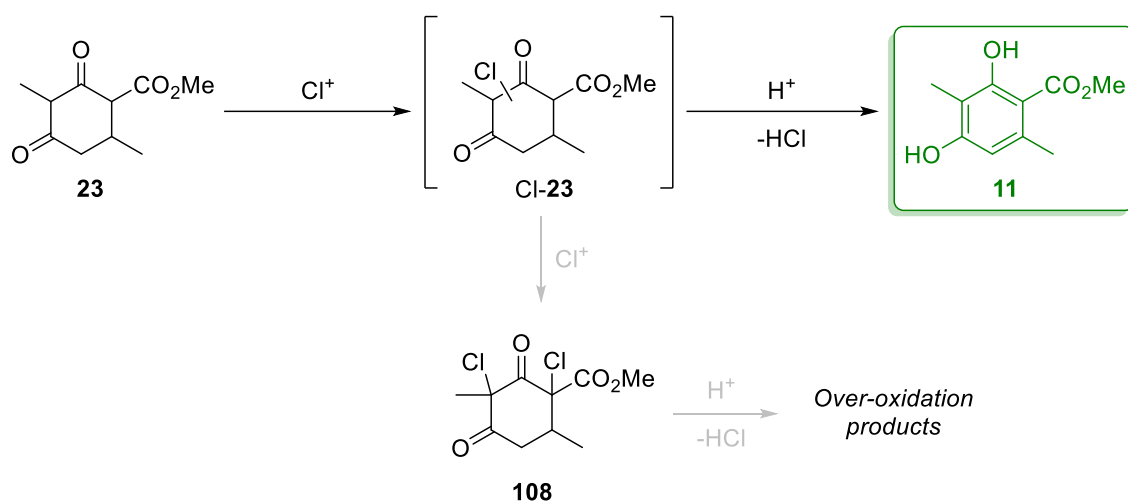


Entry ^a	Base	Solvent	T (°C) ^b	time(h)
1	PS-NMe ₃ ⁺ OH ⁻	Toluene	22 – 60	48
2	PSA-DMA	Toluene	22 – 60	48
3	DBU	Toluene	22 – 60	48
4	NaHCO ₃	MeOH	22	48
5	K ₂ CO ₃	MeOH	22	48
6	Et ₃ N	Toluene	22 – 60	48
7	PPh ₃ /Et ₃ N	Toluene	22 – 60	48
8 ^c	Et ₃ N·3HF	DMSO [0.2 M of 98]	120	14

^a All the experiments were carried out at 1 mmol scale;^b In different cases, two temperatures were screened 22 °C and 60 °C;^c Following a reported procedure.¹⁸¹

2.1.4. Alternative chlorinating agents to elemental chlorine

Along with the design of *de novo* strategies for the synthesis of Veramoss (**11**), the optimisation of the IFF's approach was also explored. As discussed earlier in the chapter 1, the most efficient processes employ the oxidation of intermediate **23** through a chlorination-dehydrochlorination reaction, where a chlorinating agent is exploited to introduce a good leaving group on the molecule (Cl-**23**), which triggers the double bond formation through its elimination (*Scheme 30*). Such dehydrochlorination occurs in acidic conditions and, once initiated, it therefore self-catalyses until the end of the process.

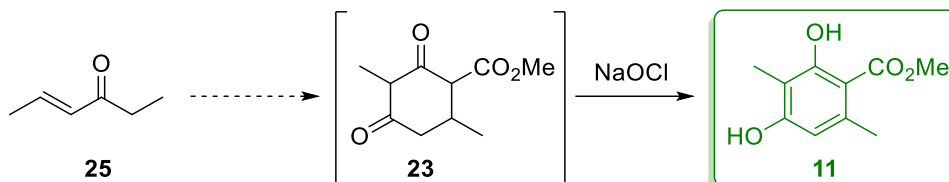


Scheme 30. Mechanism for the oxidation of intermediate **23** based on a chlorination-dehydrochlorination sequence.

Although widely employed, the chlorination-dehydrochlorination process has several drawbacks that need to be considered; poly-chlorination, and HCl removal. In addition to the amount of water required for quenching of the final product, chemical over-oxidation plays a key role in the efficiency of the process. Since the intermediate **23** presents two possible nucleophilic sites, the initially formed mono chloro species Cl-**23** can be further chlorinated to yield a di-chlorinated product **108**. The latter could then give rise to a plethora of other side reactions yielding undesired over-oxidised materials. Therefore, the nature of the chlorinating agent as well as the reaction conditions are critical variables for an effective oxidation. Under IFF's evaluation of the reaction elemental chlorine was found to be the agent of choice as it allows a better dosage control than other chemicals. Due to its toxicity, the use of elemental chlorine has been strongly restricted over the years and can only be employed in certain geographical areas where safety and environmental controls are less strictly controlled, limiting the accessible manufacturing sites.¹⁸² Accordingly, a new chlorinating agent is required to replace the hazardous chlorine gas as well as reduce the amount of water used in the process.

2.1.4.1. Sodium hypochlorite (NaOCl)

The investigation was initially focused on the oxidation of compound **23** using sodium hypochlorite under acid conditions. Under these reaction conditions hypochlorous acid (HClO) is expected to be the chlorinating agent, whereby the by-products would mainly be water and sodium chloride.^{183–189} Therefore, it can be considered a suitable replacement of elemental chlorine (*Scheme 31*).



Scheme 31. Proposed preparation of Veramoss (**11**) via hex-4-en-3-one (**25**).

The preparation of Veramoss (**11**) can be performed as a one-pot procedure which starts from the commonly referred to Veramoss ketone **25**. To avoid issues attributed to carried by-products from the first step, we considered employing pure intermediate **23**, however, during the quenching of the **Na-23** formed in the first step, inorganic phosphorous salts were also precipitating, which may be influencing the reaction and therefore needed to be accounted for. Consequently, we aimed at emulating a reaction mixture which would contain the same inorganic salts formed in the original chlorine process. Hence, intermediate **23** was treated with MeONa to form the **Na-23**, which is then quenched with polyphosphoric acid (PPA).

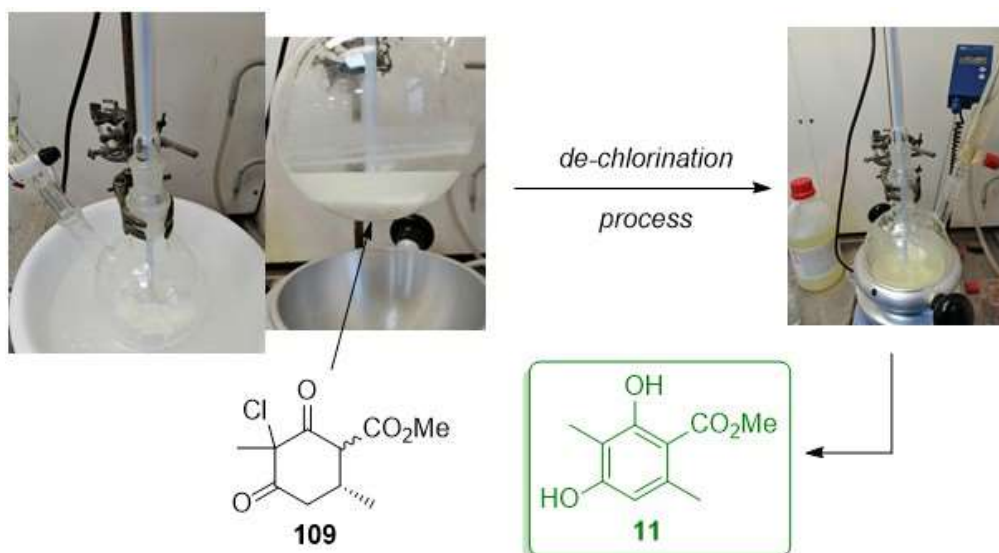
In order to gain understanding of the industrial method, we first attempted to re-create the chlorine-based process in our laboratory (*Scheme 32*). Chlorine gas was bubbled at 0 °C and the time of exposure depended on the disappearance of the **23** which was monitored via TLC. Once the chlorinated intermediates were fully formed, the mixture was heated to induce the de-chlorination.



Scheme 32. Set-up for the chlorine oxidation of **23**. The reaction formed Veramoss (**11**) and **29** as the major by-product.

Two different work-up methods were exploited in accordance with the patent procedures.^{190,191} In both cases Veramoss (**11**) was obtained in low yields along with a major by-product **29**, which can be attributed to the acidic conditions with methanol as the solvent. However, as productivity was not the main aim of testing but familiarisation of the chemistry, no further optimisation was performed.

Having gained some insight and tested the process, the same oxidation was performed replacing the toxic chlorine gas with the NaOCl and using 3.2 equivalents of polyphosphoric acid instead of the original 1.6 (to increase the acidity). The addition of the oxidizing agent was firstly carried out over 30 minutes and afterwards the suspension was heated up at 67 °C until no more intermediates were present. Upon further investigation, the white precipitate formed after the hypochlorite addition was discovered to be chloro-compound **109** as a mixture of its two isomers. As shown in *Scheme 33*, the mixture turns yellow when heated up and undergoes elimination to the desired product **11**.



Scheme 33. Pictures of the white suspension generated before and during the de-chlorination process. The suspension is the chlorinated intermediate **109**.

The liquid-liquid biphasic system was extracted with AcOEt and after concentration an orange oil was initially obtained which on standing became a solid. The latter was then crystallised from 1:1 MeOH:H₂O to obtain Veramoss (**11**) in 54% isolated yield. Although the high purity as indicated by ¹H NMR (97%), the colour did not match the material obtained from the original chlorine process (*Figure 8*).

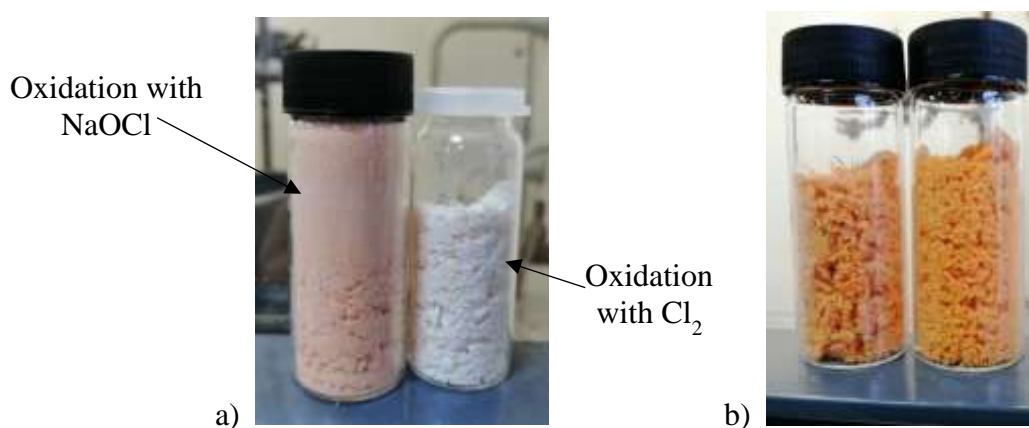
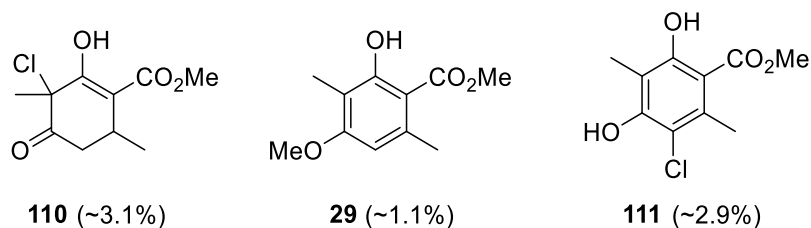


Figure 8. a) Comparison between Veramoss (**11**) obtained from NaOCl and chlorine process; b) Crude solids obtained without performing any crystallisation.

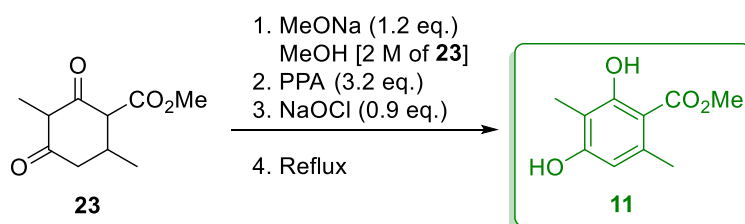
The reaction was re-run and a chromatographic purification was carried out in order to isolate the colourful by-products. Unfortunately, none of the coloured compounds were eluted from the column. Nonetheless, we managed to collect and identify some by-products, such as **29** and the chloro-compounds **110** and **111** (*Scheme 34*).



Scheme 34. Structures of several by-products obtained from the oxidation of **23** with sodium hypochlorite and the corresponding isolated yields.

The product **111** suggested an over-dosage of the chlorinating agent and therefore we attempted to reduce its quantity. It was then considered to use a lower quantity of sodium hypochlorite to yield full conversion. Nonetheless, using 0.9 equivalents of NaOCl increased the conversion to 84%. Subsequently, a small screening of the time of addition was carried out and the best reaction conditions were found to be a 5 hours (*Table 12*).

Table 12. Screening of reaction addition times for the oxidation of **23**.



Entry ^{a,b}	Addition (h)	Conv. 11 (%) ^c
1	0.5	61
2	2	71
3	5	84
4	12	60

^a The reaction were carried out on 64 mmol scale; ^b MeONa and NaOCl were slowly added at 0 °C; ^c Based on ¹H-NMR spectra employing dimethyl fumarate as internal standard.

Even though promising results were obtained from the chlorination step, the HCl elimination was found to be an issue. After the addition of NaOCl and the PPA, the reaction is composed of a 1:1 MeOH:H₂O mixture, which is the composition employed for the crystallisation in the current process. However, only a partial precipitation of Veramoss (**11**) was observed during this stage, and the final material was only isolated after methanol removal and liquid-liquid extraction with ethyl acetate. Prolonged heating times or increased water ratios did not change the amount of precipitate, suggesting the de-chlorination was only occurring partially. A further issue was concerning the difficulty in assessing the proper NaOCl concentration and therefore obtaining reproducible results. For these reasons, alternative options using other “green” chlorinating agents were considered.

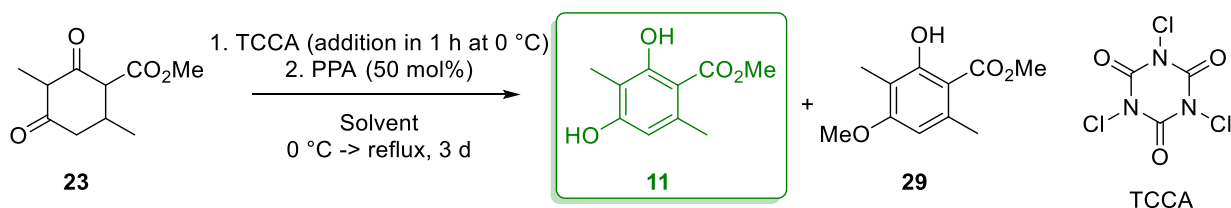
2.1.4.2. *Trichloroisocyanuric acid*

Trichloroisocyanuric acid (TCCA) has been gaining attention over the last decade as it is a valuable alternative to other toxic and unstable chlorinating agents. Its high thermal stability and active chlorine content (45.7% active chlorine vs 25-30% of other agents) make TCCA of potential use in industry as easy-to-handle and atom-economic reagent.^{192,193} TCCA is soluble in most common organic solvents such as acetone, ethyl acetate, methanol, and toluene, although its by-product (cyanuric acid) is typically insoluble and can be easily filtered off from the reaction mixture. The white solid cyanuric acid can either be safely disposed, as it slowly degrades, or alternatively recovered for recycling and reuse. TCCA has widely been described as efficient chlorinating agent for ketones, alkenes, acids, esters, arenes, heterocycles, imides, and amides for the synthesis of α -chloro ketones, esters, chlorohydrins, *N*-chloroamides, *N*-chloroimides, and chloro-substituted arenes or heterocycles¹⁹²⁻²¹⁴ It was also found to be a valuable replacement to convert acids into acid chlorides when coupled with strong Lewis bases such as triphenylphosphine in order to avoid the usage of noxious reagents such as POCl₃, PCl₅, and SOCl₂.²¹⁵⁻²²⁰ As a result, it was deemed an interesting candidate for the purposes.

A first attempt was carried out by slowly adding a solution of TCCA to a 0.07 M solution of **23** in methyl acetate (AcOMe) and MeOH. After the addition, a catalytic amount of polyphosphoric acid (50 mol%) was added. The resulting white suspension was refluxed until disappearance of the intermediate chlorinated compounds. As *Table 13* shows, Veramoss (**11**) was formed in good to excellent conversions under both conditions (*Table 13, Entries 1&2*),

however, compound **29** was also detected when methanol was employed as the solvent, probably due to a high dilution of the starting material. When the reaction was run more concentrated at 1 M, the conversion dropped dramatically (*Table 13, Entry 3*). This is probably as a consequence of the di and mono chloro version of TCCA co-precipitating from solution before conducting the desired chlorination at the higher concentration.

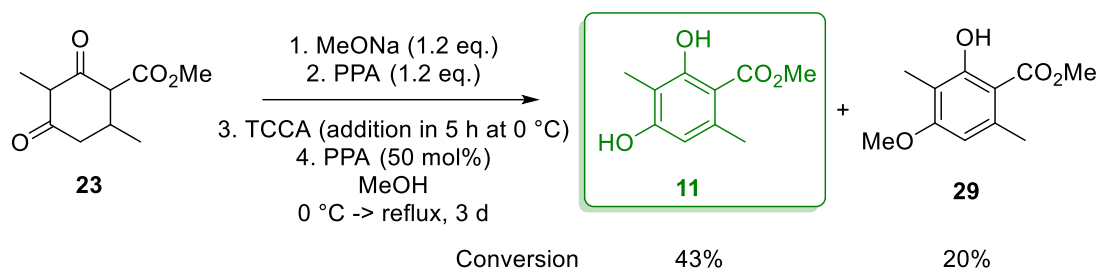
Table 13. Screening of solvent and concentration for the oxidation of Veramoss using TCCA.



Entry ^a	Solvent [Conc.]	Conv. 11 (%) ^b	Conv. 29 (%) ^b
1	AcOMe [0.07 M] ^c	85	-
2	MeOH [0.07 M] ^c	68	21
3	AcOMe [1 M] ^c	52	-

^a All the experiments were carried out on 10 mmol scale;^b Based on ¹H-NMR spectra employing dimethyl fumarate as internal standard;^c The molarity of the solvent is in respect with the moles of compound **23**.

Despite the modest outcomes obtained from the preliminary tests, we decided to deploy the TCCA addition to the “simulated” industrial conditions that were previously optimised using NaOCl (see section 2.1.4.1). A 0.4 M solution of TCCA in methanol was added to an ice-cooled reaction mixture of compound **23** over 5 hours (*Scheme 35*). By analysing the crude mixture, roughly 82% of compound **23** reacted with the chlorinating agent. Veramoss (**11**) was formed although only in low conversions (43%), along with the monomethoxy derivative **29** (20%). After crystallisation, the desired material (light yellow) was isolated in 23% yield. The outcomes could be attributed to a decomposition of TCCA in the methanol as the solution is unstable over longer storage times.²⁰⁴ We also noticed this phenomenon in other experiments run in section 2.1.4.3.



Scheme 35. The oxidation was carried in the “simulated” industrial condition previously optimised when NaOCl was employed. Conversion based on $^1\text{H-NMR}$ spectra employing dimethyl fumarate as internal standard.

It was therefore decided to perform an additional experiment using AcOMe as an alternative solvent. The TCCA addition was performed on an ice-cooled 2 M solution of **23** within 5 hours. Following the TCCA addition, the mixture was left stirring at room temperature for 24 hours but no change occurred to the mixture during this period. Surprisingly, when the mixture was heated, it turned yellow after 3 hours and the pH changed to 1 – 2. After 24 hours, all the chlorinated intermediates **109** disappeared and Veramoss (**11**) was detected in 65% conversion (*Figure 9*).

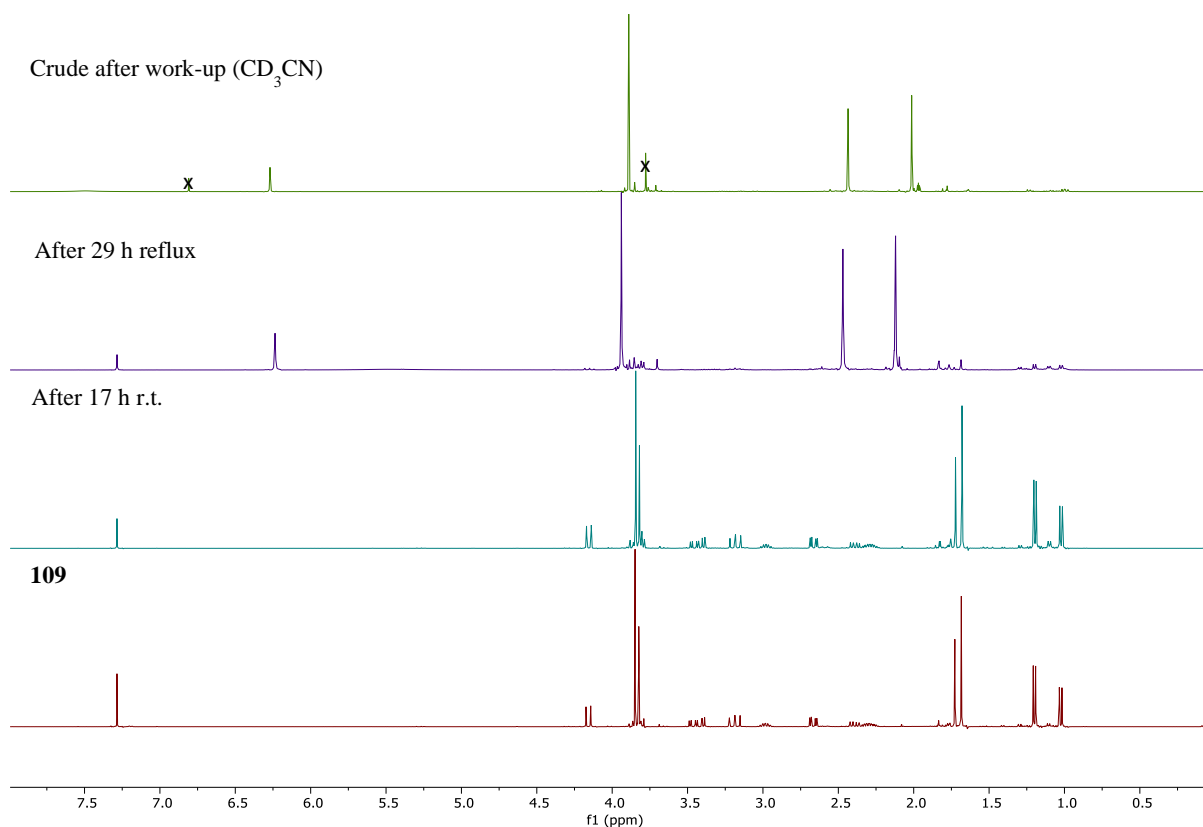
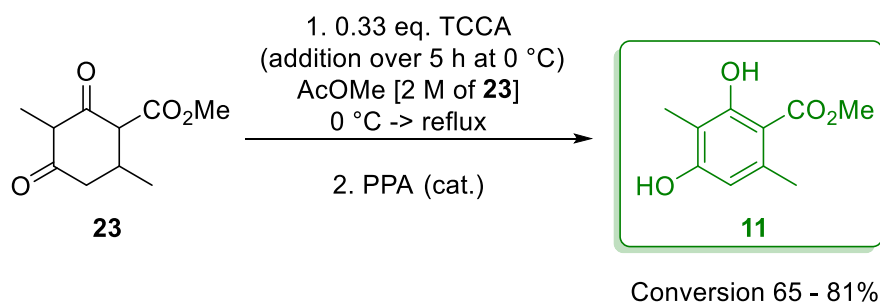
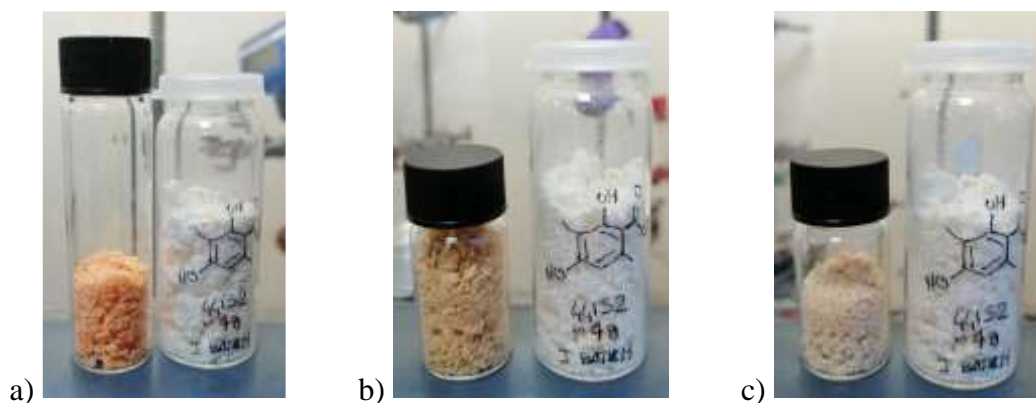


Figure 9. $^1\text{H-NMR}$ spectra for the chlorination of **23** with TCCA using AcOMe as the solvent.

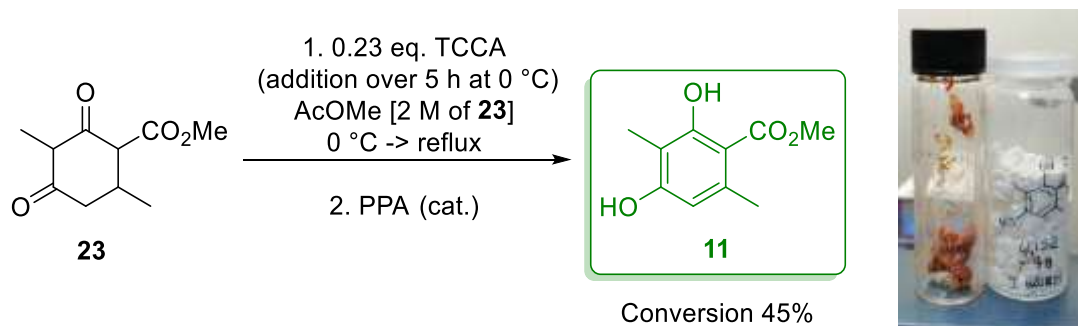
Sadly, as shown in *Scheme 36*, the final material was still orange, however less intense than the one NaOCl was yielding (*See picture a*). Surprisingly, when the reaction was repeated, the de-chlorination process did not occur without polyphosphoric acid addition. It is possible that a small amount of acid may have gone into the mixture and catalysed the de-chlorination. To our delight, the second experiment brought about a more intense yellow material after 39 hours of reflux (*See picture b*, 81% conversion). The crystallisation of the sample was performed and the final material appears to be less yellow than prior purification (*See picture c*).





Scheme 36. Preparation of Veramoss using TCCA and AcOMe. Colour comparison of the final material with the one prepared using elemental chlorine. a) First run, b) Second run, and c) Second run after crystallisation. Conversion based on $^1\text{H-NMR}$ spectra employing dimethyl fumarate as internal standard.

As the reaction was determined to work, we decided to examine whether there is any correlation between the colour formation and the equivalent of TCCA employed. Two more experiments were therefore set up where the equivalents of TCCA were set at 0.23 to 0.43. When 0.23 equivalents were used, a small amount of compound **23** remained unreacted as expected (Figure 10). After 22 hours at reflux, the initial 1:2 ratio of the two keto forms of **109** changed to 1:1 ratio, and the enol form **110** appeared along with them. As can be seen in the $^1\text{H-NMR}$ spectra shown, the unreacted compound **23** disappeared from the mixture. We then added a catalytic amount of PPA, which created a dark red Veramoss (**11**) material after 17 hours (Scheme 37). Surprisingly, the desired compound was only detected in 45% of conversion (58% purity).



Scheme 37. Preparation of Veramoss (**11**) using TCCA and AcOMe. Colour comparison of the final material (left) with the one prepared using elemental chlorine (right). Conversion based on $^1\text{H-NMR}$ spectra employing dimethyl fumarate as internal standard.

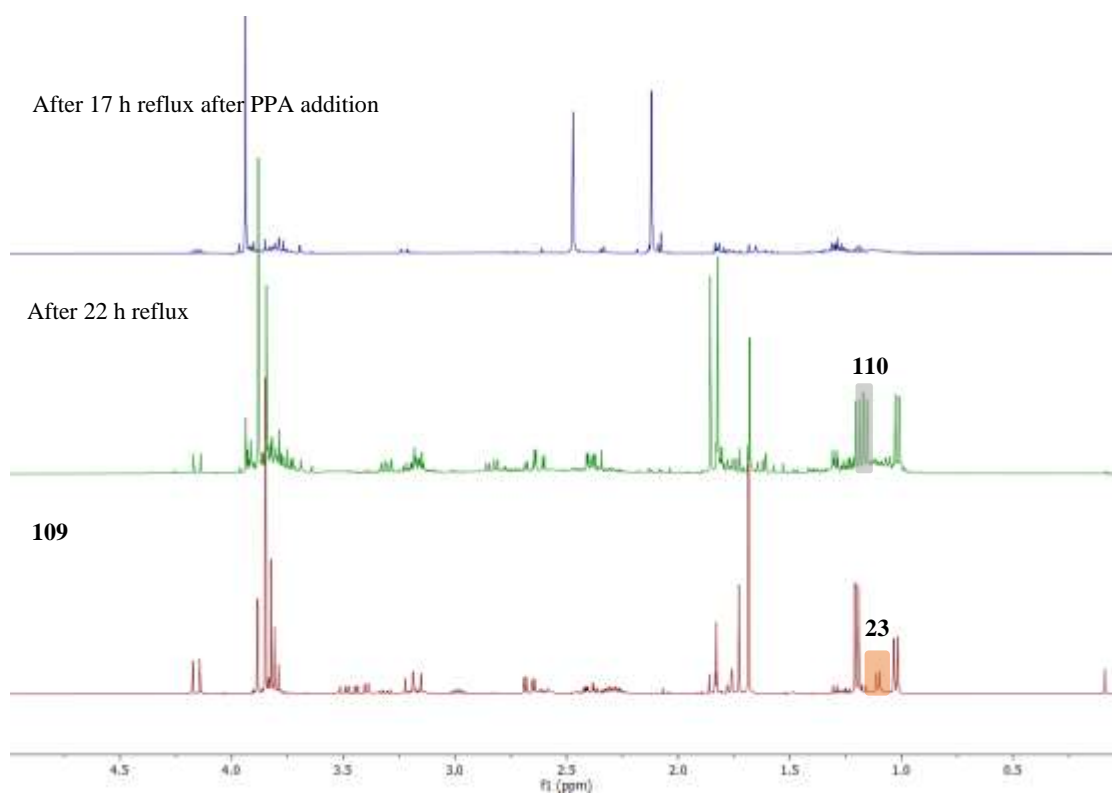
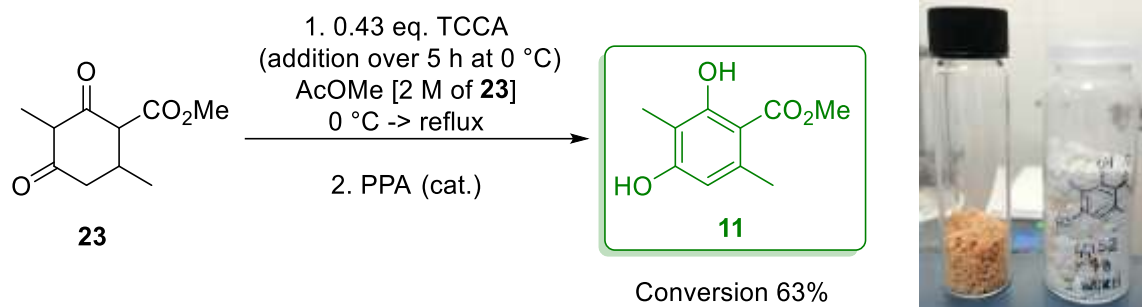


Figure 10. $^1\text{H-NMR}$ spectra oxidation of compound **23** using 0.23 equivalents of TCCA in AcOMe solvent. The area highlighted in orange and grey corresponds with the characteristic signal of the respectively Veramoss precursor **23**, and the chlorinated version **110**.

By comparison, when 0.43 equivalents of TCCA were added, no more compound **23** could be detected in the $^1\text{H-NMR}$ spectra of the crude reaction mixture, although it was noted that a notable amount of the dichlorinated **108** was observed (around 25%). The latter was found at a higher concentration after refluxing for 24 hours (*Figure 11*). Polyphosphoric acid was added and after 40 hours the mixture was worked up and Veramoss (**11**) was detected in 63% conversion and an orange final material was obtained (*Scheme 38*). The latter results would suggest the di-chloro species could be either inert or more slowly de-hydrochlorinate under these particular conditions.



Scheme 38. Preparation of Veramoss (**11**) using TCCA and AcOMe. A colour comparison of the final material (left) with the one prepared using elemental chlorine (right). Conversion based on $^1\text{H-NMR}$ spectra employing dimethyl fumarate as internal standard.

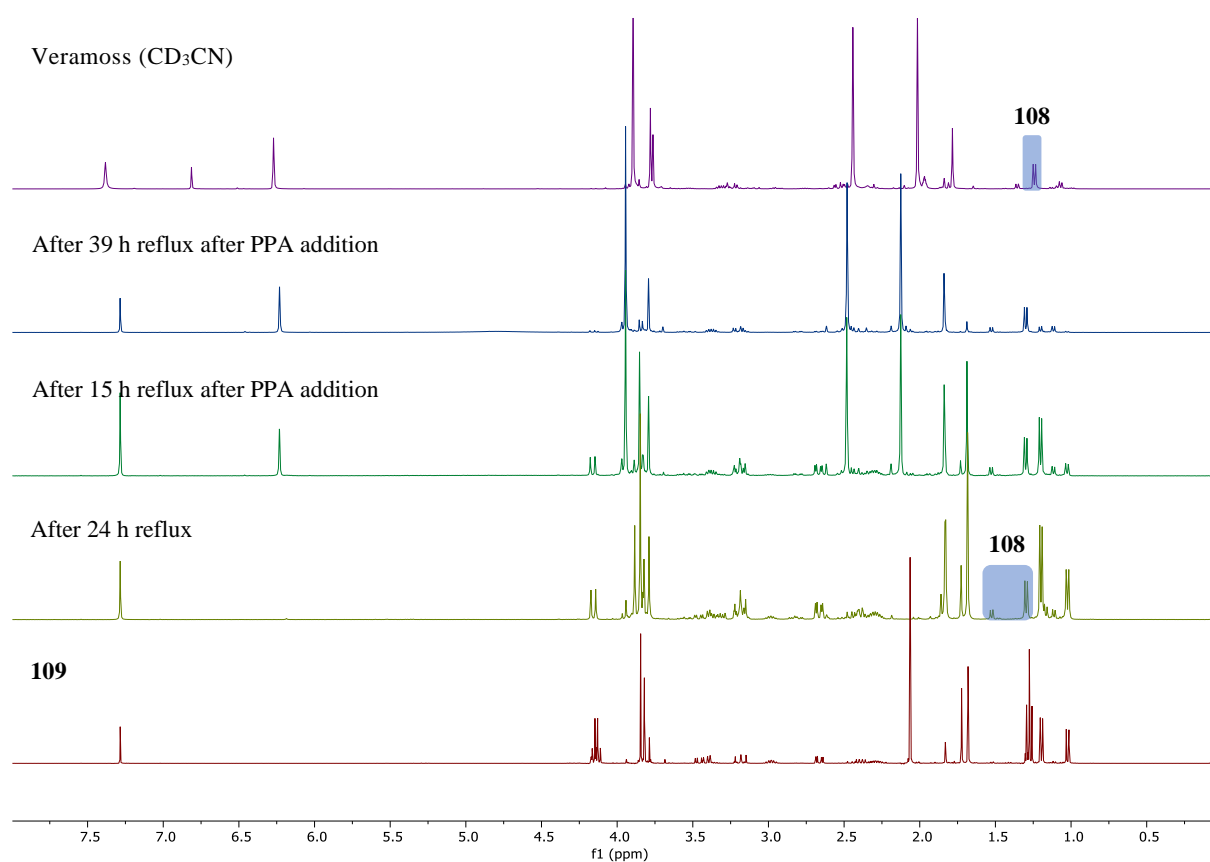
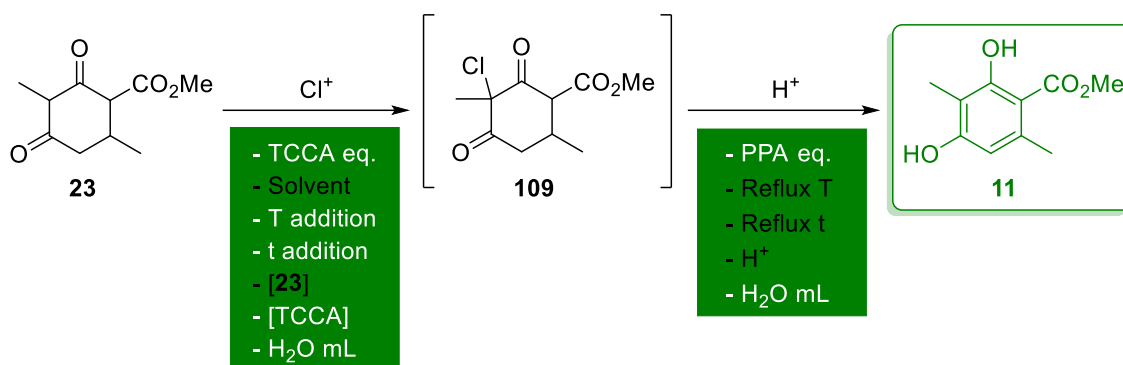


Figure 11. $^1\text{H-NMR}$ spectra chlorination of compound **23** using 0.43 eq. of TCCA in AcOMe. The area highlighted in blue corresponds with the characteristic signal of the di-chloro compound **108**.



Scheme 39. Process diagram for the oxidation of compound **23** to Veramoss (**11**).

Having acquired experimental information using one-factor-at-the-time method (OFAT), we decided a better understanding of the process could be obtained employing Design of Experiment (DoE) methodology. As depicted in *Scheme 39*, 11 identified variables could influence the final outcomes of the process, however, some of them cannot be varied as they are fixed by either the reaction conditions of the first step (Solvent, concentration of **23** in solvent, nature of the acid, Reflux Temperature (T)), or indirectly stated by other variables (Reflux time (t)). Consequently, only 6 factors remained to be investigated and Definitive Screening Design (DSD) was chosen as DoE model to employ. The applied model considers all possible second order interactions (*i.e.* temperature-time interaction) between the factors and quadratic effects (non-linear effects). It therefore enables the maximum amount of information with a low amount of experiments. The DSD is a modern three-levels experimental design developed by Jonas and Nachtsheim and implemented on different cases for the optimisation of manufacturing processes.^{221–224} The model required 17 experiments to be run and *Table 14* shows the screened reaction conditions and outcomes.

Table 14. Reaction conditions screening for DoE optimisation.

Entry ^a	t (h)	TCCA (eq.)	T (°C)	PPA (eq.)	H ₂ O ^b	[TCCA]	Conv. 11 (%) ^c
1	1	0.4	12.5	0.1	0.5	0.9	58.3
2	1	0.25	25	0.1	3	0.9	91.8
3	5	0.325	25	0.7	0.5	0.9	90.6
4	5	0.25	25	0.1	0.5	0.6	91.3
5	3	0.325	12.5	0.4	1.75	0.6	85.1
6	5	0.25	12.5	0.7	3	0.3	100
7	5	0.4	0	0.1	1.75	0.9	59.3

8	1	0.4	25	0.4	0.5	0.3	47.1
9	5	0.4	25	0.1	3	0.3	62.1
10	1	0.25	25	0.7	1.75	0.3	81.5
11	1	0.25	0	0.7	0.5	0.9	79.2
12	3	0.4	25	0.7	3	0.9	72.2
13	5	0.25	0	0.4	3	0.9	95.5
14	5	0.4	0	0.7	0.5	0.3	48.5
15	1	0.325	0	0.1	3	0.3	54.4
16	3	0.25	0	0.1	0.5	0.3	63.3
17	1	0.4	0	0.7	3	0.6	69.3

^a The experiments were carried out in 50 mmol scale; ^b Measured in mL each 50 mmol of **23**; ^c Based on ¹H-NMR spectra employing dimethyl fumarate as internal standard.

Once the designated experiments had been acquired, the model was run using JMP Pro 15. The model obtained matches the experimental results quite well ($R^2 = 0.98331$, root mean square estimate (RMSE) = 3.3596) as shown in *Figure 12*, the factors with the highest impact on process's outcome are the equivalents of TCCA used and the concentration of TCCA solution added to the reaction mixture, as their lines' slope are the steepest. The increase of chlorinating agent affects negatively the performance of the oxidation due to a rise in the formation of poly-chlorinated materials (second graph from the left, *Figure 12*), whereas employing more concentrated TCCA solution yields higher selectivity (first graph from the right, *Figure 12*). Prolonging the addition time as well as increasing the temperature improves the selectivity (first and third graph from the left, *Figure 12*). Low temperatures may be detrimental due to a solubility problem, as temperature strongly influences the solubility of the TCCA in AcOMe.

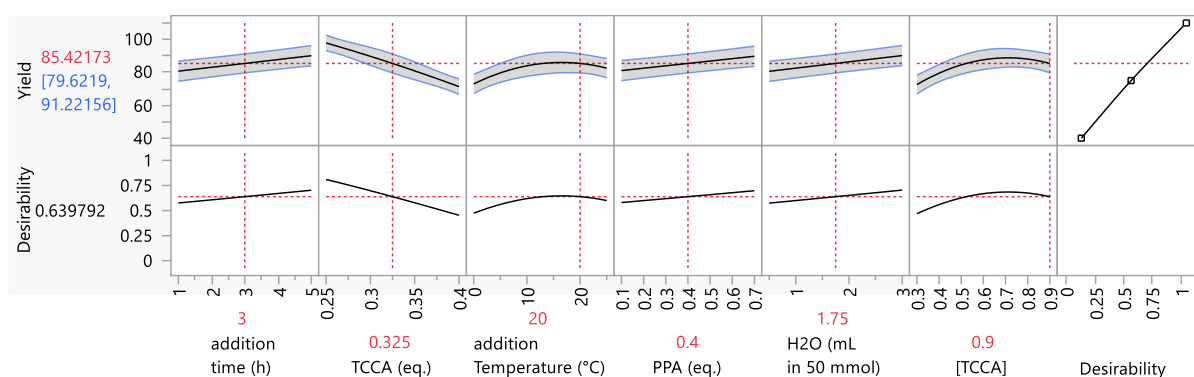


Figure 12. Graphs showing how each term influences the conversion (yield). This graph was download from JMP Pro 15. It represents the response (yield) on the y axis and the factor

(variables) on the x axis. The grey area around the black line represents the interval within there is level of confidence (95%).

The de-hydrochlorination process is affected by the quantity of acid; increasing the PPA equivalents enabled higher selectivity to be obtained. It is attributable to a fast de-hydrochlorination's rate over the side-reactions (fourth graph from the left, *Figure 12*). The amount of water also has a role in the selectivity, as it allows a better miscibility of the PPA into the reaction mixture (second graph from the right, *Figure 12*).

Having these results in hand, we next performed the reaction of *Entry 5 (Table 14)* increasing the temperature (25 °C) and the concentration of TCCA (0.9 M). To our delight, the desired material was detected in 96% conversion using these reaction conditions. Increasing the temperature to 30 °C, the selectivity decreases to 91%. Employing a larger amount of water (25 mL) also decreases the selectivity (89%).

In order to compare the final products' colour with the commercial one, the latter three batches, plus the batch from *Entry 6 (Table 14)*, were washed with water, toluene, and then crystallised from MeOH:H₂O as described by IFF's procedure. As *Figure 13* shows, one can notice the product still remains pale yellow coloured, however, closer to the white desired material than the previous methodologies. The purity of all 4 batches ranged between 95% and 98% (based on ¹H-NMR assessment).

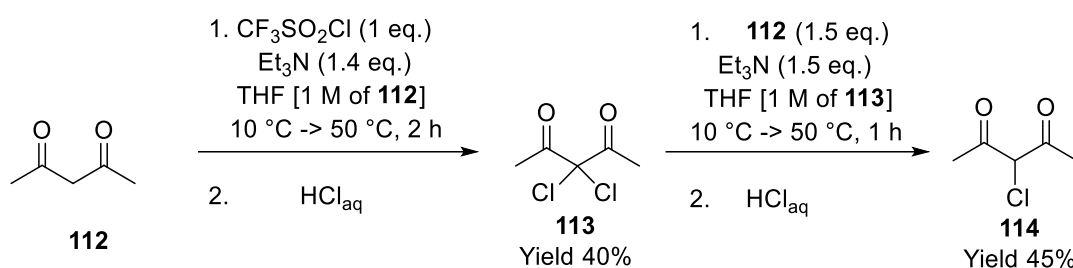


Figure 13. Colour of the batch obtained from different reaction conditions compared with the reference white Veramoss (right hand sample). The reaction conditions for the different

materials are starting from the left: 1:1 H₂O:AcOMe (95% purity); TCCA addition at 25 °C, AcOMe (98% purity); TCCA addition at 30 °C, AcOMe (98% purity); TCCA addition at 25 °C, *Table 14, Entry 6* (98% purity).

2.1.4.3. Dichlorinated compounds (**108**)

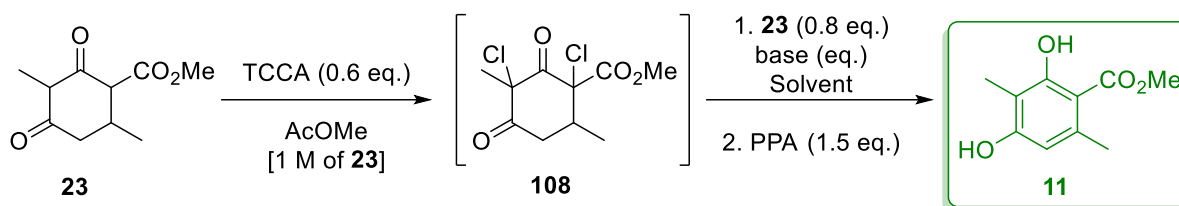
During the quest to find alternative chlorinating agents, an interesting article by Danilevich *et al.* was discovered.²²⁵ After chlorination with trifluoromethanesulfonyl chloride, the dichloroacetylacetone was used to chlorinate fresh acetylacetone under basic conditions (*Scheme 40*).



Scheme 40. Dichlorination method of acetylacetone **112** described by Danilevich *et al.*²²⁵

It was therefore decided to attempt a similar double chlorination of compound **23** using TCCA as the chlorinating agent instead of trifluoromethanesulfonyl chloride. In addition, to decrease the amount of unreacted starting material **23** in the final mixture, lower amount of the intermediate **23** (0.8 eq.) was reacted with the di-chloro species **108**. Based on this procedure, we investigated different reaction conditions as described in *Table 15*.

Table 15. Reaction conditions investigated for the dichlorination/chlorination procedure to Veramoss.



Entry ^a	Solvent	Eq.	Base	Conv. 11
1	THF	1	Et ₃ N	70
2^c	MeOH	1.1	MeONa	10
3^d	AcOMe	3.1	MeONa	44
4^d	THF	3.1	MeONa	26
5^e	THF	1.1	MeONa	17

^a All the experiments were carried out on a 25 mmol scale; ^b Based on ¹H-NMR spectra employing dimethyl fumarate as internal standard; ^c Methanol was also employed as solvent in the first chlorination step; ^d After the chlorination of **23** with TCCA, the reaction was not filtered and it was instead immediately employed as such for the subsequent step; ^e The solid cyanuric acid was removed through toluene precipitation.

The first procedure performed was to emulate the conditions described by Danilevich *et al*, yet reducing the amount of starting material **23** employed in the second step (*Table 15, Entry 1*). Once the di-chloro species **108** was formed, the cyanuric acid was filtered off and the solution concentrated. This was then slowly added as a solution in THF to a mixture of compound **23** and triethylamine. The reaction was then followed with LC-MS (ESI) and after 24 hours all the starting material **23** was fully chlorinated (*Figure 14*). The excess of PPA allowed the dehydrochlorination process to occur and the product **11** was detected in good conversion (70%). The colour of the final isolated material was noted to be similar to that obtained from the mono-chlorination with TCCA (Chapter 1, Section 2.1.4.2). As this method showed promise, the methodology was further investigated. We envisioned the possibility of performing the di-chlorination on a mixture of compound **23** in methanol with TCCA. Such a setup would allow the preparation of the precursor **23** under conditions compatible with the current IFF procedure; thus two batches of **Na-23** could be prepared (or a single batch split in two), and one 71chlorinated and to act as the chlorinating agent for the second batch. Therefore, the experiment was carried out as described (*Table 15, Entry 2*).

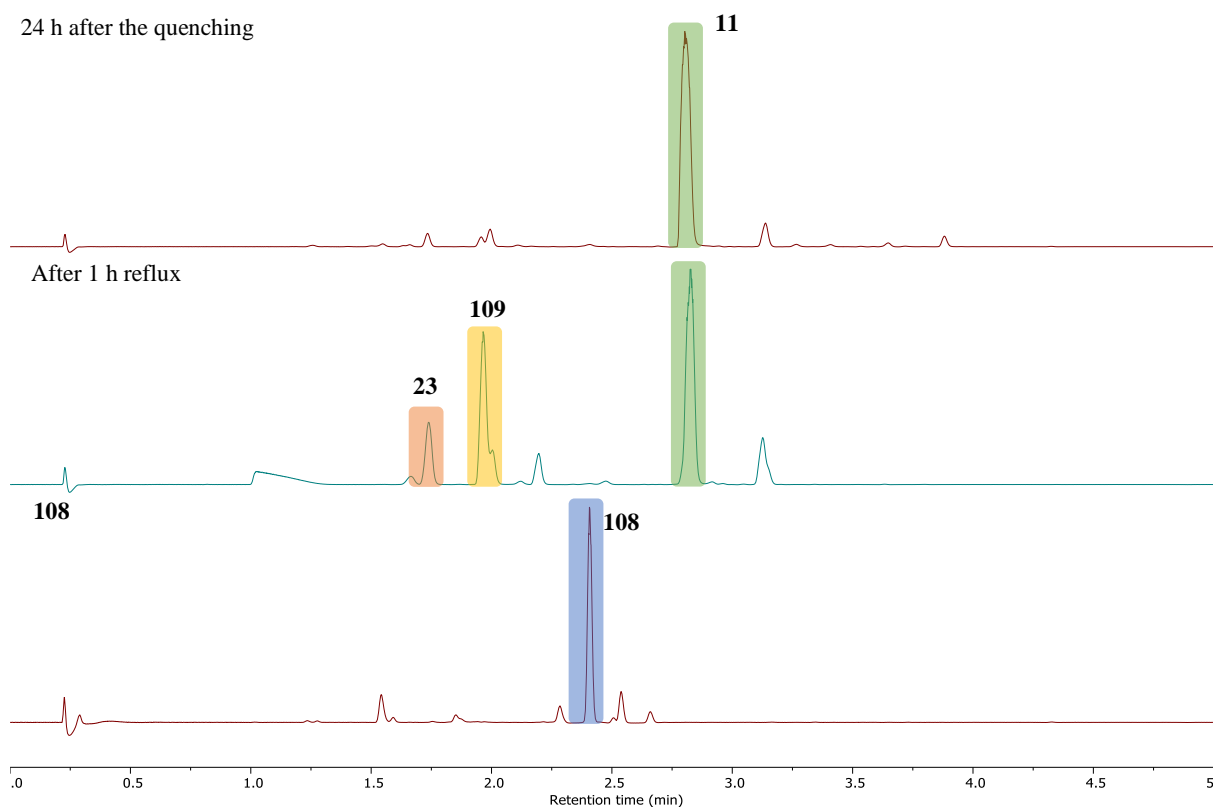


Figure 14. LC-MS chromatogram for the chlorination of compound **23** using **108** in THF with Et₃N as base (*Table 15, Entry 1*). The areas highlighted in orange, yellow, blue, and green correspond with the peaks of the respectively compounds precursor **23**, mono-chloro **109**, di-chloro **108**, and Veramoss **11**.

Unfortunately, the reaction only progressed partially (15% conversion to **11**) when the chlorination was run. The composition of the reaction mixture also did not change after 72 hours refluxing. LC-MS (ESI) analysis showed the formation of several other unidentified products during the di-chlorination step (*Figure 15*). It is already reported in the literature, solutions of TCCA in MeOH are unstable.²⁰⁴ Only a small amount of dichloro-compound was formed in the first step and therefore the starting material **23** did not fully react. We subsequently decided to investigate the reaction in the other solvent AcOMe (*Table 15, Entry 3*). In this case the mixture was not filtered after the chlorination with TCCA and instead directly used in the second step. As the by-product cyanuric acid (pK_a = 5.55) is a weaker base than the Na-**23** salt (pK_a = 8.7), an excess of base (3.1 equivalents) has to be employed to

prevent protonation of the **Na-23** salt from the acidic protons of cyanuric acid. Once quenched, the mixture was refluxed for 27 hours and Veramoss (**11**) was detected in 44% conversion.

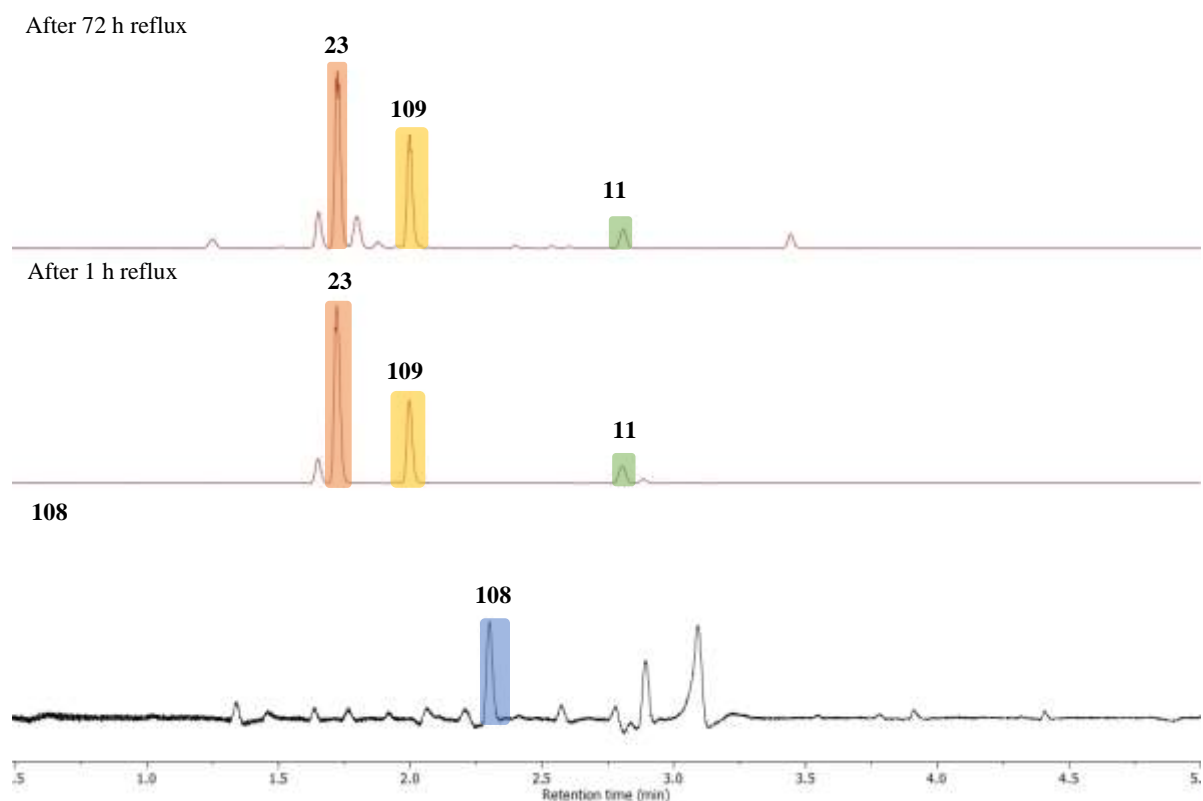


Figure 15. LC-MS chromatogram for the chlorination of compound **23** using **108** in MeOH using MeONa as base (*Table 15, Entry 2*). The areas highlighted in orange, yellow, blue, and green correspond with the peaks of the respectively compounds precursor **23**, mono-chloro **109**, di-chloro **108**, and Veramoss **11**.

In order to better understand the reaction, the experiment represented by *Entry 3* (*Table 15*) was re-run and monitored via $^1\text{H-NMR}$ sampling analysis (*Figure 16*). The di-chlorination step brought about the formation of di-chloro species **108** (2 majors and 2 minors), which was then slowly added to a mixture of **Na-23** at r.t. The exothermicity of the reaction raised the temperature up to 50 °C during the addition. After 2 hours from the addition, di-chlorinated material **108** has almost completely reacted, whereas Veramoss (**11**) appears immediately in the reaction mixture (*Figure 16*). Some **23**-related species diminished or transformed over a

further 61 hours of heating, as can be seen in the range between 1 and 1.5 ppm which changes from the initial spectra.

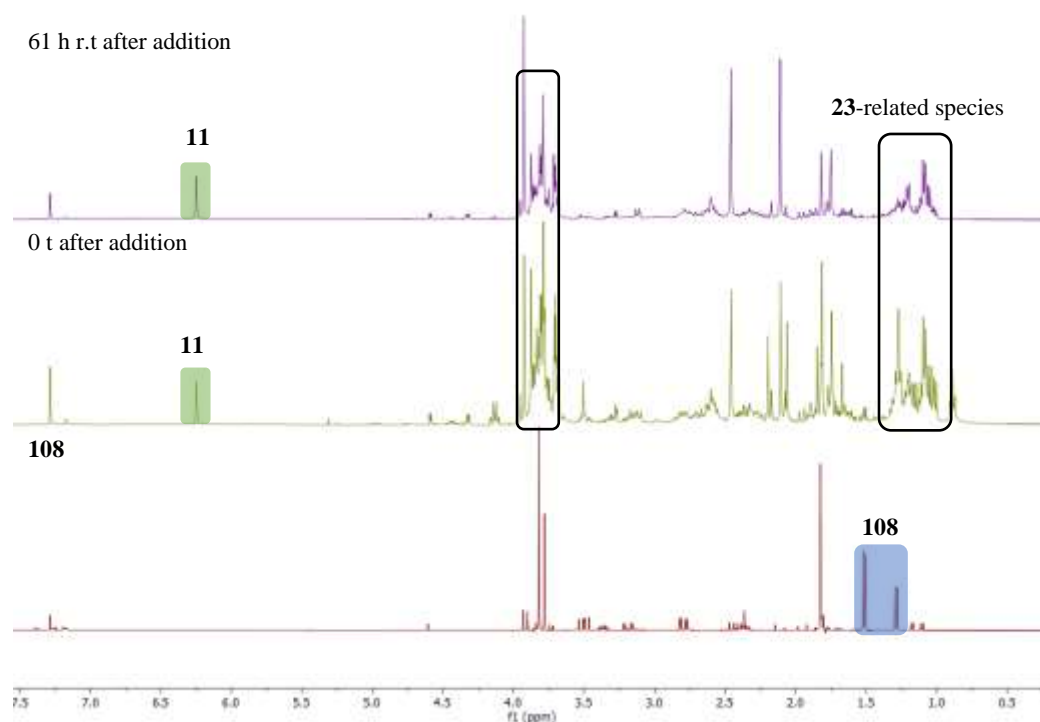


Figure 16. $^1\text{H-NMR}$ spectra monitoring for the chlorination of **23** using **108** in AcOMe using MeONa as base (*Table 15, Entry 3*). The areas highlighted in green, and blue correspond with the characteristic signals of the respectively compounds Veramoss **11**, and di-chloro **108**.

The reaction was then treated with PPA and left refluxing for a further 27 hours (*Figure 17*). It was observed that the various **23**-related species gradually disappeared as indicated by the signals between 3.5 and 4 ppm diminishing. The reaction mixture was then worked up to yield Veramoss (**11**) albeit in only 29%. It is not clear what all the different species formed during the reaction were, however it can be imagined some of them may be chlorinated. By comparing the $^1\text{H-NMR}$ spectra of reaction mixture after the addition of **108** in the Na-**23** with the one of the mono-chlorinated compounds' mixture (**109**), we could spot the presence of one of the isomers **109** (*Figure 18*). It is noteworthy, in this example it is less likely to comprehend the nature of the *Cl-23* species formed, as the stereoselectivity of chlorine exchange is unknown. In fact, it is possible all the possible regioisomers and diastereoisomers are potentially forming.

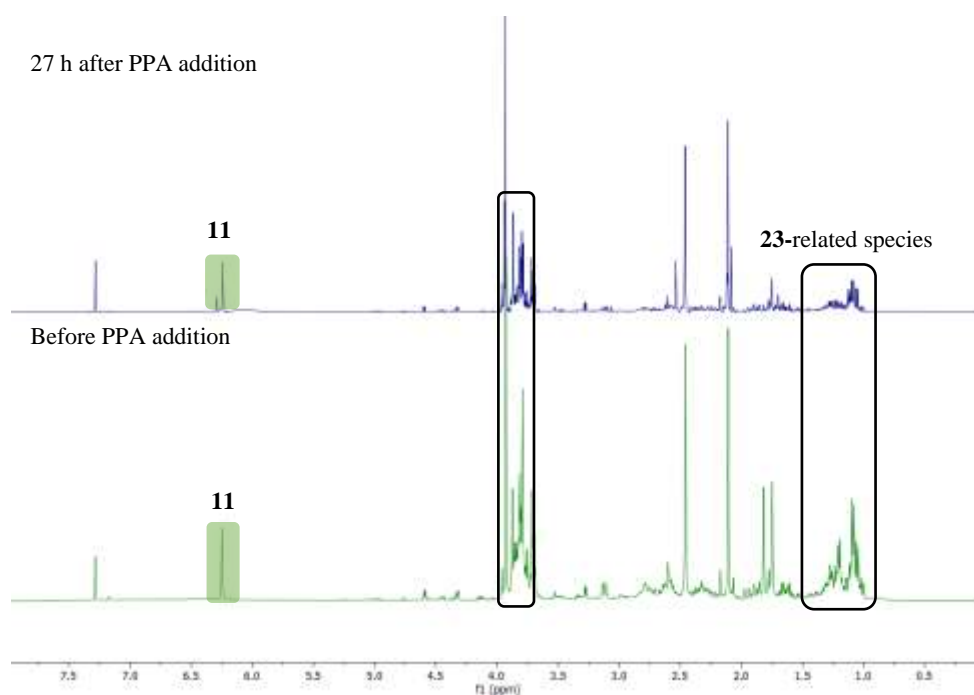


Figure 17. ^1H -NMR spectra monitoring for the chlorination of compound **23** using **108** in AcOMe using MeONa as base after PPA addition (*Table 15, Entry 3*). The area highlighted in green corresponds with the characteristic signal of the compound Veramoss **11**.

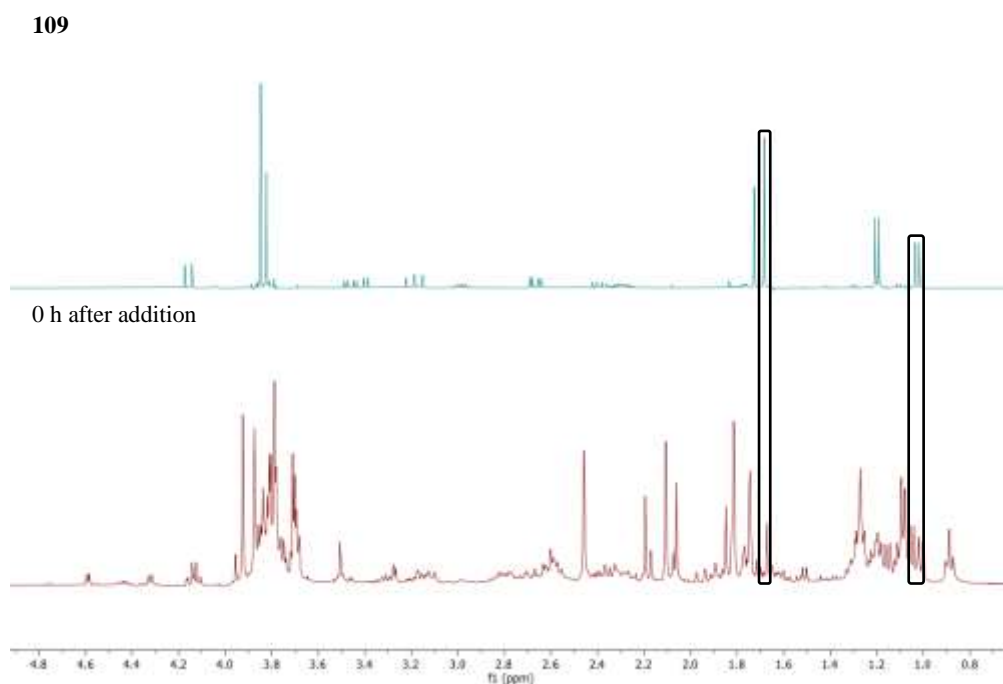


Figure 18. ^1H -NMR spectra comparison between the reaction mixtures obtained from mono-chlorination of compound **23** (**109**) and chlorination using **108** as chlorinating agent (*Table 15, Entry 3*).

The same experiment was then performed using THF instead of AcOMe as the solvent (*Table 15, Entry 4*). The reaction generates similar results as to the one in AcOMe. To control the temperature increase, the addition of **108** was performed at 0 °C and, immediately afterwards, the reaction was allowed to warm up to room temperature. Surprisingly, no reaction occurred for the first hour (*Figure 19*). The mixture was then heated to reflux and after 1 hour, the pH was found to be acidic (2 – 3), therefore already quenched. As a result, the solution was then heated for a further 22 hours to allow all the remaining chloro species to de-hydrochlorinate, however no substantial changes were noticed at this point suggesting the hydro-chlorination occurred within the first hour (*Figure 20*). Veramoss (**11**) was finally detected in 26% conversion by ^1H NMR analysis.

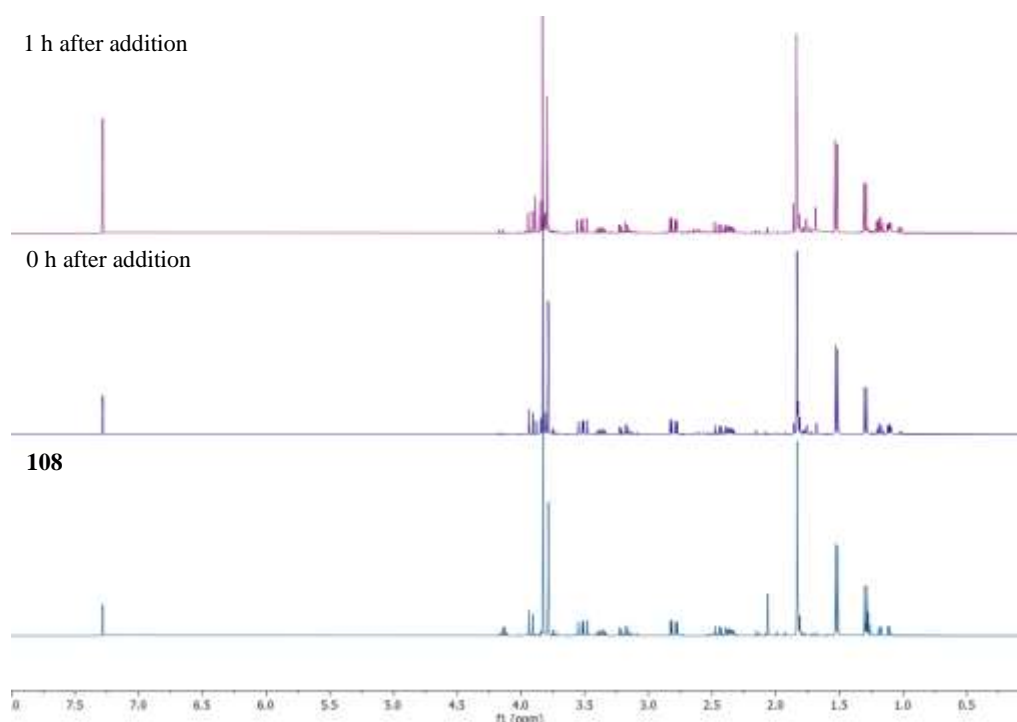


Figure 19. ^1H -NMR spectra monitoring the first 1 hour of reaction after the addition of **108** in the Na-**23** solution (*Table 15, Entry 4*).

To understand whether the residual cyanuric acid plays a role (perhaps as an acid catalyst to induce the elimination reaction), the experiment was repeated removing the cyanuric acid through a precipitation of it in toluene (*Table 15, Entry 5*). In this example, 1.1 equivalents of MeONa was then employed as no cyanuric acid was left in the mixture.

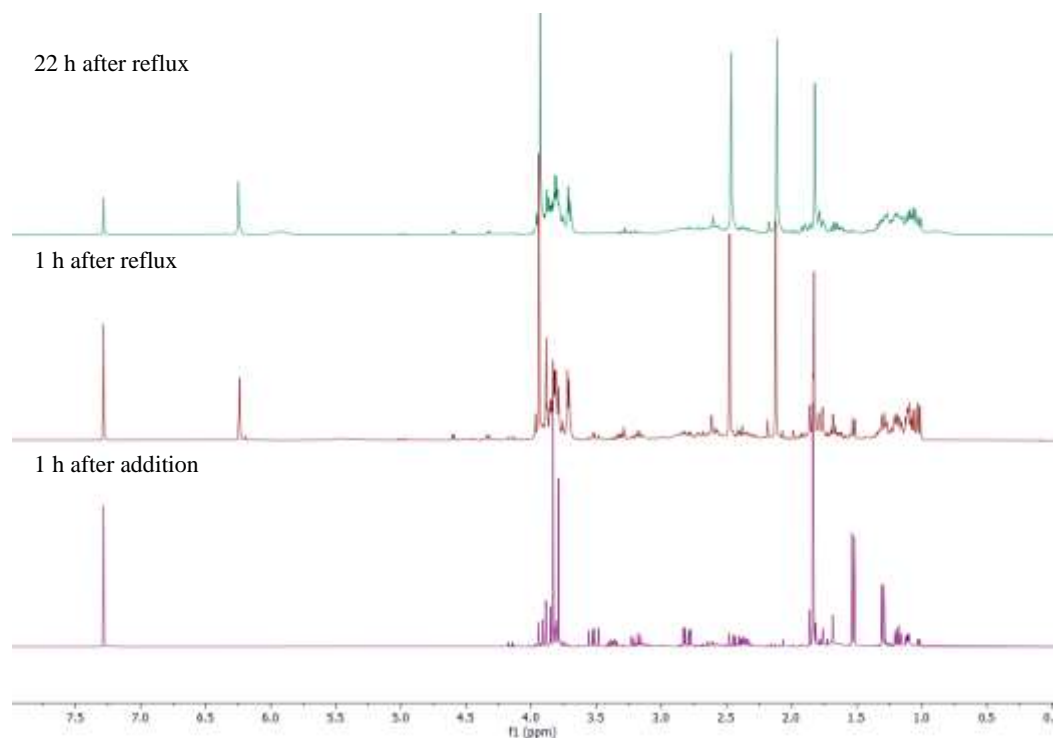


Figure 20. ¹H-NMR spectra monitoring the 22 hours of reaction after the addition of **108** in the Na-**23** solution (*Table 15, Entry 4*).

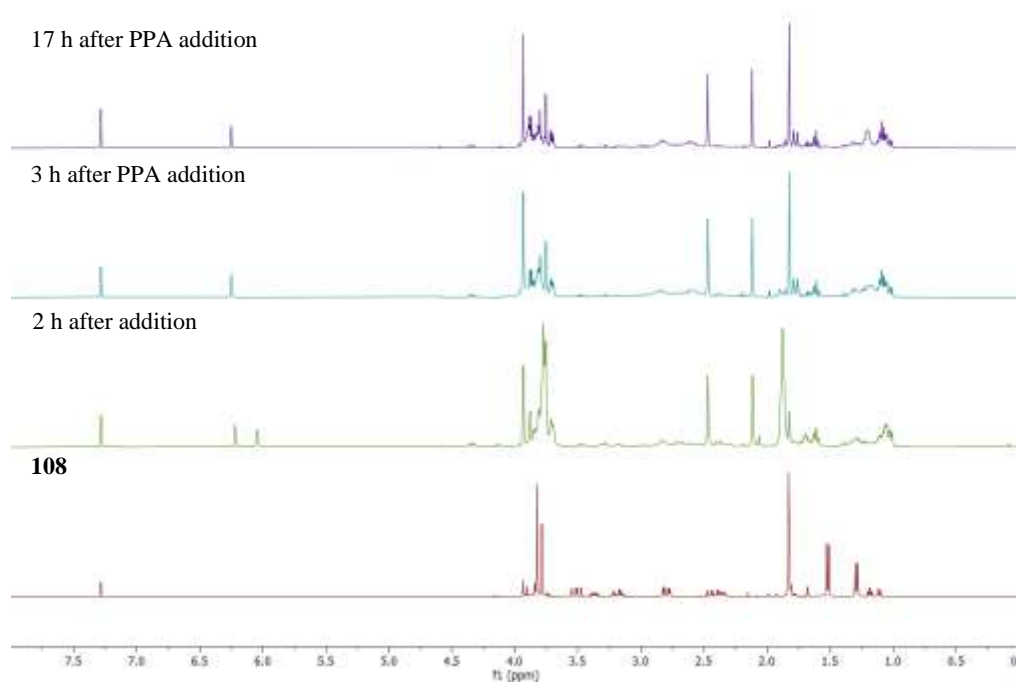


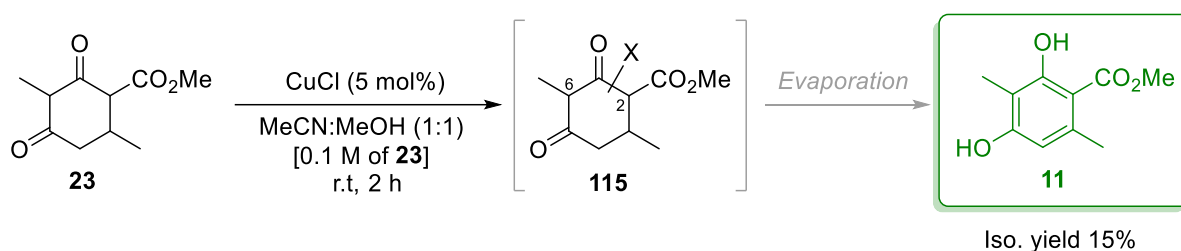
Figure 21. ¹H-NMR spectra monitoring the oxidation of compound **23** using **108** removing cyanuric acid in THF (*Table 15, Entry 5*).

In this example, no more di-chloro species **108** could be detected after 2 hours of stirring at room temperature. The resulting pH of the mixture was found to be around 5 – 6 and therefore a catalytic amount of polyphosphoric acid was added to adjust the pH to ~ 2. The white mixture was then refluxed and after 1 hour it became light yellow in colour. After 17 hours no significant changes were observed and Veramoss (**11**) was isolated in 17%.

Considering all the data acquired from the various experiments, the reaction could be strongly affected by the use of a strong base such as MeONa, because when the reaction was performed employing triethylamine, the desired material was obtained in good conversions. As MeONa is a key base for the synthesis of the intermediate **23**, the methodology was not further investigated as the reaction parameters seemed incompatible.

2.1.4.4. Aerobic oxidation

Interested in the possibilities for a catalytic oxidation, we also considered investigating an aerobic oxidation of the Veramoss precursor **23** (Scheme 41). Despite the attempts that have already been performed and described in section 2.1.1, a copper-catalysed oxidative step was still tempting. Different copper sources were therefore screened in a 1:1 mixture of acetonitrile:methanol. Copper(I) chloride was found to oxidize **23** to Veramoss in less than 2 hours (15% yield).



Scheme 41. Successful attempt of copper-catalysed oxidation of **23** to Veramoss (**11**). The exact mechanism of the process is still unknown.

Initially, the starting material **23** was believed to have oxidized to the target compound **11**, however the Veramoss was discovered to be obtained only after solvent evaporation without removing the copper salt from the solution. Before the evaporation, two products were isolated from the crude mixture. By analysis of the $^1\text{H-NMR}$ spectra, the species look rather similar. Due to their instability, these intermediates **115** are still not fully characterised and little analyses were performed, however, we were able to acquire some information. Firstly, $^1\text{H-NMR}$ spectra confirm they are neither Veramoss (**11**) nor the starting material **23**, although they have a structure similar to **23**. Secondly, Electron impact ionization (EI) technique gave a m/z 196, which is the mass of **11**, whereas LC-MS (ESI) gave a m/z 245, which accurately confirmed. As such the unknown groups could be *O*-methylated peroxide. However, the *O*-methylation could be attributed to a subsequent reaction with the solvent (MeOH), once used in the LC-MS (eluent) and also in the reaction mixture. In addition, photo-oxidation with triplet oxygen using rose Bengal as photosensitizer has formed similar products which could confirm the presence of a peroxide group in the structure.

It has also been noticed that the reaction rate increases by increasing the chloride ions concentration (addition of NaCl for instance) and that the reaction does not work using methanol as the sole solvent. A small addition of hydrochloric acid to the mixture also increase the rate of reaction, although it also brings about some additional by-product formation.

Unfortunately, after a few months of investigations, Veramoss (**11**) was not anymore isolated from the reaction mixture, and only starting material was instead detected. It is not clear the variables that caused this change. No further investigations were performed. Likewise, a Pd(OAc)₂-catalysed aerobic oxidation was also attempted, however, with no positive outcomes. Only starting material was detected even after one week of reaction.

Alongside these intriguing findings, an opportunity for a new synthesis of compound **23** was considered. Radical methylation of the 1,3-diketone had not previously been considered but several examples of metal-catalysed methylation of dicarbonyls had been published over the years.²²⁶ Specifically, copper(I)-catalysed methylation on 1,3-diketones with *tert*-butyl peroxybenzoate (TBPB) was found to occur in good yields on similar substrates such as dimedone.²²⁷ The possibility to methylate **22** to yield the precursor **23** employing similar reactions for its aerobic oxidation to Veramoss (**11**) would enable the usage of alternative raw materials. Unfortunately, a first reaction in batch produced a complex mixture of by-products from which the *O*-methylated compound **116** was isolated in 11% yield (*Figure 22*).

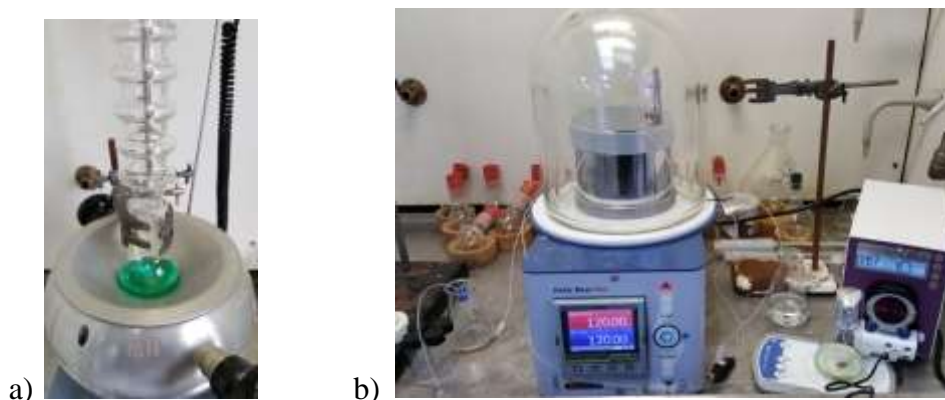
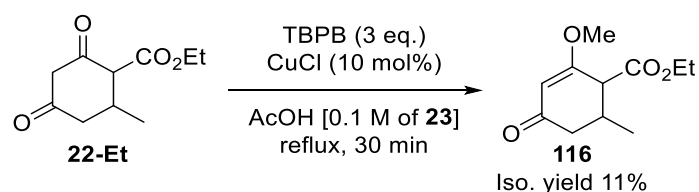
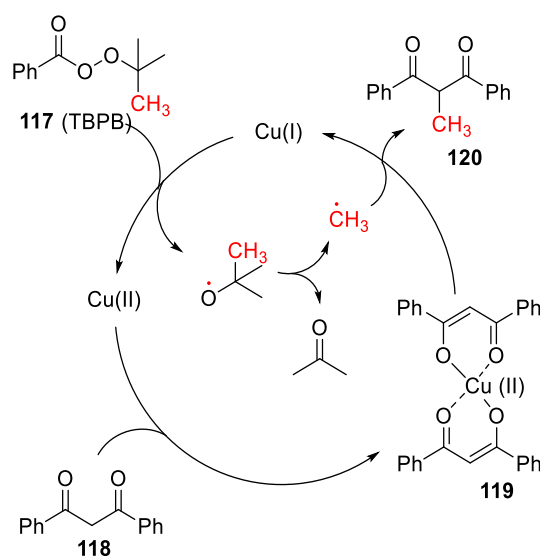


Figure 22. Copper(I)-catalysed methylation performed in batch (*a*) and in flow (*b*).

A second attempt was also performed using a flow apparatus setup (*Picture b, Figure 22*), although the same selectivity as the one in batch was detected via $^1\text{H-NMR}$ and GC-MS analysis. Additionally, when acetonitrile was used instead of acetic acid (AcOH), almost no methylation occurred, forming only multiple by-products which were not characterized. Although no other solvents were investigated, the results would imply that either acetic acid or acid conditions are required for the methylation to occur.



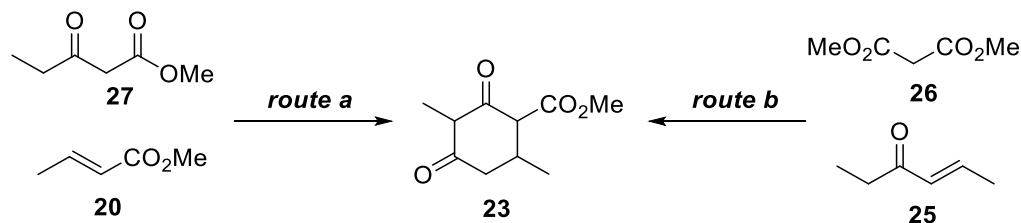
Scheme 42. Proposed mechanism for Cu-catalysed methylation of 1,3-diketones.

Following the mechanism proposed by the authors (*Scheme 42*), the enol form is required in order to obtain the Cu-substrate complex **119**, which leads to the methylation via a single electron transfer (SET) process. These conditions were probably not met when the compound **22** was employed, allowing only *O*-methylation to occur.

2.1.5. *Optimising the preparation method for compound 23*

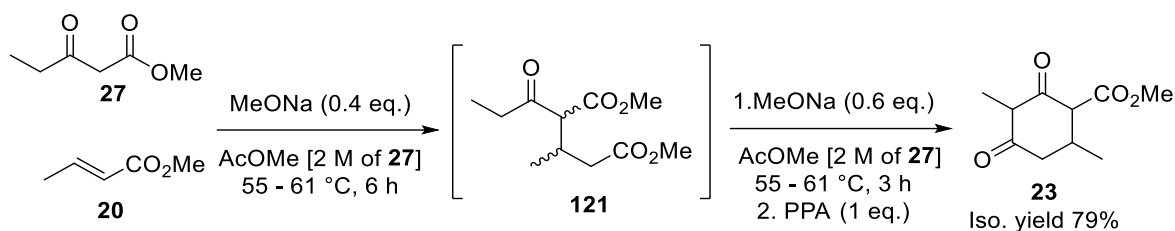
From our studies trichloroisocyanuric acid (TCCA) was found to be the chlorinating agent of choice. As described in section 2.1.4.2, the optimised conditions for the chlorination process exploits AcOMe as solvent instead of MeOH. Consequently, experiments to discover new

conditions for an effective first step of the Veramoss (**11**) preparation were needed. As already mentioned before (Chapter 1.3.1), two main possible synthetic strategies to **23** can be employed; starting from the methyl propionylacetate (**27**) and methyl crotonate (**20**) (*route a*, Scheme 43), or from hex-4-en-3-one (**25**) and dimethyl malonate (**26**) (*route b*, Scheme 43).



Scheme 43. Synthetic strategies for the preparation of **23**. The *route a* starts from **27** and **20** and the *route b* from **26** and **25**.

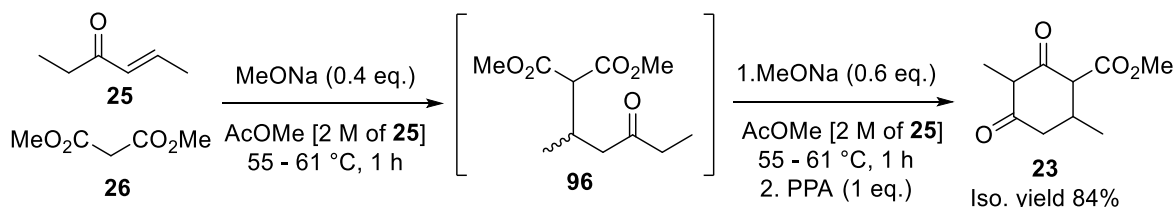
Both possibilities were then investigated employing a biphasic solid MeONa/AcOMe system instead of the monophasic MeONa/MeOH. The *route a* was first evaluated (Scheme 44). The method comprises two reaction steps where the Michael addition to **20** does not require a stoichiometric amount of base. For these reasons, only 40 mol% of solid MeONa was employed. The yellow solution was then heated at 55 – 61 °C and stirred for 6 hours or until the GC-MS showed no more starting material. The mixture was then cooled to 45 °C and the remaining base was added. On a first attempt, the mixture was cooled down to room temperature causing the precipitation of **Na-23** from the reaction mixture which required a mechanical stirrer. At the end of the MeONa addition, the mixture was kept stirring at 55 – 61 °C for 3 hours. Once it was determined that no more compound **121** was present, the mixture was cooled down prior to the polyphosphoric acid addition. Unfortunately, during the quenching, the product precipitates from the reaction and the addition of water (5 mL) was required to obtain a mobile stirring mixture. The resultant white precipitate was washed with water until pH around 5 and the Veramoss precursor **23** was isolated in 79% yield. The same experiment run using 20 mol% of MeONa but this did not go to full completion after heating for 23 hours and not even when 10 equivalents more of methyl crotonate (**20**) were added.



Scheme 44. Preparation method for **23** using methyl propionylacetate (**27**) and methyl crotonate (**20**).

In order to assess whether reducing the temperature would improve the outcomes or not, a control experiment was set up where the temperature was initially set at 25 to 30 °C. After 24 hours of stirring, no conversion to the intermediate **121** was detected. Increasing the temperature to 35 – 40 °C offered no improvements, however warming up to 40 – 45 °C brought up full conversion in roughly one hour. After the second portion of MeONa was added, the reaction was further mixed for 1 hour and quenched with PPA as already described above. In this experiment, compound **23** was isolated in 80% yield. It is noteworthy the lowest temperature the process can be operated at is 40 – 45 °C with scarce mixing efficiency due to the product's precipitation. Thus, rising the temperature to 55 – 61 °C grants more efficient mixing.

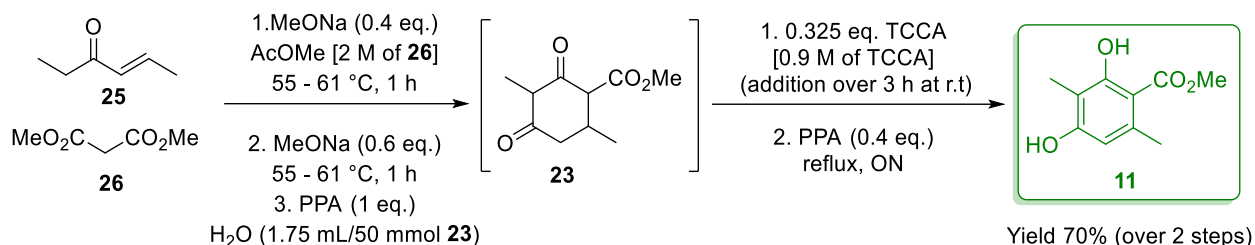
Comparing *route b* with *route a*, the Michael addition was decidedly faster (6 h vs 1 h). However, in this experiment mechanical stirring had to be employed as a magnetic stirring bar would have failed (*Scheme 45*). This strategy yielded **23** in slightly better yields than the previous one (84 vs 79%). For these reasons, the *route b* was therefore employed for the final one-pot optimisation.



Scheme 45. Preparation method for compound **23** using hex-4-en-3-one (**25**) and dimethyl malonate (**26**).

2.1.6. Final Optimisation of the one-pot preparation to Veramoss

After optimising the two steps (annulation, and oxidation) individually, it was considered to proceed to attempt the process as a one-pot methodology (*Scheme 46*).



Scheme 46. Reaction conditions employed for the one-pot procedure to Veramoss (**11**).

Our first investigations were aimed at evaluating the amount of PPA employed for the quenching of the **Na-23** salt formed. In an example test, the reaction was quenched to pH neutral (6 – 7) at the end of the first annulation step (Michael addition-Dieckmann condensation). In this case, the colour of the quenched reaction mixture was not totally white, with shades of red/pink still remaining. When TCCA addition began, the reaction mixture colour darkened to orange and then turn yellow after the addition of the remaining catalytic amount of PPA (0.4 eq.). Once concentrated, the final residue was yellow and very gooey, however, after employing IFF's purification procedure, a white solid was obtained. The process yielded 31% of white Veramoss (**11**). The low yield in this first attempt could be attributed to a partial protonation of the stage 1 material, **23**, after the first step. It was therefore thought a higher amount of PPA would be required to fully protonate the intermediate **23**, which does not get chlorinated but instead sits as sodium salt.

Consequently, a second attempt was performed, and in this example the mixture was quenched with the full 1.4 equivalents of PPA until the pH attained 1 – 2. The mixture obtained was white and a substantial amount of precipitation was produced requiring mechanical stirring to ensure agitation. The mixture was then treated with TCCA and de-hydrochlorinated. To our delight, after purification and crystallisation, a white Veramoss product **23** was again obtained although this time in an overall yield of 70%.

Having optimised the one-pot methodology, a 1 mol scale-up was performed to identify possible problems that could hamper the industrial feasibility. *Figure 23* depicts the colours and physical status of the reaction mixture throughout the whole process.

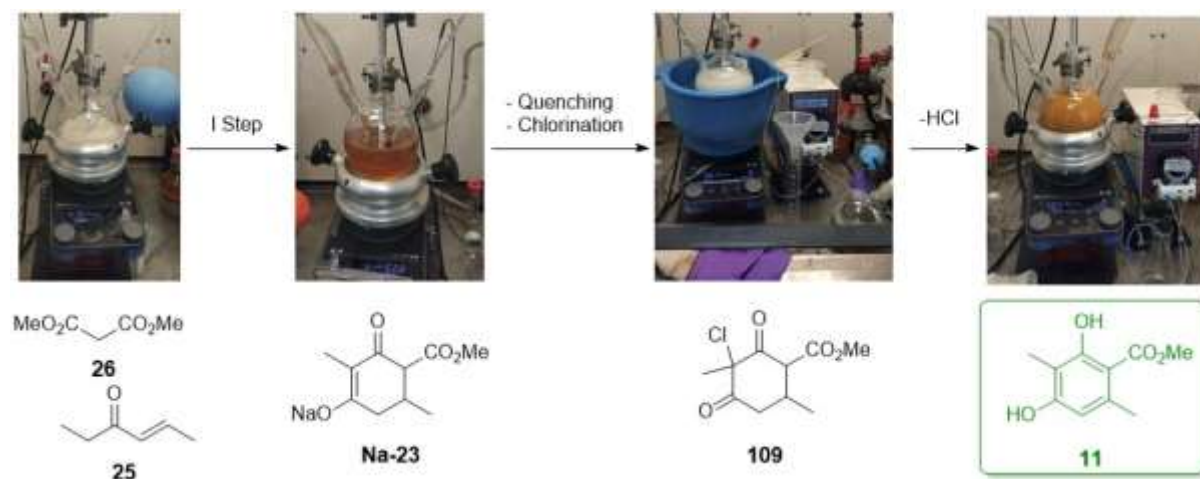


Figure 23. Pictures representing the singular steps carried out on the 1 mol scale-up.

During the processing, a few issues were encountered regarding the quenching of the sodium intermediate **Na-23**. The quenching of the first step was performed at room temperature through addition to the mixture of first water (35 mL) and second PPA (1.4 eq.). Initially, no exothermicity was observed, however, once the whole amount of the acid and water was poured into the red solution, the quenching started and the exothermicity warmed up the reaction mixture to the solvent boiling point. This situation caused partial evaporation of the solvent and the formation of big chunks of solids (phosphate salts) that compromised the homogenous stirring of the solution (*Figure 24*). The uncontrolled heating event could be attributed to an initial slow mixing rate of the viscous PPA in the water-AcOMe biphasic mixture. Due to the adiabatic temperature rise, viscosity reduces leading to more efficient mixing and exotherm, causing a partial solvent boil off of AcOMe. This phenomenon may be prevented by slowly adding the PPA in a warm reaction mixture, which improve the mixing rate and allow a better control of the heat release. Nonetheless, the process was carried on and, after chlorination and dehydrochlorination, the red solution was decanted, and the solvent recovered through vacuum distillation. The yellow residue was crystallised through the IFF purification

protocol and Veramoss (**11**) was isolated in 55% yield. The sample was then shipped to IFF in Benicarló, Spain for quality evaluation. Different analyses were performed to assess their appearance, odour characteristic, and colour (employing colourimeters for the extrapolation of L*a*b-based colour measurement values). To our delight, the analyses on the final material matches the IFF commercial specifications.

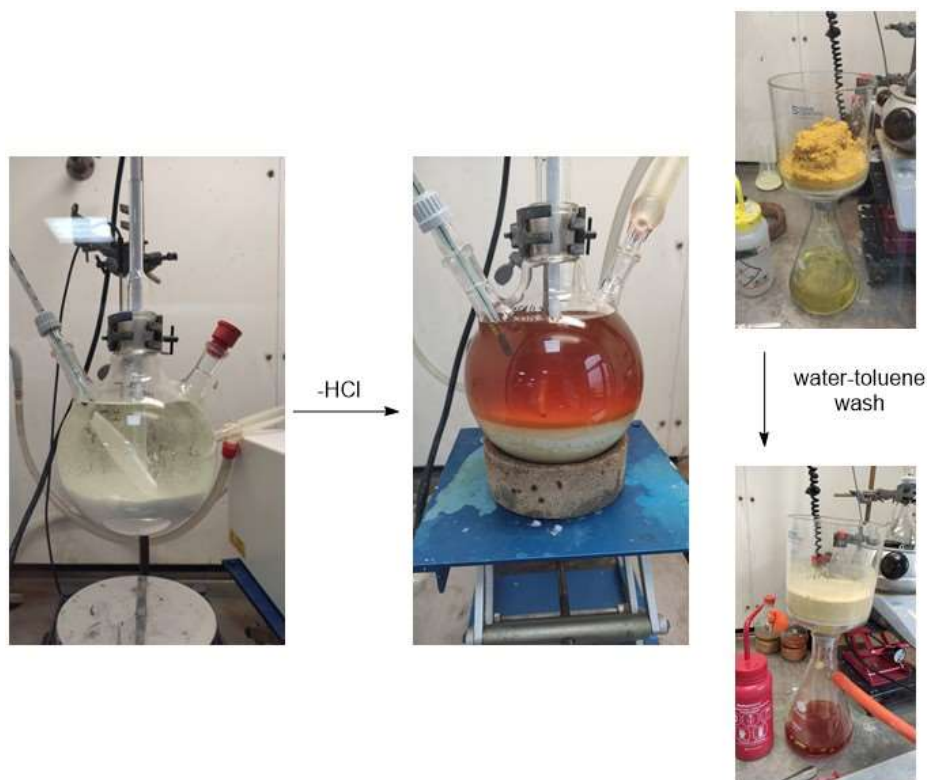


Figure 24. Pictures representing the amount of solid formed on the bottom of the flask before and after the dehydrochlorination step (left hand side) and the colour of the solid before and after the water and toluene wash (right hand side).

2.1.7. An alternative purification method for the final material

As shown in the previous section 2.1.4, the new processes of chlorination of compound **23** appeared to be forming colourful final materials whose quality would not match commercial specifications. As reported by IFF, this orange colouring has also been observed when mischarges of elemental chlorine occurs on production scale. Unfortunately, this issue provides an “out-of-spec” product, which not even the current IFF’s purification protocol seem to be

able to remove, causing a batch loss. For these reasons, it was deemed important for the project's completion to investigate an alternative downstream procedure for decolouration to reduce batch loss and wasted synthesis time.

As known products formed during phenols' oxidation, we thought it logical the colourful by-products of Veramoss (**11**) could likely have a quinone derived scaffold. Such compounds have also been reported in phenols-contaminated water treatments.²²⁸⁻²³¹ As it could be imagined, these orange quinones were reported to be highly unstable and polymerise under acidic conditions turning darker red. As a first attempt it was initially wondered whether a basic wash could possibly be useful for their removal. As Veramoss (**11**) can be deprotonated using sodium hydroxide, we attempted to use weaker inorganic bases (*Figure 25*). Sodium bicarbonate, carbonate, and phosphate dibasic were screened with sodium carbonate being revealed to be a possible candidate. Unfortunately, when performed as part of the work-up on the reaction mixture, the saturated aqueous solution did not yield a whiter product. Another attempt was also performed employing charcoal and chitosan (a linear amine-functionalised polysaccharide) as discolourising agents previously reported in literature,²²⁸⁻²³¹ however only slight discolouration was achieved.



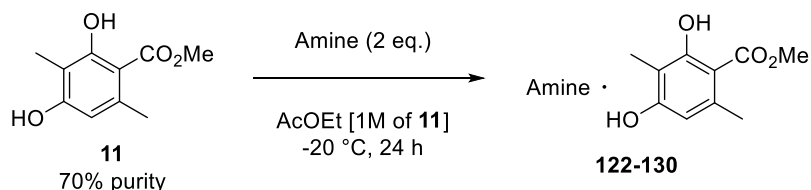
Figure 25. Comparison of colours obtained performing basic washings with sat. solution of NaHCO_3 , Na_2HPO_4 and Na_2CO_3 with the white Veramoss (**11**).

The formation of H-bonded complexes between amines and phenols are known in literature and have been widely described by Ross and co-workers in 1984.²³² Earlier on, McInnes *et al.*

described similar complexes using tetraalkylammonium hydroxy salts.²³³ This types of complexes did not find any special application until recently (2013) when Wu, Marsh and co-workers employed quaternary ammonium salts for the purification of phenol-contaminated refinery oil.²³⁴

Accordingly, the goal was to investigate the formation of a complex between Veramoss (**11**) and different amines and assess whether the former could separate from the colourful impurities. Firstly, several amines were screened, where the latter were added into a 1 M solution of orange crude Veramoss (70% purity) in AcOEt. The solutions were then stored at -20 °C for 3 days to evaluate any solid formation, and the solids were filtered and characterised. In total 11 amines were screened (based upon key indicators including toxicity/cost/solubility/stench) following this procedure and only a few examples of solid precipitation were observed (*Table 16*).

Table 16. Base screening for the formation of hydrogen-bonded complex with Veramoss.

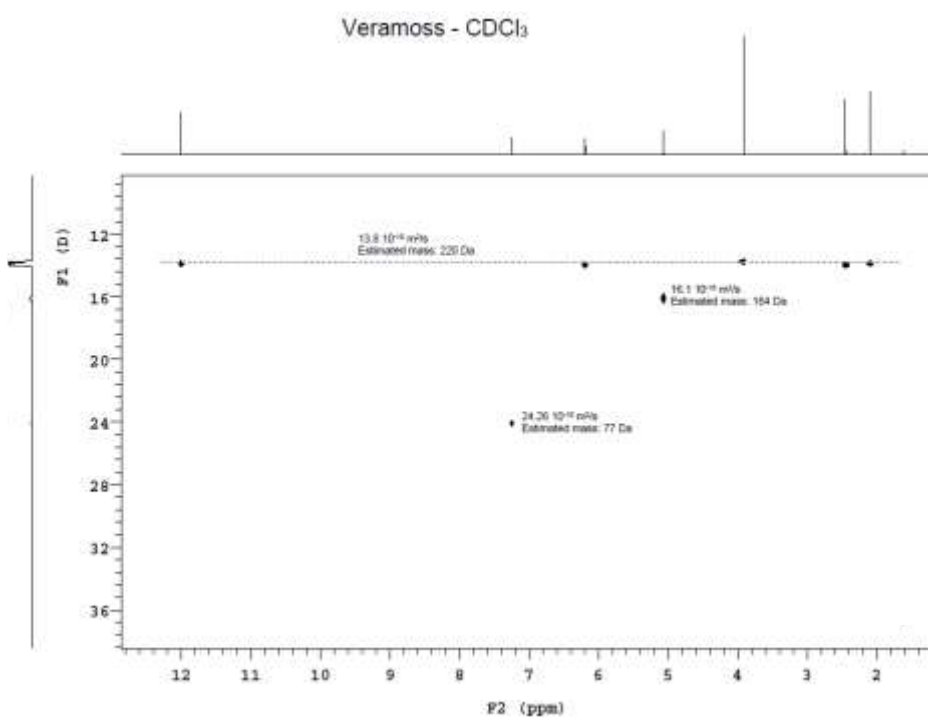


Entry ^a	Amine	Complex	Complex formation ^b	Amine:Phenol ratio ^c	Separation from impurities	Yield (%) ^d
1	NH ₃	-	No	-	-	-
2	Et ₃ N	122	Yes	-	No	-
3	<i>i</i> Pr ₂ NH	123	Yes	1:1	Yes	7
4	<i>i</i> PrNH ₂	124	Yes	-	No	-
5	<i>n</i> BuNH ₂	125	Yes	-	No	-
6	<i>n</i> Bu ₃ N	126	Yes	-	No	-
7	DBU	127	Yes	-	No	-
8	Morpholine	128	Yes	1:2	Yes	35
9	DABCO	129	Yes	1:2	Yes	99
10	tetramethylethylenediamine	130	Yes	1:2	Yes	89
11	PhNH ₂	-	No	-	-	-

^a The experiments were carried out on a 28 mmol scale; ^b Determined through spectrometric analyses; ^c Determined through SCXRD; ^d Isolated yield.

Having these results in hands, it was first attempted to evaluate the complex formation. Thanks to collaboration with Dr Aguilar-Malavia, we managed to put in place a diffusion-ordered NMR spectroscopy (DOSY) methodology capable of giving such information. The DOSY on the DABCO-Veramoss complex using different deuterated solvents (d_6 -DMSO, d_3 -MeCN, and $CDCl_3$) was first performed. The corresponding molecular weights were additionally calculated by knowing the diffusion coefficient of the species and employing the interpretation recently improved by Evans and co-workers.²³⁵

As shown in *Figure 27*, in polar solvents such as d_6 -DMSO and d_3 -MeCN, the signal peak of 1,4-diazabicyclo[2.2.2]octane (DABCO) has a different diffusion coefficient than the signal correlated with Veramoss (*Figure 26*). This is allegedly attributed to a total or partial solvation effect, as H-bond interactions of the complex are less strong than the interactions between the single molecules with the solvent. Deuterated chloroform was found to be the solvent where the complex structure is retained as also the calculated molecular weight matched the expected value (443 – 520 Da).



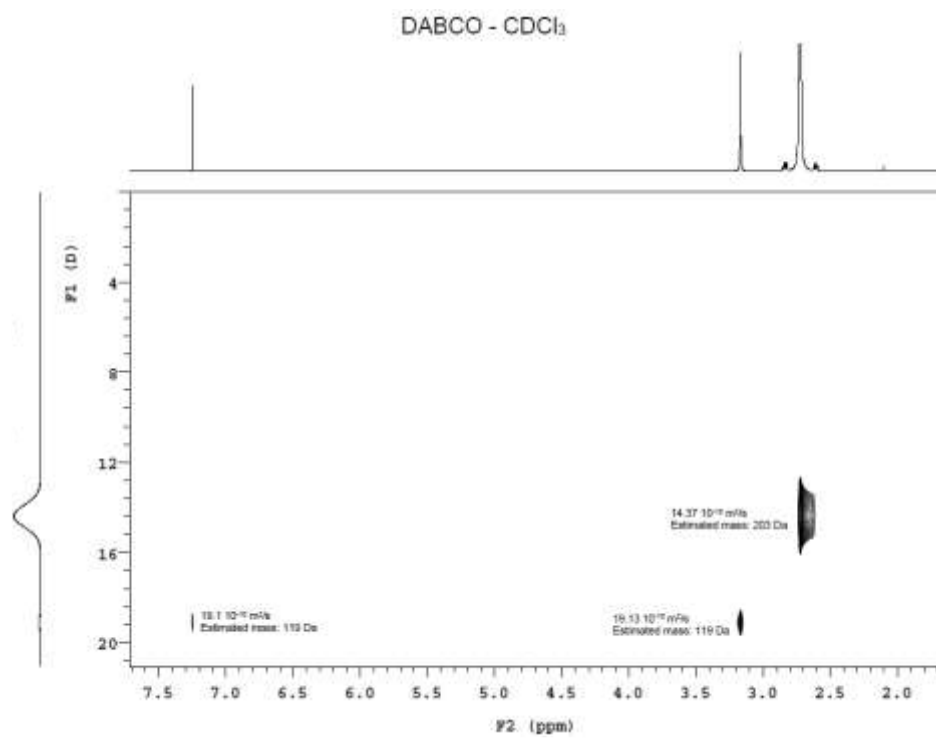
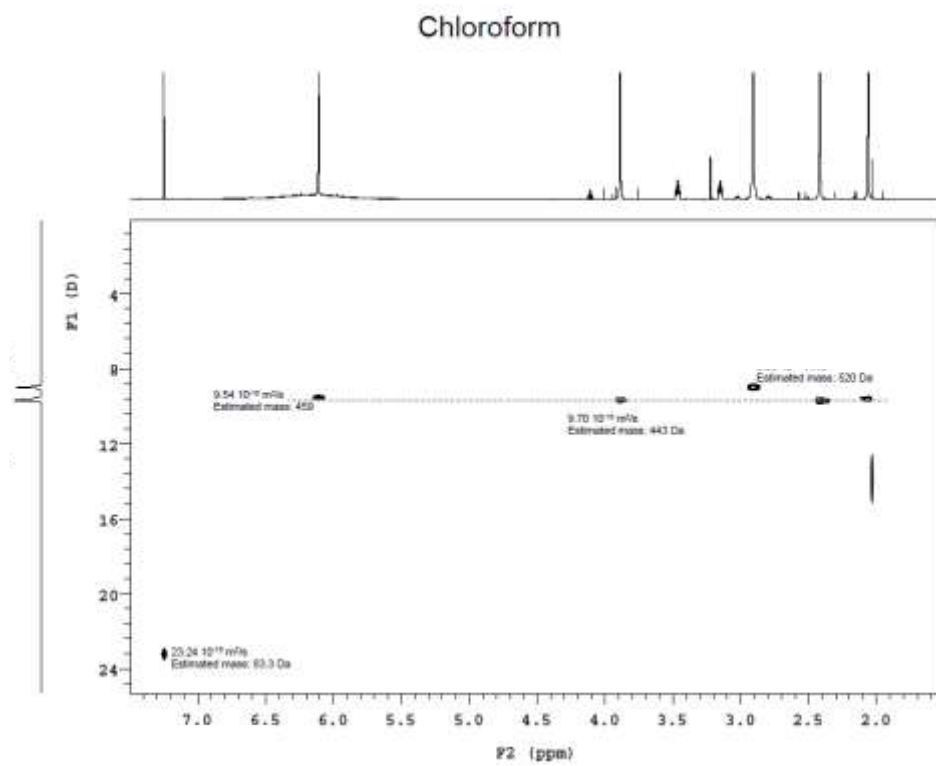


Figure 26. DOSY spectra of the single DABCO and Veramoss in CDCl₃.



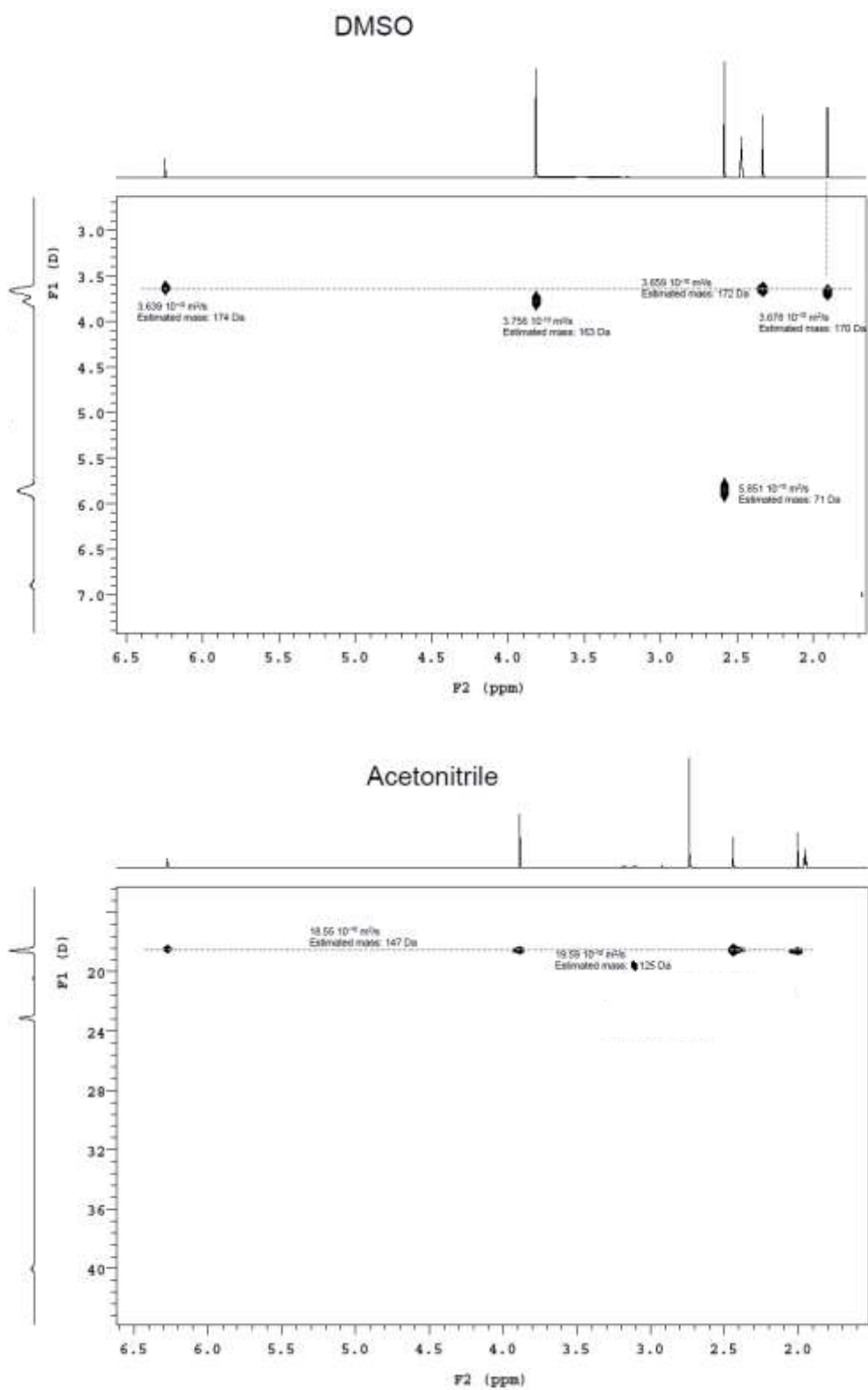


Figure 27. DOSY spectra of DABCO-Veramoss **129** complex in d_6 -DMSO, d_3 -MeCN, $CDCl_3$.

The complexes precipitating from the solution were found to be crystalline and Single crystal X-ray diffractometry (SCXRD) analyses were therefore carried out to gain more information on the structures. We noticed an H-bonding interaction between the nitrogen of the amines and the hydroxyl group of Veramoss (**11**) was present in all the isolated complexes (SCXRD depicted in the section 4.1). However, the complex between **11** and diisopropylamine (complex **123**) shows the hydrogen to be closer to the nitrogen atom than the oxygen of the phenol ring (OH distance 1.972 Å vs NH distance 0.886 Å). This data would suggest an ionic type bonding for the complex **123** instead of H-bonding as observed in the other structures (OH average distance 0.898 Å vs NH average distance 1.801 Å). Considering the p*K*_a of *i*Pr₂NH (11.07), we assumed all the acyclic trialkyl amines (*Table 16, Entries 2 – 7*) are forming low-boiling point salts with the product. This is also strongly validated by the DOSY spectra, as tributylamine and triethylamine both forms complexes with the targeted material.

Having the complexes in hands, we investigated possible conditions to recover the pure Veramoss (**11**). As pointed out in the DOSY experiments, polar solvents could possibly destabilise the H-bonded complex. Nonetheless, acidic solution may also protonate the basic site of the amine, leaving free Veramoss (**11**) to be recovered. Additionally, taking example from the IFF's purification procedure, water could be also used as anti-solvent to let the desired material precipitate out. Having these thought in mind, we carried out various initial de-complexation procedures exploiting acetic acid, 1 M HCl solution, water, and MeOH/H₂O system. As shown in *Figure 28*, the complex proved to be insoluble in water and thus no pure Veramoss (**11**) was recovered (*A in Figure 28*). When the 1 M HCl solution was employed, the desired material was successfully recovered (*B in Figure 28*). To our delight, methanol and water was found to be efficient to break up the complex and allow isolation of **11** (*D in Figure 28*). Consequently, MeOH/H₂O system was chosen to be scaled up employing a reddish coloured DABCO-Veramoss **129** complex of 95% purity. The quality of the material did not influence the final colour outcome, which remained white. Following this method, white Veramoss (**11**) was recovered in 98% isolated yield.

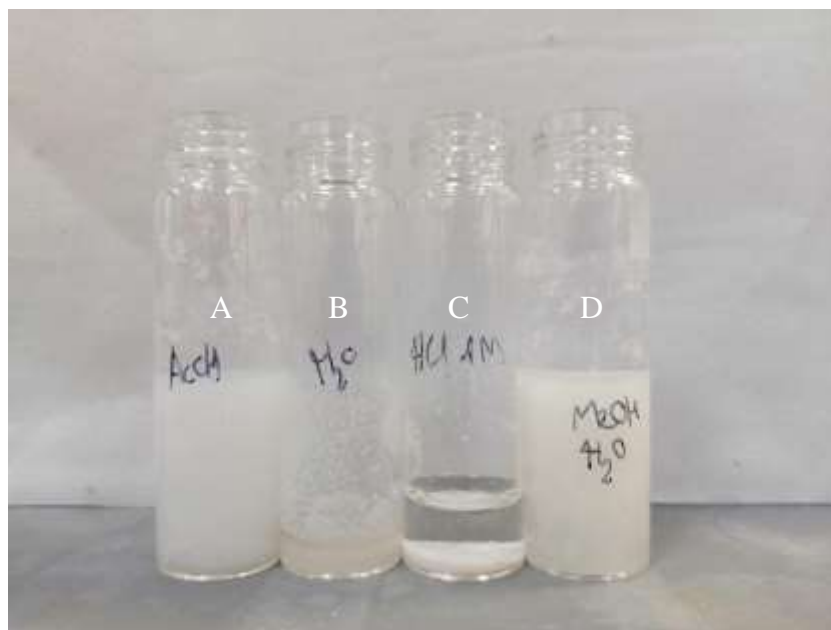


Figure 28. Attempted DABCO-Veramoss de-complexation using acetic acid-H₂O (A), water (B), 1 M HCl solution (C), and MeOH-H₂O system (D).

Having proved the potentiality of the process, we next aimed at improving the methodology to be applied at an industrial scale. The main drawback of the MeOH/H₂O system stands in the amount of solvent required in order to solubilise the material. Unfortunately, only partial de-complexation was detected when lower amount of methanol solvent was employed. To overcome the problem, the solubility of DABCO-Veramoss complex in different solvents at their boiling point was screened (*Table 17*). As proved in the laboratory, the de-complexation can be carried out by means of slow additions of water to the solution to enhance the crystalline state of the precipitate.

Table 17. Solubility screening of DABCO-Veramoss complex **129**.

Entry ^a	Solvent	Concentration (M of 129)
1	DMF	2.64
2	DMSO	1.5
3	iPrOH	0.22
4	MeOH	0.264
5	MeCN	0.132
6	THF	0.260
7	AcOEt	0.122

^aThe experiments were carried out on 0.2 mmol scale employing boiling solvents.

As shown in *Table 17*, the complex has moderate solubility in most solvents screened. For these reasons, it was decided to investigate the de-complexation method on another complex which performed well: TMEDA-Veramoss **130**. The latter has a 10-fold higher solubility in MeOH (2 M vs 0.2 M), however the tetramethylethylenediaminium salt (TMEDA^{H+}) proved to co-precipitate with the desired material. To remove the base, the solid needs to be washed through acidic waters (aqueous HCl solution).

The purification method using TMEDA was performed on a larger scale (30 g) and AcOEt was employed as solvent of choice. The complex TMEDA-Veramoss was filtered and subsequently dissolved in MeOH where water was slowly added over 2 hours to obtain a white precipitate. The white solid was washed with a diluted HCl solution to remove the remaining TMEDA salt and the desired material was isolated white in 60% yield. The rate of water addition in the de-complexation was found to be of paramount importance as a too fast addition could cause a co-precipitation of the complex **130**, and resulting in a product inheriting pink shades.

2.1.8. *Summary and Conclusions*

Over the last 3 years, the research project has achieved several goals. Firstly, three alternatives for the synthesis of the target molecule Veramoss (**11**) were investigated starting from widely accessible and cheap building blocks such as acetaldehyde, butanone, dimethyl oxalate, and malonate. Beside their potential, several issues were encountered that did not allow completing the full synthesis, therefore confirming the IFF approach from **25** to be the best choice at present.

Nevertheless, the IFF process still relies on the use of elemental chlorine to halogenate the *in situ* formed intermediate **23**. It was then considered to find a more easy to handle and environmental-friendly replacement whereby the process would inherit safety and greenness. After investigating two possible chlorinating agents (NaOCl, TCCA), TCCA was chosen as best candidate, and the oxidation step (chlorination-dehydrochlorination) was then optimised by employing DoE model (DSD). With the new optimised methodology in hands, compound **23** was oxidised to Veramoss (**11**) in 91 - 96% conversion with final material having 98% purity (NMR). The one-pot process was also scaled up to 1 mol yielding white Veramoss within commercial QC specifications in 55% (*Figure 29*).

It was noted over-oxidation of compound **23** causes a red shade colour to permeate the final material **2** which then invalidate the batch for commercial purposes. Our efforts highlighted a possible complexation-decomplexation process which at present seems to be highly selective for the particular compound and inevitably yielding white pure Veramoss (**11**) in excellent recovery. Several amines were investigated narrowing down the choice to two principal diamines; TMEDA, and DABCO. As the complex with TMEDA is more soluble in the screened solvent (AcOEt, and MeOH), the latter was taken as the more viable choice. A scale-up of the methodology allowed to the decolouration of the orange material, gaining Veramoss in higher purity in 60% recovered yield (*Figure 29*).

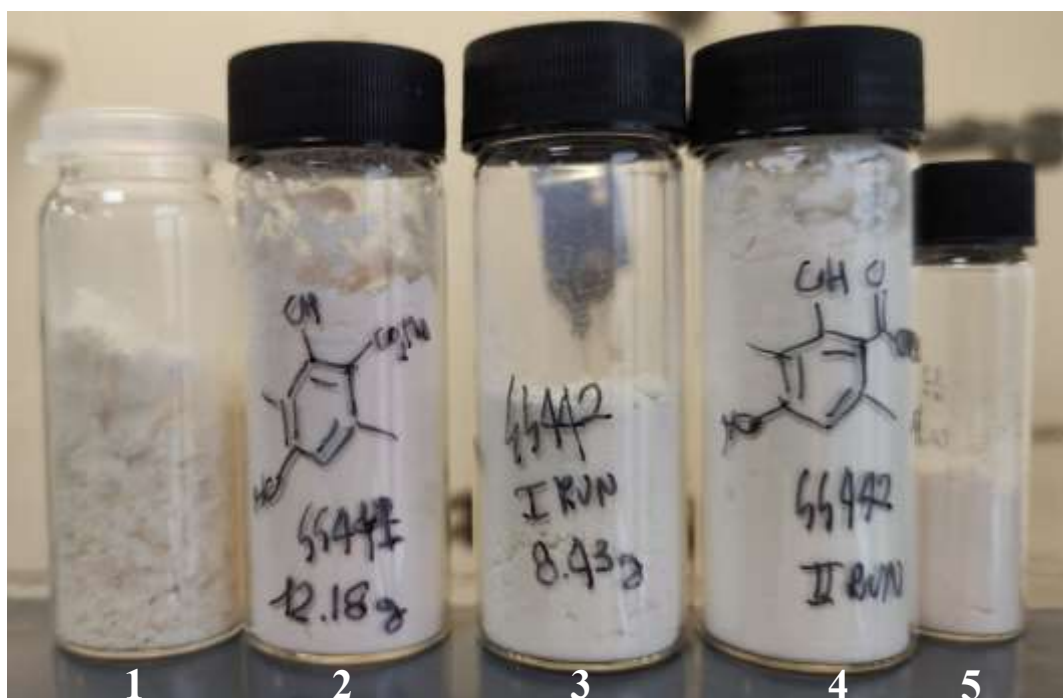
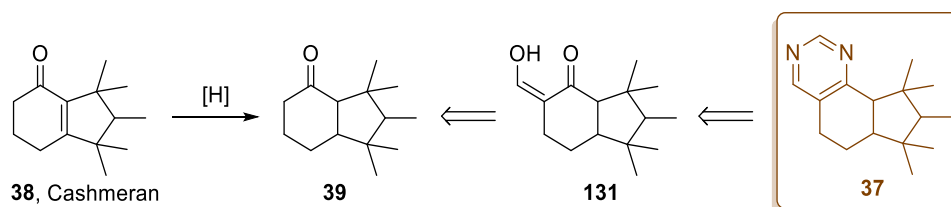


Figure 29. Picture of the four batches of crystallised Veramoss material yielded through the methodologies developed thanks to the IFF collaboration with Durham University. Samples of **11** obtained employing; elemental chlorine (1), de-colouration method on an orange over-oxidised material (2), de-complexation using only acidic waters (5). one-pot process first attempt (3), and second attempt (4).

2.2. Ambertonic

2.2.1. Ambertonic via formyl-dihydro-cashmeran: Route C

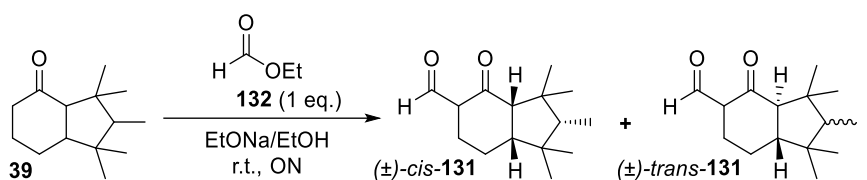
As depicted in *Scheme 47*, the first proposed alternative synthesis to Ambertonic™ starts from dihydro-cashmeran (**39**), a raw material easily accessible from IFF through hydrogenation of Cashmeran (**38**). The route consists of preparing a formylated material (**131**) which is finally transformed into the desired pyrimidine-functionalised scaffold **37**. Pyrimidine rings are widely employed in medicinal chemistry and a handful of methodologies have been described for their preparation.^{236–243} However, common methodologies employ functionalised ketones as starting materials, and particularly 1,3-dicarbonyl compounds are mostly selected. For these reasons, our initial efforts were aimed at developing optimised and valuable reaction conditions to the formyl-dihydro-cashmeran **131**.



Scheme 47. The suggested synthesis for the preparation of Ambertonic™ (**37**).

2.2.1.1. Process development for the formylation of Dihydro-Cashmeran (39)

Following the initial proposed *Route A*, the formylation of the compound **39** was first examined. The formylation of enolates are well-known in the literature with the de-protonation of the acidic formylated product playing a key role in the overall success of the process by driving the equilibrium towards this product. The preparation of **131** was initially performed using ethyl formate (**132**) and sodium ethoxide as the base. The reaction was conducted at a preparative scale of 1 mol (*Scheme 48*), yielding a dark red oily mixture found to be composed of roughly 60%_{w/w} of **131** with the rest being dihydro-cashmeran (**39**), therefore equating to 55% conversion.

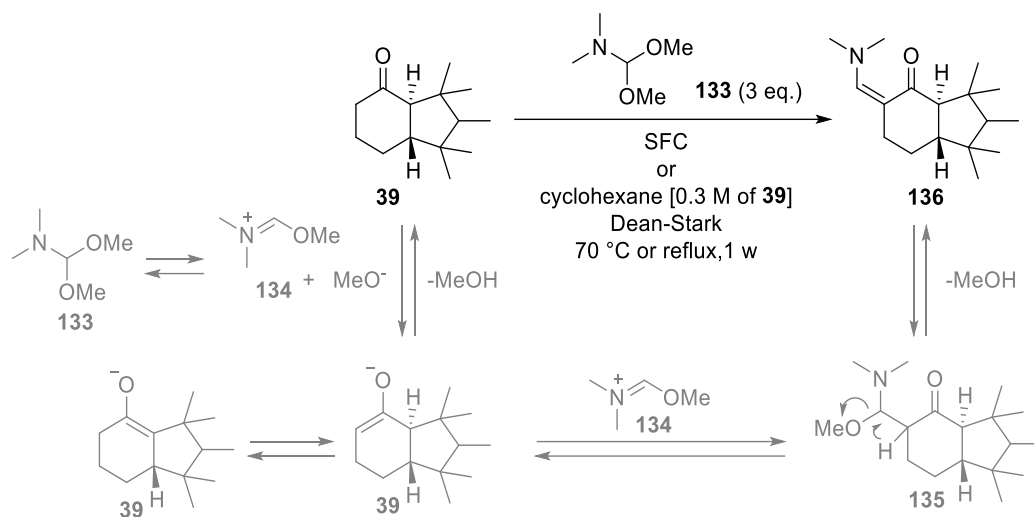


conversion to **131**: 55% (*cis:trans* 2:8)

Scheme 48. Preparation of **131** via Claisen condensation and the mixture obtained after vacuum distillation.

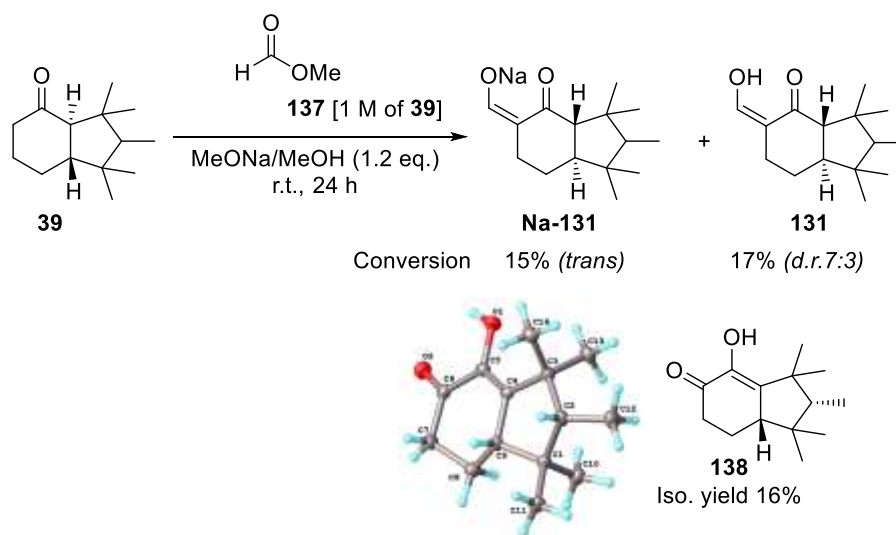
The final mixture was found difficult to purify due to the similar properties of the components. Vacuum distillations, column chromatographic separation, and acid-base extractions (using Na_2CO_3 and NaHCO_3) only managed to allow access to a slightly purer sample of the final material (e.g. distillation yielded 70%_{w/w} of **131** in **39**).

As the formylation with ethyl formate was troublesome, other options were also considered to efficiently yield synthetically equivalent analogues. Accordingly, the synthesis of the *N,N*-dimethylenaminone derivative **136** was pursued (*Scheme 49*). This transformation is widely described in literature as it enables the formylation to take place under mild conditions.^{244–247} The derivatives are generally prepared by heating the ketone with the *N,N*-dimethyl formamide dimethyl acetal (DMF-DMA) at 70 °C. Thus, the same conditions were initially employed for the synthesis of **136**, however, no reaction was observed even after 1 week and further addition of DMF-DMA. As the reaction is governed by methanol removal (see mechanism depicted in *Scheme 49*), azeotropic removal employing cyclohexane and a Dean-Stark apparatus was also attempted, however with no improvement in results occurred. In fact, in all the experiments, only starting material was recovered.



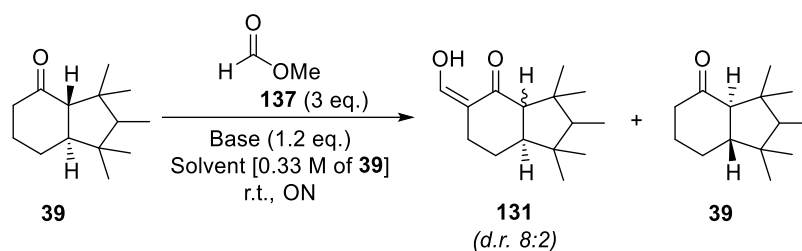
Scheme 49. Reaction conditions attempted for the preparation of the enaminone derivative **136** (black line) and proposed mechanism for the reaction (grey line).

Having unsuccessfully attempted a different formylation, our attention returned to the original procedure, however, this time changing a few parameters and reagents. First, a different formylating agent, namely, methyl formate (**137**) was employed. This was also used as the solvent of the reaction in order to help shift the equilibrium toward the **Na-131** product. Under these conditions, a white precipitate was formed, which was determined to be roughly a 1:1 mixture between the α -oxo ketone **138** and **Na-131**. The compound **138** was then isolated via crystallisation in a 1:1 MeOH:water mixture in 16%. The structure of compound **138** was confirmed by SCXRD structure and 2-D NMR spectra and its formation was attributed to the presence of oxygen in the system as the reaction was not carried out under inert conditions (*Scheme 50*). It is known that enolates can react with triplet oxygen forming 2-oxo-ketones as the final products.^{248,249} The remaining **131** was obtained via quenching of the reaction mixture and extracting it with EtOAc. Worse results were obtained when the same experiment was performed using ethyl formate as the reagent/solvent.



Scheme 50. Formylation of compound **39** using methyl formate (**137**) as the solvent for the formation of molecule **138** as well as the target **131**. Conversion based on $^1\text{H-NMR}$ spectra employing dimethyl fumarate as internal standard.

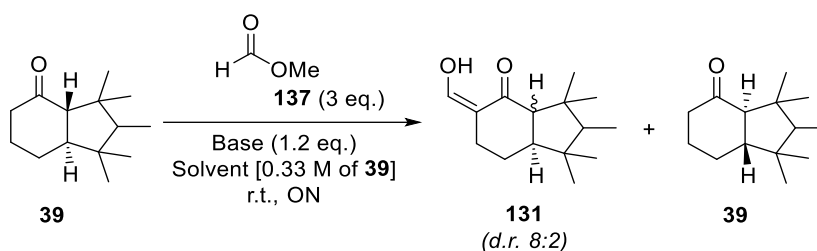
Having gained a new appreciation regarding the formylation reaction, we next evaluated the possibility of varying the identity of the base. Originally, the reaction was carried out utilising a 5 M solution of MeONa in methanol as base. Thus, we believed a screening of different organic and inorganic bases under solid/liquid biphasic conditions would be relevant for a deeper understanding of the reaction (*Table 18*). The overall procedure was also changed; instead of adding the methyl formate to a **39**/MeONa methanolic solution, a solution of **39** was slowly added to a heterogeneous mixture of MeONa and methyl formate (**137**) in the solvent. Furthermore, a different work-up was also employed which allowed efficient separation of **39** from the desired product. This will be discussed in detail below.

Table 18. Screening of the base for the formylation of **39**.

Entry ^a	Base	Solvent ^b	Yield to 131 (%) ^c	Conversion (%) ^c	131 Purity (%) ^c
1	NaH	Et ₂ O	-	0	-
2 ^d	K ₂ CO ₃	Et-	-	0	-
3	CaO	Me-	-	0	-
4	<i>t</i> -BuOK	Et ₂ O	54	70	90

^a All the experiments were carried out on a 10 mmol scale; ^b Concentration of 0.33 M; ^c based on ¹H-NMR spectra using dimethyl fumarate as internal standard; ^d In this experiment the ethyl formate **132** was employed instead of **137**.

To our delight, the use of *t*-BuOK as the base allowed the desired product to be isolated in 54% yield and 90% purity (*Table 18, Entry 4*). Additionally, different reaction conditions were investigated and MeONa in hexane was revealed to be the best conditions (*Table 19, Entry 4*). After quenching the reaction into water, the **Na-131** salt partially precipitated from the mother liquor and, after filtration, it was discovered to be the pure *trans*-isomer. To optimise the reaction workup, it was decided to wash the solid mixture with water and hexane and acidify the solid to be extracted with EtOAc. The procedure allowed isolation of compound **131** in 62% yield and 93% purity (*Table 19, Entry 5*). The method was further improved upon decreasing the quantity of methyl formate employed (*Table 19, Entry 6*).

Table 19. Screening of different solvents and alkoxide bases for the synthesis of **131**.

Entry ^a	Base	Solvent ^b	Yield (%) ^c	Conv. (%) ^c	Purity (%) ^c
1	<i>t</i> -BuOK	Toluene	33	56	83
2	<i>t</i> -BuOK	Hexane	52	67	83
3	EtONa	Hexane	40	90	93
3 ^d	MeONa	Hexane	21	33	83
4 ^e	MeONa	Hexane	85	94	100 ^f –92
5 ^g	MeONa	Hexane	62	90	93
6 ^{g,h}	MeONa	Hexane	74	94	95

^a All experiments were carried out on 10 mmol scale; ^b Concentration of 0.33 M; ^c Based on ¹H-NMR spectra employing dimethyl fumarate as internal standard; ^d A solution 5 M of MeONa in MeOH was used; ^e Obtained as precipitate (**Na-131**) and liquid (**131**); ^f **Na-131** obtained as only the *trans*-isomer; ^g The solid was filtered and then dissolved in water (500 mL); ^h 1.2 eq. of methyl formate were used.

Having determined a set of optimised reaction conditions, a scale-up of the reaction to 100 mmol was performed (*Figure 30*). The formylated compound **131** was obtained in 73% yield and in 94% of purity (*d.r.* 95:5). Sadly, by monitoring the purity of the compound, a gradual decrease of its purity over 2 weeks of its preparation was observed. Several products were detected by GC-MS along with **131**. The product was later found stable for longer time if stored at low temperature (1 – 5 °C).

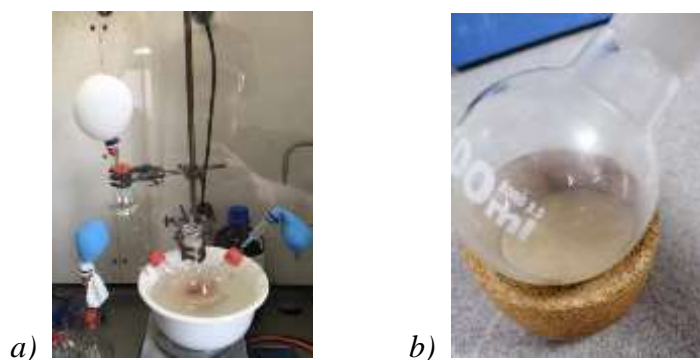
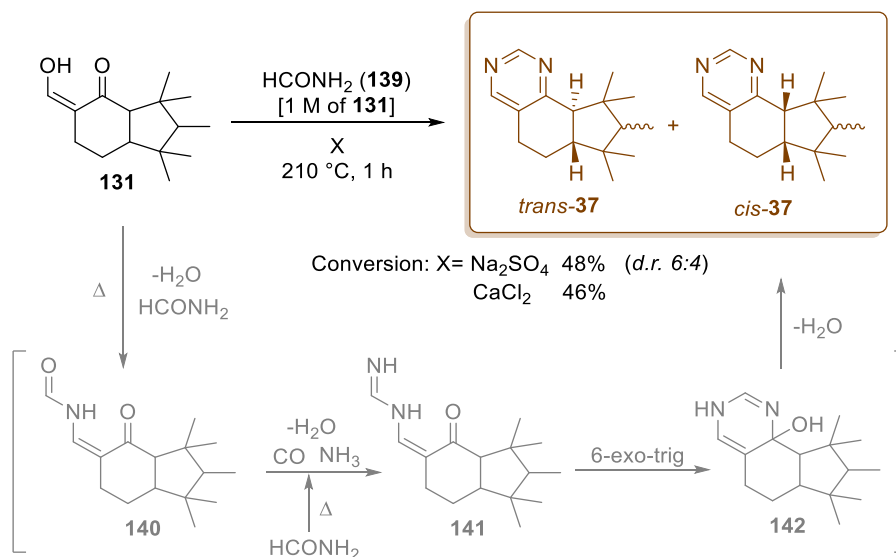


Figure 30. a) Formylation performed on 100 mmol scale. The procedure exploits the addition of **39** solution to a heterogeneous mixture of MeONa, methyl formate in hexane. b) The pure **131** was discovered to be a low-melting point solid.

Later studies performed by our industrial collaborators on preparative scale found the lab-scale optimised conditions were yielding mixtures difficult to stir with mechanical systems, impeding the completion of the reaction. This problem was attributed to the formation of extremely insoluble aggregates which were generating unstirrable bulky blocks. To prevent this issue, other solvents needed to be investigated. Ethers such as 1,2-dimethoxyethane (DME), *bis*(2-methoxyethyl)ether (triglyme), tetrahydrofuran (THF), and 4-methyl-tetrahydropyran (4-Me-THP) are well-known to be chelating agents for alkali metals and their efficiency were therefore examined in this system (*Table 20*).²⁵⁰

2.2.1.2. Pyrimidine ring formation

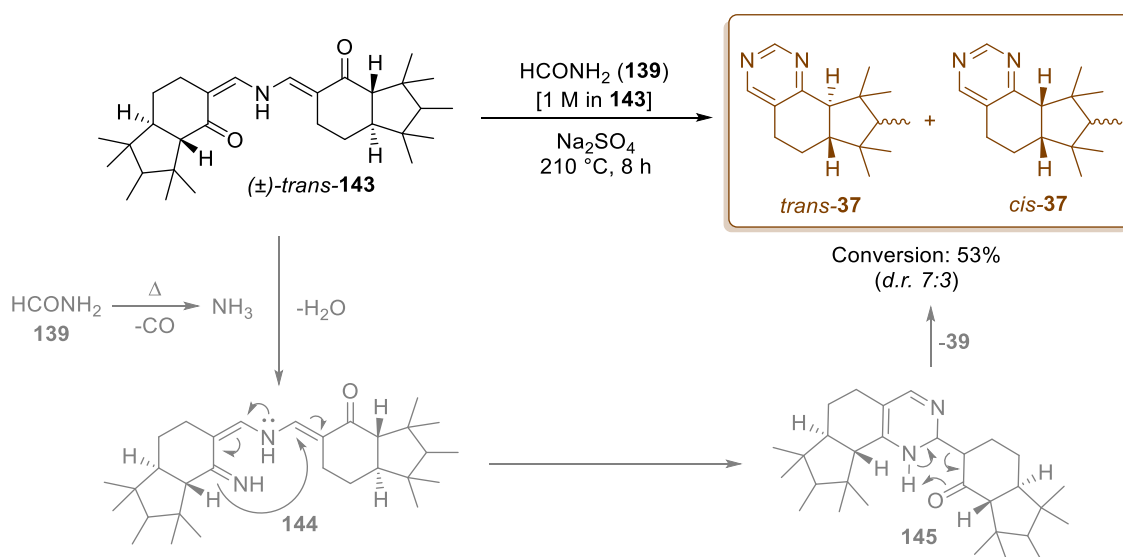
To rapidly assess the feasibility of the designed *Route A*, the subsequent stage of the process was investigated alongside with the formylation. As already mentioned previously, several synthetic methodologies for pyrimidine ring formation have been described in the literature, in particular, Bredereck *et al.* developed an efficient method starting from 1,3-diketones. The procedure consists of heating at 220 – 240 °C a mixture of the diketone along with sodium sulfate, formamide (**139**), and 2-*n*-butoxyethanol (solvent).²⁵² The reaction was therefore reproduced using our substrate of interest **131** and after 1 hour of heating no more starting material was noted by TLC and LC-MS analysis. The reaction mixture was biphasic with the top layer containing the two diastereoisomers in a ratio 6:4 *trans*:*cis* (*Scheme 51*). The mechanism has not been studied so far due to the multiple possible pathways; however, a postulated sequence starts with the introduction of the formamide on the more reactive carbonyl group with a release of water. At high temperatures (above 168 °C), formamide decomposes to carbon monoxide and ammonia, which reacts with the *N*-formyl intermediate **140** to give the formamidine **141**. The latter undergoes a 6-*exo*-*trig* cyclisation yielding the tricyclic material following dehydration producing the desired material **37**.



Scheme 51. Preparation of Ambertonic™ from **131** and formamide following the procedure of Bredereck *et al.* The proposed mechanism of the reaction is hereby depicted in grey line.

Conversions based on $^1\text{H-NMR}$ spectra employing dimethyl fumarate as internal standard. X can be sodium sulfate or calcium chloride.

The purification of the crude mixture was carried out via distillation and this allowed the collection of the desired compound in up to 78% purity; unfortunately, no better result could be obtained even after double distillation. The conversion to AmbertonicTM was acceptable at 48%. The same results were obtained when changing the sodium sulfate for CaCl_2 as a potentially more dehydrating agent (46%). An attempt to crystallise the mixture from EtOH brought about the discovery of the compound **143**. In order to determine whether this compound is an intermediate or a by-product, the pure dimer **143** was heated at 210 °C and after 8 hours AmbertonicTM was isolated in 53% yield (*Scheme 52*).



Scheme 52. Compound **143** subjected to the reaction conditions for the preparation of AmbertonicTM (black line). Proposed mechanism for the decomposition (grey line). Conversion based on $^1\text{H-NMR}$ spectra employing dimethyl fumarate as internal standard.

A further experiment was therefore set up in order to better understand this observation and implication on the mechanism of formation. As can be seen in *Figure 31*, the dimer **143** converts to AmbertonicTM over the first 5 hours of heating but then reaches a plateau. After 1 hour, **39** is detected although vanishing roughly 4 hours later. Thus, **143** could be considered

as an intermediate which progresses to a half yield of Ambertonic™, whereas the other half essentially decomposes, and potentially contributes to the formation of additional by-products (see mechanism *Scheme 52*).

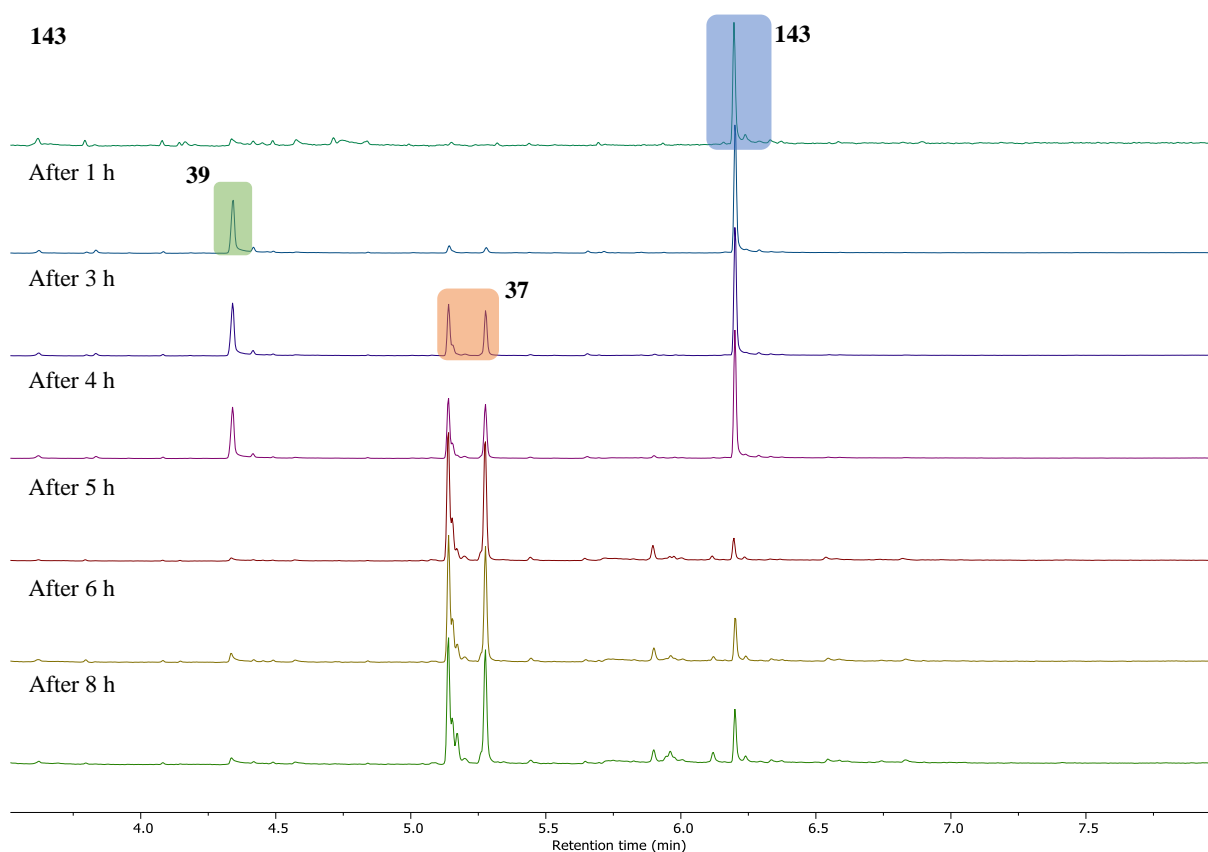


Figure 31. GC-MS spectra of the dimer **143** and control of the reaction described in *Scheme 52*. The peak highlighted in the green, orange, and blue area represent respectively dihydro-cashmeran **39**, the two isomers of **37**, and the dimer **143**.

It was then deemed important to determine the other intermediates of this reaction, therefore, the mixture was monitored carefully via GC-MS sampling every 10 minutes. During this experiment, other intermediates were also detected such as proposed species **140** and **146**. As can be observed in *Figure 32*, after 10 minutes Ambertonic™ is formed along with structures **143**, **140**, **146** and a small amount of **39**, which again tends to disappear during the reaction. After roughly 30 minutes some intermediates are still detected and the mixture remains similar

for the remaining duration of the time. All the peaks from 6.2 min to 9.4 min have m/z equal to 453 or 453+18 which could be attributed to the isomers of **143** and their hydrated forms.

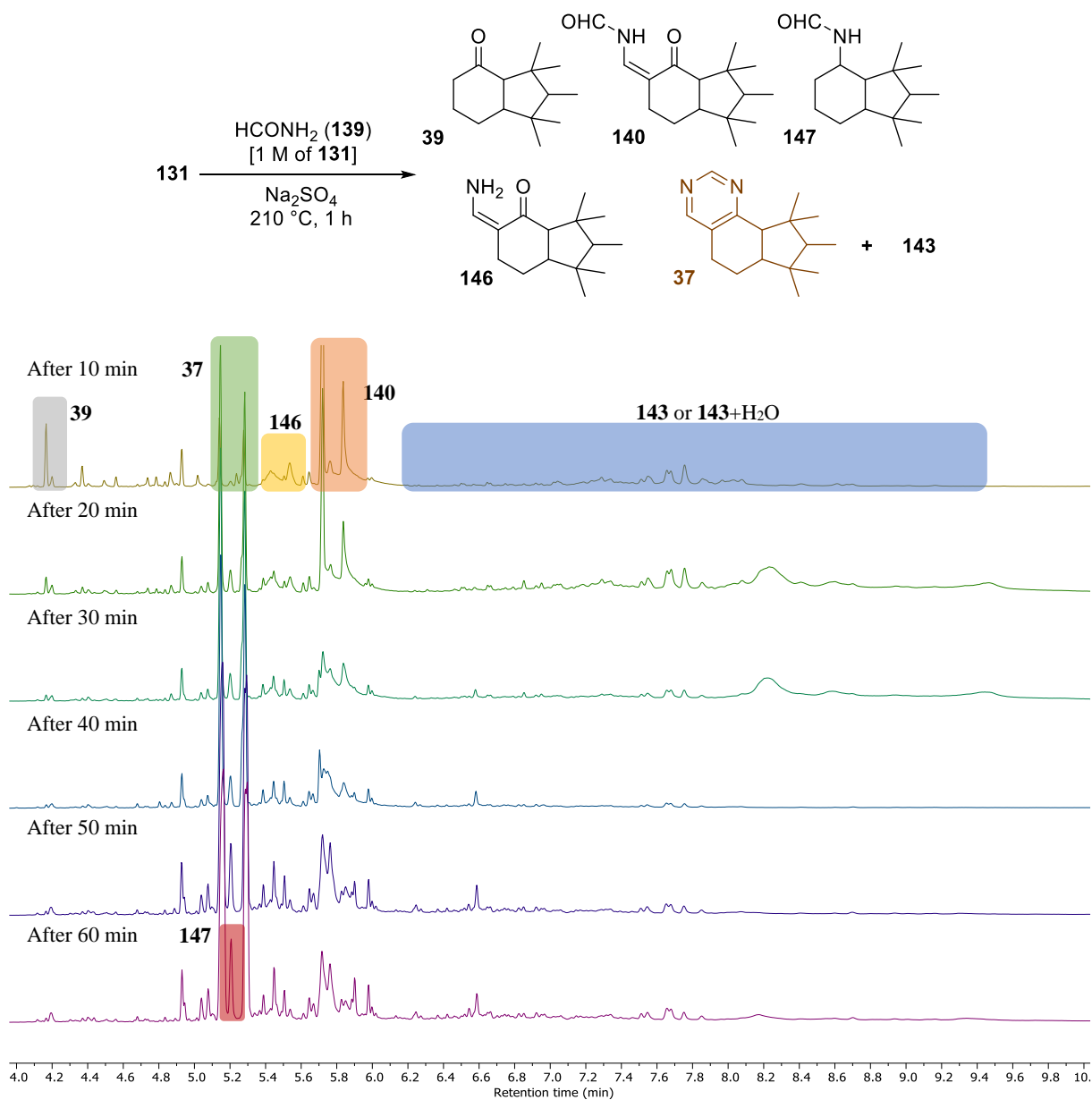
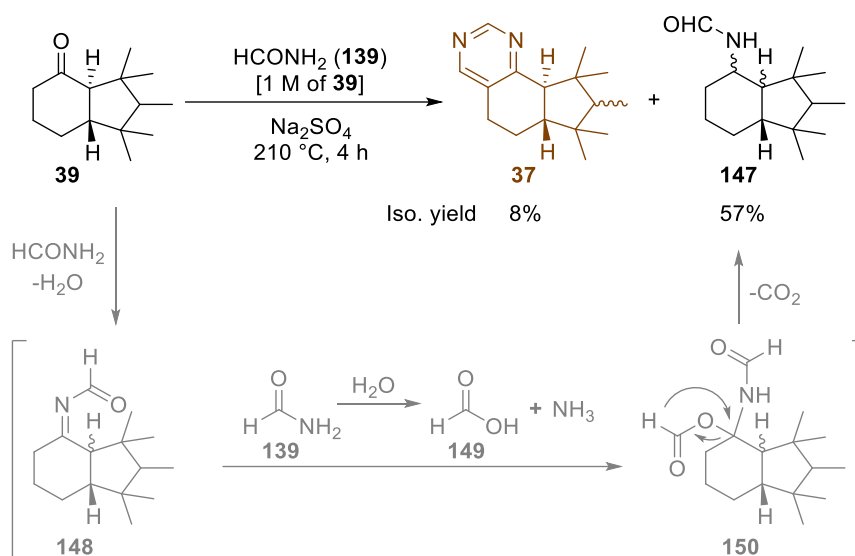


Figure 32. GC-MS control of the reaction. The peak highlighted in the grey, green, yellow, orange, blue, and red area represent respectively dihydro-cashmeran **39**, the two isomers of **37**, the compound **146**, the intermediate **140**, the dimer **143**, and the by-product **147**.

To reveal whether compound **39** forms Ambertonic™ with formamide, the former was treated under the same reaction conditions (*Scheme 53*). Surprisingly, Ambertonic™ was isolated in only poor yields (8%) and the main product was instead compound **147**.



Scheme 53. Attempt to obtain Ambertonic™ from **39** using formamide. The proposed mechanism for the formation of **147** is hereby depicted in grey lines.

This compound may imply a Leuckart reaction is occurring.^{253,254} The reaction could be attributed to the presence of dihydro-cashmeran **39** and the hydrolysis of formamide into ammonium formate at high temperature. The latter compound was also identified in *Figure 32* and it appears to be forming during the reaction. By comparing the $^1\text{H-NMR}$ spectra of this characterised new compound **147** with the previously obtained Ambertonic™ distillate (74% purity), we discovered the Leuckart's product **147** could be the reason for the difficult purification as it has physical properties similar to the final material (*Figure 33*).

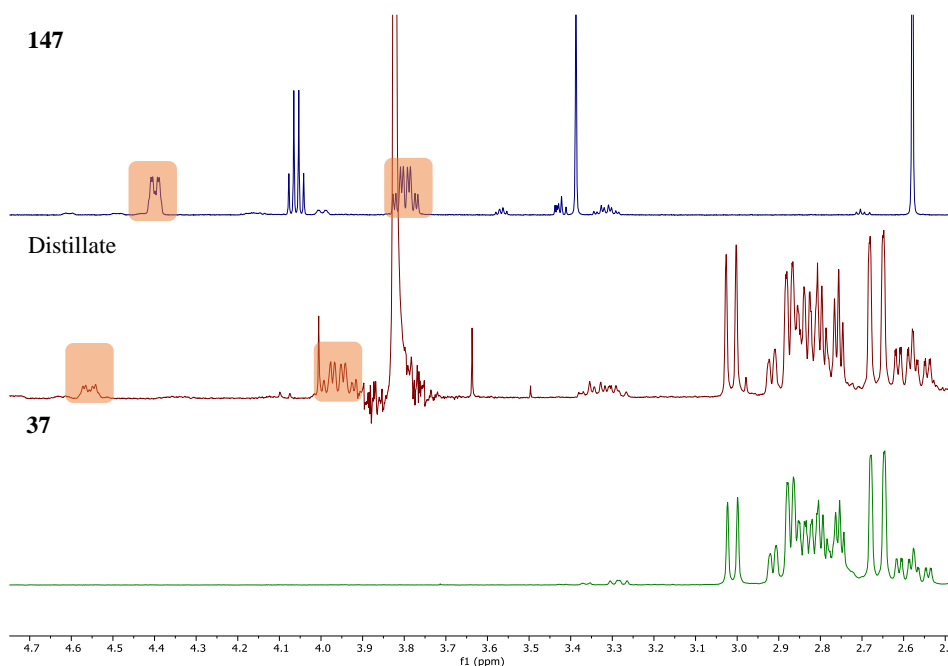


Figure 33. $^1\text{H-NMR}$ spectra of the distillate obtained from the crude reaction compared with AmbertonicTM (**37**) and the *N*-formyl compound **147**. The spectra of **147** is in acetonitrile- d_3 instead of chloroform- d .

Until this moment, a mixture 60 %_{w/w} of **131** in **39** was employed for the investigation due to the difficulties in preparing and isolating a purer sample of **131** (see section 2.2.1.1). Once optimised a more efficient procedure to **131**, the pyrimidine ring reaction step was carried out with this new pure material and **37** was obtained as a white solid in 91% purity after vacuum distillation. The overall isolated yield was 65%, although a small amount of Leuckart reaction **147** was still detected ($^1\text{H-NMR}$ spectra shows a roughly 95:5 ratio AmbertonicTM:**7**). As described above, this compound could be forming from the decomposition of the dimers **143** which were also still observed in the distillation residue (*Figure 34*).

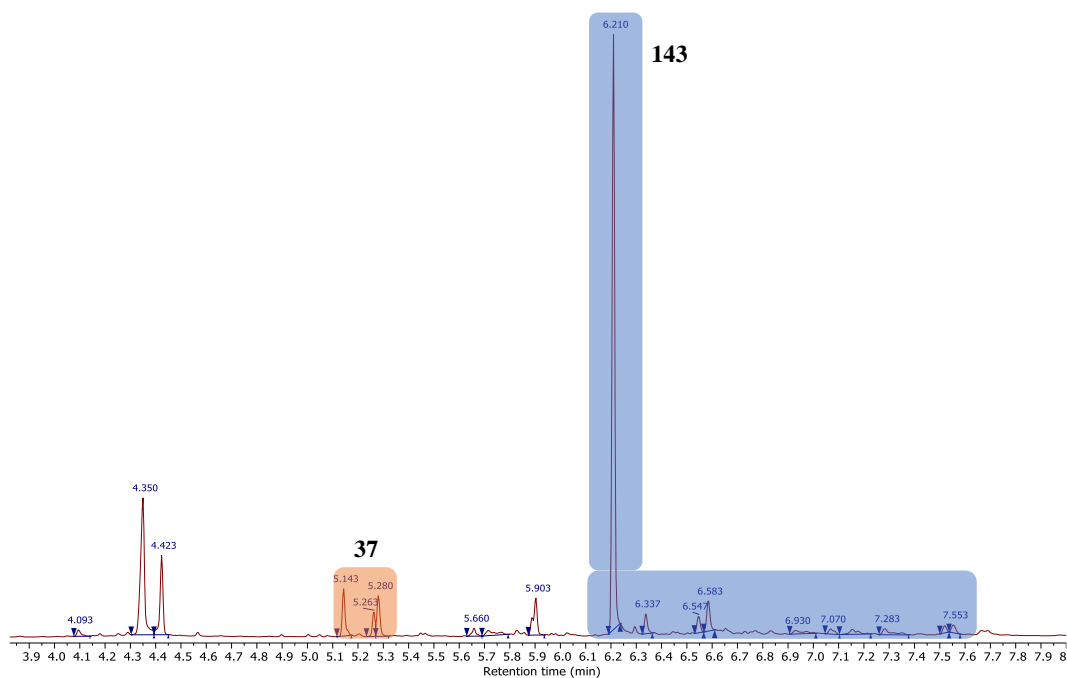


Figure 34. GC-MS spectra on the distillation residue which shows the dimers **143** and Ambertonic™ in small amount. The peak highlighted in the orange, and blue area represent respectively the two isomers of **37**, and the dimers **143**.

Encouraged by these promising results, we then opted in understanding the effect of the temperature on the reaction selectivity. Initial studies performed at low temperatures (100 – 120 °C) showed only formation of dimer **143** was detected instead of Ambertonic™. This suggests higher temperatures may be necessary for the cyclisation to occur. For a rapid and simple examination, in the earlier experiments the temperature of the reaction was controlled by the hold temperature of the hotplate, and no internal measurements were carried out. We therefore first repeated the previous experiment to measure the internal reaction temperature to establish a starting point for the screening. We discovered when the hotplate was set up at 210 °C the internal mixture was heated up to 180 °C. For these reasons, we reckoned it noteworthy to investigate temperatures ranged between 150 and 200 °C to better appreciate the reaction and optimise the method. The experiments were carried out without using CaCl₂ in order to simplify the work-up process for direct analysis (*Figure 35*).

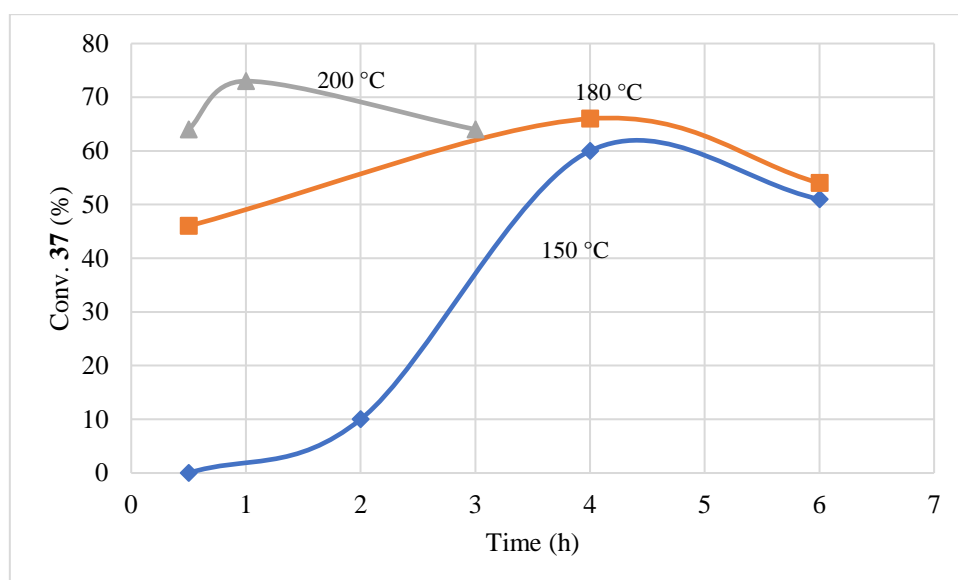
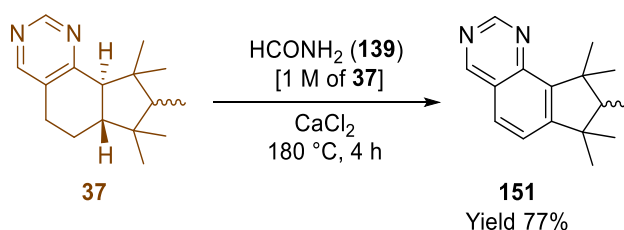


Figure 35. Screening of the reaction conditions for the synthesis of Ambertonic™. Conversion based on ¹H-NMR spectra employing dimethyl fumarate as internal standard.

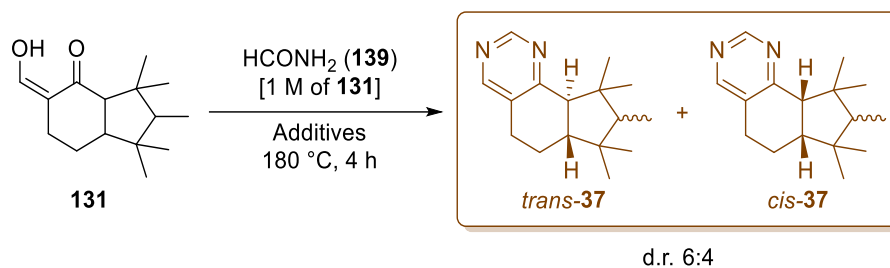
As shown in *Figure 35*, the conversion rises with increasing temperature; probably due to a faster cyclisation rate. However, longer reaction times shows reduction of Ambertonic™ (from 66% to 54% after 2 hours at 180 °C). To explain the singularity, a pure sample of Ambertonic™ was placed under the same reaction conditions. After 4 hours at 180 °C, a new fully oxidised quinazoline analogue (*dehydro*-Sinfonide, **151**) was isolated in 77% yield (*Scheme 54*). Thus, Ambertonic™ oxidizes when heated under the reaction conditions. As 200 °C would present a challenging temperature to reach both in lab and at plant scale, we decided to employ a temperature of 180 °C & 4 h as the optimised reaction conditions.



Scheme 54. *Trans*-Ambertonic™ placed in the reaction conditions forms *dehydro*-Sinfonide (**151**).

Having optimised the temperature, we then performed a screening of different potential additives to improve the reaction selectivity. As can be seen in *Table 21*, the dehydrating agent plays a key role in the reaction outcomes. The latter may be preventing the hydrolysis of formamide to ammonium formate keeping the amount of water low during the reaction (*Table 21, Entry 1*). An acid catalyst such as $\text{Zn}(\text{OAc})_2$ does not improve the reaction performance, on the contrary the mixture appeared to be darker and was more difficult to purify (*Table 21, Entry 11*). This may be attributed to the formation of hydrogen cyanide and its polymers derivatives. It is described in the literature, acid catalysis decomposes formamide in hydrogen cyanide decreasing the decarbonylation process.²⁵⁵ Surprisingly, the addition of ammonium acetate did not encourage the pyrimidine formation (*Table 21, Entry 4*), therefore, an extra source of ammonia does not reduce the formation of the dimer **143**. Other than sodium sulfate and calcium chloride, additional dehydrating agents were also evaluated such as common zeolites (MS 3Å and MS 4Å) and sodium chloride (*Table 21, Entries 8 – 10*). However, the results still show a better achievement utilising calcium chloride (*Table 21, Entry 3*). The outcome was also compared to the sodium sulfate initially employed as reported in the literature (*Table 21, Entry 2*).²⁵² When molecular sieves were employed, the work-up proved to be problematic due to the formation of emulsion in the phase separation and therefore low conversions may be attributing to such issue (*Table 21, Entries 8&9*). As mentioned earlier, the reaction mixture comprises of two phases; formamide, and compound **131**. To improve the mixing and active surface area between the reactants, as reported by Bredereck *et al*, the reagents were diluted in a high boiling point solvent such as 2-*n*-butoxyethanol. When the experiment was performed, instead of a dark brown tar usually obtained under SFC, a clear red solution was obtained, however, comparable results were obtained (*Table 21, Entry 5*). To reduce the amount of dimer **143** in the reaction, we also attempted to slowly add either formamide or **131** into the reaction mixture to decrease the probability of dimerization, although with no improvements (*Table 21, Entries 6&7*).

Table 21. Screening of the reaction conditions for the Ambertonic™ synthesis.



Entry ^a	Additives/Solvents	Conv. 37 (%) ^b
1	-	66
2	Na ₂ SO ₄	70
3	CaCl ₂	73
4^c	NH ₄ OAc	63
5	CaCl ₂ /2- <i>n</i> -butoxyethanol	68
6^d	CaCl ₂ /2- <i>n</i> -butoxyethanol	65
7^e	CaCl ₂ /2- <i>n</i> -butoxyethanol	57
8	MS 3Å	54
9	MS 4Å	52
10	NaCl	64
11^f	Zn(OAc) ₂	42

^a The experiments were carried out on 10 mmol scale; ^b Based on ¹H NMR spectra employing dimethyl fumarate as internal standard; ^c 1 equivalent was used; ^d A solution of **131** in the solvent was added to a mixture of CaCl₂ and formamide at 180 °C over 2 hours; ^e Formamide was slowly added to a mixture of **131**, CaCl₂ in the solvent; ^f The reaction was performed on 1 mmol scale with 10 mol% of zinc(II) acetate.

As the industrial collaborators were also interested in developing the synthetic preparation of Sinfonide, an unsaturated Ambertonic™ analogue (**153**), the same cyclisation reaction was also briefly studied starting from its formyl-cashmeran derivative **152**. As can be seen from *Figure 36*, **151** was found to be a main by-product in this procedure. It can be noticed that the amount of *dehydro*-Sinfonide (**151**) increases as the reaction progresses. In this case, only one temperature was examined; 3 hours at 180 °C resulted to be the best conditions for the reaction, although 6% of **151** was also formed.

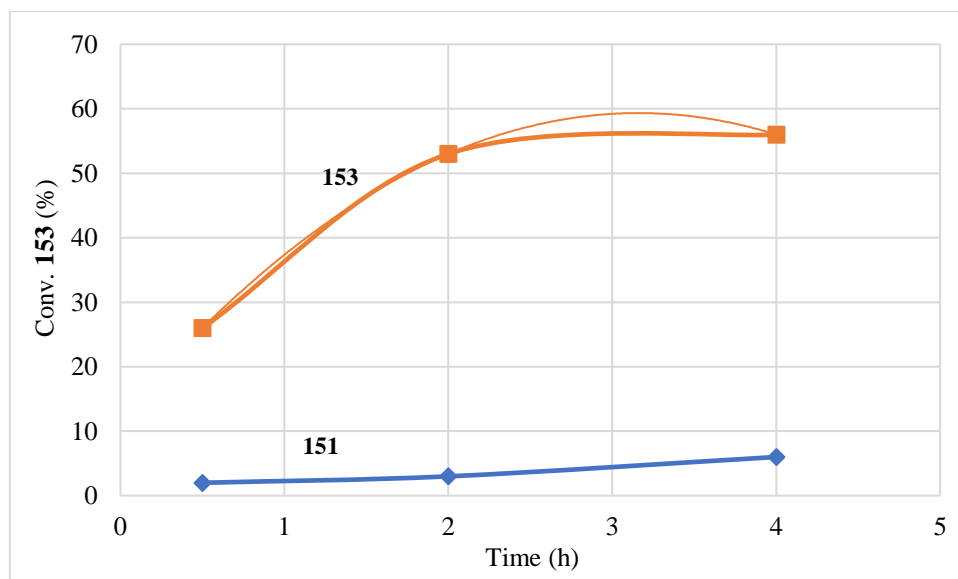
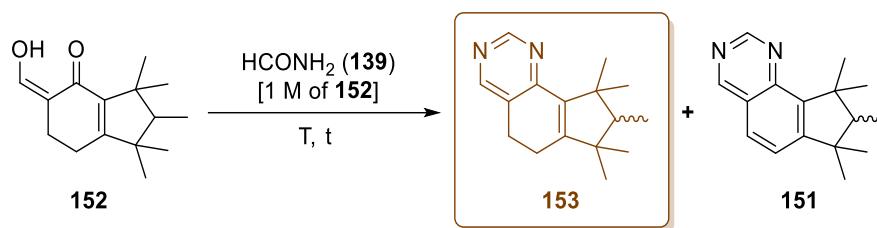
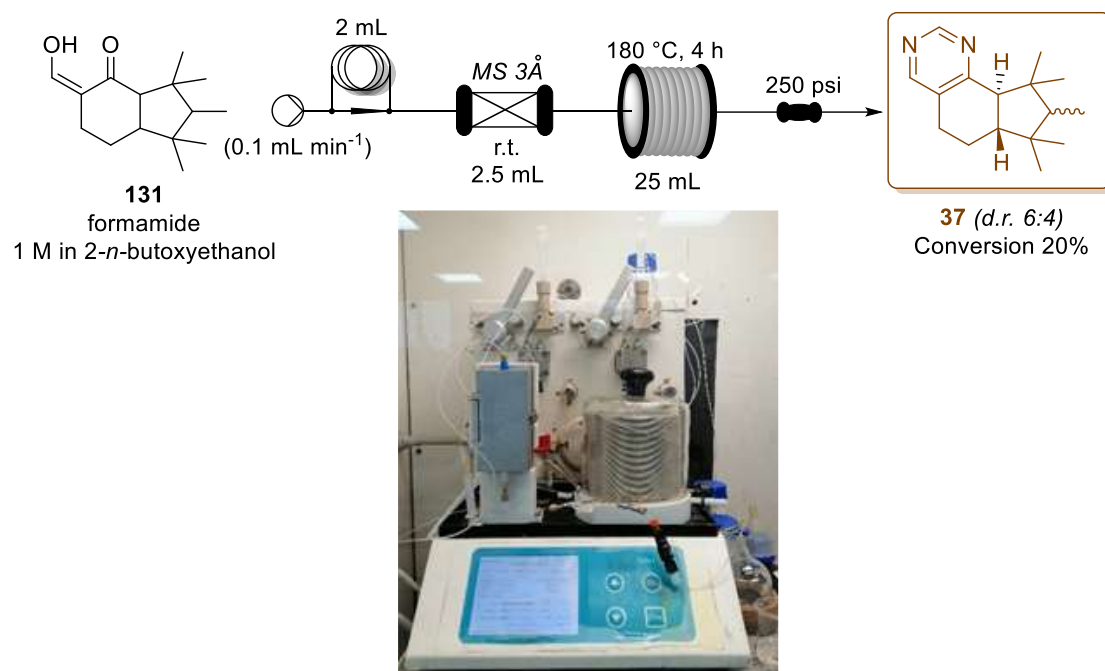


Figure 36. Screening of the reaction conditions for the synthesis of Sinfonide **153**. Conversion based on $^1\text{H-NMR}$ spectra employing dimethyl fumarate as internal standard.

2.2.1.3. A flow set-up for the pyrimidine formation

The positive outcomes as obtained using 2-*n*-butoxyethanol as the solvent made us think of a possible flow approach for this last stage. Thus, we set up a flow apparatus (Uniqsis FlowSyn) based on the batch conditions. A process flow diagram is described in *Scheme 55*.



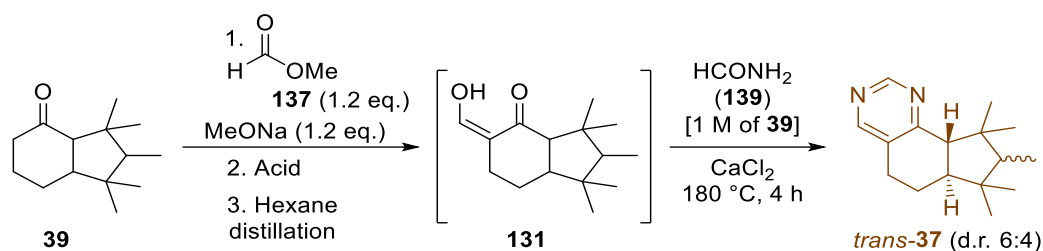
Scheme 55. Flow setup for the synthesis of Ambertonic™. Conversions based on ¹H-NMR spectra employing dimethyl fumarate as internal standard.

In order to dehydrate the solution, a packed column filled with molecular sieves was integrated before the reactor coil. Attempts to utilise packed columns of calcium chloride (using a 1:1 mixture of CaCl₂ and sand) resulted in line blockages of either the stainless steel coil reactor or the tubing after the column. Once exiting the column, the stream was directed into a 25 mL stainless steel coil reactor maintained at a temperature of 180 °C. The chosen residence time was transposed from the optimised batch reaction. When we employed the amount of formamide utilised under batch conditions (1 mL for 1 mmol of **131**), this brought about a high pressure build-up, tripping the max pressure working of the HPLC pumps. This premature stoppage prevented us from collecting the product stream. We therefore lowered the amount of formamide (800 vs 1000 μL/mmol of **131**) to prevent the over-pressure. Unfortunately, the setup was no more efficient than the batch process. Under the flow optimised conditions, Ambertonic™ was obtained in 20% yield.

2.2.1.4. *Toward a one-pot procedure*

Having optimised individually the two steps of the process, we decided to develop a one-pot procedure where the **Na-131** salt was not isolated. The intermediate was instead quenched with an acid and then immediately utilised in the next stage (*Table 22*). As the cyclisation step requires high temperatures, the solvent employed in the initial stage was distilled off from the reaction mixture and therefore could be recovered for re-use.

Having performed the first one-pot trial, we were glad to observe the formation of Ambertonic™ in good yields (56%, *Table 22, Entry 1*). As we know from the previous chapter (section 2.2.1.1), the formyl-dihydro-cashmeran **131** could potentially be decomposing during the intermediate step, and therefore we attempted an optimisation of the latter (*Table 22*). Consequently, different acids (polyphosphoric acid and sulfuric acid) and distillation temperatures (95 °C and 36 °C) were studied, however, the changes did not seem to improve the outcomes (*Table 22, Entries 1 – 3*). To further optimise the methodology, we also considered the possibility of reducing the amount of formamide as it may impact on the purification step, due to formation of emulsions and undesirable by-products. When smaller quantities were employed, solidification of the reaction mixture occurred, possibly due to a complete decomposition/evaporation of the formamide (*Figure 37*). In order to avoid this issue, the same experiment was performed employing 2-*n*-butoxyethanol as a solvent, yielding similar results (*Table 22, Entry 4*). As expected, when a larger amount of chemical was employed, the extraction of the product proved substantially harder due to the formation of emulsions, and causing low isolations (*Table 22, Entry 5*).

Table 22. Screening of reaction conditions for one-pot synthesis of Ambertonic™.

Entry ^a	Acid	Vol. formamide (mL)	Conv. 37 (%) ^b
1 ^c	PPA	20	56
2 ^d	PPA	20	58
3	H ₂ SO ₄	20	55
4	PPA	5	17 (22) ^e
5	PPA	40	40

^a The experiments were carried out on 20 mmol scale; ^b Based on ¹H-NMR spectra employing dimethyl fumarate as internal standard; ^c The distillation was performed at 95 °C (hotplate's temperature) at atmospheric pressure; ^d The distillation was carried at 36 °C (hotplate's temperature) at 190 mbar; ^e Conversion obtained when 20 mL of 2-*n*-butoxyethanol was added before starting the second step.

**Figure 37.** Block of solid yielded when 5 mL of formamide was employed.

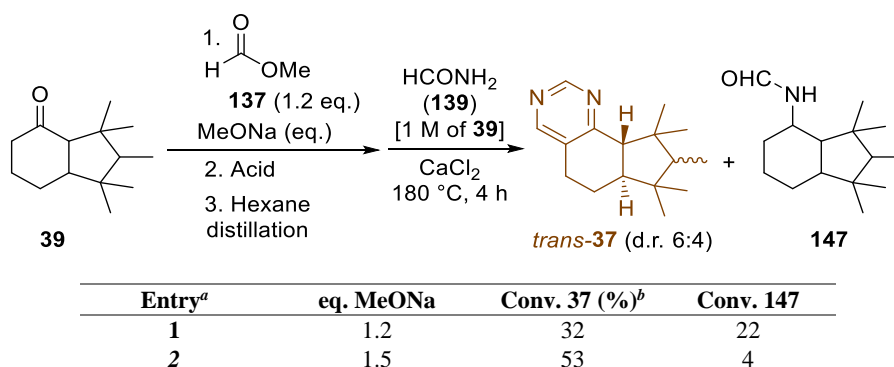
Having established the principle of a one-pot procedure for the synthesis of Ambertonic™, we considered to examine the final purification (*Figure 38*). As the reaction mixture is biphasic, the organic layer (top) can be directly separated from the other layer (bottom). In this way the desired product is then distilled.



Figure 38. Apparatus used for the one-pot procedure of the synthesis of **37**. In the flask two layers can be noticed; the bottom layer is mainly formamide along with CaCl_2 and the top layer is where the product is distilled from.

Unfortunately, the initial distillation of the organic layer provided the target compound **37** but contaminated with the Leuckart's product **147**, showing the same issue initially encountered (section 2.2.1.2). These outcomes suggest a small amount of **39** was remaining unreacted from the first step (Table 23). As a consequence, an increase amount of MeONa was employed (1.5 equivalents) this had the effect of dramatically decreasing the impurity formation (Table 23, Entry 2).

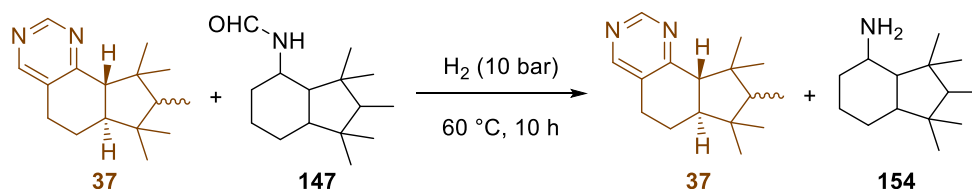
Table 23. Screening of reaction conditions for the synthesis of compound **37**.



^a The experiments were carried out on 20 mmol scale; ^b Based on ¹H-NMR spectra employing dimethyl fumarate as internal standard.

As our industrial collaborators were finding it challenging to avoid the formation of this impurity, a down-stream procedure for its removal was therefore perceived to be a good option and was thus taken in consideration. Several deprotecting procedures for formides have been described in literature.²⁵⁶ Sadly, classic acid or base catalysis did not allow for the efficient hydrolysis of this particular formyl group, moreover oxidation of Ambertonic™ (**37**) to Sinfonide (**153**) occurred under many of the acidic conditions tested. For these reasons, we attempted to develop a hydrogenolysis method. Several catalysts were screened on a mixture of 69% Ambertonic™ (**37**) and 17% of compound **147**. As can be seen in *Table 24*, none of the catalysts allowed us to achieve our outlined aim.

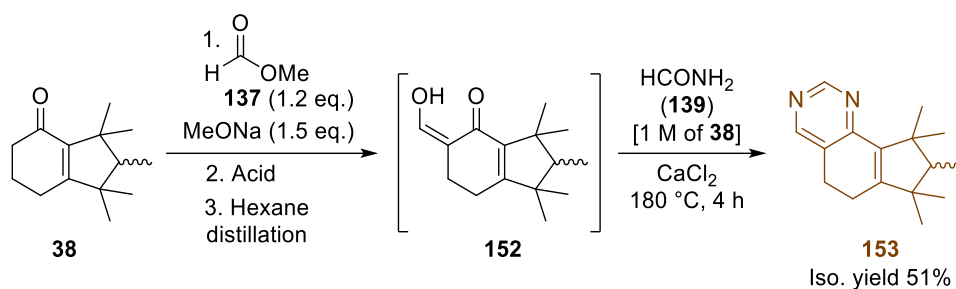
Table 24. Screening of catalysts for the hydrogenation of a mixture **37** and **147**.



Entry ^a	Leuckart's (%) ^b	Catalyst
1	19	-
2	18	Pd/C
3	15	Pt/C
4	16	Ru/C
5	19	Wilkinson's
6	15	Pd encat
7	19	Ni/C

^a The experiments were carried out on 20 mmol scale; ^b Based on ¹H-NMR spectra employing dimethyl fumarate as internal standard.

As we were also optimising a procedure for compound **153**, we therefore applied the same preparative method for the preparation of Sinfonide (**153**). The same procedure was performed on the substrate **38** and Sinfonide (**153**) was isolated in 51% yield (*Scheme 56*).



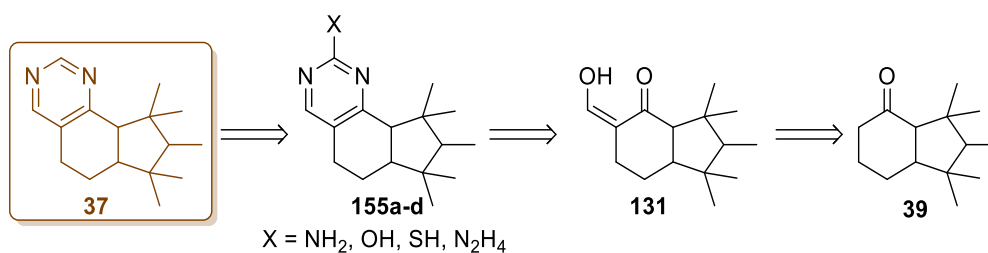
Scheme 56. One-pot procedure applied to Cashmeran (**38**) to yield Sinfonide (**153**).

Therefore, having solved the issue with mixing in the formylation step (see section 2.2.1.1), and having optimised the reaction conditions for the one-pot procedure, we performed the experiment employing 4-methyl-tetrahydropyran (4-Me-THP) replacing hexane as the initial solvent. To our delight, the process yielded the desired materials **37** and **153** without loss of yield (58% and 51% respectively).

2.2.2. Alternative strategies to the pyrimidine scaffold: Route D

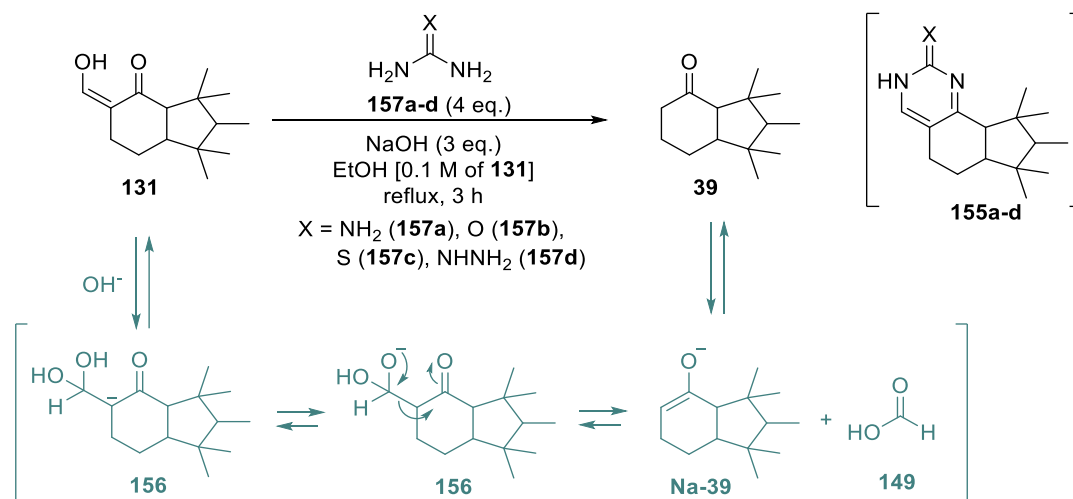
2.2.2.1. Starting from dihydro-cashmeran

The first attempted alternative strategy to AmbertonTM was via a 2-substituted pyrimidine derivative **155**, where X could be an amino, thiol or hydroxyl group, which could be subsequently removed either via a reductive or oxidative step to yield the final product (*Scheme 57*).^{257–266}



Scheme 57. Retrosynthetic pathway for the synthesis of **37** through scaffolds **155a-d**.

The preparation of the different pyrimidine derivatives started off by preparing the amino-pyrimidine **155a**, pyrimidinone **155b**, pyrimidin-thio-one **155c**, and hydrazinopyrimidine **155d**. In the literature, the methods used to prepare such species are miscellaneous, however, most of them employ basic conditions.^{267–275} Thus, the formyl dihydro-cashmeran **39** and corresponding urea derivative (**157a-d**) were treated with sodium hydroxide in ethanol (*Scheme 58*). Unfortunately, from these conditions none of the compounds **155** were formed and, according to GC-MS monitoring, the starting material **131** was instead converted into the dihydro-cashmeran **39** after 3 hours. It was then discovered the elimination of the formyl group under acidic and basic aqueous condition has been described in the literature.^{276,277} In fact, compound **131** decomposed fully after 2 hours when treated with a NaOH solution in EtOH, forming dihydro-cashmeran. It could therefore be speculated that a possible mechanism of the decomposition occurs through the addition of a hydroxyl anion to the formyl group. The driving force of the reaction is the formation of formic acid, which allows the protonation of the enolate **Na-39**.

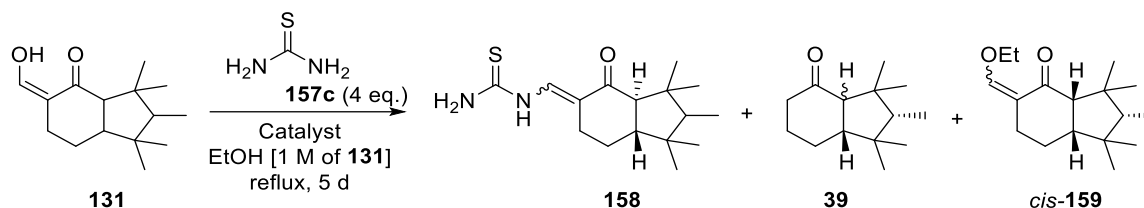


Scheme 58. Screening of the preparation of **155b-d** in basic conditions using thiourea, urea, and aminoguanidine bicarbonate (black line). Suggested decomposition pathway for **131** in basic conditions (grey line).

Focusing on the preparation of the pyrimidin-thio-one **155c**, we decided to investigate the addition of thiourea under several reaction conditions (*Table 25*). Firstly, the reaction was performed in ethanol under neutral conditions (*Table 25, Entry 1*). Unfortunately, the

experiment was found to be sluggish and did not yield the desired derivative **155c**. In fact, chromatographic purification of the crude mixture allowed the isolation of the products **39**, **159**, and **158**. The latter was identified with spectroscopic analysis as the enaminone derivative. The *cis*-isomers of **131** seem to be less reactive with thiourea (**157c**), probably due to the steric hindrance of the pentamethyl-cyclopentyl ring. When acid conditions were employed, the enaminone **158** was not formed, instead, the hydrolysed material Cashmeran **39** was detected as main component via GC-MS (EI), probably due to the presence of trace water in the solvent (*Table 25, Entries 2*). Higher temperatures and SFC did not improve the reaction, even though a small portion of **158** was identified (*Table 25, Entry 3*). As some of the intermediate **158** was observed forming in the reaction at 78 °C, we wondered whether an increase of temperature may lead to the cyclisation step. Therefore, the reaction was performed in 1,4-dioxane at 160 °C and 181 °C (through sealed microwave reactions), however, none of the desired compound **155c** was detected (*Table 25, Entries 4&5*). Although a VERY stinky smell of rotten egg was instead noted, which would suggest thiourea (**157c**) decomposition.

Table 25. Reaction conditions attempted for the preparation of the pyrimidin-thio-one **155c**.

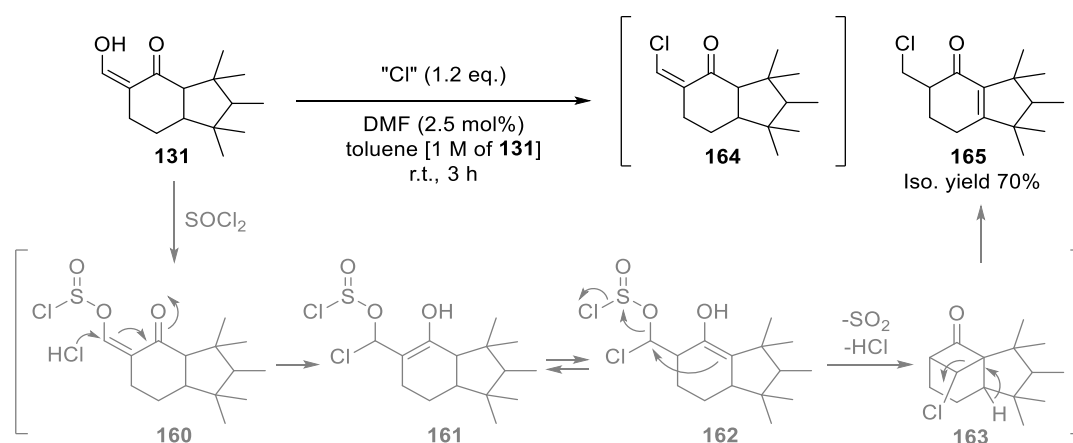


Entry ^a	Catalyst (mol%)	Time (h)	Temp. (°C)	Conv. (%) ^b	Yield 158 (%) ^b (<i>Z:E</i> ratio)	Yield 39 (%) ^b	Yield 159 (%) (<i>Z:E</i> ratio)
1	-	120	78	50	12 (4:6) ^c	-	13 (6:4) ^c
2	H ₂ SO ₄ (10)	1	78	100	-	85	-
3^d	H ₂ SO ₄ (10)	1	150	100	-	85	-
4^{e,g}	-	1	160	100	-	-	-
5^{e,g}	-	1	181	100	-	-	-

^aThe experiments were carried out in a 10 mmol scale; ^bBased on GC relative area percentage (RAP); ^cIsolated yield; ^dReaction performed under solvent-free conditions; ^eReaction performed employing 1,4-dioxane as solvent; ^gThe experiment was performed in the microwave.

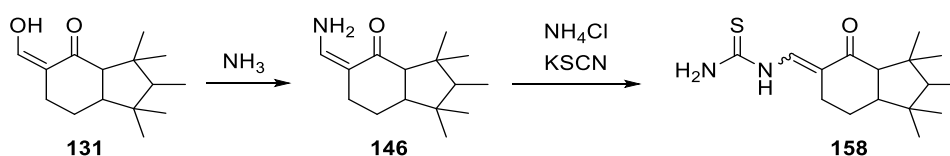
As the possibility for a cyclisation of **158** into **155c** was still of significant interest, we resolved to test other strategies to this intermediate. The latter could then be evaluated for the cyclisation

under different conditions. Following a few interesting procedures from the literature,²⁷⁸ we examined the preparation of **158** through a derivative such as the chloro analogue **164** which would allegedly be more reactive with thiourea (*Scheme 59*). Surprisingly, every attempt to obtain compound **164** (using thionyl chloride and chloroacetyl chloride at low temperatures and diluted conditions) instead formed the isomer **165**, which was identified via NMR and mass spectrometry analysis. The product may be forming due to a rapid isomerisation of the enol **161** to the more stable enol **162**, which cyclised into an unstable chloro-cyclobutene intermediate and rapidly ring-opening to form the product **165**.



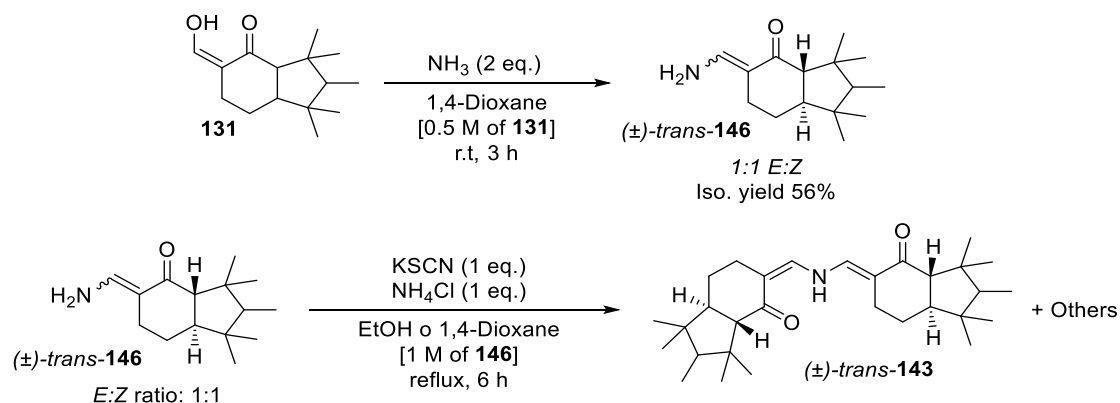
Scheme 59. Attempted synthesis of compound **164** from **131**. The "Cl" is derived from the SOCl_2 or chloroacetyl chloride. A proposed mechanism for the generation of product **165** is depicted in grey.

Since the first synthesis to the intermediate **158** was ineffective, we considered to venture an alternative preparation. The route consists of forming the 3-amino-enone compound **146** which reacts with potassium thiocyanate and ammonium chloride to obtain the enaminone **158** (*Scheme 60*).



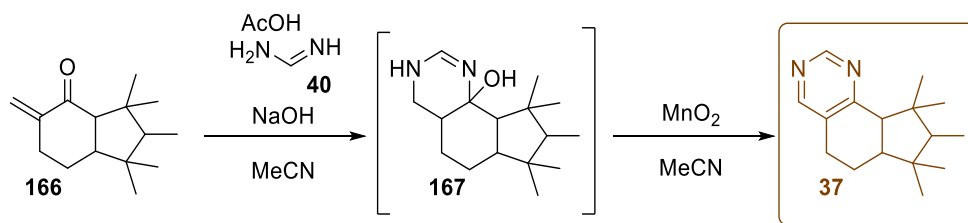
Scheme 60. Proposed alternative pathway to **155c** via the 3-amino-enone **146**.

Hence, the compound **146** was prepared from **131** using an ammonia solution in 1,4-dioxane. (*Scheme 61*). The thiocyanate addition and cyclisation experiment was carried out in two different solvents: EtOH and 1,4-dioxane. Sadly, both of the trails ended in a mixture of different compounds where the main product could be identified as the dimer **143**.



Scheme 61. Reaction conditions for the preparation of the 3-amino-enone **146** and attempt of the preparation of **155c**.

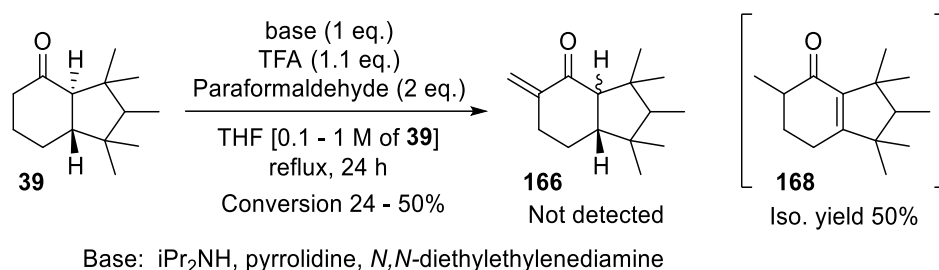
A dihydropyrimidine system had been prepared from α,β -unsaturated ketones by Shibata and Funabiki *et al.* in 1999.²⁷⁹ Following this procedure, a strategy was elaborated where an *exo*-methylene compound **166** was prepared to obtain the pyrimidine precursor **167**, which would gain Ambertonic™ (**37**) after a dehydration-oxidation step (*Scheme 62*).



Scheme 62. Synthetic strategy for the synthesis of Ambertonic™ starting from the *exo*-olefin **166**.

Hence, a screening for the preparation of the *exo*-ene compound **166** was carried out. The procedures for α -methylenation are miscellaneous and described on many different

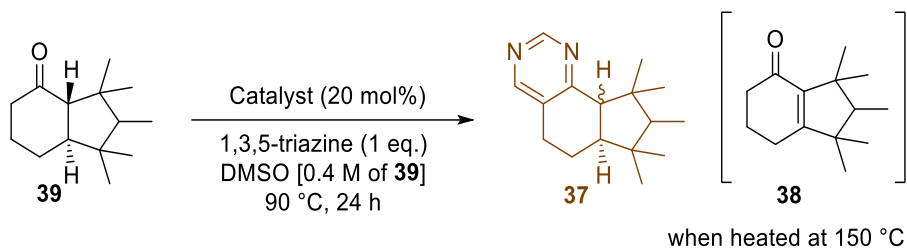
substrates.^{280–284} We decided to focus on a catalytic approach using triflate ammonium salts which would enable the process to be as efficient as possible and less hazardous through the use of paraformaldehyde instead of the aqueous solution.²⁸⁰ Unfortunately, the screening of different amines did not lead to higher conversions than 50% and the main product isolated in traces was the rearranged compound **168** in 50% yield (*Scheme 63*). We allegedly propose a similar mechanism to the one depicted in *Scheme 59* for such rearrangement.



Scheme 63. Attempts of methylenation of starting material **39** which mainly lead to compound **168**.

Having experienced difficulties in efficiently forming intermediates of **39**, it was considered valuable to investigate the pyrimidine ring formation directly starting from starting material **39**. As an example, several *electron-inverse-demand Hetero-Diels-Alder* reactions between ketones and 1,3,5-triazine have been used to obtain pyrimidine rings.^{285,286} The reaction conditions were therefore reproduced using substrate **39** (*Table 26*). Unfortunately, the first attempt performed using the reported highest performing catalyst (prolinamide) did not furnish any of the desired species **37**, instead it only resulted in its oxidation to Cashmeran (**38**) at the higher temperatures (*Table 26, Entry 1*). Changing the catalyst to pyrrolidine a slight improvement was noticed (*Table 26, Entry 2*). Using other bases such as morpholine and benzylamine did not result in any better results (*Table 26, Entries 3 – 4*). As can be seen in *Figure 39*, the main component of all the crude mixtures remains compound **39**. A test experiment to validate the general conditions using cyclohexane as the substrate was also carried out and was shown to successfully form the pyrimidine ring structure in good conversion (50%) as described in literature. The outcomes may suggest the carbonyl group of compound **39** is less reactive.

Table 26. Attempts to perform *electron-inverse-demand Hetero-Diels-Alder* reaction and the catalysts screened.



Entry ^a	Catalyst	Conv. 37 (%) ^b
1	prolinamide	-
2	pyrrolidine	6
3	morpholine	-
4	benzylamine	-

^a The experiments were carried out on 2 mmol scale; ^b Based on ¹H-NMR spectra employing dimethyl fumarate as internal standard.

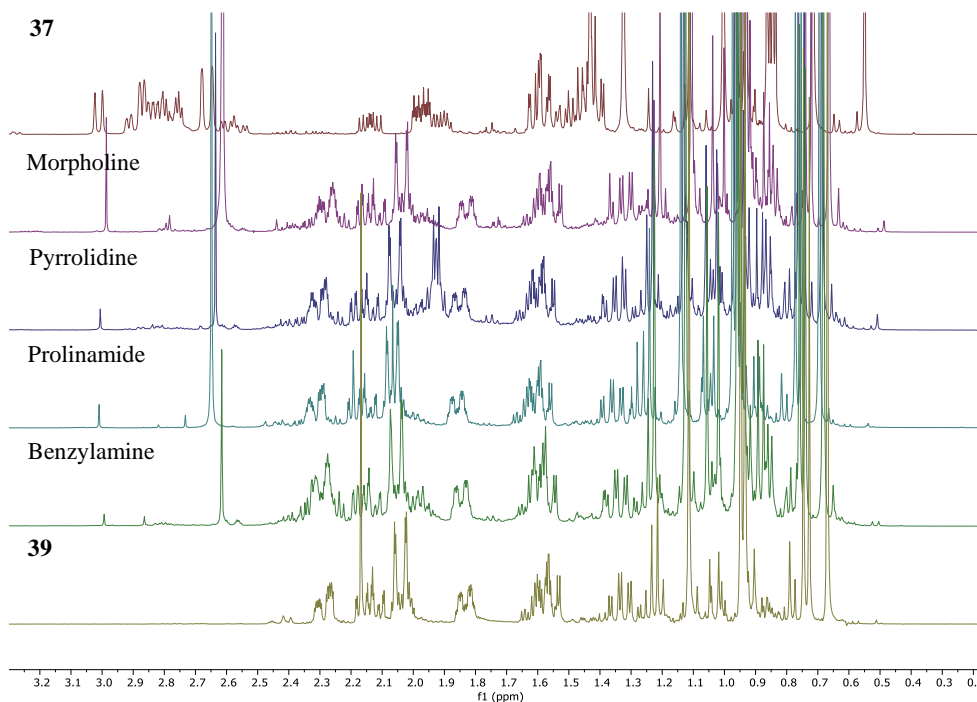
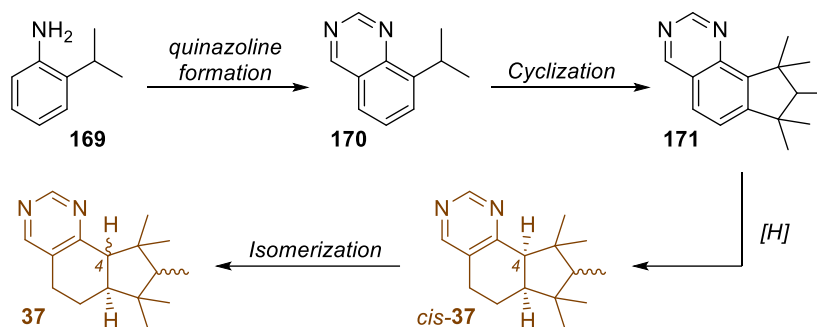


Figure 39. ¹H-NMR spectra of the reaction mixture using different amines compared with **39** and Ambertonic™ (**37**).

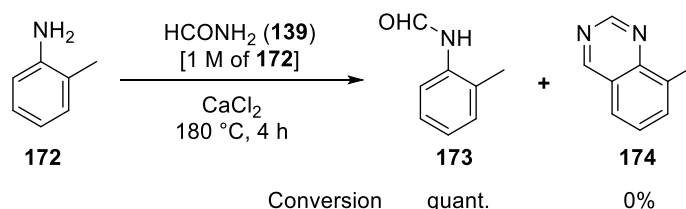
2.2.2.2. Changing the starting material

Having explored possible routes from dihydro-cashmeran **39**, we evaluated a synthetic preparation commencing from an entirely different and simplified starting material. We proposed the use of readily available 2-isopropylaniline (**169**) where the isopropyl group could be exploited for the construction of the indane ring and the amino group as a constituent of the pyrimidine moiety (*Scheme 64*).^{287,288}



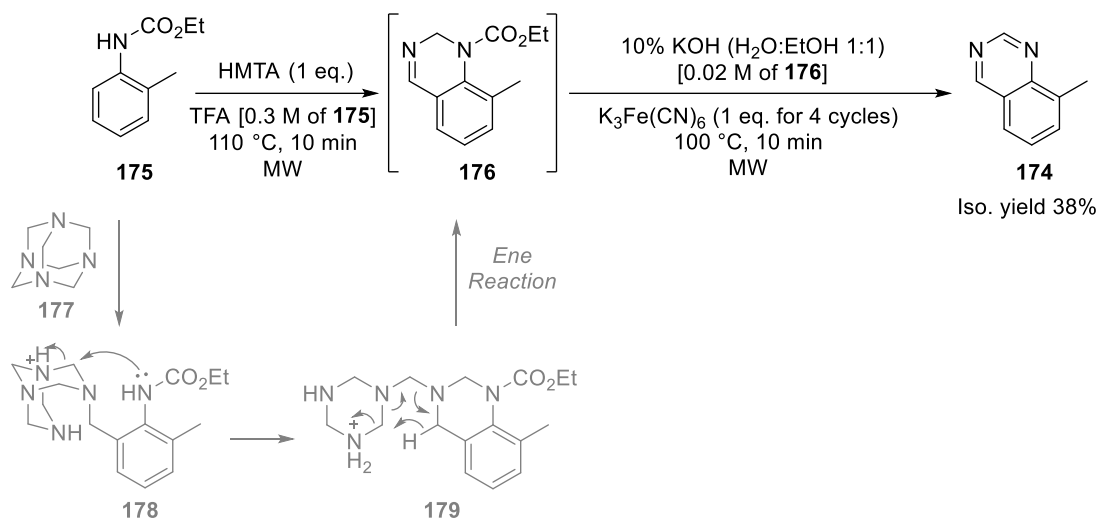
Scheme 64. Proposed synthetic strategy starting from 2-isopropylaniline (**169**).

Very few examples of quinazoline preparation methods based upon 2-substituted anilines have been reported in literature.^{289–292} We thus commenced on a screening program of reaction conditions to evaluate the quinazoline ring formation. However, due to the temporary unavailability of aniline **169**, *o*-toluidine (**172**) was instead employed. We therefore assessed a possible formation of the quinazoline scaffold **174** using a cited Brederick set of conditions (section 2.2.1.2),^{252,293} however, under these conditions only the *N*-formylation was obtained (*Scheme 65*).



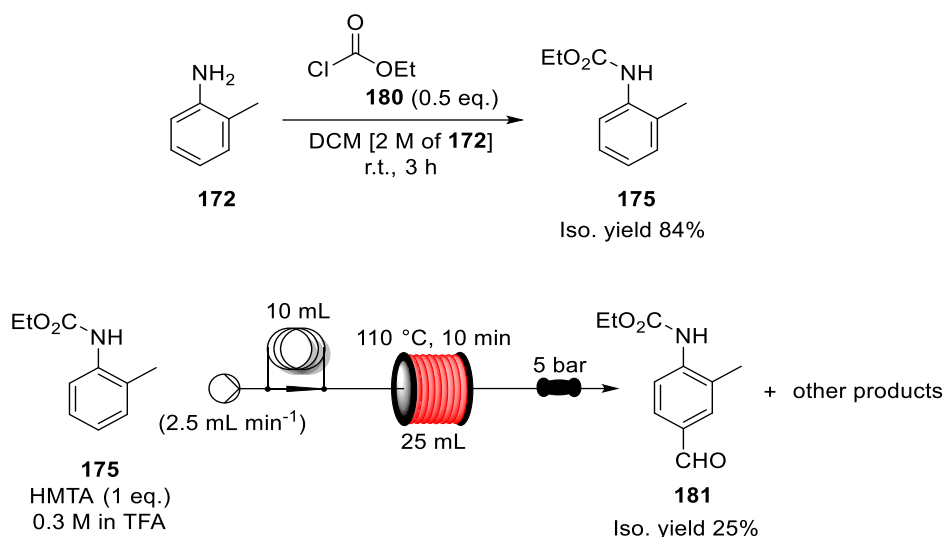
Scheme 65. Attempted quinazoline **174** formation under Brederick conditions. Conversion based on $^1\text{H-NMR}$ spectra employing dimethyl fumarate as internal standard.

We then opted to test a literature method reported by Zanatta *et al.* The methodology starts from the synthesis of the ethyl carbamate intermediate **175** (Scheme 66).^{289,290} The authors proposed an initial acid-mediated *ortho*-formylation to form the intermediate **179** which then transforms into the dihydro-quinazoline compound **176** via an ene reaction. The method had been already applied on the aniline **172** reporting a 38% isolated yield.



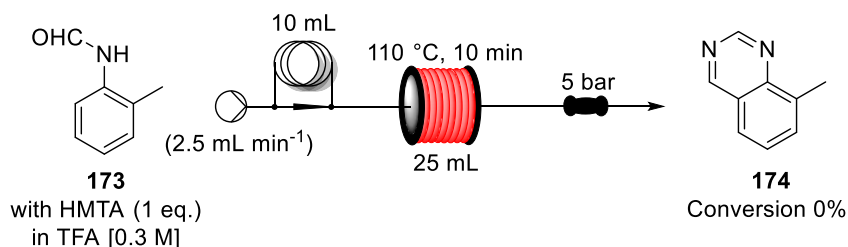
Scheme 66. Reaction conditions for the formation of quinazoline **174** following the literature of Zanatta *et al.* (black). The proposed mechanism is also depicted in grey.

Based on the reported procedure, we first prepared the *N*-protected intermediate **175** through condensation with ethyl chloroformate (**180**). With quantities of compound **175** in hand, the subsequent step was attempted in a PTFE coil flow reactor instead of exploiting the microwave reactor as indicated in the literature (Scheme 67) as it was thought it could be an interesting example of a continuous system for the formation of pyrimidine rings. The reaction was performed at different temperatures (90 – 100 – 110 °C) and different residence times (10 – 30 – 60 minutes). At temperatures below 110 °C only starting material was recovered whereas at 110 °C a complex mixture was obtained where the *para*-formylation product **181** was isolated as a major product.



Scheme 67. Attempted preparation of quinazoline **174** exploiting flow apparatus.

These outcomes were attributed to the steric hindrance at the *ortho*-position with respect to the *para*-position. Considering the proposed mechanism of the reaction, it was meaningful to attempt the cyclisation using the formyl group rather than the designated carbamate group in **175**. Unfortunately, compound **173** reacted under the Zanatta conditions brought about a complex mixture where no desired product could be detected (*Scheme 68*).



Scheme 68. Attempted synthesis of quinazoline **174** from the formyl amide **173**.

2.2.3. X-Ray structure of Ambertonic™ and the nature of its “selective” configuration

Along with being able to optimise a preparative method for the targeted fragrance Ambertonic™ (**37**), we were also able to obtain an SCXRD structure. After performing several attempts at

crystallisation on the *cis/trans* mixture, we decided to purify the mixture via flash chromatography. To our delight, we were able to isolate a single crystal suitable for the purpose and confirm the presence of the pyrimidine ring and the relative configuration as *anti* between the protons at C-6 and C-2 (*Figure 40*).

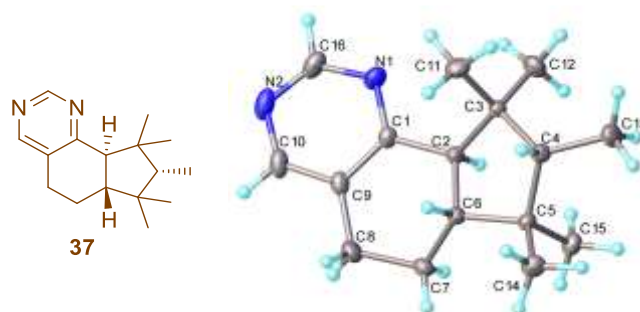
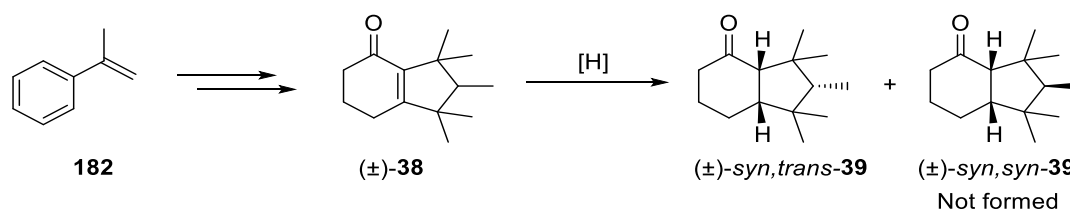


Figure 40. Single crystal X-ray structure of the *trans*-isomer of Ambertonic™.

Additional information can also be extracted from the 3-D structure regarding the relative *syn* configuration between the protons in the C-6 and C-4 positions. Taking into account that the proton in C-2 can be easily epimerised, the latter configuration gives us key information on the selectivity of the previous hydrogenation step which forms the intermediate **39** (*Scheme 69*).



Scheme 69. The key intermediate **39** is synthesised from Cashmeran (**38**) via hydrogenation.

As mentioned, dihydro-cashmeran (**39**) is prepared from catalytic hydrogenation of Cashmeran (**38**), a musky odorant patented by IFF in 1973.²⁹⁴ The symmetry of the starting material implies the two faces are diastereotopic and therefore two pairs of diastereoisomers (*syn,trans-39* and *syn,syn-39*) could be formed. However, only the *syn,trans* pair seems to be forming. This *trans*-selectivity appears to derive from a spatial rearrangement of the methyl C-13 on the cyclopentane ring as shown in *Figure 41*. The SCXRD structure of **38** shows a propensity for

the methyl C-13 to sit in an equatorial-like position and, therefore, contorts the ring so that the vicinal methyl groups (C-11, C-14) on the *Si* face are positioned closer to the double bond than the methyl groups on the *Re* face (C-12, C-15).

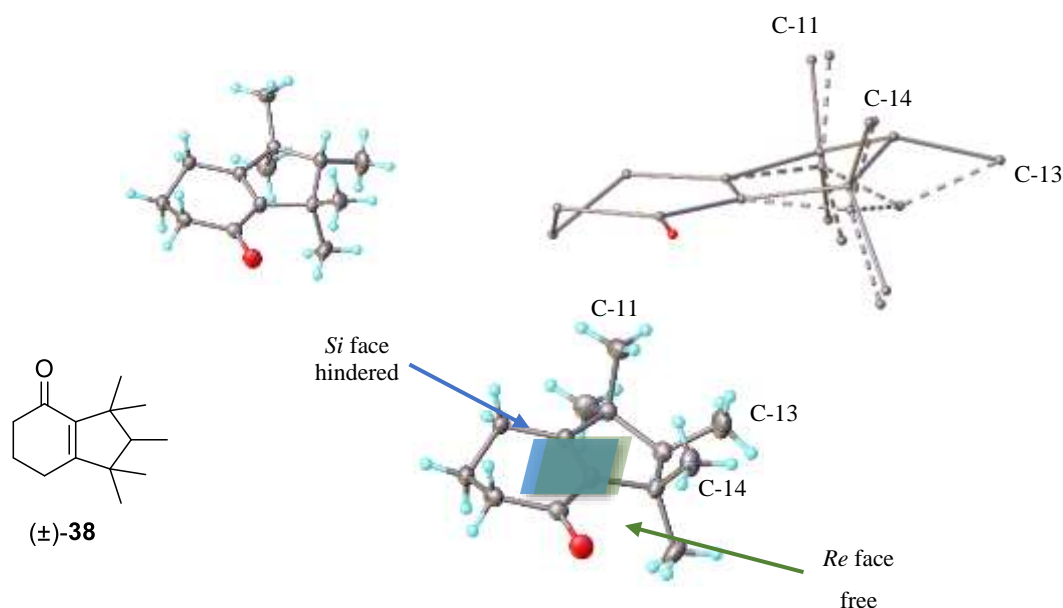


Figure 41. Single crystal X-Ray structure of Cashmeran (**38**). It can be noticed the momentous role the methyl C-13 plays in settling the shape of the cyclopentane ring.

DFT-based computational studies performed by Prof. Fernando P. Cossío *et al.* also confirmed the different energetic barrier for the addition of the hydrogen on the two faces which seem to be enough to explain the selectivity.²⁹⁵

2.2.4. Resolution and characterisation of the enantiomers

As very little information has previously been gathered regarding the olfactory property of the main *cis/trans* products, IFF and ourselves were also interested in performing an enantiomeric resolution of the main *trans* isomer of Ambertonic™. After first screening different solvent conditions, we managed to perform a successful chiral LC separation (Instrument: PerkinElmer Series 200 with diode array detector (DAD) at 254 nm; Column: Daicel ChiralPak IA 250 x 4.6 mm; Eluent: 98% cyclohexane: 2% dichloromethane; Flowrate: 0.8 mL/min) and obtained the enantiomers **37-A** and **37-B**, called as such for their order of elution. To characterise the

two enantiomers, we decided to acquire a Circular Dichroism (CD) spectra. The spectra were recorded on a 3×10^{-3} M solution of **37-A** and **B** in chloroform (*Figure 42*).

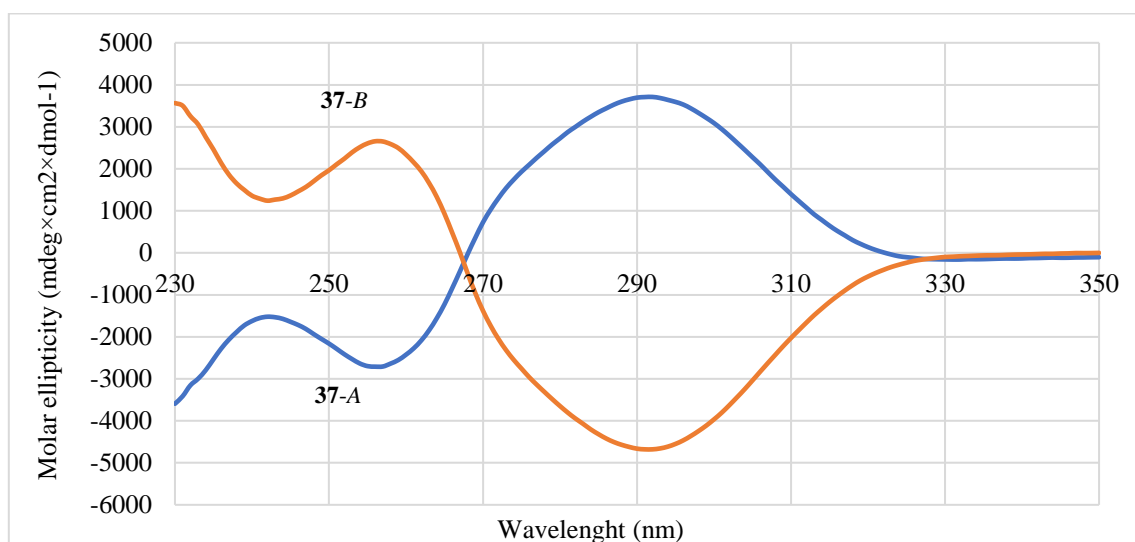
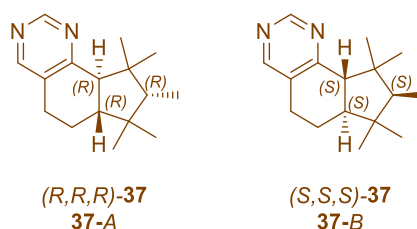


Figure 42. CD spectra acquired for the two enantiomers **37-A** and **37-B**.

It is described in the literature that it is possible to determine the absolute configuration of a chiral compound by comparing the experimental data with that obtained via DFT calculations.^{296–298} With the assistance of Prof. Fernando P. Cossío *et al.*, a time dependent-DFT single-point calculations on the optimised structures of the two enantiomers was carried out by means of the Gaussian 09 software, and these calculations allowed to compute the CD spectra of both enantiomers.²⁹⁵ By comparison of the CD computational and experimental spectra, the enantiomer isolated **37-A** was found to correspond to a configuration (*R,R,R*), whereas, **37-B** matches with the molecule (*S,S,S*)-**37** (*Scheme 70*).



Scheme 70. Assessment of the absolute configuration for the two enantiomers isolated of *trans*-Ambertonic™.

Unfortunately, evaluation of the olfactory properties carried out by the IFF through a GC-sniff apparatus revealed only a slight difference in olfactory strength between the two enantiomers, however with no significant difference in their odour profile when compared with the original mixture.

2.2.5. *Summary and Conclusions*

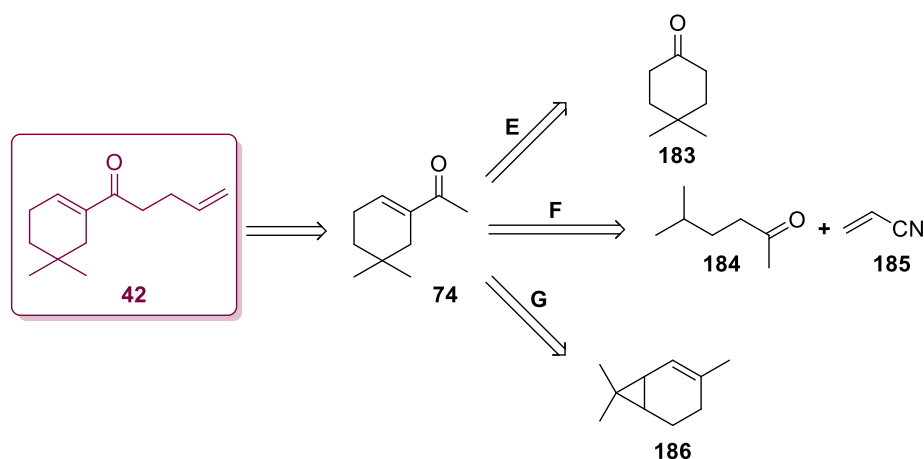
During our studies, five different routes to Ambertonic™ (**37**) were designed and explored in the laboratory; four (section 2.2.1 – 2.2.2.1) of which started from an advanced derivative Cashmeran (**38**) and one from a simple aniline building block (section 2.2.2.2). The investigations have generated a lot of knowledge on the chemical reactivity of precursor **39**. For instance, the formylation of compound **39** initially failed to go to completion due to the existence of an equilibrium between the starting material **39** and the final product **131**. This may be due to a higher thermodynamic stability of the former, i.e. compound **39**. Such problems were finally solved by employing different solvents to shift the reaction equilibrium and reduce the amount of unreacted material **39**. Meanwhile, the formyl-dihydro-cashmeran **131** was employed to examine possible cyclisation conditions. After several different attempts, we were able to design an efficient methodology based on a publication by Bredereck *et al.* This procedure allowed us to isolate the final material in 66% yield when temperature and reaction times were properly adjusted (180 °C & 4 h). Due to the reaction kinetics, the step was also investigated under continuous-flow conditions employing a stainless steel coil reactor, however the desired product was only obtained in low yield. Following further detailed investigation of the process, we managed to develop a one-pot, two step, methodology starting from material **39** and enabling isolation of the final target in 53 – 58% with a *trans/cis* ratio of 6:4. The quality of the final material was found to be highly dependent on the amount of unreacted material left after the first formylation step, as the latter could then form a by-product difficult to separate from the final Ambertonic™ (**37**). The optimised methodology was further exploited on Cashmeran (**38**) as the starting material for the preparation of a similar derivative named Sinfonide (**153**) isolated in 51% yield.

Further investigations have discovered the nature of the relative *anti*-configuration between the methyl group and the proton at position C-4 (See *Figure 40*), which is due to a stereoselective

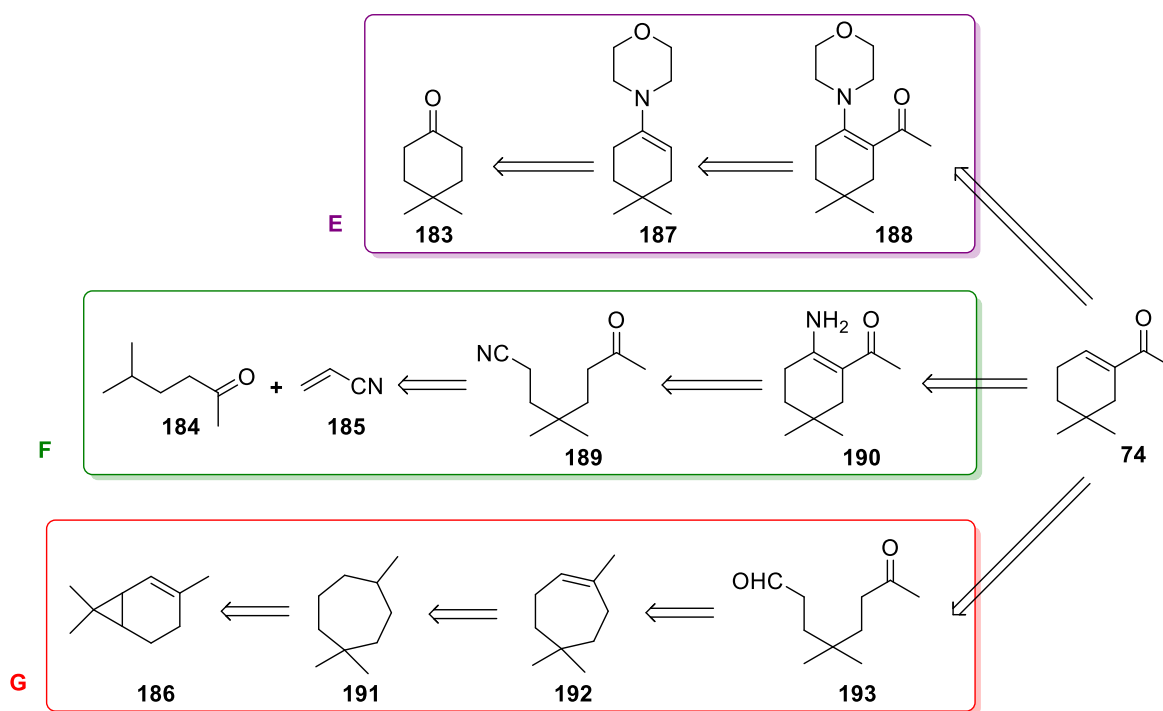
hydrogenation of Cashmeran (**38**) to the intermediate **39**. A separation of the racemic *trans*-configured Ambertonic™ to its two enantiomers was performed to investigate a possible difference in olfactory properties from the *cis/trans* mixture, however, no significant difference was revealed between the two enantiomers and the mixture based upon IFF testing.

2.3. Galbascone

Three new routes to Galbascone (**42**) were conceived during the project (*Scheme 71*). The strategies were designed to converge on the key intermediate, the dehydroherbac (**74**). The raw materials for these proposed retrosynthetic strategies are acrylonitrile (**185**), 4,4-dimethylcyclohexanone (**183**), 5-methyl-hexan-2-one (**184**), and 3-carene (**186**), all of which are widely available building blocks.

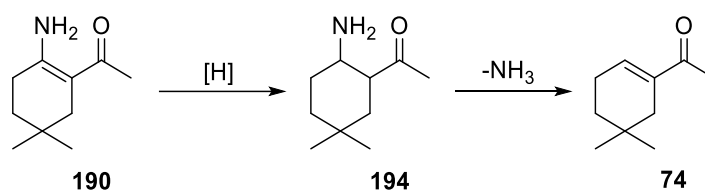


Scheme 71: Proposed retrosynthetic pathways for *de novo* synthesis of Galbascone (**42**).



Scheme 72. Potential retrosyntheses for the synthesis of key intermediate **74**.

As can be seen from the *Scheme 72*, all routes start from different basic raw materials and require different types of chemistry. Routes E and F have not quite - similar intermediates (**188** & **190**) undergoing a de-amination process to furnish the unsaturated ketone **74**. The latter procedure depicted in *Scheme 73* consists of an enamine hydrogenation (**190** → **194**) followed by an elimination of the amine (**194** → **74**).

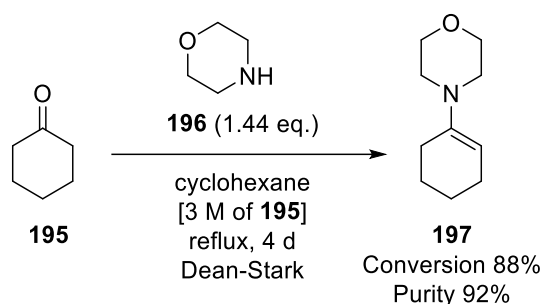


Scheme 73. De-amination process from intermediate **190** to the unsaturated ketone **74**.

2.3.1. Galbascone from 4,4-dimethylcyclohexanone (183): Route E

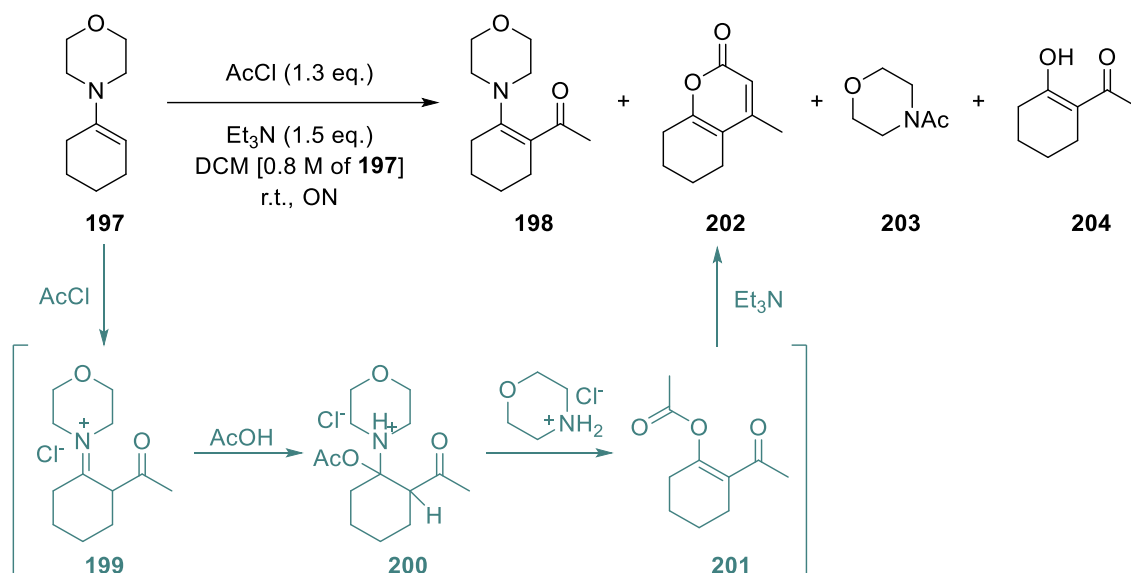
The preparative route E starting from 4,4-dimethylcyclohexanone (**183**) first involves the formation of enamine derivative **187**, which can be acetylated to form the enamionone **188** (Scheme 72). The intermediate can then undergo de-amination to form the unsaturated ketone **74**. Due to laboratory availability, it was decided to first establish the conditions employing cyclohexanone (**195**) as starting material instead of the more expensive material **183**.

Consequently, the representative enamine **197** was prepared from ketone **195** and morpholine (**196**) in cyclohexane employing a Dean-Stark apparatus for the azeotropic removal of water. After 4 days under reflux, the intermediate **197** was obtained in 88% yield and 92% purity where the remaining part was starting material **195** (Scheme 74).



Scheme 74. Preparation of the enamine **197** from cyclohexanone (**195**) and morpholine (**196**). Conversion based on $^1\text{H-NMR}$ spectra employing 1,2-dimethoxybenzene as internal standard.

Having quantities of enamine **197** in hand, the acetylation to form enamionone **198** was attempted. The procedure followed was modified from the work of Tunoglu *et al.* (Scheme 75).²⁹⁹ A solution of **197** in dichloromethane (DCM) was treated with acetyl chloride allowing the temperature to rise to 35 – 40 °C. After 18 hours of stirring at room temperature, the crude mixture was analysed via LC-MS (ESI) and $^1\text{H-NMR}$ spectra and gave indication of the formation of the desired material **198**.

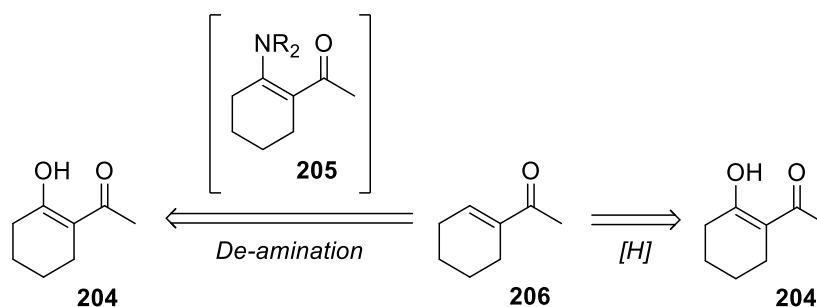


Scheme 75. Attempted acetylation of compound **197** to prepare enaminone **198**.

The mixture was then divided into 3 separate batches to evaluate the purification step. We firstly attempted vacuum distillation (170 °C and 7 mbar) but only the *N*-acetyl-morpholine (**203**) and the 2-acyl-cyclohexanone (**204**) were isolated but unfortunately as a 1:1 mixture. A second distillation under lower pressure and temperature (50 °C and 0.5 mbar) produced the same mixture 1:1 **203:204** of distillate. Finally, the third batch was purified through chromatography using triethylamine-deactivated silica enabling the isolation of compound **204** (18%_{w/w} of the crude) and the 4-methyl-tetrahydrocumarin (**202**) (9%_{w/w} of crude). Based on such ratios, we could speculate the reaction yields the compounds **204** and **202** in respectively 25% and 10%. The formation of **202** may be attributed to the high water content in the reaction which allow for acetic acid in the system. The proposed mechanism for the formation of **202** is depicted in *Scheme 75*. The acetic acid reacts with the iminium **199** forming intermediate **200**, and ultimately generating the *O*-acetyl compound **201**. The latter may then cyclise to compound **202** through base-catalysed condensation. Consequently, it was decided to prepare the 1,3-diketone **204** via the same methodology, however hydrolysing the enaminone intermediate **198** after acetylation. Once hydrolysed and purified, compound **204** was isolated in 67% yield. The experiment was carried out twice, and was found to be highly reproducible. In light of these results, the failing of the former preparation may be attributed to either a high

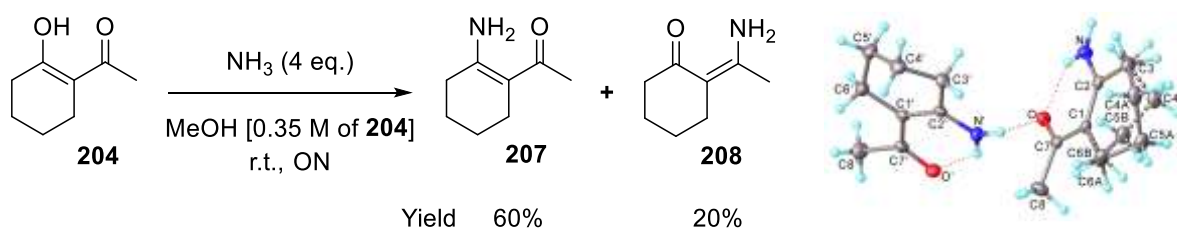
level of residual water in the reaction or decomposition during the isolation probably due to the presence of other impurities (triethylamine & acetic acid).

Two main strategies could be applied to synthesise the desired α,β -unsaturated ketone **206** from the 1,3-dicarbonyl compound **204** (*Scheme 76*): the direct reduction of the carbonyl, and the foregoing described de-amination (section 2.3). In both approaches, the main issue is achieving an high selectivity for nucleophilic addition on the dicarbonyl system.



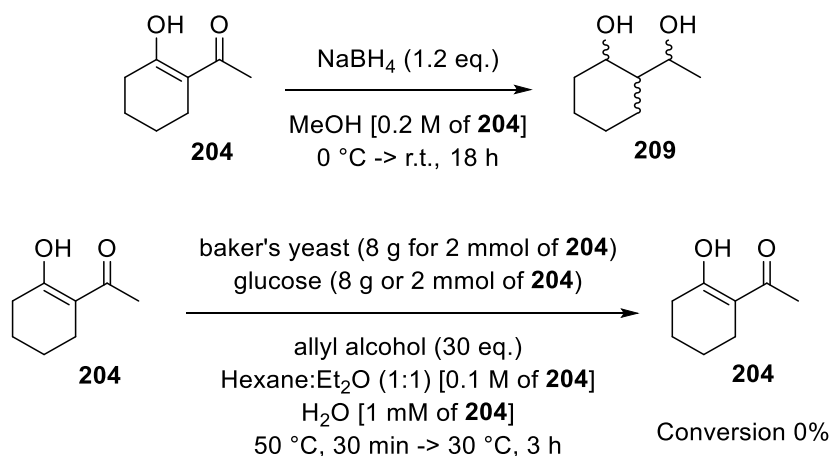
Scheme 76. Proposed strategies for the synthesis of the α,β -unsaturated ketone **206**.

We therefore attempted direct amination with ammonia on compound **204** and, pleasingly, the desired material **207** was isolated in 60% yield along with 20% of the alternative addition product **208** (*Scheme 77*). The two isomers were identified through 2D-NMR spectra and obtaining a SCXRD structures of **207** and **208**.



Scheme 77. Reaction conditions for the preparation of the enaminone **207**. On right hand side is depicted the SCXRD structure of the desired material **207**. SCXRD of compound **208** depicted in experimental part.

Having both compounds **204** and **207** in hand, we next attempted the reduction step. Firstly, we attempted a selective reduction of the di-carbonyl **204** employing sodium borohydride and baker's yeast (*Scheme 78*). When one equivalent of sodium borohydride was added in the methanolic solution of **204**, the reduction was found sluggish and unselective and only fully reduced material **209** was detected by LC-MS (ESI) after 24 hours (*Figure 43*). The addition of a further equivalent of sodium borohydride generated a complex mixture containing only fully reduced compounds as evidenced by the ^{13}C -NMR spectra which did not show any signal around 200 ppm. Due to the complexity of the mixture, no further investigations were performed to isolate the compounds **206**. When employing the baker's yeast-based reduction developed by Yusufoglu *et al.*, no reaction occurred (*Scheme 78*).³⁰⁰



Scheme 78. Reaction conditions attempted for the selective reduction of compound **204** to the desired material **206**.

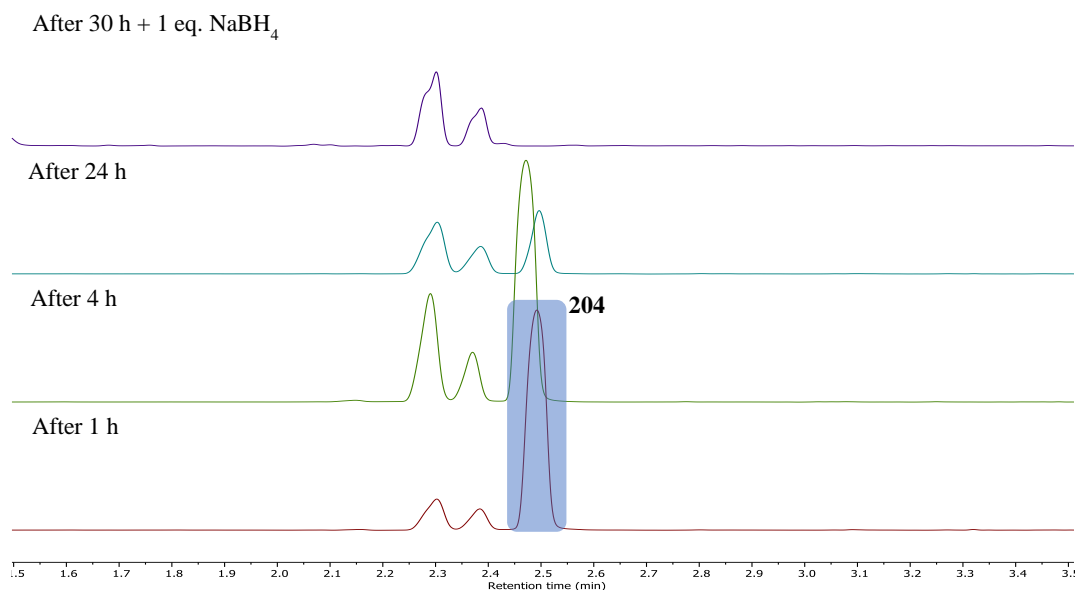
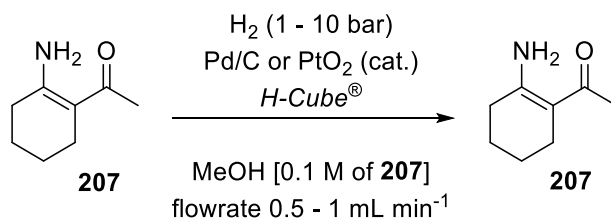


Figure 43. LC-Chromatogram monitoring the reaction mixture for the reduction of **204** using sodium borohydride as reducing agent. The peak highlighted in the blue area represents 1,3-diketone compound **204**.

We then elected to examine the reduction of enaminone **207**, following a literature article described by Zhang and co-workers.²⁹⁹ Reduction with two different catalysts (Adam's catalyst and Pd/C) were investigated under different reaction conditions (up to 50 °C and 10 bar) employing the H-Cube[®] apparatus. Unfortunately, these experiments showed no conversion of starting material **207** (Scheme 79).

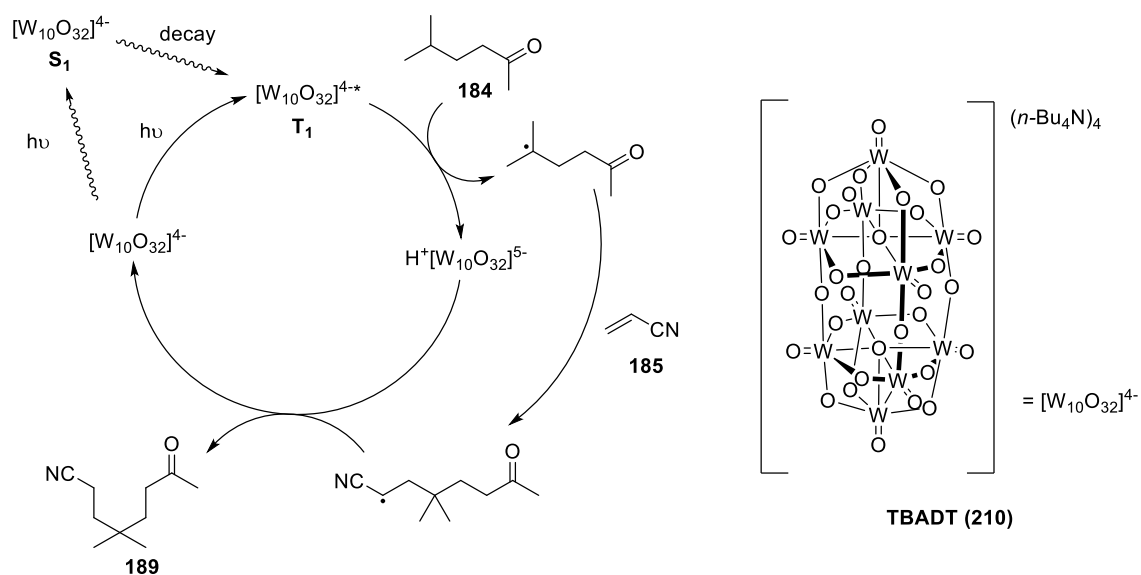


Scheme 79. Reaction conditions for the reduction of enaminone **207**.

2.3.2. Galbascone from 5-methyl-hexan-2-one and acrylonitrile: Route F

This particular synthetic strategy relies on a photocatalysed CH-activation reaction as described by Fagnoni, Ryu and co-workers.^{301,302} The reaction consists of a Hydrogen Atom Transfer (HAT) induced by a photocatalyst (PC) in its excited reactive state.^{303–305} In this example, tetrabutylammonium decatungstate (TBADT) was employed as PC.³⁰⁶ The mechanism of the reaction is depicted in *Scheme 80*. The light absorption process occurring to the decatungstate anion creates an excited singlet state (S_1), which rapidly decays to a lower-energy triplet state (T_1). Once in the T_1 state, the PC oxidises the substrate through hydrogen abstraction. In the example of 5-methyl-hexan-2-one (**184**), the γ -abstraction is favourable as its transition state favours the formation of the most stable 3° radical. The secondary substrate acrylonitrile (**185**) acts as radical acceptor forming a new resonance stabilised radical intermediate which then undergoes hydrogen abstraction regenerating the PC.

Continuous-flow photoreactions have been widely described in the literature as the high surface-to-volume ratio provided by the flow system permits very efficient irradiation compared to a batch-mode setup, therefore reducing reaction time and improving selectivity.^{307,308}

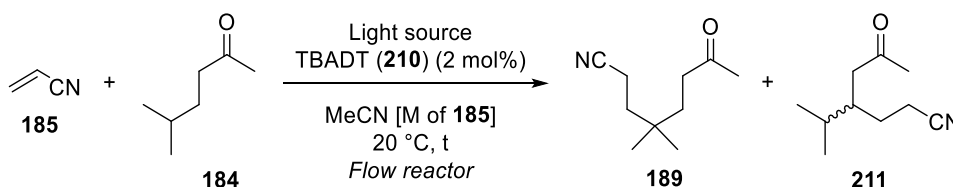


Scheme 80. Literature mechanism for hydrogen atom transfer reaction between **184** and **185** catalysed by TBADT.

The first step of the synthesis was performed following a flow setup described by Fagnoni, Ravelli and co-workers.³⁰⁹ A 0.1 M solution of ketone **184** (10 eq.), **185** (1 eq.), and TBADT **210** (2 mol%) in acetonitrile (MeCN) was pumped through a 10 mL perfluoroalkoxy alkane (PFA) coil reactor irradiated by a 125 W medium pressure Hg Lamp. The acetonitrile as solvent was employed to solubilise the photocatalyst which is otherwise insoluble in the ketone **184**.

As shown in *Table 27*, several setups were investigated to increase the efficiency and boost productivity. It was observed that increasing the amount of ketone **184** effects the efficiency of the process more than prolonging the reaction times (*Table 27, Entries 1 – 4*). To increase the productivity, the minimum amount of solvent was employed (0.38 M) reducing the conversions to 46% (*Table 27, Entry 5*). To our delight, changing the light source to a 62 W LED 365 nm increases the efficiency to 74% conversion (*Table 27, Entry 6*). This result may be due to a high intensity output on the wavelength that activates the PC (16W radiant power). A scale-up of the reaction allowed to concentrate the solution further to 0.48 M (*Table 27, Entry 7*) yielding **189** in 63% isolated yield (productivity = 630 mg h⁻¹) however, after purification, the desired material **189** was discovered to be in a mixture 95:5 with its β -abstraction product **211**. It should be noted though that the excess ketone **184** can be recovered via distillation.

Table 27. Screening of reaction conditions for the preparation of **189** in flow.

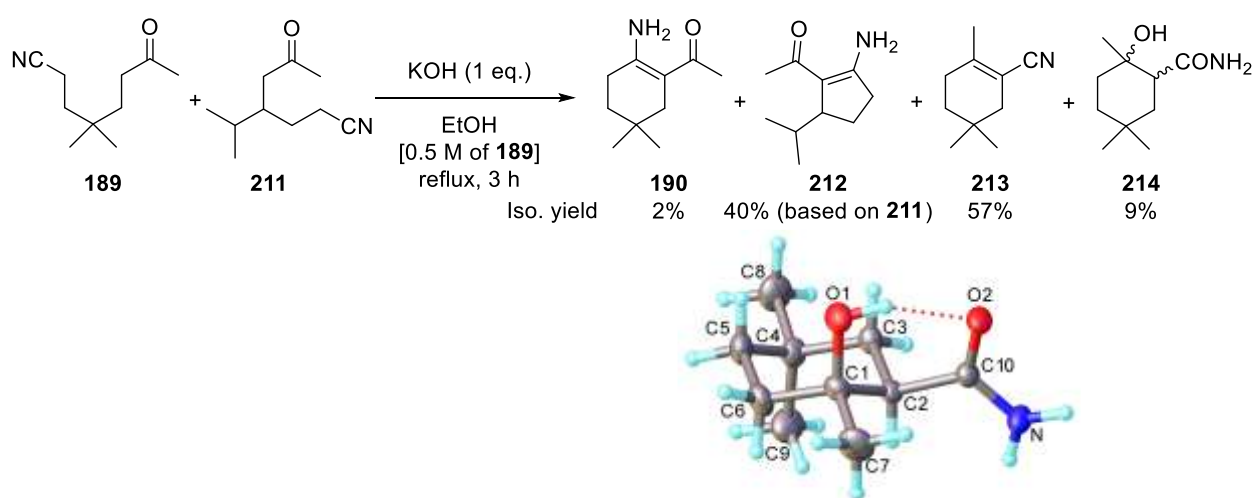


Entry ^a	Eq. 184	[M]	Rt (min)	Light source	Conv. 189 (%) ^b
1	5	0.1	24	125 W Hg lamp	23
2	5	0.1	48	125 W Hg lamp	30
3	10	0.1	24	125 W Hg lamp	40
4	10	0.1	48	125 W Hg lamp	55
5	10	0.38	48	125 W Hg lamp	46
6	10	0.38	48	62 W LED 365 nm	74
7 ^c	10	0.48	48	62 W LED 365 nm	63 ^d

^aThe experiments were carried out on 5 mmol scale;^bConversions based on ¹H NMR spectra employing 1,2-dimethoxybenzene as internal standard;^c The experiment was performed on 40 mmol scale;^d Isolated as a mixture 95:5 **189:211**.

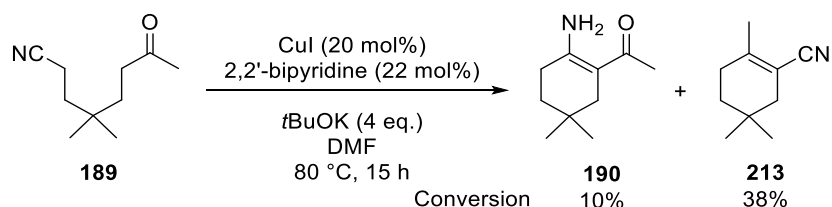
Having access to compound **189**, the subsequent planned Thorpe-Ziegler cyclisation was investigated. Nucleophilic attacks on the nitrile groups are not that common as they are not good electrophiles. For these reasons, Lewis acids based upon copper,^{310,311} nickel,^{312,313} rhenium,³¹⁴ and zinc^{315–317} have been employed to facilitate the attack. In addition, Rukavishnikov *et al.* had described a base-driven cyclisation on a similar substrate to yield 5-membered ring enamines.³¹⁸

The experiment was initially monitored using LC-MS (ESI) and several peaks appeared during the reaction. After purification over silica gel, the desired material **190** was found, although in only traces (20 mg from a 6 mmol amount of **189**). The major product isolated was **213** which forms via α -deprotonation of the nitrile and electrophilic attack on the carbonyl group. Over time, the compound **213** hydrolyses to yield the amide **214**, which was also isolated and characterised including by SCXRD (structure shown in *Scheme 81*). From the chromatographic separation, enaminone **212** was also isolated and it was discovered to be forming within the first 15 minutes of the reaction as Rukavishnikov *et al.* describes in their article.³¹¹



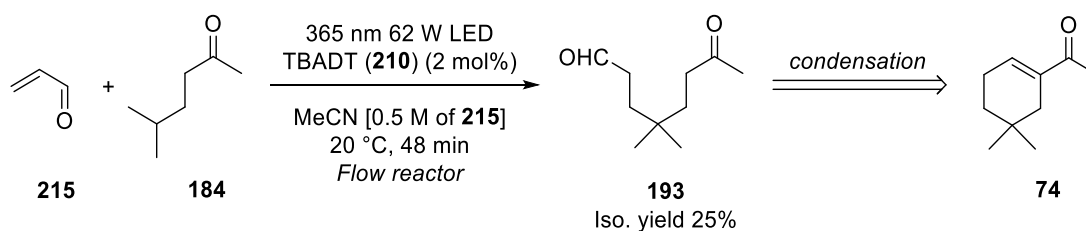
Scheme 81. Reaction conditions and products isolated from the attempt to synthesis **190** employing Rukavishnikov's methodology.³¹¹ SCXRD structure of compound **214** is herein depicted.

Attempts to use a stronger base such as *t*BuOK was found to increase the conversions to the by-product **213** (55%). To increase the enol-to-nitrile attack, we decided to investigate a copper-catalysed process as published by Yamamoto, Bao, Yu, and co-workers in 2013 (*Scheme 82*).³¹⁰ The methodology notably improved the yield of **190** (10%), however the by-product **213** remains the main material (38%).



Scheme 82. Reaction conditions for the keto-nitrile cyclisation of **189** to the enaminone **190**. Conversion based on ¹H-NMR employing 1,2-dimethoxybenzene as internal standard.

As the ketone **189** proved challenging to cyclise as desired, we decided to explore different radical acceptors. For instance, we envisioned acrolein as a potential candidate since the obtained product **193** would be only one-step away from dehydroherbac **74** (*Scheme 83*). Applying the optimal conditions previously found for compound **189**, we carried out the photo-catalysed reaction. The latter yielded a mixture of different materials where only the desired compound **193** was identified and isolated in 25%.

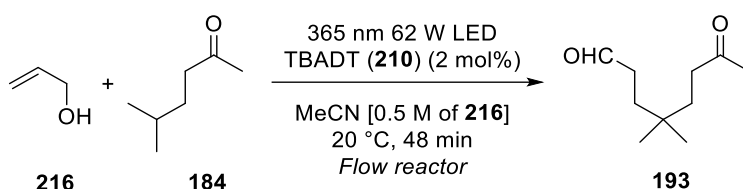


Scheme 83. Reaction conditions for the preparation of intermediate **193** from acrolein **215**.

To avoid the use of acrolein as a toxic substrate, allyl alcohol (**216**) was instead investigated as potential precursor. As can be seen from *Table 28*, when the experiment was carried out, the product **193** was detected in 1.4% (*Table 28, Entry 1*). The formation of **193** could be attributed

to an oxidation of the alcohol groups by oxygen. In fact, enriching the amount of oxygen in the solution, the conversion of **193** doubled (*Table 28, Entry 2*).

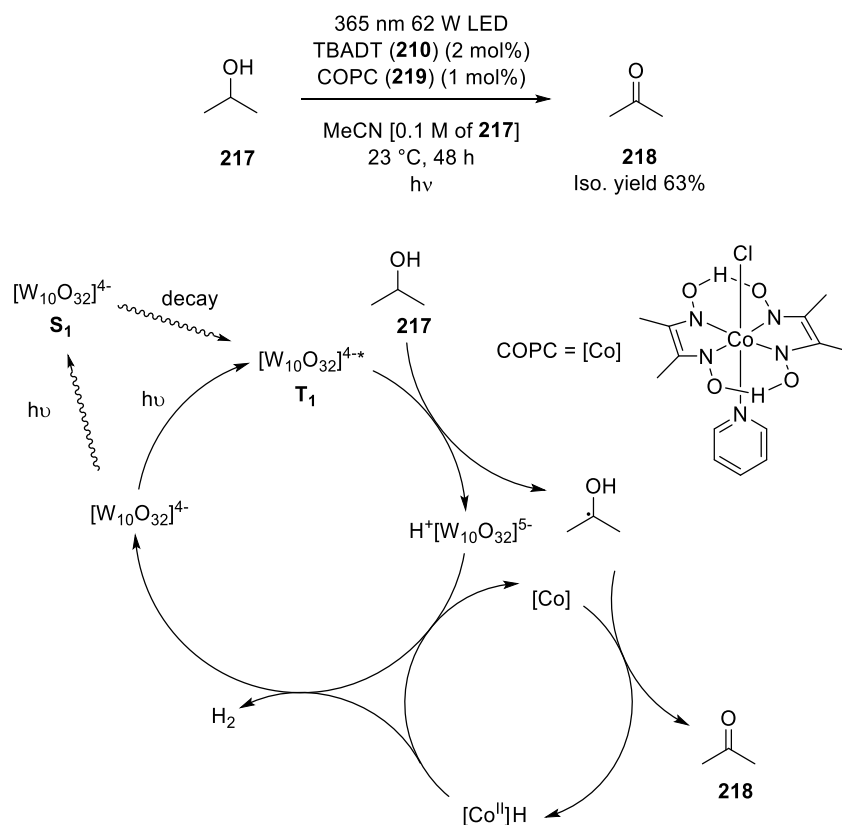
Table 28. Alternative reaction conditions for the preparation of **193** starting from allyl alcohol (**216**).



Entry ^a	Additive	t (min)	Conv. 193 (%) ^b
1	-	48	1.4
2	O ₂	48	3.5
3	COPC	48	0
4 ^c	<i>t</i> -butyl hydroperoxide (1 eq.)	48	9
5 ^c	<i>t</i> -butyl hydroperoxide (1 eq.)	100	14
6 ^c	<i>t</i> -butyl hydroperoxide (1 eq.)	238	13
7	<i>t</i> -butyl hydroperoxide (2.5 eq.)	100	9
8	cumene hydroperoxide (2 eq.)	100	10
9	H ₂ O ₂ (1 eq.)	100	11
10	H ₂ O ₂ (2.5 eq.)	100	0

^aThe experiments were carried out on a 5 mmol scale; ^bBased on ¹H NMR spectra employing 1,2-dimethoxybenzene as internal standard; ^cThe experiments were carried out on 2.5 mmol scale.

Sorensen and co-workers developed a dehydrogenation of saturated alkanes and alcohols employing TBADT as PC and cobaloxime pyridine chloride (COPC, **219**) as co-catalyst.³¹⁹ The mechanism of the reaction is similar to the one described in *Scheme 84*, where the radical formed by HAT undergoes hydrogen abstraction to form the metal-hydride complex [Co^{II}]-H and the desired alkene or ketone. The metal hydride formed is then regenerated by the reduced TBADT species by releasing hydrogen gas.



Scheme 84. Proposed mechanism for the dehydrogenation promoted by TBADT (**210**) and COPC (**219**).

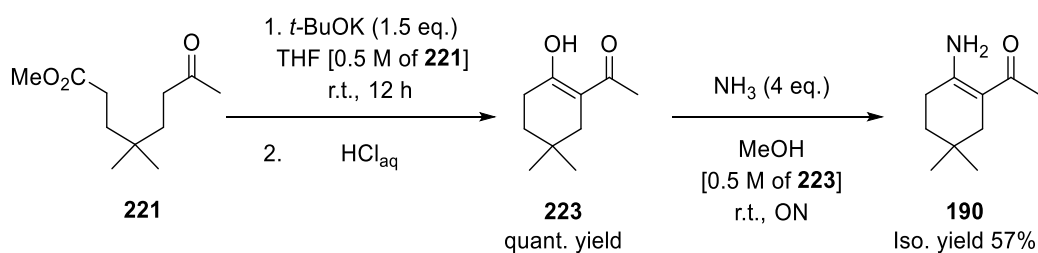
Unfortunately, in our example the addition of COPC as an additional oxidising agent decreases the conversion, suggesting an active oxygen species is likely promoting the process. For these reasons, we decided to employ a *tert*-butyl hydroperoxide aqueous solution as an oxidising agent. Under these reaction conditions, the desired compound **193** was detected in 9%, along with several other products that could allegedly be hydroperoxide intermediates (*Table 28, Entry 4*). Longer residence times up to 100 minutes improves the conversions to 14%, however, this levels off over longer times (*Table 28, Entries 5&6*). An increase of the hydroperoxide to 2.5 eq. slightly reduced the selectivity, allowing **193** to be detected in only 9% conversion (*Table 28, Entry 7*). A fast screening of different hydroperoxide derivatives was also evaluated. Cumene hydroperoxide and hydrogen peroxide were investigated, however, these gave similar results (*Table 28, Entries 8 – 10*).

While these attempts did not achieve an acceptable outcome, we once again decided to change the radical acceptor. Therefore, we investigated the use of methyl acrylate (**220**) which has already been described by Fagnoni and co-workers as a successful radical acceptor. The preparation of the methyl acrylate adduct **220** was performed using the same optimised conditions employed for acrylonitrile (**185**) and the desired keto-ester **221** was isolated in 50% yield (*Scheme 85*). In this example, a significant amount of the double addition keto-diester **222** was also isolated (50%), which was not detected when acrylonitrile was employed. The reason could be attributed to a higher reactivity of the methyl acrylate compared to the acrylonitrile.



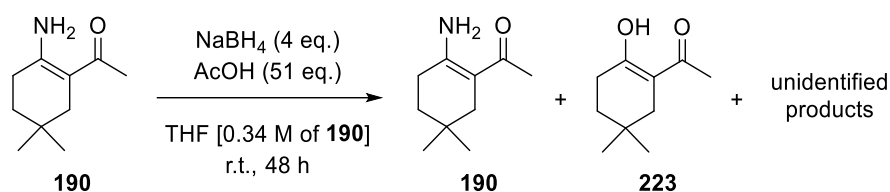
Scheme 85. Reaction conditions towards the synthesis of the keto-ester compound **221**.

Having the keto-ester **221** in hand, we exploited a Claisen cyclisation to target the 1,3-dicarbonyl compound **223**. Two different reaction conditions were screened: MeONa in methanol solution, and the biphasic *t*-BuOK in THF. Unfortunately, the first conditions investigated (MeONa/MeOH) did not form the final material even after 2 days of stirring, whereas quantitative conversion was yielded with *t*-BuOK/THF after 12 hours (*Scheme 86*). The amination step to **190** was carried out by adding a methanolic ammonia solution to a solution of **223** in methanol. The reaction yielded the final material in 57%, surprisingly lower than its de-methylated derivative **207** (section 2.3.1).



Scheme 86. Reaction conditions for the synthesis of **190** in steps from the keto-ester **221**.

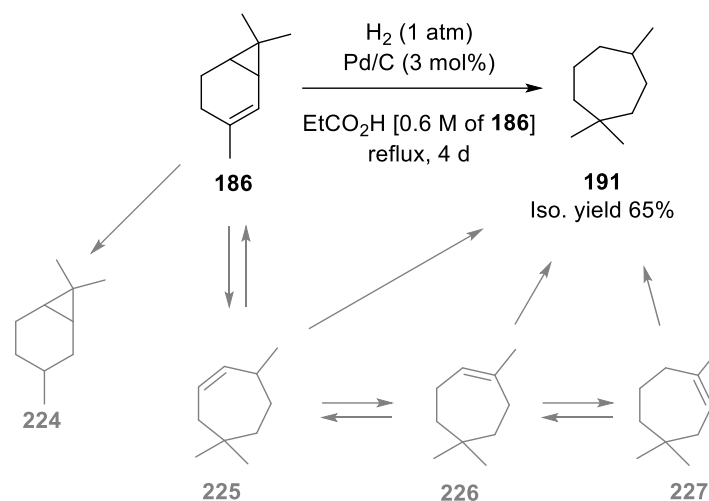
As also attempted in chapter 2, section 2.3.1 for the de-methylated material, the de-amination process was investigated on compound **190** employing catalytic hydrogenation in ethanolic solution. Unfortunately, Pd/C and PtO₂ both proved unsuitable for the reduction step, in fact only hydrolysed product **223** and the enaminone **190** were detected in the reaction mixture. The H-CUBE[®] was also employed to allow an increase of hydrogen pressure (10 bar), however, again the same results were obtained. Consequently, we decided to exploit the reduction using borohydride chemistry as previously described by Manfredini *et al.*^{320,321} A triacetoxymethylborohydride complex made *in situ* was exploited for the reduction, however after 2 days of stirring, a complex mixture comprising the hydrolysed compound **223** and the enaminone starting material was obtained (*Scheme 87*). Analysing the mixture with ¹³C NMR, we noticed no new quaternary carbons were present in the mixture as well as no boron (¹¹B NMR spectra recorded), which would suggest a complete reduction of both enamine and carbonyl group.



Scheme 87. Reaction conditions for the reduction of **190** employing sodium borohydride.

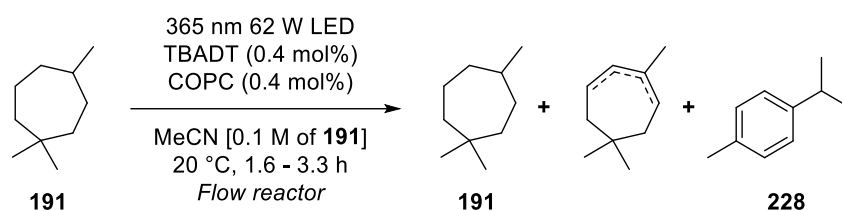
2.3.3. Galbascone starting from 3-carene: Route G

Another strategy taken into consideration was the use of 3-carene (**186**) as the starting material for dehydroherbac (**74**). Based on this approach, we started by reducing the 3-carene in propionic acid utilizing Pd/C under a hydrogen atmosphere. The procedure was first applied by Crocker *et al.* in 1966.³²² The authors proposed a ring-opening of the cyclopropane and subsequent hydrogenation of the dehydrocycloheptanes formed (*Scheme 88*). As such the experiment was conducted on a 100 mmol scale and after 4 days yielded the trimethylcycloheptane (**191**) in 65%.



Scheme 88. Reaction conditions for the synthesis of **191** from 3-carene (**186**) and the proposed mechanism described by Crocker in 1966.

Having **191** in hand, we investigated the photo-catalysed dehydrogenation described in the earlier section 2.3.2 on **191**. The hypothesis was that since the substrate **191** has a tertiary carbon for the formation of a stable radical, selectivity should be achieved. Unfortunately, the reaction did not bring about the desired result, even when long residence times (3.3 hours) were employed (*Scheme 89*). The mixtures obtained were composed mainly of unreacted starting material **191** but with other over-oxidised material whose *m/z* matches the *p*-cymene (**228**), based upon the extent of reaction no isolation was attempted.

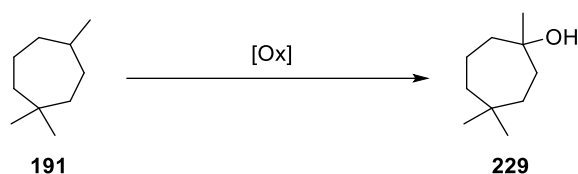


Scheme 89. Reaction conditions for the TBADT/COPC-catalysed dehydrogenation of **191**.

Similar oxidations on tertiary carbons have been described in the literature for the synthesis cholestane derivatives by Mincione *et al.* in 1992 and for the preparation of a Vitamin D₃ analogue by Fuchs and co-workers in 2012.^{323–325} In these two examples, dioxirane was

employed as the oxidant. Different from Mincione approach, Fuchs' methodology forms the dioxirane *in situ* from Oxone and 1,1,1-trifluoroacetone (TFA) and occurs in only 6 hours compared with using the dioxirane derivative of acetone (*Table 29, Entry 1*). The trifluoromethyldioxirane (TFDO) is more volatile than the dimethyldioxirane (DMDO) and for these reasons it is easier to be prepared *in situ*. To our delight, the desired compound **229** was successfully synthesised in 36% yield. Unfortunately, when the reaction was run employing DMDO as *in situ* formed oxidant, no desired material **229** was found (*Table 29, Entry 2*).

Table 29. Reaction conditions for the hydroxylation of **229**.



Entry ^a	Reaction conditions	Conv. 229 (%) ^b
1	TFA (20 eq.), Oxone (6 eq.), NaHCO ₃ (12 eq.), MeCN:H ₂ O (10:1) [0.1 M of 191], 5 to 10 °C, 6 h	36% ^c
2	Acetone (20 eq.), Oxone (6 eq.), NaHCO ₃ (12 eq.), MeCN:H ₂ O (10:1) [0.1 M of 191], 5 to 10 °C, 18 h	-
3	O ₃ <i>t</i> BuOMe [0.16 M of 191], - 78 °C	traces
4	<i>m</i> CPBA (1 eq.), CHCl ₃ [1.25 M of 191], reflux, 18 h	28% ^c

^a The experiments were carried out on a 10 mmol scale; ^b Based on ¹H-NMR spectra employing 1,2-dimethoxybenzene as internal standard; ^c Isolated yield.

Due to the restricted laboratory availability of the TFA and the low efficiency of the method, other reaction conditions for the desired hydroxylation were investigated such as the usage of peracids and ozone as alternative oxidants. The ozone-driven oxidation was noted as being described by Mazur *et al.* although providing low selectivity when methylcyclohexane was oxidised in solution.³²⁶ In fact, improved conversions and selectivity were reported when the hydrocarbons were absorbed on silica gel due to a better ozone uptake and contact area.³²⁷ However, later in 2015 Khalitova *et al.* published an efficient methodology for the ozone hydroxylation of methylcyclohexane.³²⁸ Inspired by these results, we decided to attempt to reproduce the procedure on our target **191**, however, the desired material was detected only in

traces by GC-MS analysis along with a large amount of residual starting material (*Table 29, Entry 3*).

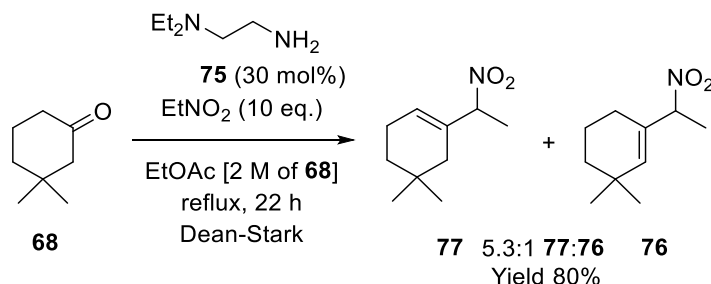
Additionally, in 1985, Schneider and co-workers developed a peracid hydroxylation of hydrocarbons.³²⁹ The authors claimed faster reaction rates were obtained when peroxybenzoic acids carrying electron-withdrawing groups were employed probably due to the formation of a better acid leaving group. To our delight, the reaction carried out on **191** did indicate the formation of the desired material **229**, albeit in low yield (*Table 29, Entry 4*).

Due to limited time (Covid restrictions) and low amounts of material **229** gathered in this last step, we were unable to further proceed with this particular investigation.

2.3.4. Galbascone from 3,3-dimethylcyclohexanone: Route H

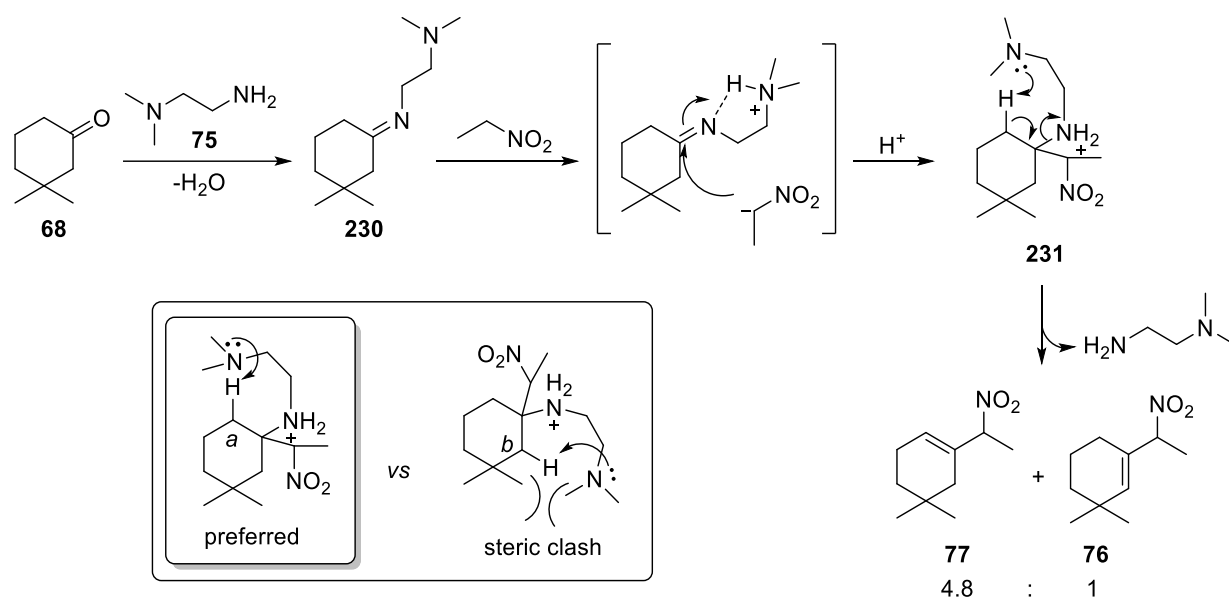
2.3.4.1. A deep understanding

The preliminary optimised conditions developed in a former collaboration between Durham University and IFF are depicted in *Scheme 90*. As can be seen, 22 hours was required for the reaction to reach a satisfying conversion to the final materials **76** and **77**. However, as already noted in the chapter 1, section 1.3.3, decomposition of the desired material **77** takes place under the reaction conditions, changing the isomer composition in the final mixture and reducing the overall efficiency of the process due to the irreversible loss of material. Consequently, investigating the performance of the reaction over time would help gain a better understanding of the kinetic of the reaction/side reactions and thus help establish the best conditions for the process.



Scheme 90. Reaction conditions for the Henry reaction of **68** to the nitro compounds **76** and **77**.

The previous study proposed a mechanism for the reaction as depicted in *Scheme 91*. The reaction initially undergoes imine formation between the ketone **68** and *N,N*-diethylethylenediamine (**75**). Deprotonation of the nitro compound and its subsequent attack on the iminium group forms the β -nitroamine intermediate **231**. Compound **231** is then proposed to undergo an E_2 elimination to form the final regioisomeric compounds **76** and **77**, and regenerating the amine catalyst **75**. The nature of the selectivity is believed to emerge from the steric hindrance of the aliphatic group on the tertiary amine (*Scheme 91*). This selectivity would mainly promote elimination of the α -proton over the more hindered transition state to remove the β -proton.



Scheme 91. Proposed mechanism for the preparation of the allylic nitro compounds **76** and **77**.

Having the proposed mechanism in mind, we initially investigated the importance of the concentration comparing the reactions in benzene at 0.2 M of **68**, as previously run, with a new reaction performed at 1 M of **68**. In *Figure 44*, it can be seen that concentration has a strongly impact on both the reaction time and the efficiency of the reaction.

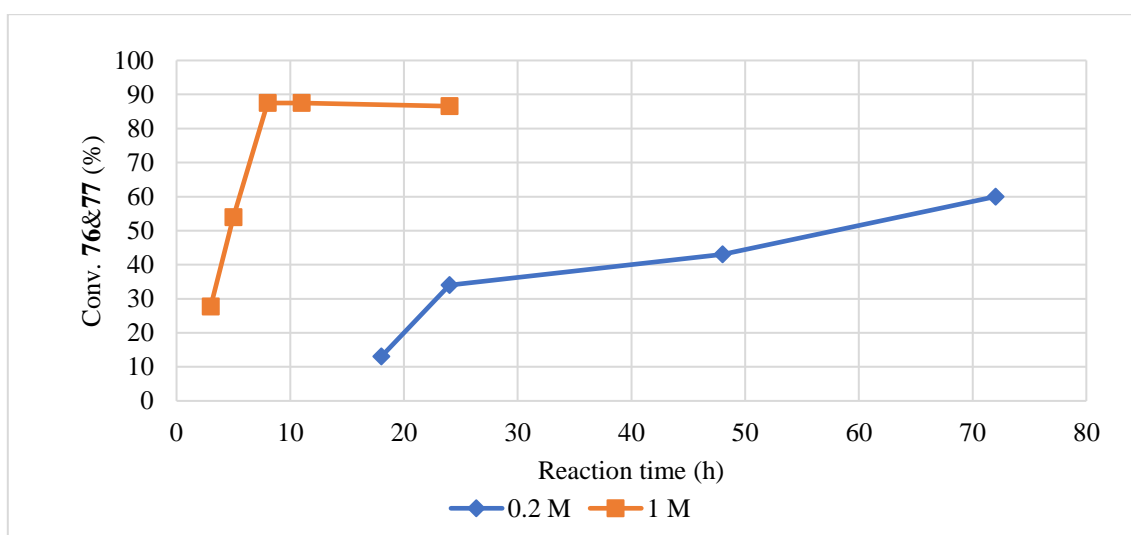


Figure 44. Conversion of **77** and **76** in relation with the reaction time under different concentrations. The experiments were carried out on a 25 mmol scale. Conversions estimated by GC-MS through a calibration curve.

We then considered it of value to investigate the variation of the reaction rate in different solvents considering the transition state energies may be affected by the polarity of the solvent. As can be seen from *Figure 45*, reactions carried out in apolar hydrocarbon solvents such as benzene, toluene, and cyclohexane tend to reach full conversion slower than those reactions performed utilising more polar solvents like EtOAc, 4-methyltetrahydropyran (4-Me-THP), and 2-methyltetrahydrofuran (2-Me-THF). *Figure 46* shows how the ratio of the two isomers **76** and **77** changes over time in the various solvents. The formation of the desired compound **76** is initially favoured over the isomer **77**, however, it slowly interconverts as the reaction time increases. Despite these data, ethyl acetate was still found to be the optimal solvent, as it provides the best selectivity (ratio **77:76**, 5.4:1) and efficiency (87.5%) after 8 hours of reaction time.

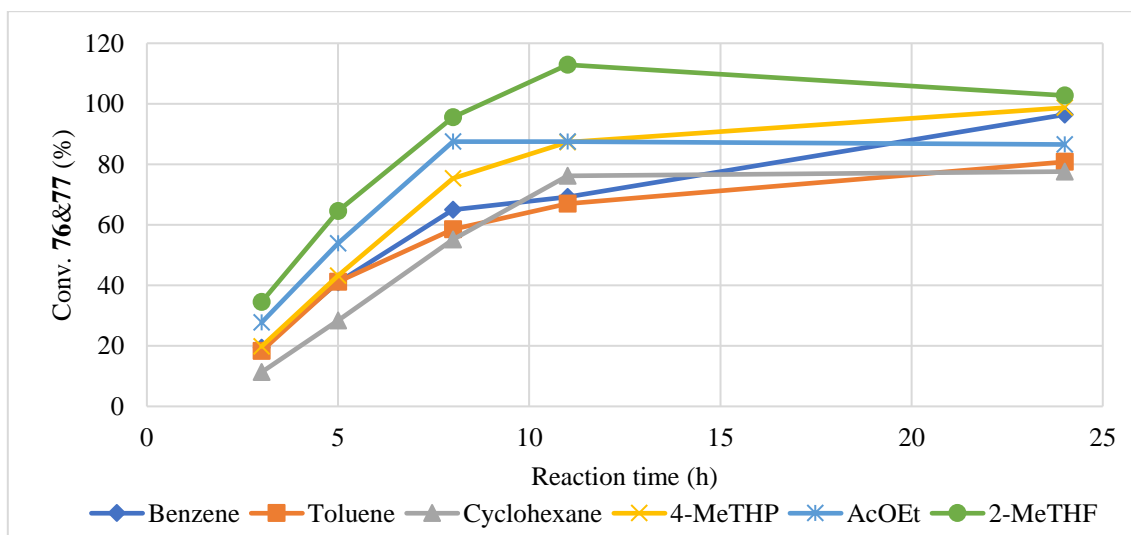


Figure 45. Conversion of **76** and **77** in relation with the reaction time in different solvents. The experiments were carried out on a 25 mmol scale. Conversions estimated by GC-MS through a calibration curve.

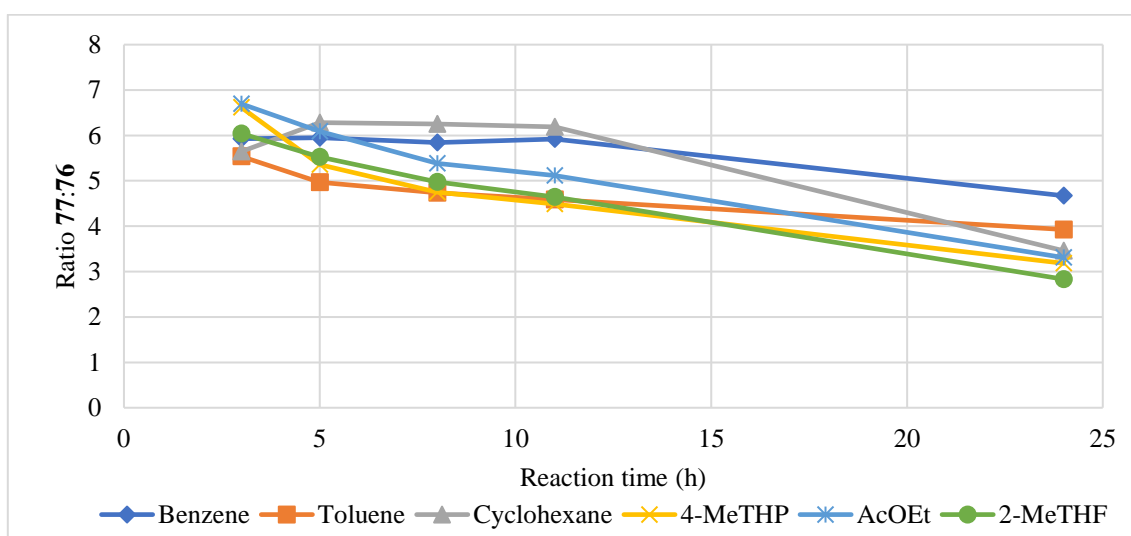


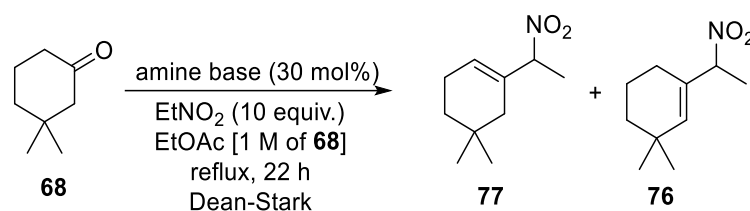
Figure 46. Ratio **77:76** in relation with the reaction time in different solvents. The experiments were carried out on a 25 mmol scale.

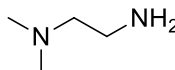
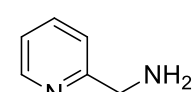
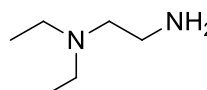
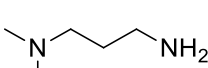
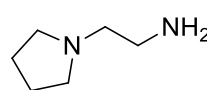
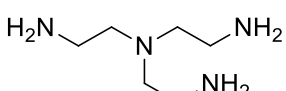
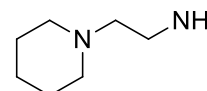
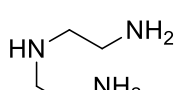
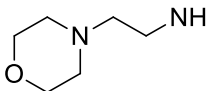
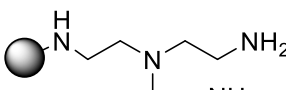
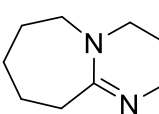
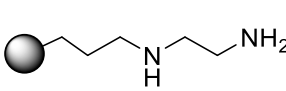
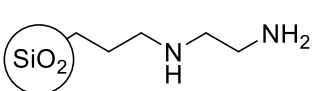
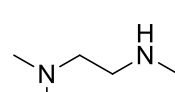
In the initial study, the nature of the catalyst was also investigated and *N,N*-diethylethylenediamine (**75**) as well as 1-(2-aminoethyl)pyrrolidine (**233**) were identified as

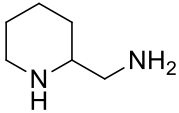
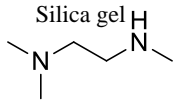
good catalysts (*Table 30, Entries 2&3*). The higher boiling points (b.p. of **75** = 146 °C, b.p. of **233** = 170 °C, b.p. of **232** = 105 °C) and higher steric hindrance of the ethylenediamines **75** and **233** yielded better selectivity than the *N,N*-dimethylethylenediamine (**232**) previously reported in the literature. The improved selectivity shown by catalyst **233** could be attributed to an increase in the energy gap between the transition states for the two possible de-protonation steps due to its higher level sterics and limited conformational freedom of the ring. Many other catalysts were also investigated to increase knowledge of the reaction (*Table 30, Entries 4 – 5 & 8 – 13*). To further validate the imine-based mechanism proposed in *Scheme 91*, we considered performing other control experiments. A strong non-nucleophilic amine such as 1,8-diazabicyclo[5.4.0]undec-7-ene (DBU, **236**) was tested to analyse whether simple basic conditions were necessary (*Table 30, Entry 6*), and, a primary amine such propylamine (**237**) and a tertiary amine (triethylamine, **238**) were screened to assess the need for the ethylenediamine-type of moiety (*Table 30, Entry 7*). No reaction were detected in all of these tests.

The *tris*-amine **245** had previously been investigated as polymer-supported catalyst, however, the results had been poor. The lower yields obtained from other homogenous *tris*-amine derivatives (**243** and **244**) suggested a supported catalyst more similar to **232** should be considered (*Table 30, Entries 12 – 14*). Consequently, we examined a polymer-supported ethylenediamine **246**, although the outcomes were unsatisfying (*Table 30, Entry 15*). Inspired by reports by Kobayashi *et al.* on heterogenous catalysis relating to condensations reaction in flow, we decided to investigate their preferred catalyst 3-(ethylenediamino)propyl-functionalised silica gel (**247**).^{168,169} To our delight, the reaction gave some promise with partially formation of the product, albeit with low **77:76** ratio (3.5:1) (*Table 30, Entry 16*). The activity of the latter may be explained by a higher surface area compared to the polymer-bound catalyst and therefore better accessibility of the ethylenediamine active moiety. Another possible explanation may be the bi-functionality of the silica support providing some Brønsted acidic sites as well as the amine functionality thus promoting the catalysis (acid catalysis). Interestingly, no reaction was detected when only silica gel was used (*Table 30, Entry 17*), or when silica and ethylene diamine were combined (*Table 30, Entry 18*).

Table 30. Base screening for the irregular nitro-aldol reaction of 3,3-dimethylcyclohexanone.



Entry ^a	Base (<i>b.p.</i>)	Conv. 76&77 (%) ^b	Entry	Base	Conv. 76&77 (%) ^b
1	 232 105 °C	87 (4.9)	10	 241	0 -
2	 75 146 °C	56 (5.3)	11	 242	5 (4.1)
3	 233 170 °C	81 (8.2)	12	 243	30 (4.2)
4	 234 186 °C	70 (4.8)	13	 244	29 (2.5)
5	 235 224 °C	32 (3.6)	14	 245	<1 -
6	 236	0 ^c -	15	 246	0 ^c -
7	<i>n</i> PrNH ₂ 237 Et ₃ N 238	0 ^c -	16	 247	29 ^c (3.5)
8	 239	6 (3.1)	17	Silica gel	0 ^c -

9		240	42 (3.4)	18		8 -
---	---	------------	-------------	----	---	--------

^a Reactions carried out on 50 mmol scale at 1.0 M; ^b Yield estimated by GC-MS using *n*-pentadecane as an internal standard; ^c Conversion based on ¹H-NMR spectra employing 1,2-dimethoxybenzene as internal standard.

Considering the three most active catalysts (**75**, **232** & **233**) and the solid catalyst (**247**) depicted *Table 30*, we decided to monitor how the formation of the two isomers **76** and **77** changes over a 24 hours reaction period (*Figure 47* & *Figure 48*). As one might expect, the heterogenous catalyst reaches full conversion after longer reaction times than the corresponding homogenous catalysts due to a diffusion-dependent reaction rate. The selectivity does not significantly change throughout the reaction period (3:1 after 3 h vs 2.8:1 after 24 h) suggesting the steric environment around the active site does not allow a high preference toward any deprotonation site.

The catalysts **75** and **233** presented the highest selectivity (**77:76** ratio: ~ 9:1) after 5 hours, albeit with low conversions (40 – 65%). After 8 hours, catalyst **233** increased to a peak conversion whilst essentially conserving the selectivity (8.5 vs 9.5). The selectivity of catalyst **75** instead dropped to 5.3 under-performing the initial catalyst **232** (87% vs 56% conversion after 8 h). Interestingly, conversion of **76** and **77** did not change over 24 hours of monitoring when catalyst **232** was employed, only reduction of the ratio **77:76**. This may suggest a conversion of the kinetic isomer **77** to the thermodynamic isomer **76**.

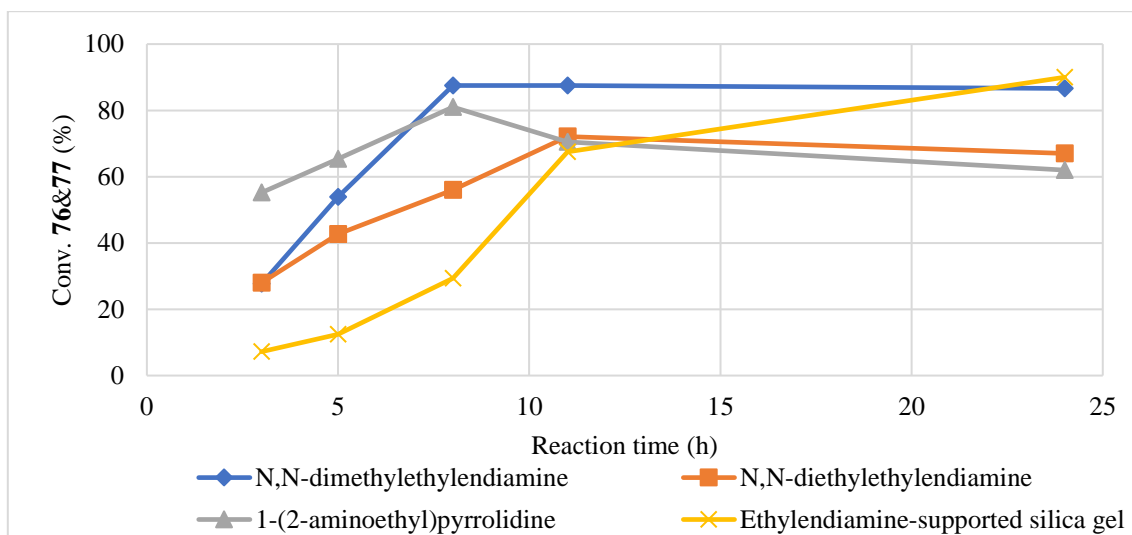


Figure 47. Conversion of **76** and **77** in relation with reaction time employing different catalysts. The experiments were carried out on a 25 mmol scale. Conversions estimated by GC-MS through a calibration curve.

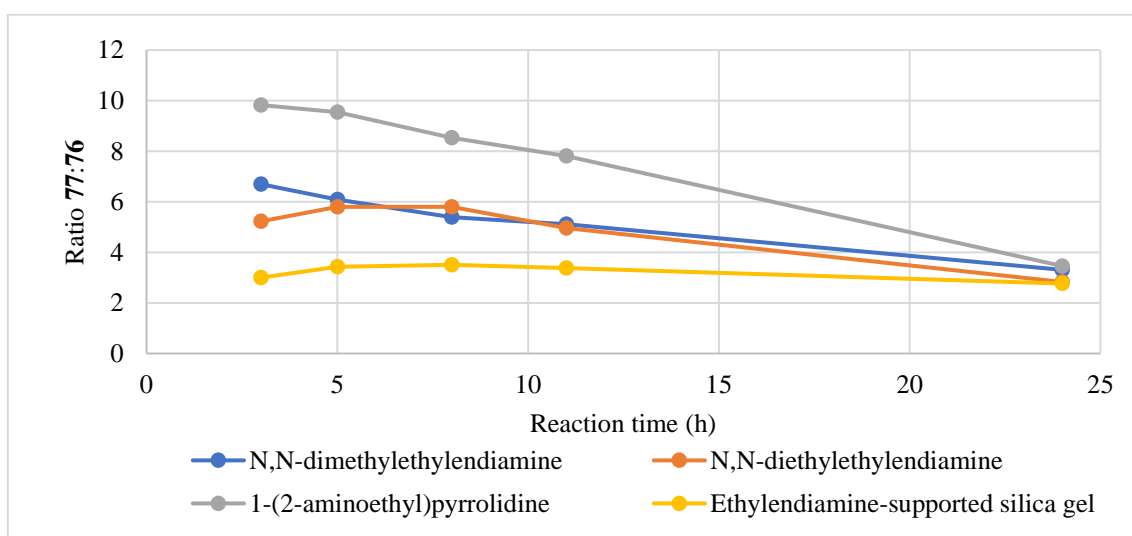
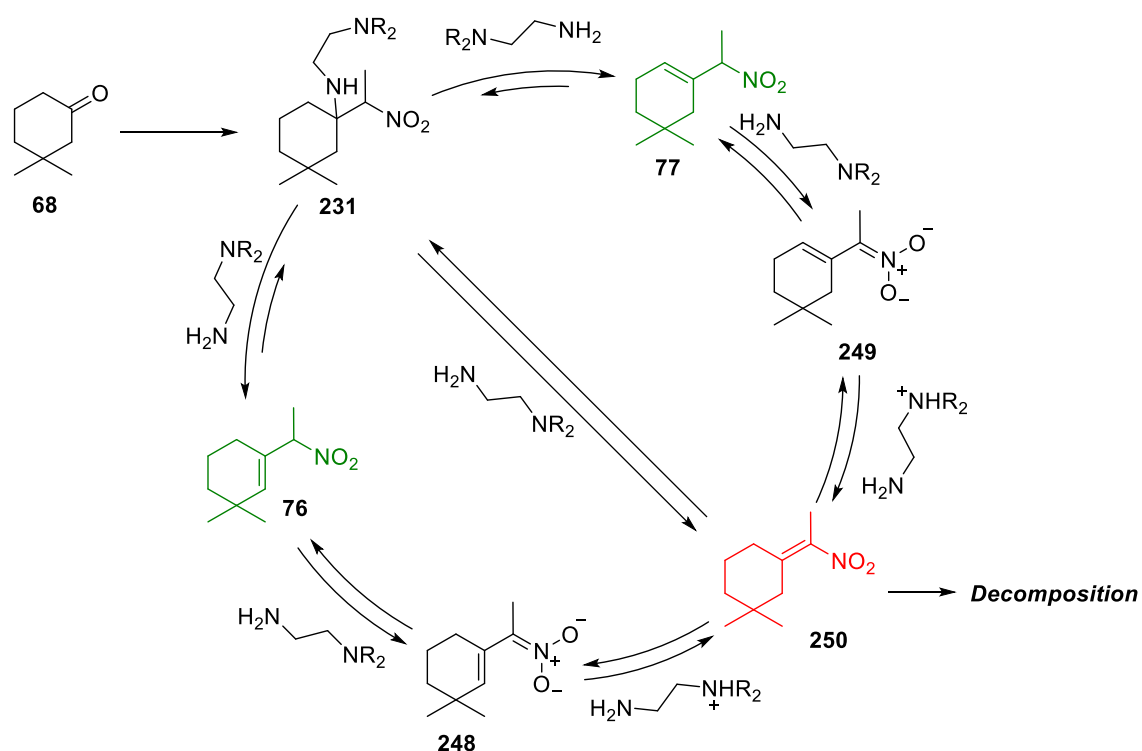


Figure 48. Ratio **77:76** in relation with the reaction time in different catalysts. The experiments were carried out on a 25 mmol scale.

Combining the new data with the previous observations and findings, we proposed a possible mechanism for the decomposition of the final compounds **76** and **77** (*Scheme 92*). Once

formed, the β -nitro-amine **231** eliminates to yield the two allylic nitro isomers **76** and **77**. The basicity of the amino group on the ethylenediamine could deprotonate the isomers **76** and **77** to form the corresponding nitrates **248** and **249**. Deprotonation of the nitrates **248** and **249** can then bring about formation of the α,β -unsaturated nitro molecule **250**, which undergoes decomposition. It is noteworthy that the elimination of intermediate **231** could also yield the undesired material **250**. It is important to note that these reactions are all potentially reversible and their kinetic rates are strictly dependent upon the nature of the catalyst. In fact, *N,N*-dimethylethylenediamine (**232**) does not cause decomposition of the allylic materials over 24 hours of monitoring however, the more bulky catalyst **75** and **233** do. This may be due to a less steric hindrance of the alkyl groups on the tertiary amine moiety, which allows the undesired material **250** to be interconverted into one of the two isomers **76** and **77**. During the monitoring, a small peak having the same *m/z* ratio as **76** and **77** was observed in all the three experiments, however, it rapidly disappears over time suggesting rapid decomposition.



Scheme 92. Proposed mechanism for the decomposition of the final materials **76** and **77**.

Having established a greater knowledge regarding the catalyst, we decided to investigate the relevance of the nitroethane. It is in fact reported by Tamura *et al.* the importance of keeping

high excess of nitroethane to increase the reaction kinetics.¹⁴⁵ However, from an industrial implementation strategy nitroethane content in the reaction mixture should be minimised to prevent hazardous situations (flammable, Acute toxicity (oral, inhalation) and noted as a potential explosive material). Consequently, reaction mixtures with lower amount of nitroethane were monitored over 24 hour periods (*Figure 49*). As can be seen, a decrease of nitroethane in the reaction mixture strongly influence the reaction kinetics and this may be due to a change of the reaction temperature (less nitroethane will mean low boiling point of the reaction mixture nitromethane forms an azeotrope) as well as a reduction of one of the reactants. As mentioned initially, the concentration of the reaction was found to be highly important for the reaction kinetics. For these reasons, we determined that it would be valuable to perform an experiment with less nitroethane (2.5 eq. instead of 10 eq.) and more concentrated (2.5 M instead of 1 M). The reaction reached 61% conversion and gave a 5.8:1 ratio **77:76** after 11 hours of reaction. These conditions would allow the reduction in the amount of solvent and nitroethane employed, increasing the productivity (28 vs 13 g/100 mL).

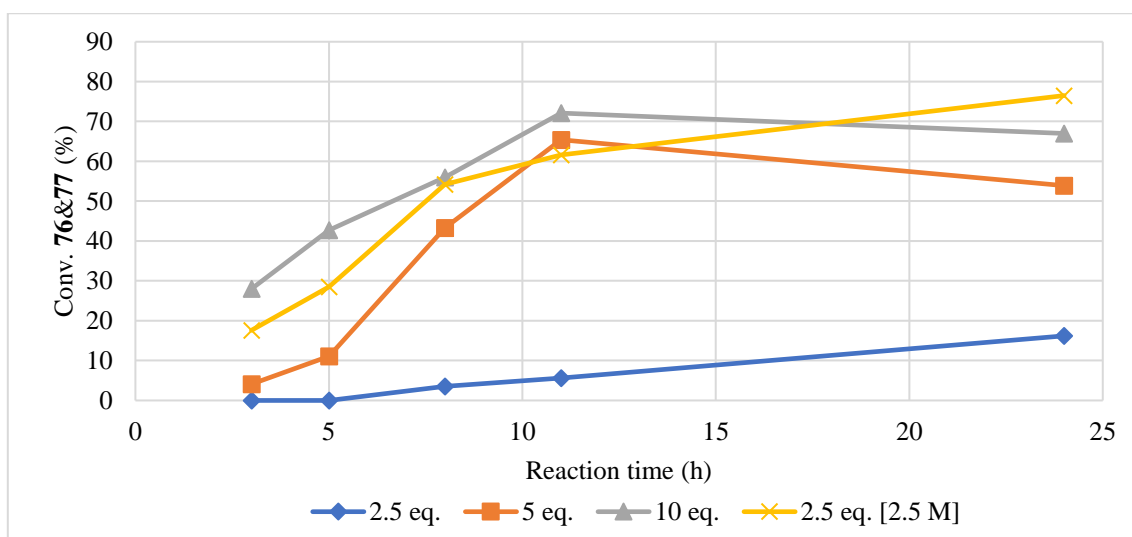


Figure 49. Conversion of **76** and **76** in relation with the reaction time when changing the amount of nitroethane. The experiments were carried out on a 25 mmol scale. Conversions estimated by GC-MS through a calibration curve.

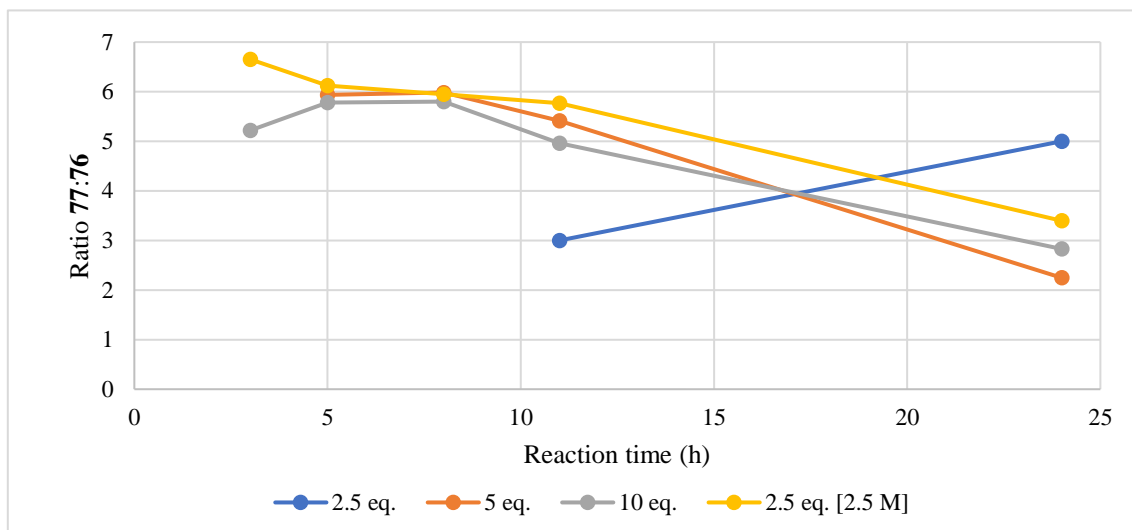


Figure 50. Ratio **77:76** in relation with the reaction time changing the way of addition of the catalyst. The experiments were carried out on a 25 mmol scale.

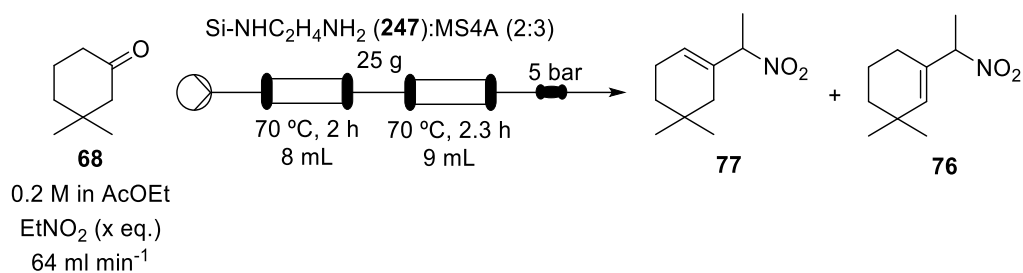
2.3.4.2. Exploring a continuous approach

Having found a suitable heterogeneous catalyst for the reaction, the catalyst reuse was considered. As already widely discussed above, the batch mode reaction had shown different key parameters, such as optimal water removal, catalyst loading, nitroethane's stoichiometry, and reaction time. A flow apparatus was therefore considered using a packed bed reactor of the catalyst. Indeed, similar condensation reactions requiring water removal had already been implemented under flow by Kobayashi *et al.*^{168,169} The group prepared a blend of catalyst and dehydrating agents (calcium chloride or molecular sieves) to ensure the amount of water produced was promptly removed from the system. Following Kobayashi's example, we set up a similar apparatus employing molecular sieves 3Å powder as the dehydrating agent (*Figure 51*).



Figure 51: Setup for the continuous-flow preparation of the nitro olefin **77**.

To assess whether the ratio of **77:76** increases with a reduced reaction time, and a high catalyst/substrate ratio, a more diluted solution of the starting material **68** was employed (0.2 M vs 1 M). To prevent solvent expansion (boiling), a modified 100 psi BPR was placed at the end of the glass reactor, which kept the system pressure around 3.6 bar. As the other key parameters (catalyst loading, water removal) could not be easily changed due to the system setup, only the amount of the nitroethane was therefore taken into consideration as a parameter. As such the equivalents were varied from 1.25 to 10 but in each case the final material **77** was only detected in low yields (*Table 31, Entries 1&3*).

Table 31: Flow setup for the investigation of continuous-flow preparation of **77**.

Entry ^a	EtNO ₂ (eq.)	Conv. 76&77 (%) ^b	Ratio 77:76
1	1.25	2	5.6
2	5	2	6.4
3	10	3	5.8

^aThe experiment was carried out on a 1.5 mmol scale; ^bConversions estimated by GC-MS based upon a calibration curve.

2.3.5. Summary and Conclusions

During the project, we investigated three potential synthetic approaches for the preparation of the Galbascone precursor **42**. The proposed methodologies started from different raw materials such as acrylonitrile (**185**), 4,4-dimethylcyclohexanone (**183**), 5-methyl-hexan-2-one (**184**), and 3-carene (**186**). These approaches encompass various type of chemical transformations such as amination, Claisen condensation, hydrogenation, oxidation, and photocatalysed CH-activation.

Despite our attempts, two of the three approaches proved to be unfeasible due to the difficulty in the de-amination of the final enamionone intermediates (section 2.3.1 and 2.3.2). While investigating a photocatalysed CH activation, we encountered an opportunity to directly formulate the final ketone through acrolein (**215**) and 5-methyl-hexan-2-one (**184**) under continuous-flow conditions, although attempts to improve upon the poor yields only brought about the formation of unidentified by-products.

The route C (section 2.3.3) starting from 3-carene (**186**) was only partially explored due to restricted laboratory time. Nonetheless, the isolation of the tertiary alcohol intermediate **229** through an oxidative CH-activation reaction allows us to perform one of the key steps of the synthetic approach. This indicates a chance for this approach in the future. It is noteworthy

though that the full synthesis still requires three more steps to be performed and the selective elimination as well as the aldol cyclisation to the final product which may all require careful optimisation. As such much work is still to be done before a verdict can be made on this route.

Along with designing new approaches, the optimisation of a previously devised methodology was also performed (section 2.3.4). Kinetic studies were pursued on the amino-catalysed nitro-Aldol reaction allowing a better understanding of the process and enabling us to propose a possible decomposition pathway for the final products (**76** & **77**), which seems to be directly correlated with the level of steric hindrance of the ethylenediamine catalyst. Furthermore, we also engineered a process reduction of the hazardous nitroethane reagent without losing selectivity or efficiency. It was found that the reagent reduction can be compensated for by increasing the concentration of the reaction solution. Inspired by work of Kobayashi *et al.*, we also attempted to devise a continuous-flow approach employing an ethylenediamine-supported silica gel (**247**) as heterogeneous catalyst and molecular sieves as the dehydrating agents. Unfortunately, our flow setup only allowed to detect the desired material in poor yields.

3. Conclusions and outlooks

The aim of this doctoral project was to evaluate new routes for the preparation of three key fragrance ingredients [Veramoss (**11**), Ambertonic (**37**), Galbascone (**42**)] all currently manufactured by the IFF facilities at Benicarlò in Spain. For each target compounds several speculative alternative routes were proposed and experimentally evaluated.

For the Veramoss target, a two steps process starting from hex-4-en-3-one (**25**) and dimethyl malonate (**26**) is currently being employed for the manufacturing of the material. The process comprises of a conjugate addition/Claisen cyclisation step to a precursor material **23**, which is then oxidised to Veramoss through a chlorination-dehydrochlorination stage employing elemental chlorine. The need for an alternative synthetic approach was therefore aimed at removing the toxic elemental chlorine as reagent, improving the quality of the final material by preventing over-oxidation, and reducing the cost of goods by starting from cheaper raw materials. Three unprecedented routes were explored during the project.

Methyl crotonate (**20**) and ethyl acetoacetate (**21**) were employed for the synthesis of a key intermediate 1,6-dihydro-orsellinate **Et-22** whose oxidation was attempted by introducing a methyldene group in position 3 on the cyclohexandione ring (Chapter 2, section 2.1.1.). After several attempts employing paraformaldehyde in different reaction conditions, it was clear the *exo*-olefin desired material **78** could not be isolated due to its extreme reactivity in the reaction mixture. Consequently, to obtain a more stable intermediate for the alkylation, it was made an effort to firstly oxidise the 1,6-dihydro-orsellinate **Et-22** to its aromatic material **Et-34**. Unfortunately, all the oxidising conditions screened during the project did not allow to obtain the orsellinate material **Et-34** efficiently (best condition yielded 7% of **Et-34**). In fact, in the conditions where the latter **Et-34** was formed, a significant amount of over-halogenated materials were noted as well.

Dimethyl malonate (**26**), acetaldehyde (**91**), and 2-butanone (**90**) were also explored as alternative cheap starting materials to gain the key precursor **23** (Chapter 2, section 2.1.2.). A dimethyl ethylidenemalonate intermediate **89** was firstly prepared from malonate **26** and acetaldehyde **91** and consequently employed in a conjugate addition/Claisen cyclisation stage to **23**. A preparative methodology for the compound **89** was developed employing polystyrene-supported dimethylamine as catalyst in a flow-continuous approach (38% yield), however only moderate conversion (up to 50%) was obtained leaving a substantial amount of unreacted materials **26** and **91** in the reaction mixture. The presence of the latter materials was found to hamper the isolation of a pure product via distillation due to side condensation reactions occurring during the procedure. Nevertheless, pure dimethyl ethylidenemalonate **89** was isolated via column chromatography to evaluate the subsequent cyclisation stage which was found to be challenging. Several catalysts (morpholine, diisopropylamine, *N,N*-diethylethylenediamine, Cu(OTf)₂, proline) as well as strong base (LDA) were explored for the reaction and no desired material **23** was isolated in these examples.

As 2-butanone still remains a valuable raw material, a *route b* strategy to Veramoss **11** was also explored (Chapter 2, section 2.1.3.). The key goal of this synthetic pathway was to prepare the 3-chloro-hex-4-en-3-one (**98**) and attempt a conjugate addition/Claisen cyclisation with dimethyl malonate (**26**) to gain a chlorinated analogue of **23** (**97**) which could undergo to dehydrochlorination to the desired Veramoss. The design of the synthesis started from the preparation of the chloro-ene **98** material. The developed methodology for the latter employs 2-butanone, acetaldehyde, and dimethyl oxalate (**101**) in a 4 steps procedure, where the first

two steps could be performed without isolating the intermediate **100**, and yielded the pure desired compound 4-acyl-3-hydroxyl-2,5-dihydrofuran-2-one (**99**) in 53%. The last two steps of the procedure involves a chlorination of the compound **99** with TCCA and consequent base-driven rearrangement which yielded the chloro-ene material **98** in 76% (40% over the four steps). Unfortunately, after having developed the procedure to the chloro-ene **98**, the cyclisation with dimethyl malonate was attempted gaining a cyclopropane material **106** as only product. An additional attempt to employ this strategy was also performed through dehydrochlorination of **98** to an alkyne derivative, however no desirable outcomes were obtained. Future works may be focused on exploiting the optimised methodology for the preparation of the compound **99**. The ability of the latter to rearrange into α,β -unsaturated ketone materials may be an opportunity to develop an alternative green process to hex-4-en-3-one (**25**), key raw material to Veramoss.

Along with scouting *de novo* strategies, efforts on improving the current manufacturing process was also performed (Chapter 2, section 2.1.4.). In particular, the project focused on finding an alternative chlorinating agent to the toxic chlorine gas. Sodium hypochlorite, TCCA, and the dichloro-species **108** were employed as alternative agents in the chlorination of the precursor **23**. Despite the results obtained from sodium hypochlorite and the di-chloro species **108**, experiments employing TCCA yielded desirable conversion to Veramoss. After an initial OFAT approach study, a DoE was performed which allows to spot the optimised conditions for an efficient chlorination process. After having optimised the first step to the precursor **23** in a different solvent (AcOMe), the chlorination stage with TCCA was performed in a one-pot process from the starting material **25** and **26**. To our delight, the desired Veramoss was isolated in 55% yield with purity found to be within specification for IFF commercial purpose. Further works may be focused on applying this optimised methodology on other challenging fragrance materials currently manufactured employing similar oxidation process as well as attempt a scale up for production to estimate the feasibility of the procedure.

In addition, an alternative purification methodology for crude Veramoss was developed exploring the affinity of some amines to form H-bonded complex with phenols (Chapter 2, section 2.1.5.). The H-bonded complexes were characterised via DOSY $^1\text{H-NMR}$ analysis as well as SCXRD and it was found amines with $\text{p}K_a$ over 11 (diisopropylamine, triethylamine, tributylamine) did form ionic salts instead. After choosing DABCO and TMEDA as valuable amines, a procedure was developed where the amine-phenol complex could be weakened to

recover the pure Veramoss material **11**. The methodology allowed to purify 70% purity final material into 95% purity white crystals in good-to-excellent yield (60 – 98%). Future works may be focused on finding an efficient down stream procedure for the recovery of the used amine to allow the purification treatment to be sustainable and low-budget. Furthermore, orsellinate materials have been gaining interest due to their biological activity in the pharmaceutical industry which could exploit such purification system. It may be therefore promising to look at alternative examples where such purification methodology is essential for industrial production.

The second target the doctoral project focused on was the musky, amber fragrance material Ambertonic (**37**). As newly patent synthetic odorant, the development of a preparative procedure is still ongoing. A one step process involving formamidine acetate (**40**) and an hydrogenated version of Cashmeran™ (**38**) was developed by the sponsor, however a substantial amount of reagents was needed to yield the desired material only in 68%. The goal of project was to design alternative synthetic routes and optimised them for possible industrial applications. Consequently, five synthetic routes were designed: four of which started from the same hydrogenated Cashmeran™ **39**, and one from an aniline building block (Chapter 2, section 2.2.2.2.).

The hydrogenated version of Cashmeran™ **39** was exploited as building block due to its availability in bulk volumes on site. The four adopted synthetic strategies aimed at constructing the pyrimidine ring missing from the original scaffold of the material **39**. The main idea was to prepare an intermediate of **39**, through either formylation (compound **131**) or olefination (compound **166**), to exploit for the formation of the pyrimidine ring (Chapter 2, section 2.2.2.1.). Additionally, an *electron-inverse-demand Hetero-Diels-Alder* reaction with 1,3,5-triazine for direct preparation of the heterocyclic ring was also screened with desirable outcomes. After several efforts on preparing the above mentioned intermediates **131** and **166**, an efficient preparative method to the formyl compound was developed and applied for the subsequent pyrimidine ring formation to Ambertonic **37** (Chapter 2, section 2.2.1.1.). The latter was then obtained by reacting the material **131** with formamide at high temperatures. Dimerization of the starting material **39** and decomposition of the final material were observed so an optimisation of the reaction conditions (180 °C & 4 h) were also performed (Chapter 2, section 2.2.1.2.). A feasibility investigation to combine the two optimised steps was performed and Ambertonic was obtained in good yield (56%). The one-pot procedure was optimised to

prevent the formation of a *N*-formyl amide material **147** whose presence hamper the purification of the final product (Chapter 2, section 2.2.1.4.). The preparative methodology allowed to isolate both Ambertonic **37** and its commercial analogue Sinfonide **153** in good yield (53 – 58% yield) from respectively the hydrogenated Cashmeran™ **39** and Cashmeran™. Future works may be focused on exploit the optimised methodology on different fragrance material of interest for the sponsor as well as other material where an efficient pyrimidine ring formation procedure is required for bulk production.

Alongside with the main goal, side investigations were also undergoing. For instance, the acquisition of the SCXRD structure of the main *trans*-isomer of Ambertonic revealed the relative configuration of the methyl group in position 2 on the indene scaffold. Such configuration was directly attributed to an *anti*-selectivity of the hydrogenation on the starting material **38**. As the main *trans*-isomer of Ambertonic was isolated, a resolution of the racemic mixture was also exploited to evaluate possible olfactory difference of the enantiomers with the original material. Unfortunately, no significant changes in their olfactory profile was noted.

The last discussed target was a fruity, green odorant Galbascone (**42**). The latter is a synthetic fragrance part of the ketone family and its synthesis is still a challenge for many organic synthetic chemists. Galbascone (**42**) is currently being produced from dehydrolinalool (**60**) through dehydration and cyclisation to obtain a 1:1 mixture of two isomers in low yield (38%). The aim of the project was therefore to develop more efficient and selective synthetic pathways to the key intermediate dehydroherbac **74** and optimised a previously developed methodology to assess the feasibility for industrial application. Three alternative synthesis to Galbascone were designed and explored during the project.

Two of these synthetic route aim at preparing similar enaminone compounds (**207** & **190**) to adopt for a two steps de-amination process previously described in literature on different substrates. 4,4-dimethylcyclohexanone (**183**) was employed in an attempt to form such the targeted enaminone compound **207**, however its isolation was found to be difficult (Chapter 2, section 2.3.1.). The enaminone compound **207** was eventually obtained through a two steps acetylation-amination method, albeit with low yields (40% over two steps and two column chromatography). To evaluate a more selective and quick route to the enaminone material, 5-methyl-hexan-2-one (**184**) and acrylonitrile (**185**) were also exploited to prepare the similar intermediate **190** (Chapter 2, section 2.3.2.). The strategy employed a photo-catalysed reaction,

which was optimised in a flow-continuous approach, for the synthesis of a keto-cyano intermediate **189**. The optimised procedure allowed to isolate the material **189** in high yield (63%) and throughput (630 mg h⁻¹). Unfortunately, the Torpe-Ziegler reaction to prepare the enaminone material **190** was not effective due to competitive thermodynamic condensation reaction favouring the unsaturated nitrile compound **213**. After changing the starting materials and adopting Claisen cyclisation and amination reaction, the 1,3-dicarbonyl compound **190** was isolated and exploited for the selective de-amination step. Unfortunately, none of the screened reductive conditions allowed to isolate the desired final material **74**.

A final attempt to Galbascone was performed by employing 3-carene as raw material by hydrogenation and CH-activation reaction (Chapter 2, section 2.3.3.). After obtaining the trimethylheptane compound **191** through hydrogenation of 3-carene (65% yield), several attempt of CH-activation reactions were performed and it was found the trifluoromethyldioxirane *in-situ* prepared strategy was yielding the hydroxyl material **229** in moderate yields (36%). Unfortunately, due to restriction in time and product **229** availability, no further works were performed. As the possibility to exploit a cheap raw material such as 3-carene is tempting, future works should be focused on evaluate the subsequent selective elimination step to the dehydrated compound **192**. Such stage may result challenging due to the multiple site where the elimination could occur. Therefore, a thorough screening of different bases and leaving groups may allow to obtained the desired material. Additionally, further works may investigate the possibility to directly rearrange the starting material 3-carene into the dehydrated compound **192** reducing the reaction steps.

Alongside with these alternative routes, a previously developed two steps preparative methodology starting from 3,3-dimethylcyclohexanone (**68**) was also explored (Chapter 2, section 2.3.4.). In particular, the first nitro aldol condensation to prepare the allylic nitro compound **77** was evaluated to improve its selectivity and productivity. Time-monitoring experiments exploiting different reaction conditions allowed to reduce the reaction times (from 24 h to 8 h), decrease the amount of nitroethane employed (from 10 eq. to 2.5 eq.) as well as double the productivity (from 13 to 28 g/100 mL). The investigation also allowed to have a better understanding of the mechanism for the decomposition of the desired material **77**.

Flow chemistry is becoming a valuable tool in organic chemistry with the aim of continuous manufacturing directed at reduction in cost and waste. Continuous methodologies were

evaluated during the doctoral project. As described above, an heterogeneous polymer-supported Knoevenagel condensation for the preparation of dimethyl ethylidenemalonate compound **89** was developed and described in section 2.1.2. The simple flow apparatus allowed to recover and recycle the catalyst and quickly scale up the procedure for the route investigation. The pyrimidine ring formation to Ambertonic **37** was also exploited in flow as it was found to be highly dependent by the reaction time and temperature, however the desired material was only detected in 20% yield (Chapter 2, section 2.2.1.3.). A photo-catalysed preparative reaction to the intermediate **189** was also developed and quickly optimised for the purpose (Chapter 2, section 2.3.2.).

Future works should be focused on scouting new sustainable and efficient synthesis routes suitable for continuous manufacturing and, therefore, applying a quality-by-design (QbD) strategy rather than a series of continuous improvements used in existing methodologies based on batch approaches. As already described in the first section of this thesis, the F&F industry mainly comprises of manufacturing organisations based on essentially bulk chemical synthesis. For these reasons, ICM facilities would be a crucial step forward to reduce the costs and be globally competitive.

4. Experimental Procedures

Unless otherwise stated, all solvents were purchased from Fisher Scientific and used without further purification. Dry solvents were obtained by filtration through a dehydrated column of Al₂O₃. Substrates, their precursors, and reagents were purchased from either Alfa Aesar, Sigma Aldrich, Fluorochem, TCI, Carbosynth or Acros Organics. Dihydro-Cashmeran (**39**), Cashmeran (**38**), hex-4-en-3-one (**25**) were supplied as raw materials by IFF and used as received.

¹H NMR spectra were recorded on either Bruker Avance-400, Varian VNMRS-700 or Varian VNMRS-500 instruments and are reported relative to residual solvent: CDCl₃ (δ 7.26 ppm), DMSO-*d*₆ (δ 2.50 ppm), MeOD-*d*₄ (δ 3.31 ppm), MeCN-*d*₃ (δ 1.94 ppm). ¹³C NMR spectra were recorded on the same instruments and are reported relative to CDCl₃ (δ 77.16 ppm) and DMSO-*d*₆ (δ 39.52 ppm), MeOD-*d*₄ (δ 49.00 ppm), MeCN-*d*₃ (δ 1.32 ppm). Data for ¹H NMR

are reported as follows: chemical shift (δ / ppm) (multiplicity, coupling constant (Hz), integration). Multiplicities are reported as follows: s = singlet, d = doublet, t = triplet, q = quartet, sept. = septet, m = multiplet, app. = apparent. Data for ^{13}C NMR are reported in terms of chemical shift (δ_{C} / ppm). DEPT-135, COSY, HSQC, HMBC, PSYCHE and NOESY experiments were used in structural assignments for key molecules.

IR spectra were obtained using a Perkin Elmer Spectrum Two UATR Two FT-IR Spectrometer (neat, ATR sampling) with the intensities of the characteristic signals being reported as weak (w, <20% of tallest signal), medium (m, 21–70% of tallest signal) or strong (s, >71% of tallest signal).

Both low and high resolution mass spectrometry were performed using the indicated techniques. Low resolution gas chromatography mass spectrometry (GC-MS Polar compounds) was performed on a Shimadzu QP2010-Ultra equipped with an Rxi-17Sil MS column (0.15 μm x 10 m x 0.15 mm) in EI mode carrier Helium (0.41 mL min^{-1} flowrate) with gradient oven temperature from 50 $^{\circ}\text{C}$ to 300 $^{\circ}\text{C}$ in 5 minutes and injection volume 0.5 μL and 25:1 Split:Splitless ratio. Low resolution gas chromatography mass spectrometry (GC-MS Nonpolar compounds) was performed on a Shimadzu QP2010-Ultra equipped with an Rxi-5Sil MS column (0.15 μm x 10 m x 0.15 mm) in EI mode carrier Helium (0.41 mL min^{-1} flowrate) with gradient oven temperature from 50 $^{\circ}\text{C}$ to 300 $^{\circ}\text{C}$ in 5 minutes and injection volume 0.5 μL and 25:1 Split:Splitless ratio. Low and high resolution atmospheric solids analysis probe mass spectrometry (ASAP-MS) was performed using a Waters LCT Premier XE. Low resolution liquid chromatography mass spectrometry (LC-MS) was performed using a Waters TQD mass spectrometer and an Acquity UPLC BEH C18 1.7 μm column (2.1 mm x 50 mm) in ESI mode with a MeCN:Water (0.1% formic acid) as mobile phase in gradient conditions (ramping from 95:5 to 5:95 MeCN:Water (0.1% formic acid) in 4 minutes). ESI-HRMS was performed using a Waters QtoF Premier mass spectrometer. For accurate mass measurements the deviation from the calculated formula is reported in ppm and mDa. The mass deviation tolerance is 3 mDa following the Journal of Organic Chemistry Authors' guidelines.³³⁰ Melting points were recorded on an Optimelt automated melting point system with a heating rate of 1 $^{\circ}\text{C}/\text{min}$ and are reported uncorrected.

Reactions were conducted in flow using the following equipment Vapourtec SF-10 (peristaltic), Polar bear plus FlowTM, Vapourtec UV-150 easy-MedChem along with standard

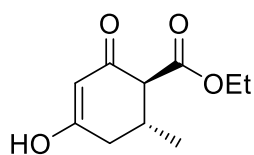
PTFE tubing and reactor coils. Microwave reactions were performed using a Biotage Initiator+ microwave reactor.

SiO₂ column chromatography was performed using Sigma Aldrich silica gel (grade 9385, pore size 60A) and standard manual column apparatus. For TLC, Sigma Aldrich glass-backed plates were used and visualisation was performed using UV-irradiation or a KMnO₄ stain. Organic solutions were concentrated under reduced pressure using a Buchi rotary evaporator and hi-vacuum was achieved using an Edwards RV5 pump and Schlenk line. Kugelrohr distillation was performed using a Buchi Glass Oven B-3585 and vacuum distillation was performed using a Buchi V-700 vacuum pump equipped with a V-850 vacuum controller attached to a standard distillation pig setup.

4.1. Veramos

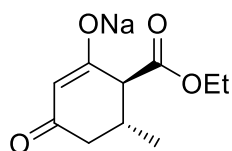
*General Procedure for the preparation of 22-Et and 23*¹⁴⁶

To a 2.75 M solution of EtONa (1.1 mol, 1.1 eq.) in EtOH (400 mL), ethyl acetoacetate (**21-Et**) or **11** (1 mol, 1 eq.) was added dropwise over 30 minutes. Then methyl crotonate (**20**) (106 mL, 1 mol, 1 eq.) was slowly added into the red solution over 15 minutes. The reaction mixture stirred under reflux for 7 hours. The mixture was then concentrated under vacuum to gain a white powder which was dissolved in water (500 mL) and acidified with conc. Hydrochloric acid (38%). The aqueous phase was extracted with EtOAc (3 × 150 mL) and the combined organic solution was washed with brine, dried over Na₂SO₄ and concentrated *in vacuo*.

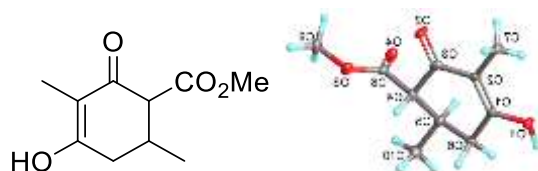


*Ethyl 2-methyl-4,6-dioxocyclohexanecarboxylate (22-Et)*³³¹ yellowish powder (98.1 g, 45% yield). ¹H NMR (400 MHz, DMSO-*d*₆) δ 11.38 (s, 1H), 5.22 (s, 1H), 4.12 (q, *J* = 7.1 Hz, 2H), 3.05 (d, *J* = 10.1 Hz, 1H), 2.42 – 2.14 (m, 1H), 1.19 (t, *J* = 7.1 Hz, 3H), 0.96 (d, *J* = 5.9 Hz, 3H). ¹³C NMR (101 MHz, DMSO-*d*₆) δ 193.8, 178.4, 171.0, 103.0, 60.6, 60.2, 35.7, 31.9, 19.5, 14.6. LC-MS (ESI+) *R*_t = 1.55 min *m/z* [M+H]⁺ = 199.5. HR-MS calculated for C₁₀H₁₅O₄

199.0970, found 199.0974 ($\Delta = 0.4$ mDa; 2.0 ppm). FT-IR (neat) ν (cm^{-1}) 2948 (m), 1701 (C=O, s), 1530 (C=O, s), 1453 (m), 1416 (m), 1351 (s), 1336 (m), 1301 (s), 1287 (m), 1267 (s), 1189 (m), 1148 (m), 1039 (s), 823 (s). Melting point: 73.1 – 87.5 °C (EtOAc), literature: 99 – 101 °C.³³¹



Sodium 6-(ethoxycarbonyl)-5-methyl-3-oxocyclohex-1-enolate (Na-22): The white precipitate obtained from the mixture was filtrated and left to dry over 48 h to yield **Na-22** as a white powder (121.1 g, 50% yield). ¹H NMR (500 MHz, DMSO-*d*₆) δ 4.37 (s, 1H), 4.01 (q, $J = 7.0$ Hz, 2H), 2.63 (d, $J = 11.3$ Hz, 1H), 2.15 (dtd, $J = 11.3, 6.4, 4.5$ Hz, 1H), 1.90 (dd, $J = 15.9, 4.5$ Hz, 1H), 1.72 (dd, $J = 15.9, 12.2$ Hz, 1H), 1.14 (t, $J = 7.0$ Hz, 3H), 0.82 (d, $J = 6.4$ Hz, 3H). ¹³C NMR (126 MHz, DMSO-*d*₆) δ 190.65, 186.68, 173.38, 99.69, 61.04, 59.54, 44.45, 32.42, 20.73, 14.70. LC-MS (ESI-) $R_t = 1.5$ min m/z [M-H] = 197.2. HR-MS calculated for C₁₀H₁₃O₄ 197.0814, found 197.0802 ($\Delta = -1.2$ mDa; 0.5 ppm). FT-IR (neat) ν 2948 (O-H, m), 1701 (C=O, s), 1530 (C=O, s), 1453 (m), 1416 (m), 1351 (s), 1336 (m), 1302 (s), 1287 (m), 1267 (s), 1254 (m), 1225 (m), 1216 (s), 1189 (m), 1148 (s), 1039 (s), 882 (m), 823 (s) cm^{-1} . Melting point: 248.3 – 256.9 °C (EtOH).



Methyl 3,6-dimethyl-2,4-dioxocyclohexanecarboxylate (23):³³² yellowish powder (207 g, 95% yield). ¹H NMR (400 MHz, DMSO-*d*₆) δ 10.68 (s, 1H), 3.62 (s, 3H), 3.16 – 3.01 (m, 1H), 2.50 – 2.38 (m, 1H), 2.37 – 2.24 (m, 2H), 1.53 (s, 3H), 0.92 (d, $J = 6.2$ Hz, 3H). ¹³C NMR (101 MHz, DMSO-*d*₆) δ 193.41, 172.30, 171.63, 108.99, 59.77, 51.95, 36.43, 31.36, 19.70, 7.73. LC-MS (ESI+) $R_t = 1.28$ min m/z [M+H] = 199.3 HR-MS calculated for C₁₀H₁₅O₄ 199.0970, found 199.0971 ($\Delta = 0.1$ mDa; 0.5 ppm). FT-IR (neat) ν 3062 (w, OH), 2965 (w, CH), 2931 (w, CH), 2652 (w), 1730 (s, C=O), 1388 (s, CH), 1366 (s, CH), 1318 (s), 1242 (s, CN), 1203 (s), 1152 (s), 1077 (s), 990 (m), 802 (m), 651 (m) cm^{-1} . Melting point: 158.8 – 160.6 °C (EtOAc), literature: 143 – 145 °C.³³² Crystal Data for C₁₀H₁₄O₄ (M = 198.21 g/mol):

orthorhombic, space group $Pna2_1$ (no. 33), $a = 14.1800(15) \text{ \AA}$, $b = 12.8303(12) \text{ \AA}$, $c = 5.3183(5) \text{ \AA}$, $V = 967.58(16) \text{ \AA}^3$, $Z = 4$, $T = 120 \text{ K}$, $\mu(\text{MoK}\alpha) = 0.105 \text{ mm}^{-1}$, $D_{\text{calc}} = 1.361 \text{ g/cm}^3$, 13090 reflections measured ($4.282^\circ \leq 2\theta \leq 54.998^\circ$), 2216 unique ($R_{\text{int}} = 0.0585$, $R_{\text{sigma}} = 0.0474$) which were used in all calculations. The final R_1 was 0.0509 ($I > 2\sigma(I)$) and wR_2 was 0.1286 (all data). Operator reference number: 19srv231.

*General procedure to gain compound 78 through 79*³³³

In a round bottom flask filled with EtOH (40 mL), **22-Et** (1.98 g, 10 mmol, 1 eq.), and paraformaldehyde (601 mg, 20 mmol, 2 eq.), dimethylamine hydrochloride (915 mg, 11 mmol, 1.1 eq.) was added. The mixture was stirred under reflux until the disappearance of the starting material as monitored by TLC (Eluent: DCM:MeOH 95:5). The solvent was removed *in vacuo* and the residue checked via LC-MS (ESI) and $^1\text{H-NMR}$. A second experiment was performed using piperidine (296 μL , 3 mmol, 0.3 eq.) as catalyst and acetic acid (57 μL , 1 mmol, 0.1 eq.).

General procedure to attempt alkylation of Na-22 with paraformaldehyde

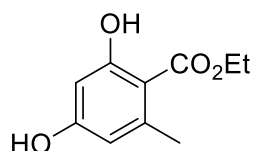
To a solution of paraformaldehyde (300.3 g, 10 mol, 1 eq.) in the EtOH (10 mL) under reflux, was slowly added a solution of **Na-22** (2.2 g, 10 mmol, 1 eq.) in EtOH (10 mL). The reaction mixture was then stirred under reflux for 30 minutes and monitored via LC-MS (ESI). In all the cases a white powder was obtained. All the other reaction conditions and temperatures are described on *Table 5*.

*Oxidation of 22-Et using CuBr₂ in excess*¹⁵⁴

To a solution of **22-Et** (1.98 g, 10 mmol, 1 eq.) in MeCN (10 mL), was added in one portion copper(II) bromide (4.5 g, 20 mmol, 2 eq.). The reaction was then stirred for 4 hours under reflux. The brown mixture was concentrated under vacuum to obtain a brown residue, which was partitioned between water (10 mL) and EtOAc (10 mL). The organic phase was removed and the aqueous phase was extracted with EtOAc ($3 \times 10 \text{ mL}$). The residue was then analysed through (GC-MS polar compounds) reporting the RAP of the compounds **82** ($R_t = 5.26 \text{ min}$ (major isomer) – 5.28 min (minor isomer)), **22-Et** ($R_t = 3.63 \text{ min}$), and **34-Et** ($R_t = 5.08 \text{ min}$). The results are depicted in *Scheme 19*.

*General procedure for the preparation of 34-Et*³³⁴

To an ice-cooled solution of **22-Et** (1.98 g, 10 mmol, 1 eq.), acetic anhydride (2.83 mL, 30 mmol, 3 eq.) in acetic acid (6 mL), was added dropwise a solution of bromine (500 μ L, 10 mmol, 1 eq.) in acetic acid (1 mL). After 1 hour of stirring under reflux, hydrobromic acid (33% sol. in acetic acid, 178 μ L, 1 mmol, 0.1 eq.) and water (2 mL) were poured into the reaction mixture. The reaction was stirred for a further 30 minutes and then allowed to cool to room temperature. The mixture was poured into water (20 mL) and extracted with Et₂O (3 \times 20 mL). The combined organic phase was washed with water (20 mL) and saturated NaHCO₃ aqueous solution (20 mL) until there was no more bubbling occurred. The solution was dried over Na₂SO₄ and concentrated under vacuum to gain a white powder. The residue was purified via flash chromatography (Eluent: hexane:chloroform 9:1) to yield **34-Et** (1.12 g, 57% yield).



Ethyl 2,4-dihydroxy-6-methylbenzoate (34-Et):³³⁵ White solid (R_f = 0.4, hexane:chloroform 9:1). ¹H NMR (400 MHz, Chloroform-*d*) δ 6.30 (dd, *J* = 2.6, 0.5 Hz, 1H), 6.25 (dt, *J* = 2.6, 0.8 Hz, 1H), 4.42 (q, *J* = 7.1 Hz, 2H), 2.52 (s, 3H), 1.43 (t, *J* = 7.1 Hz, 3H). ¹³C NMR (101 MHz, Chloroform-*d*) δ 171.73, 165.27, 160.28, 144.04, 111.37, 101.28, 61.33, 24.36, 14.24. GC-MS (EI) R_t = 5.06 min m/z [M]⁺ = 196.1. HR-MS calculated for C₁₀H₁₃O₄ 197.0814, found 197.0816 (Δ = 0.2 mDa; 1.0 ppm). FT-IR (neat) ν 3352 (br, OH), 2981 (w), 2937 (w, CH), 1637 (s, C=O), 1601 (s), 1583 (s), 1504 (m), 1483 (m), 1463 (m), 1454 (m), 1403 (m), 1379 (m), 1317 (m), 1218 (s), 1173 (s), 1125 (s), 1077 (m), 834 (m) cm⁻¹. Melting point: 110.3 – 124.3 °C (Et₂O), literature: 135 – 136 °C (EtOH).³³⁵

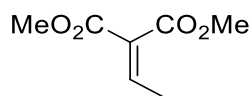
*Oxidation of 22-Et using CuCl₂ and LiCl in excess*¹⁵⁵

To a solution of **22-Et** (1.98 g, 10 mmol, 1 eq.) in MeCN (100 mL), copper(II) chloride (1.27 g, 30 mmol, 3 eq.) and lithium chloride (4.03 g, 30 mmol, 3 eq.) were added. The reaction mixture was then stirred under reflux and monitored via LC-MS (ESI). After stirring overnight, the mixture was allowed to cool to room temperature. The solvent was removed under vacuum and the residue was partitioned between water (20 mL) and Et₂O (20 mL). The organic phase was removed and the aqueous phase was extracted with Et₂O (2 \times 20 mL). The combined organic phases was washed with brine (10 mL), dried over Na₂SO₄ and concentrated *in vacuo*

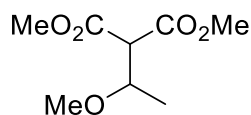
to furnish a brown oil. The oil was purified via flash chromatography (Eluent: hexane:chloroform 9:1) to isolate **34-Et** as a white solid (137 mg, 7% yield).

*General procedure as applied to reaction condition screening for the synthesis of compound **89***

In a 100 mL round bottom flask containing dimethyl malonate (**26**) (11.4 mL, 100 mmol, 1 eq.) in MeOH (50 mL) was added acetaldehyde (**91**) (5.6 mL, 100 mmol, 1 eq.). Na₂SO₄ (3 g) or trimethyl orthoformate (0.1 – 0.5% mol) were added to the solution as dehydrating additives. The catalyst (3 or 50 mol%) was added to the reaction mixture and it was stirred at room temperature for 1 or 72 hours. The reaction mixture was filtrated to remove the catalyst and concentrated to yield a yellow oil, which was analysed via ¹H-NMR and GC-MS nonpolar compounds (EI). One of the residue (*Entry 12, Table 7*) was purified via flash chromatography (Eluent: hexane:AcOEt gradient from 85:15 to 65:35) to yield the products **93** (888 mg, 4.7% yield), **89&95** (as a 4:6 mixture, 365 mg, 0.8% yield), **92** (320 mg, 1.1 % yield), and **94** (130 mg, 0.4% yield).

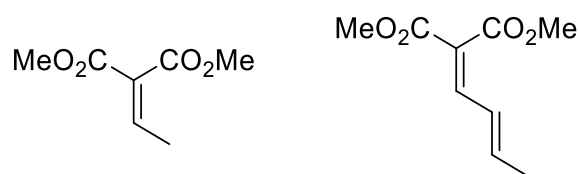


*Dimethyl 2-ethylidenemalonate (89):*¹⁶⁴ Isolated through vacuum distillation as a yellow liquid (R_f = 0.7, hexane:AcOEt 85:15). ¹H NMR (600 MHz, Chloroform-*d*) δ 7.10 (q, *J* = 7.3 Hz, 1H), 3.81 (s, 3H), 3.75 (s, 3H), 1.93 (d, *J* = 7.3 Hz, 3H). ¹³C NMR (151 MHz, Chloroform-*d*) δ 165.75, 164.31, 145.78, 128.93, 52.26, 52.18, 15.64. GC-MS (EI) R_t = 3.32 min m/z [M]⁺ = 158.1 HR-MS calculated for C₇H₁₁O₄ 159.0657, found 159.0661 (Δ = 0.4 mDa; 2.5 ppm). FT-IR (neat) ν 2957 (w, CH), 1724 (s, C=O), 1670 (w, C=C), 1436.73 (s), 1383 (m), 1358 (m), 1263 (s), 1223 (s), 1128 (s), 1024 (m), 1004 (m), 827 (w), 727 (w) cm⁻¹. b.p. 120 °C & 18 mbar, literature: 105 °C & 17 mbar.¹⁶⁴

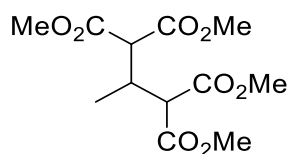


Dimethyl 2-(1-methoxyethyl)malonate (93): Yellow liquid (R_f = 0.5, hexane:AcOEt 85:15). ¹H NMR (600 MHz, Chloroform-*d*) δ 3.99 – 3.90 (m, 1H), 3.74 (s, 3H), 3.72 (s, 3H), 3.49 (d, *J* = 8.7 Hz, 1H), 3.33 (s, 3H), 1.23 (d, *J* = 6.2 Hz, 3H). ¹³C NMR (151 MHz, Chloroform-*d*) δ

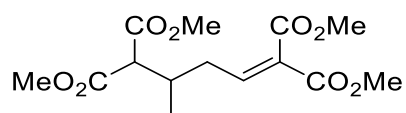
167.98, 167.54, 75.39, 58.16, 56.89, 52.51, 52.49, 16.90. GC-MS (EI) $R_t = 3.30$ min m/z $[M-CH_3OH]^+ = 158.1$ HR-MS calculated for $C_8H_{15}O_5$ 191.0919, found 191.0926 ($\Delta = 0.7$ mDa; 3.7 ppm). FT-IR (neat) ν 2957 (m, CH), 1734 (s, C=O), 1436 (s), 1218 (m), 1178 (m), 1144 (m), 1021 (m), 822 (w), 755 (w) cm^{-1} .



Dimethyl 2-allylidene malonate (95): Red oil ($R_f = 0.7$, hexane:AcOEt 85:15) Isolated as a 60:40 mixture **89:95**. 1H NMR (700 MHz, Chloroform-*d*) δ 7.35 (d, $J = 11.6$ Hz, 1H), 6.52 (ddq, $J = 14.8, 11.6, 1.7$ Hz, 1H), 6.34 (dq, $J = 14.8, 6.8, 0.8$ Hz, 1H), 3.83 (s, 3H), 3.77 (s, 3H), 1.90 (dd, $J = 6.8, 1.7$ Hz, 3H). ^{13}C NMR (176 MHz, Chloroform-*d*) δ 165.16, 146.14, 145.00, 127.18, 122.57, 52.27, 52.21, 19.07. GC-MS nonpolar compounds (EI) $R_t = 4.01$ min m/z $[M]^+ = 184.1$ HR-MS calculated for $C_9H_{13}O_4$ 185.0814, found 185.0818 ($\Delta = 0.4$ mDa; 2.2 ppm).



Tetramethyl 2-methylpropane-1,1,3,3-tetracarboxylate (92):³³⁶ Colourless oil ($R_f = 0.35$, hexane:AcOEt 85:15). 1H NMR (600 MHz, Chloroform-*d*) δ 3.74 (s, 12H), 3.65 (d, $J = 7.0$ Hz, 2H), 3.00 (q, $J = 7.0$ Hz, 1H), 1.10 (d, $J = 7.0$ Hz, 3H). ^{13}C NMR (151 MHz, Chloroform-*d*) δ 168.69, 168.43, 53.94, 52.58, 52.43, 32.84, 14.33. GC-MS nonpolar compounds (EI) $R_t = 4.97$ min m/z $[M-MeOH]^+ = 259.1$ HR-MS calculated for $C_{12}H_{19}O_8$ 291.1080, found 291.1082 ($\Delta = 0.2$ mDa; 0.7 ppm). FT-IR (neat) ν 2957 (m, CH), 1730 (s, C=O), 1435 (m), 1268 (m), 1223 (m), 1212 (m), 1155 (s), 1069 (m), 1025 (m) cm^{-1} .



Tetramethyl 4-methylpent-1-ene-1,1,5,5-tetracarboxylate (94): Yellow oil ($R_f = 0.2$, hexane:AcOEt 85:15). 1H NMR (600 MHz, Chloroform-*d*) δ 7.05 – 6.96 (m, 1H), 3.82 (d, $J =$

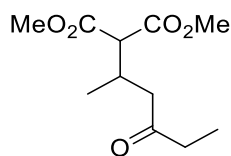
1.0 Hz, 3H), 3.78 (d, $J = 1.0$ Hz, 3H), 3.74 – 3.71 (m, 6H), 3.29 (dd, $J = 7.6, 1.0$ Hz, 1H), 2.52 – 2.44 (m, 2H), 2.34 – 2.25 (m, 1H), 1.01 (d, $J = 6.6$ Hz, 3H). ^{13}C NMR (151 MHz, Chloroform-*d*) δ 168.68, 165.51, 164.05, 147.14, 129.61, 56.49, 52.46, 52.41, 52.28, 34.17, 32.98, 17.26. GC-MS nonpolar compounds (EI) $R_t = 5.53$ min m/z $[\text{M-MeOH}]^+ = 284.1$ HR-MS calculated for $\text{C}_{14}\text{H}_{21}\text{O}_8$ 317.1236, found 317.1244 ($\Delta = 0.8$ mDa; 2.5 ppm). FT-IR (neat) ν 2956 (w, CH), 1727 (s, C=O), 1435 (s), 1221 (m), 1153 (m), 1057 (m), 931 (w), 828 (w), 728 (w) cm^{-1} .

General procedure to apply for the reaction condition screening for the synthesis of 89 with flow apparatus.

In 50 mL conical flask, dimethyl malonate (11.4 mL, 100 mmol, 1 eq.) and acetaldehyde (5.6 mL, 100 mmol, 1 eq.) were solubilised in MeOH (50 mL). Using a Vapourtec SF-10 peristaltic pump (blue peristaltic tubing), the mixture was streamed in a Diba Omnifit column (15 mm x 100 mm) filled up with 6.7 grams of PS-DMA at a flow rate of $800 \mu\text{L min}^{-1}$ in order to achieve a contact time for the mixture of 12.5 minutes (Volume of filled column = 10 mL). The system was allowed to reach the steady state conditions (2 reactor process volumes) and then 7 mL of the mixture (10 mmol) was collected in a second 50 mL conical flask. The mixture was then concentrated under vacuum and analysed via ^1H -NMR spectra. Different reaction conditions and residence times were investigated as depicted in *Table 8*.

General procedure for the attempt to obtain 96 from 90 and 89

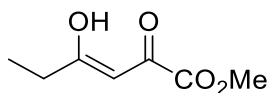
To freshly distilled diisopropylamine (3.4 mL, 24 mmol, 1.2 eq.) in dry THF (60 mL), was added a 1.6 M solution of *n*-butyllithium in hexanes (13.7 mL, 22 mmol, 1.1 eq.) at -78 °C. The mixture was stirred for 1 minute and a solution of 2-butanone (**90**) (1.79 mL, 20 mmol, 1 eq.) in dry THF (40 mL) was slowly added at -78 °C. After stirring for 15 minutes, a solution of compound **89** (3.8 g, 24 mmol, 1.2 eq.) in dry THF (40 mL) was slowly added to the mixture. The solution was stirred at -78 °C and then allowed to warm to room temperature. After 1 hour of stirring, the solution was quenched with a saturated solution of NH_4Cl (100 mL). The THF was removed under vacuum and the organic material extracted with EtOAc (3×50 mL). The combined organic layer was washed with water, brine, dried over Na_2SO_4 , and concentrated under vacuum. The residue was purified through flash chromatography (Eluent: Hexane:AcOEt 8:2) to yield the compound **96** (829 mg, 15% yield).



Dimethyl 2-(4-oxohexan-2-yl)malonate (96):³³⁷ Colourless oil (Rf = 0.44, Hexane:AcOEt 8:2). ¹H NMR (400 MHz, Chloroform-*d*) δ 3.72 (d, *J* = 0.9 Hz, 6H), 3.41 (d, *J* = 6.7 Hz, 1H), 2.86 – 2.73 (m, 1H), 2.64 (dd, *J* = 17.1, 5.0 Hz, 1H), 2.49 – 2.31 (m, 3H), 1.04 (t, *J* = 7.3 Hz, 3H), 1.01 (d, *J* = 6.8 Hz, 3H). ¹³C NMR (101 MHz, Chloroform-*d*) δ 210.07, 169.20, 169.16, 56.02, 52.51, 52.50, 46.32, 36.46, 29.18, 17.93, 7.86. LC-MS (ESI+) Rt = 2.76 min m/z [M+H]⁺ = 231.1. HR-MS calculated for C₁₁H₁₉O₅ 231.1232, found 231.1246 (Δ = 1.4 mDa; 6.1 ppm). FT-IR (neat) ν 2976 (CH, w), 2955 (CH, w), 2884 (CH, w), 1732 (C=O, s), 1713 (C=O, s), 1460 (w), 1436 (m), 1247 (m), 1196 (s), 1156 (s), 1117 (m), 1023 (m) cm⁻¹.

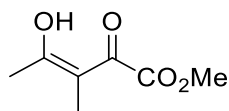
*General procedure for the synthesis of 100 and 102*¹⁷⁷

To an ice-cooled suspension of dimethyl oxalate (**101**) (5.9 g, 50 mmol, 1 eq.) and sodium methoxide (3.24 g, 60 mmol, 1.2 eq.) in diethyl ether (50 mL), 2-butanone (**90**) (4.5 mL, 50 mmol, 1 eq.) was slowly added over 30 minutes. The mixture was then allowed to warm to room temperature and left stirring for 24 hours. The reaction mixture was quenched with conc. hydrochloric acid (38%) until pH 1 and extracted with diethyl ether (3 × 50 mL). The combined organic phase was treated with brine (50 mL), dried over Na₂SO₄, and concentrated under vacuum. The residue was then purified through flash chromatography (Eluent: Hexane:AcOEt 6:4) to yield the compounds **100** (3.08 g, 39% yield) and **102** (2.05 g, 26% yield). Different reaction conditions were also evaluated where the reaction mixture was concentrated before quenching with conc. HCl until pH 1 as depicted in *Table 10*.



Methyl 2,4-dioxohexanoate (100): Colourless oil (Rf = 0.65, Hexane:AcOEt 6:4). ¹H NMR (599 MHz, Acetonitrile-*d*₃) δ 6.38 (s, 1H), 3.82 (s, 3H), 2.57 (q, *J* = 7.4 Hz, 2H), 1.10 (t, *J* = 7.4 Hz, 3H). ¹³C NMR (151 MHz, Acetonitrile-*d*₃) δ 206.42, 165.64, 163.46, 102.66, 53.56, 35.03, 8.66. LC-MS (ESI+) Rt = 1.76 min m/z [M+H]⁺ = 159.3. HR-MS calculated for C₇H₁₁O₄ 156.0657, found 159.0648 (Δ = -0.9 mDa; -5.7 ppm). FT-IR (neat) ν 3235 (w, OH), 2916 (w,

CH), 2848 (w), 1753 (s, C=O), 1721 (s, C=O), 1648 (m), 1437 (m), 1353 (m), 1305 (m), 1266 (m), 1220 (m), 1165 (s), 1112 (s), 1021 (s), 854 (m), 775 (m), 625 (m) cm^{-1} .



methyl 3-methyl-2,4-dioxopentanoate (102): White solid ($R_f = 0.25$, Hexane:AcOEt 6:4). ^1H NMR (599 MHz, Acetonitrile- d_3) δ 7.13 (s, 1H), 3.06 (s, 3H), 1.77 (s, 3H), 1.53 (s, 3H). ^{13}C NMR (151 MHz, Acetonitrile- d_3) δ 167.63, 140.60, 128.53, 108.14, 50.67, 23.66, 8.34. LC-MS (ESI+) $R_t = 1.42$ min m/z $[\text{M}+\text{H}]^+ = 159.3$. HR-MS calculated for $\text{C}_7\text{H}_{11}\text{O}_4$ 159.0657, found 159.0655 ($\Delta = -0.2$ mDa; -1.3 ppm). FT-IR (neat) ν (cm^{-1}) 3264 (w, OH), 2997 (w, CH), 2960 (w, CH), 2926 (w, CH), 1767 (s, C=O), 1721 (s, C=O), 1462 (w), 1396 (w), 1353 (m), 1305 (m), 1222 (m), 1164 (s), 1114 (m), 1063 (m), 1021 (s), 887 (m), 853 (m), 776 (m), 625 (w), 508 (m) cm^{-1} . Melting point: 83.8 – 89.1 $^\circ\text{C}$ (EtOAc).

One-pot procedure for the synthesis of 99¹⁷⁷

To an ice-cooled suspension of dimethyl oxalate (**101**) (12.0 g, 102 mmol, 1 eq.) and sodium methoxide (6.6 g, 122 mmol, 1.2 eq.) in diethyl ether (102 mL), was slowly added butanone (**90**) (9.13 mL, 102 mmol, 1 eq.) over 30 minutes. The mixture was then allowed to warm to room temperature and left stirring for 24 hours. The reaction mixture was partitioned with water (150 mL) and the aqueous phase was cooled to 5 $^\circ\text{C}$. Acetaldehyde (**91**) (11 mL, 204 mmol, 2 eq.) was added in one portion raising the temperature to ~ 15 $^\circ\text{C}$. The mixture was then stirring for 75 minutes at 5 $^\circ\text{C}$. The yellow solution was quenched with conc. hydrochloric acid (38%) to pH 1 and the precipitate formed filtered and dried under vacuum. The yellowish solid was crystallised from a 1:1 mixture of $\text{H}_2\text{O}:\text{MeOH}$ to yield white crystals of **99** (9.20 g, 53% yield).

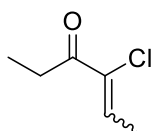


3-Hydroxy-5-methyl-4-propionylfuran-2(5H)-one (99): White crystal. ^1H NMR (599 MHz, $\text{DMSO}-d_6$) δ 5.12 (q, $J = 6.4$ Hz, 1H), 2.86 – 2.72 (m, 2H), 1.38 (d, $J = 6.4$ Hz, 3H), 0.99 (t, $J = 7.3$ Hz, 3H). ^{13}C NMR (151 MHz, $\text{DMSO}-d_6$) δ 195.91, 169.36, 148.82, 124.52, 75.36, 35.04,

19.77, 7.71. LC-MS (ESI+) $R_t = 1.42$ min m/z $[M+H]^+ = 171.1$. HR-MS calculated for $C_8H_{11}O_4$ 171.0657, found 171.0646 ($\Delta = -1.1$ mDa; -6.4 ppm). FT-IR (neat) ν 3450 (w, OH), 3260 (w, OH), 2982 (w, CH), 2946 (w), 1737 (s, C=O), 1634 (s), 1444 (s), 1376 (s), 1334 (s), 1213 (s), 1169 (s), 1118 (m), 1046 (m), 950 (w), 866 (m), 784 (w), 694 (m), 598 (m) cm^{-1} . Melting point: 83.9 – 86.3 °C (MeOH:H₂O, 1:1). Crystal Data for $C_8H_{12}O_5$ ($M = 188.18$ g/mol): monoclinic, space group $P2_1/c$ (no. 14), $a = 5.2952(3)$ Å, $b = 13.9259(7)$ Å, $c = 12.5367(7)$ Å, $\beta = 102.176(2)^\circ$, $V = 903.66(9)$ Å³, $Z = 4$, $T = 120$ K, $\mu(Mo\ K\alpha) = 0.116$ mm⁻¹, $D_{calc} = 1.383$ g/cm³, 15755 reflections measured ($4.428^\circ \leq 2\theta \leq 60.072^\circ$), 2661 unique ($R_{int} = 0.0429$, $R_{\sigma} = 0.0321$) which were used in all calculations. The final R_1 was 0.0552 ($I > 2\sigma(I)$) and wR_2 was 0.1200 (all data). Operator reference number: 20srv219.

*General procedure for the synthesis of compound 98*¹⁷⁷

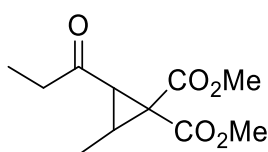
To a stirred solution of compound **99** (8.78 g, 46.7 mmol, 1 eq.) in a 3:1 mixture of MeOH:H₂O (100 mL), trichloroisocyanuric acid (3.91 g, 15.2 mmol, 0.325 eq.) was added portion wise at room temperature. After the addition was complete the reaction mixture was stirred for 1 hour and the resulting suspension was filtered off and the filtrate cooled to 0 °C. Sodium bicarbonate was slowly added (13.70 g, 163.4 mmol, 3.5 eq.) and then vigorously stirred for 45 minutes. The methanol was removed from the reaction mixture under vacuum and the aqueous phase extracted with EtOAc (3 × 50 ml). The combined organic phase was washed with brine, dried over Na₂SO₄, and concentrated to yield **98** (4.70 g, 76% yield).



4-Chlorohex-4-en-3-one (98): Dark yellow oil. ¹H NMR (600 MHz, Chloroform-*d*) δ 7.04 (q, $J = 6.9$ Hz, 1H), 2.77 (q, $J = 7.2$ Hz, 2H), 1.97 (d, $J = 6.9$ Hz, 3H), 1.12 (t, $J = 7.3$ Hz, 3H). ¹³C NMR (151 MHz, Chloroform-*d*) δ 195.17, 135.55, 134.67, 32.03, 15.31, 8.42. LC-MS (ESI+) $R_t = 1.96$ min m/z $[M+H]^+ = 133.7$ (100%)/ 135.7 (30%). HR-MS calculated for $C_6H_{10}OCl$ ³⁵ 133.0420, found 133.0443 ($\Delta = 2.3$ mDa; 17.3 ppm). FT-IR (neat) ν 2981 (CH, w), 2942 (CH, w), 2879 (CH, w), 1687 (C=O, s), 1619 (C=C, s), 1459 (m), 1378 (m), 1271(m), 1192 (m), 1167 (m), 1102 (w), 1058 (w), 946 (w), 891 (w), 851 (C-Cl, s), 791 (s), 698 (m), 576 (w) cm^{-1} .

General procedure for the attempted synthesis of Veramoss from compound **98**

To an ice-cooled suspension of sodium methoxide (489 mg, 9.05 mmol, 1.2 eq.) in THF (4 mL), was added slowly dimethyl malonate (**26**) (996 mg, 7.54 mmol, 1.0 eq.). After 10 minutes at 0 °C, compound **98** (1.0 g, 7.54 mmol, 1.0 eq.) was added and the red mixture was then stirred at r.t. for 12 hours. The suspension was quenched with hydrochloric acid (1 M) until pH 1 and then extracted with AcOEt (3 × 20 mL). The combined organic phase was washed with brine, dried over Na₂SO₄, and concentrated under reduced pressure. The residue was then purified by flash chromatography (Eluent: Hexane:AcOEt 8:2) to yield **106** (361 mg, 21% yield).



Dimethyl 2-methyl-3-propionylcyclopropane-1,1-dicarboxylate (106): Colourless oil (R_f = 0.35, Hexane:AcOEt 8:2) ¹H NMR (600 MHz, Chloroform-*d*) δ 3.76 (s, 3H), 3.71 (s, 3H), 2.76 (d, *J* = 7.1 Hz, 1H), 2.62 (qd, *J* = 7.3, 3.3 Hz, 2H), 2.37 (dq, *J* = 7.0, 6.4 Hz, 1H), 1.21 (d, *J* = 6.4 Hz, 3H), 1.06 (t, *J* = 7.3 Hz, 3H). ¹³C NMR (151 MHz, Chloroform-*d*) δ 206.22, 167.43, 167.07, 53.10, 52.69, 44.57, 39.75, 37.86, 28.33, 11.43, 7.72. LC-MS (ESI+) R_t = 1.89 min m/z [M+H]⁺ = 229.1. HR-MS calculated for C₁₁H₁₇O₅ 229.1076, found 229.1099 (Δ = 2.3 mDa; 10.0 ppm). FT-IR (neat) ν 2963 (CH, w), 2954 (CH, w), 1733 (C=O, s), 1708 (C=O, s), 1436 (m), 1340 (w), 1292 (m), 1258 (m), 1211 (s), 1145 (s), 1109 (m), 1024 (m) cm⁻¹.

General procedure for the attempt to synthesis the alkyne **107** from **98**

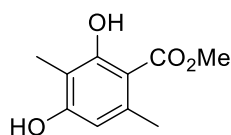
To a solution of **107** (132 mg, 1 mmol, 1.0 eq.) in the desired solvent (2 mL), the specific base was added (2.0 eq.). The mixture was then stirred at the desired temperature for 14 – 48 hours analysing the mixture every 2 hours via GC-MS nonpolar compounds (EI). The results are depicted in *Table 11*.

General procedure for the oxidation of Veramoss (**11**) with chlorine gas

NOTE: The chlorine gas for the following reaction was obtained using KMnO₄ and aqueous conc. HCl exploiting the following reaction: 4 KMnO₄ + 16 HCl → 2 KCl + 2 MnCl₂ + 8 H₂O

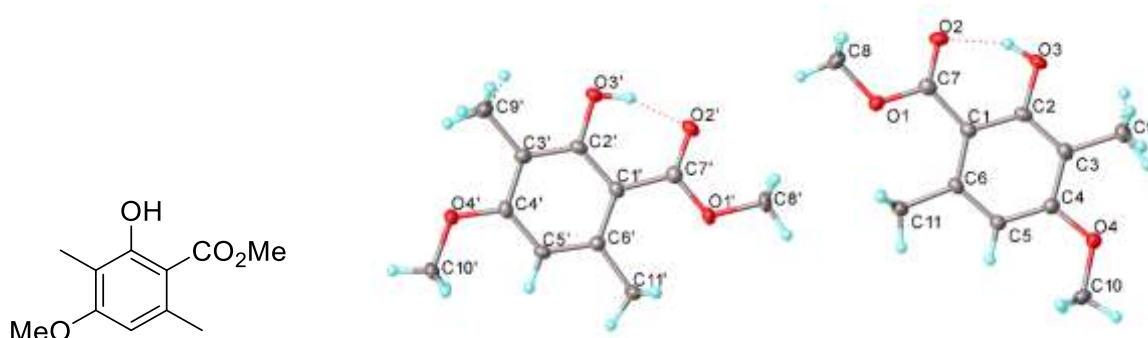
+ 5 Cl₂. The generated gas was first bubbled through water to reduce the HCl content in the chlorine.

To a mixture of compound **23** (9.9 g, 50 mmol, 1.0 eq.) in MeOH (13 mL), was added a 5 M solution of MeONa in MeOH (12 mL, 60 mmol, 1.2 eq.) at 0 °C. After 10 minutes of stirring, polyphosphoric acid (13.0 g, 80 mmol, 1.6 eq.) was slowly added to the solution (The viscous oil was first heated at 80 °C before the dropwise addition). Chlorine gas was bubbled through the solution until disappearance of the starting material **23** as indicated by TLC (Eluent: Hexane:AcOEt 8:2; R_f of **23** = 0.16, R_f of Cl-**23** = 0.45). At this stage two different work-up conditions were applied: **Conditions A**-The solvent was evaporated under reduced pressure and the residue was then solubilised in toluene (100 mL) and a saturated solution of NaHCO₃ (100 mL) was added until neutralisation of the aqueous layer. The organic phase was extracted with a 2 M solution of NaOH (3 × 25 mL) and then the solvent was evaporated under reduced pressure and the residue was purified via flash chromatography (Eluent: 15% AcOEt in Hexane) to obtain compound **29** (847 mg, 8% yield). The solid was crystallised from MeOH. The original aqueous phase was acidified with conc. Hydrochloric acid (38%) and the resulting white precipitate filtrated to yield Veramoss (**11**) (1.96 g, 20% yield); **Conditions B**-The solution was heated under reflux until disappearance of the intermediates Cl-**7** on TLC (Eluent: Hexane:AcOEt 8:2; R_f of Cl-**23** = 0.40 to 0.2, R_f of **11** = 0.56). Water (100 mL) was added and the mixture stirred, over 1 hour the solution turned yellow. The reaction was allowed to cool to room temperature where a precipitate forms. The yellow precipitate was filtered, washed with water until the washings reached pH 7, and then washed with toluene (500 mL) until disappearance of the yellow colour. The resultant white solid was then crystallised from a 1:1 mixture of MeOH:H₂O to yield Veramoss (981 mg, 10% yield).



Methyl 2,4-dihydroxy-3,6-dimethylbenzoate (11):³³² White crystal (R_f = 0.56, Hexane:AcOEt 8:2). ¹H NMR (400 MHz, DMSO-*d*₆) δ 11.69 (s, 1H), 10.11 (s, 1H), 6.28 (s, 1H), 3.84 (s, 3H), 2.36 (s, 3H), 1.95 (s, 3H). ¹³C NMR (101 MHz, DMSO-*d*₆) δ 172.31, 162.26, 160.48, 139.23, 110.97, 108.57, 104.33, 52.30, 23.95, 8.42. GC-MS polar compounds (EI) R_t = 5.00 min m/z [M]⁺ = 196.1 HR-MS calculated for C₁₀H₁₃O₄ 197.0814, found 197.0836 (Δ = 2.2 mDa; 11.2

ppm). FT-IR (neat) ν 3370 (br, OH), 3180 (br, OH), 2958 (w, CH), 1618 (s, C=O), 1608 (s), 1498 (m), 1440 (s), 1371 (m), 1308 (s), 1291 (s), 1271 (s), 1198 (s), 1178 (m), 1108 (m), 1059 (m), 1031 (s), 991 (m), 941 (m), 825 (w), 725 (m) cm^{-1} . Melting point: 135.5 – 138.4 °C (MeOH), literature: 143 – 145 °C.³³²

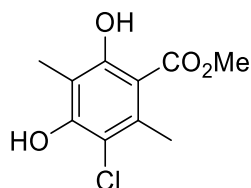


Methyl 2-hydroxy-4-methoxy-3,6-dimethylbenzoate (29).³³⁸ White solid (R_f = 0.67, hexane:AcOEt 8:2). ^1H NMR (700 MHz, Chloroform- d) δ 11.82 (s, 1H), 6.27 (s, 1H), 3.92 (s, 3H), 3.85 (s, 3H), 2.53 (s, 3H), 2.07 (s, 3H). ^{13}C NMR (176 MHz, Chloroform- d) δ 172.70, 162.24, 161.54, 140.26, 111.01, 106.00, 105.62, 55.59, 51.92, 24.78, 7.94. LC-MS (ESI+) R_t = 3.19 min m/z $[\text{M}+\text{H}]^+$ = 211.5. HR-MS calculated for $\text{C}_{11}\text{H}_{15}\text{O}_4$ 211.0970, found 211.0971 (Δ = 0.1 mDa; 0.5 ppm). FT-IR (neat) ν 2952 (w, C-H), 2924 (w, C-H), 2855 (w), 1646 (s, C=O), 1624 (s), 1608 (m), 1575 (s), 1438 (s), 1401 (s), 1367 (s), 1300 (s), 1235 (s), 1197 (s), 1135 (s), 1003 (m), 803 (s) cm^{-1} . Melting point: 89.8 – 92.5 °C (MeOH), literature: 93.5 °C.³³⁸ Crystal data for $\text{C}_{11}\text{H}_{14}\text{O}_4$ (M = 210.22 g/mol): triclinic, space group P-1 (no. 2), a = 7.8320(8) Å, b = 10.8772(11) Å, c = 12.7976(13) Å, α = 107.084(3)°, β = 91.175(3)°, γ = 101.539(3)°, V = 1017.40(18) Å³, Z = 4, T = 120 K, $\mu(\text{MoK}\alpha)$ = 0.104 mm^{-1} , D_{calc} = 1.372 g/cm^3 , 11705 reflections measured ($4.372^\circ \leq 2\theta \leq 49.996^\circ$), 3578 unique (R_{int} = 0.0309, R_{sigma} = 0.0403) which were used in all calculations. The final R_1 was 0.0424 ($I > 2\sigma(I)$) and wR_2 was 0.1161 (all data). Operator reference number: 19srv047.

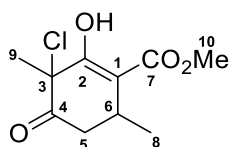
General procedure for the oxidation of Veramoss (11) with sodium hypochlorite

To a mixture of compound **23** (9.9 g, 50 mmol, 1.0 eq.) in MeOH (13 mL), was added a 5 M solution of MeONa in MeOH (12 mL, 60 mmol, 1.2 eq.) at 0 °C. After 10 minutes of stirring, polyphosphoric acid (26 g, 160 mmol, 3.2 eq.) was slowly added to the solution (The viscous oil was first heated to 80 °C for the dropwise addition). An 18%_{w/v} solution of NaOCl was added to the mixture at 0 °C until disappearance of starting material **7** was determined by TLC

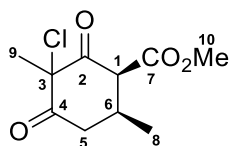
(Eluent: Hexane:AcOEt 8:2; Rf of **23** = 0.16, Rf of Cl-**23** = 0.45). The resulting yellow solution was heated to 67 °C and stirred until disappearance of the chlorinated intermediate on TLC (Eluent: Hexane:AcOEt 8:2; Rf of **11** = 0.56). The mixture was allowed to cool and then concentrated under vacuum and a 5 grams portion of the batch was purified via flash chromatography (Eluent: gradient Hexane:AcOEt 9:1 to 1:1) to yield Veramoss (**11**) (Rf = 0.45, 3 g, 64.5% yield) and additional by-products **111** (Rf = 0.67, 159 mg, 2.9% yield), **29** (Rf = 0.75, 57 mg, 1.1% yield), and **110** (Rf = 0.28, 173 mg, 3.1% yield).



Methyl 3-chloro-4,6-dihydroxy-2,5-dimethylbenzoate (111).³³⁹ White solid (Rf = 0.67, Hexane:AcOEt 8:2). ¹H NMR (700 MHz, Chloroform-*d*) δ 11.71 – 11.66 (m, 1H), 6.15 (s, 1H), 3.94 (s, 3H), 2.59 (d, *J* = 0.7 Hz, 3H), 2.17 (d, *J* = 0.8 Hz, 3H). ¹³C NMR (176 MHz, Chloroform-*d*) δ 172.09, 161.04, 153.96, 135.80, 113.81, 110.65, 106.52, 52.33, 19.88, 8.87. LC-MS (ESI+) Rt = 2.58 min m/z [M+H]⁺ = 231.2(100%)/ 233.2 (30%). HR-MS calculated for C₁₀H₁₂O₄³⁵Cl 231.0424, found 231.0411 (Δ = -1.3 mDa; -5.6 ppm).



Methyl 3-chloro-2-hydroxy-3,6-dimethyl-4-oxocyclohex-1-ene-1-carboxylate (110): Yellow oil (Rf = 0.28, Hexane:AcOEt 8:2). ¹H NMR (700 MHz, Chloroform-*d*) δ 12.42 (s, 1H, OH), 3.86 (s, 3H, **10**), 3.28 (ddd, *J* = 12.9, 6.9, 0.6 Hz, 1H, **5**), 3.16 (pd, *J* = 6.9, 2.2 Hz, 1H, **6**), 2.37 (dd, *J* = 12.9, 2.2 Hz, 1H, **5**), 1.80 (s, 3H, **9**), 1.00 (dd, *J* = 6.9, 0.6 Hz, 3H, **8**). ¹³C NMR (176 MHz, Chloroform-*d*) δ 200.30 (**4**), 172.06 (**7**), 167.06 (**2**), 104.21 (**1**), 62.61 (**3**), 52.55 (**10**), 41.74 (**5**), 27.96 (**6**), 22.08 (**8**), 21.50 (**9**). LC-MS (ESI+) Rt = 3.16 min m/z [M+H]^{+v} = 233.2 (100%)/ 235.2 (30%). HR-MS calculated for C₁₀H₁₄O₄Cl³⁵ 233.0581, found 233.0582 (Δ = 0.1 mDa; 0.4 ppm).



Methyl 3-chloro-3,6-dimethyl-2,4-dioxocyclohexane-1-carboxylate (109): Isolated as a white solid directly from the reaction mixture before heating to reflux. Isolated as a 6:4 mixture *trans*:*cis* isomer. *cis*-isomer: ^1H NMR (600 MHz, Chloroform-*d*) δ 3.79 (s, 3H, **10**), 3.42 (dd, $J = 16.4, 5.3$ Hz, 1H, **5**), 3.36 (d, $J = 7.0$ Hz, 1H, **1**), 2.96 (hd, $J = 7.1, 5.3$ Hz, 1H, **6**), 2.36 (ddd, $J = 16.4, 7.6, 0.7$ Hz, 1H, **5**), 1.70 (s, 3H, **9**), 1.00 (d, $J = 7.0$ Hz, 3H, **8**). ^{13}C NMR (151 MHz, Chloroform-*d*) δ 199.52 (**4**), 195.81 (**2**), 167.97 (**7**), 68.94 (**3**), 60.15 (**1**), 52.96 (**10**), 41.81 (**5**), 26.54 (**6**), 19.73 (**8**), 19.79 (**9**). *trans*-isomer: ^1H NMR (600 MHz, Chloroform-*d*) δ 4.13 (d, $J = 12.5$ Hz, 1H, **1**), 3.82 (s, 3H, **10**), 3.15 (dd, $J = 14.7, 13.6$ Hz, 1H, **5**), 2.64 (dd, $J = 14.7, 4.3$ Hz, 1H, **5**), 2.32 – 2.22 (m, 1H, **6**), 1.66 (s, 3H, **9**), 1.17 (d, $J = 6.3$ Hz, 3H, **8**). ^{13}C NMR (151 MHz, Chloroform-*d*) δ 198.66 (**4**), 196.54 (**2**), 168.74 (**7**), 67.88 (**3**), 58.74 (**1**), 52.50 (**10**), 42.58 (**5**), 28.65 (**6**), 20.24 (**8**), 18.07 (**9**). LC-MS (ESI+) Rt = 3.15 min m/z $[\text{M}+\text{H}]^{+\text{v}} = 233.2$ (100%)/ 235.2 (30%). HR-MS calculated for $\text{C}_{10}\text{H}_{14}\text{O}_4\text{Cl}^{35}$ 233.0581, found 233.0583 ($\Delta = 0.2$ mDa; 0.9 ppm).

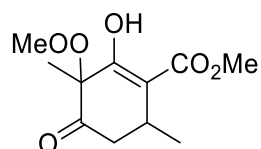
General procedure for the oxidation of 23 to Veramoss (11) using di-chlorinated compounds 108

To a solution of compound **23** (4.96 g, 25 mmol, 1.0 eq.) in MeOAc (25 mL), was added portion-wise TCCA (3.87 g, 15 mmol, 0.6 eq.). After stirring for 1 hour the mixture was filtered and the solution added to a solution containing **23** (3.96 g, 20 mmol, 0.8 eq.) and triethylamine (2.53 mL, 25 mmol, 1 eq.) in THF (20 mL). The combined mixture was stirred for 24 hours and quenched with PPA (3.14 g, 40 mmol, 1.5 eq.). The THF was removed under vacuum and the residue partitioned between EtOAc (50 mL) and water (50 mL). The organic layer was washed with brine, dried over Na_2SO_4 , and concentrated. The results are depicted in *Table 15*.

General procedure for the oxidation of compound 23 to Veramoss (11) using CuCl as catalyst

To a 250 mL round bottom flask containing a 1:1 mixture of MeCN:MeOH (100 mL), compound **23** (1.98 g, 10 mmol, 1.0 eq.) and copper(I) chloride (50 mg, 0.5 mmol, 0.05 eq.) were added in one portion. The clear light green solution was stirred for 3 hours at room temperature. The mixture was concentrated *in vacuo* and the residue was partitioned between

water (10 mL) and AcOEt (10 mL). The organic phase was removed and the aqueous phase was extracted with AcOEt (2 × 10 mL). The combined organic phase was washed with brine (10 mL), dried over Na₂SO₄ and concentrated to yield Veramoss (**11**) as yellowish powder (294 mg, 15% yield).



Methyl 3,6-dimethyl-(methylperoxy)-2,4-dioxocyclohexanecarboxylate (115): Was isolated by quenching the reaction with PS-TsOH and the yellow solution concentrated under vacuum and purified via flash chromatography (Eluent: Toluene:MeCN 9:1) to yield **115** (258 mg). Yellow oil (R_f = 0.5, Toluene:MeCN 9:1). One compound was isolated pure. ¹H NMR (400 MHz, Chloroform-*d*) δ 3.87 (s, 3H), 3.34 – 3.22 (m, 1H), 2.80 (dd, *J* = 19.4, 6.5 Hz, 1H), 2.32 (s, 3H), 2.18 (dd, *J* = 19.4, 1.6 Hz, 1H), 1.34 (d, *J* = 7.0 Hz, 3H). ¹³C NMR (101 MHz, Chloroform-*d*) δ 200.59, 166.87, 163.26, 150.69, 149.58, 52.38, 41.33, 30.75, 20.44, 20.19. LC-MS (ESI+) Rt = 2.0 min m/z [M+H]⁺ = 245.3. HR-MS calculated for C₁₁H₁₇O₆ 245.1025, found 245.1040 (Δ = 1.5 mDa; 6.1 ppm). The other compound was isolated as a mixture with the previous (R_f = 0.5 – 0.33, Toluene:MeCN 9:1, 631 mg). ¹H NMR (400 MHz, Acetonitrile-*d*₃) δ 3.88 (s, 3H), 3.04 (qd, *J* = 6.9, 1.6 Hz, 1H), 2.69 (dd, *J* = 19.5, 6.5 Hz, 1H), 2.04 (dd, *J* = 19.5, 1.6 Hz, 1H), 1.25 (d, *J* = 6.9 Hz, 3H).

General procedure of photo-oxidation of compound 23 using rose Bengal

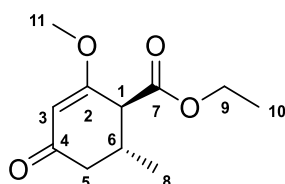
A solution of compound **23** (527 mg, 2.66 mmol, 1.0 eq.) and Rose bengal sodium salt (509 mg, 0.5 mmol, 0.19 eq.) in MeOH (100 mL) was pumped through the photoreactor (LED lamp 530 nm) at 5 mL min⁻¹. The collected stream was concentrated under vacuum and analysed by ¹H-NMR and LC-MS (ESI).

General procedure for methylation of 22-Et using CuCl as a catalyst

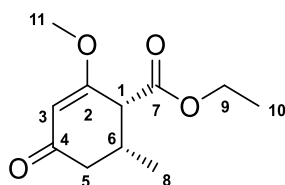
In Batch: To a suspension of **22-Et** (400 mg, 2 mmol, 1.0 eq.) and copper(I) chloride (20 mg, 0.2 mmol, 0.1 eq.) in acetic acid (20 mL), was added *tert*-butyl peroxybenzoate (1.14 mL, 6 mmol, 3.0 eq.). The green mixture was stirred under reflux for 30 minutes and then allowed to cool at room temperature. The solvent was removed *in vacuo* and the residue partitioned

between DCM (5 mL) and a saturated NaHCO₃ aqueous solution (5 mL). The organic phase was removed and the aqueous phase was extracted with DCM (2 × 10 mL). The combined organic phase was washed with water (10 mL), brine (10 mL), dried over Na₂SO₄ and concentrated *in vacuo* to obtain a yellow oil. The crude was purified via flash chromatography (Eluent: acetone:Et₂O:hexane 1.4:0.6:8) to gain **116** (45 mg, 11% yield).

In Flow: In a 50 mL round bottom flask equipped with a stirring bar, a solution of **22-Et** (400 mg, 2 mmol, 1.0 eq.) in AcOH or MeCN (20 mL) was placed. Copper(I) chloride (20 mg, 0.2 mmol, 0.1 eq.) and *tert*-butyl peroxybenzoate (1.14 mL, 6 mmol, 3.0 eq.) were added in one portion to the mixture. The solution was pumped through a 10 mL-coil at 120 °C using a peristaltic pump. The flow rate was set to allow the mixture to stay at 120 °C for 15, 30, 45 or 60 minutes. The collected green solution was concentrated under vacuum and analysed via ¹H-NMR and GC-MS polar compounds (EI).



Trans-ethyl 2-methoxy-6-methyl-4-oxocyclohex-2-enecarboxylate (trans-116): Yellow oil (R_f = 0.62, Acetone:Et₂O:hexane 1.4:0.6:8). ¹H NMR (700 MHz, Acetonitrile-*d*₃) δ 5.40 (d, *J* = 1.2 Hz, 1H, **3**), 4.24 – 4.14 (m, 2H, **9**), 3.70 (s, 3H, **11**), 3.23 (dd, *J* = 8.8, 1.2 Hz, 1H, **1**), 2.51 – 2.44 (m, 1H, **6**), 2.40 (dd, *J* = 16.5, 4.4 Hz, 1H, **5**), 2.09 (dd, *J* = 16.5, 10.7 Hz, 1H, **5**), 1.25 (t, *J* = 7.1 Hz, 3H, **10**), 1.05 (d, *J* = 6.7 Hz, 3H, **8**). ¹³C NMR (176 MHz, Acetonitrile-*d*₃) δ 196.93 (**4**), 173.38 (**2**), 170.59 (**7**), 102.42 (**3**), 61.07 (**9**), 56.14 (**11**), 53.16 (**1**), 42.68 (**5**), 32.19 (**6**), 18.53 (**8**), 13.46 (**10**). GC-MS (EI) R_t = 4.83 min *m/z* [M]⁺ = 212.1 HR-MS calculated for C₁₁H₁₇O₄ 213.1127, found 213.1130 (Δ = 0.3 mDa; 1.4 ppm).



Cis-ethyl 2-methoxy-6-methyl-4-oxocyclohex-2-enecarboxylate (cis-116): Yellow oil (R_f = 0.62, Acetone:Et₂O:hexane 1.4:0.6:8). ¹H NMR (700 MHz, Acetonitrile-*d*₃) δ 5.42 (s, 1H, **3**),

4.23 – 4.14 (m, 2H, **9**), 3.70 (s, 3H, **11**), 3.35 (d, $J = 5.6$ Hz, 1H, **1**), 2.54 – 2.44 (m, 1H, **6**), 2.39 (dd, $J = 16.6, 13.6$ Hz, 1H, **5**), 2.20 (dd, $J = 16.6, 4.4$ Hz, 1H, **5**), 1.25 (t, $J = 7.1$ Hz, 3H, **10**), 1.05 (d, $J = 6.9$ Hz, 3H, **8**). ^{13}C NMR (176 MHz, Acetonitrile- d_3) δ 198.03 (**4**), 174.10 (**2**), 169.43 (**7**), 103.00 (**3**), 61.12 (**9**), 56.08 (**11**), 50.51 (**1**), 40.54 (**5**), 30.63 (**6**), 17.46 (**8**), 13.54 (**10**). GC-MS polar compounds (EI) $R_t = 4.89$ min m/z $[\text{M}]^+ = 212.1$ HR-MS calculated for $\text{C}_{11}\text{H}_{17}\text{O}_4$ 213.1127, found 213.1130 ($\Delta = 0.3$ ppm; 1.4 ppm).

General Procedure for the preparation of compound 23 employing methyl acetate as the solvent (route A)

To a heterogeneous mixture of MeONa (5.5 g, 102 mmol, 0.4 eq.) in methyl acetate (68.5 mL), was slowly added to the reaction mixture methyl propionylacetate (**27**) (32 mL, 255 mmol, 1.0 eq.). After the addition, methyl crotonate (**20**) (27.1 mL, 255 mmol, 1.0 eq.) was slowly added (the reaction was exothermic and warmed the reaction to 50 °C). The reaction was then warmed to 55 – 61 °C and stirred until no more starting materials were detected by GC-MS nonpolar compounds (EI) (R_t of **27** = 2.53 min, R_t of **121** = 4.13 min) (around 6 hours). The reaction cooled to 45 °C and MeONa (8.3 g, 153 mmol, 0.6 eq.) was added portion-wise. The mixture was then warmed to 55 - 61 °C and stirred for 3 hours or until no more intermediate **121** was detected in the GC-MS nonpolar compounds (EI). The reaction was then allowed to cool to 40 – 45 °C, water (5 mL) and polyphosphoric acid (21.3 g, 255 mmol, 1.0 eq.) was added to the mixture. The white precipitate formed was filtered and washed with water until the mother liquor was neutral.

General Procedure for the preparation of compound 23 employing methyl acetate as solvent (route B)

To a heterogeneous mixture of MeONa (5.5 g, 102 mmol, 0.4 eq.) in methyl acetate (69.1 mL), was slowly added dimethyl malonate (**26**) (29.1 mL, 255 mmol, 1.0 eq.) at room temperature. Slow addition of 4-hexen-3-one (**25**) (29.1 mL, 255 mmol, 1.0 eq.) caused an exothermic heating of the reaction to 50 °C. The reaction was warmed to 55 – 61 °C and stirred until no more starting materials were detected in the GC-MS nonpolar compounds (EI) (R_t of **25** = 2.40 min, R_t of **96** = 4.30 min) (around 1 hour). The reaction was cooled to 45 °C and MeONa (8.3 g, 153 mmol, 0.6 eq.) was added portion-wise. The mixture was warmed to 55 – 61 °C and

stirred for 1 hour or until no more intermediate **96** was detected in the GC-MS nonpolar compounds (EI). The reaction was cooled to 40 – 45 °C, water (5 mL) and polyphosphoric acid (21.3 g, 255 mmol, 1.0 eq.) were added in the mixture. The white precipitate was filtered and washed with water until neutralisation of the mother liquor.

*Procedure for the one-pot preparation of Veramoss (**11**) from compounds **25** and **26** employing TCCA*

To a heterogeneous mixture of MeONa (21.6 g, 400 mmol, 0.4 eq.) in methyl acetate (271 mL), was slowly added dimethyl malonate (**26**) (114.4 mL, 1 mol, 1.0 eq.) at room temperature. Next, 4-hexen-3-one (**25**) (114.2 mL, 1 mol, 1.0 eq.) was slowly added which caused an exothermic heating to 50 °C. The reaction was then heated to 55 – 61 °C and stirred until no more starting materials were detected in the GC-MS nonpolar compounds (EI) (Rt of **25** = 2.40 min, Rt of **96** = 4.30 min) (around 1 hour). The reaction was cooled to 45 °C and MeONa (32.4 g, 600 mmol, 0.6 eq.) was added portion-wise. The mixture again was warmed to 55 - 61 °C and stirred for 1 hour or until no more intermediate **96** was detected in the GC-MS nonpolar compounds (EI). The reaction was then allowed to cool to 40 – 45 °C, water (35 mL) and polyphosphoric acid (117 g, 1.4 mol, 1.4 eq.) were added to the mixture. The reaction was cooled to 12.5 °C and a 0.9 M solution of TCCA (83.7 g, 325 mmol, 0.325 eq.) in methyl acetate (361 mL) was slowly added to the mixture at a flow rate of 2 mL/min over 3 hours. After the addition, the mixture was warm to reflux and stirred for 16 hours. The reaction was allowed to cool to room temperature and the solid filtered off from the mixture. The red solution was then concentrated under vacuum and the residue washed with water until neutralisation of the mother liquor (around 6.5 L). The pale yellow solid was then washed with toluene (1 L) to gain a white material which was dried under vacuum overnight. The material was then crystallised from MeOH (195 mL plus 2 g of tartaric acid) at 55 °C slowly adding water (142 mL) over 4 hours and cooling the mixture over 6 hours to room temperature to gain pure Veramoss (**11**) (110 g, 55% yield).

JMP data output for Definitive Screening Design performed on Veramoss oxidation

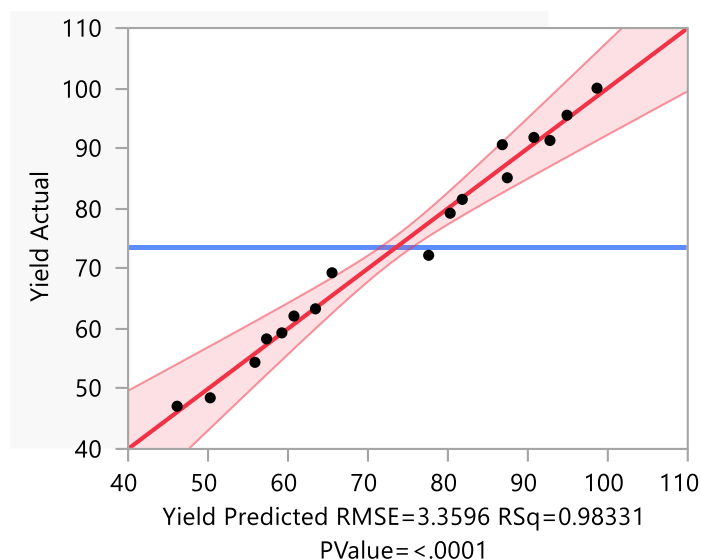


Figure 52. Comparison between the actual yield and the yield predicted by the model. RMSE and Rsq are depicted below the graph.

Table 32. Estimates for each term involved in the model.

Term	Estimate	Std Error	t Ratio	Prob> t
Intercept	87.427586	2.719351	32.15	<.0001
addition time (h)(1,5)	4.6928571	0.897891	5.23	0.0012
TCCA (eq.)(0.25,0.4)	-13.27143	0.897891	-14.78	<.0001
addition Temperature (°C)(0,25)	4.7928571	0.897891	5.34	0.0011
PPA (eq.)(0.1,0.7)	4.3428571	0.897891	4.84	0.0019
H ₂ O (mL in 50 mmol)(0.5,3)	4.7857143	0.897891	5.33	0.0011
[TCCA](0.3,0.9)	6.4285714	0.897891	7.16	0.0002
[TCCA]*[TCCA]	-8.62069	2.205685	-3.91	0.0058
addition Temperature (°C)*addition Temperature (°C)	-7.47069	2.205685	-3.39	0.0116
TCCA (eq.)*TCCA (eq.)	-0.82069	2.205685	-0.37	0.7208

Table 33. Effect summary of the model predicted by the JMP.

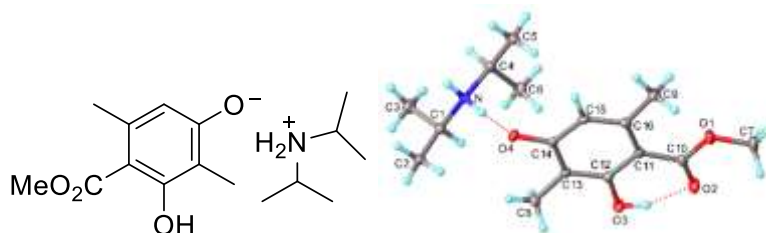
Source	LogWorth	PValue
TCCA (eq.)(0.25,0.4)	5.809	0.00000
[TCCA](0.3,0.9)	3.736	0.00018
addition Temperature (°C)(0,25)	2.967	0.00108
H ₂ O (mL in 50 mmol)(0.5,3)	2.964	0.00109
addition time (h)(1,5)	2.915	0.00122
PPA (eq.)(0.1,0.7)	2.725	0.00188
[TCCA]*[TCCA]	2.234	0.00584
addition Temperature (°C)*addition Temperature (°C)	1.934	0.01165
TCCA (eq.)*TCCA (eq.)	0.142	0.72084

General procedure for the synthesis of the complexes **122-130**

To a solution of compound **11** (70% purity, 28 g, 100 mmol, 1.0 eq.) in AcOEt (100 mL) or MeOH (50 mL), was added the desired base (2.0 eq.) in one portion. The dark purple mixture was then stored at -20 °C for 24 hours and the solid formed filtered. The solid was then crystallised from the required solvent.

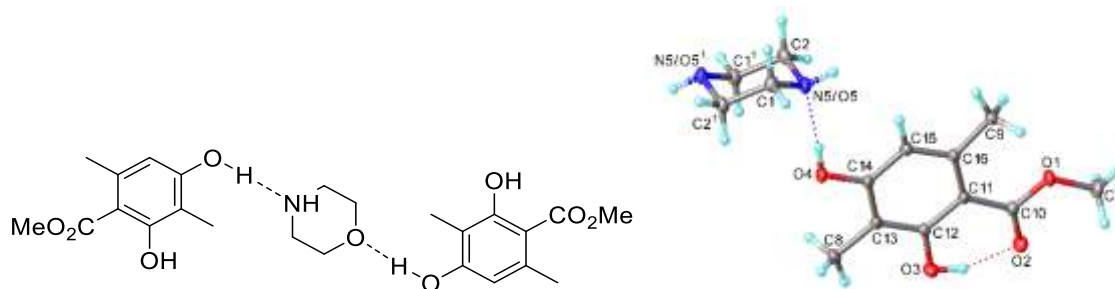
General procedure for the recovery of **11** from the complexes **122-130**

After having obtained a clear solution of compounds **129** or **130** (roughly 100 mmol) in MeOH (50 mL or 500 mL) heated under reflux, the mixture was allowed to cool to 40 °C. Water (200 mL or 500 mL) was then added to the warm solution over 30 minutes. Once the addition had finished, the mixture was allowed to cool to room temperature and filtered. The solid residue was washed with water (200 mL) and dried under vacuum to yield Veramoss **11** as a white crystal.

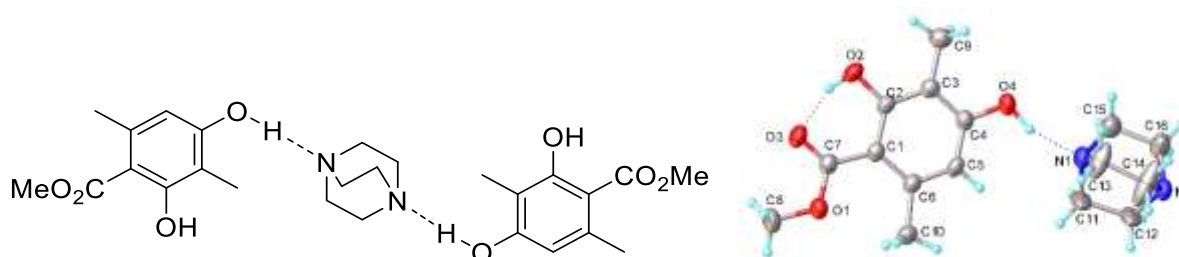


iPr₂NH-Veramoss Complex (**123**): White crystal (2.1 g, 7% yield). ¹H NMR (600 MHz, Chloroform-*d*) δ 6.17 (s, 1H), 3.89 (s, 3H), 3.02 (sept, *J* = 6.3 Hz, 2H), 2.42 (s, 3H), 2.08 (s, 3H), 1.11 (d, *J* = 6.4 Hz, 12H). ¹³C NMR (151 MHz, Chloroform-*d*) δ 172.83, 163.35, 160.13, 139.72, 111.34, 109.53, 104.26, 51.74, 45.55, 24.31, 8.09. LC-MS (ESI+) Rt = 2.14 min *m/z* [M+H]⁺ = 197.6. HR-MS calculated for C₁₀H₁₃O₄ 197.0814, found 197.0837 (Δ = 2.3 mDa; 11.7 ppm). IR (neat) ν 2980 (CH, w), 2930 (CH, w), 2881 (CH, w), 2731 (CH, w), 2731 (CH, w), 2436 (w), 1625 (C=O, s), 1531(m), 1448 (m), 1396 (m), 1385 (m), 1317 (m), 1290 (m), 1266 (s), 1189 (m), 1149 (m), 1127 (m), 1103 (m), 1028 (m), 883 (w), 802 (s), 637 (s) cm⁻¹. Melting point: 84.7 – 89.1 °C (MeOH). Crystal structure data for C₁₆H₂₇NO₄ (*M* = 297.38 g/mol): triclinic, space group P-1 (no. 2), *a* = 7.8043(3) Å, *b* = 9.5260(4) Å, *c* = 11.4834(5) Å, α = 77.2244(17)°, β = 73.9230(17)°, γ = 80.1805(17)°, *V* = 794.56(8) Å³, *Z* = 2, *T* = 120 K, μ(Mo Kα) = 0.088 mm⁻¹, *D*_{calc} = 1.243 g/cm³, 14528 reflections measured (3.756° ≤ 2θ ≤ 59.994°), 4626 unique (*R*_{int} = 0.0331, *R*_{sigma} = 0.0412) which were used in all

calculations. The final R_1 was 0.0545 ($I > 2\sigma(I)$) and wR_2 was 0.1323 (all data). Operator reference number: 20srv228.

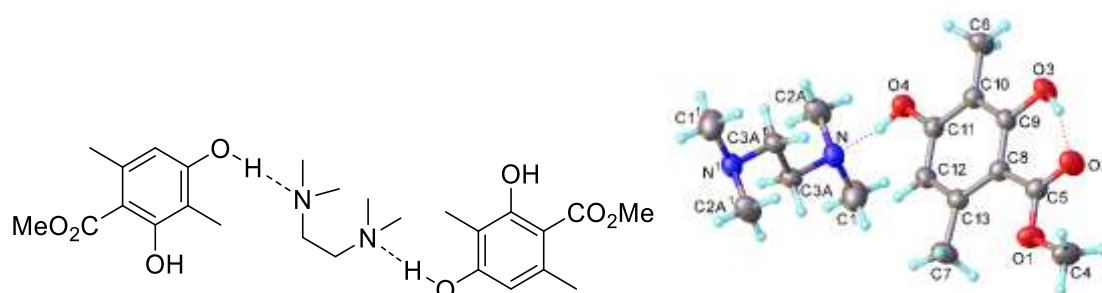


Morpholine-Veramoss Complex (128): Brown pale crystal (8.4 g, 7% yield). ^1H NMR (600 MHz, Chloroform- d) δ 6.16 (s, 2H), 3.91 (s, 6H), 3.77 – 3.71 (m, 4H), 2.98 – 2.91 (m, 4H), 2.44 (s, 6H), 2.09 (s, 6H). ^{13}C NMR (151 MHz, Chloroform- d) δ 172.76, 163.34, 158.92, 140.09, 110.76, 109.00, 104.98, 67.72, 51.89, 46.03, 24.28, 7.90. LC-MS (ESI+) R_t = 2.68 min m/z $[\text{M}+\text{H}]^+$ = 197.5. HR-MS calculated for $\text{C}_{10}\text{H}_{13}\text{O}_4$ 197.0814, found 197.0817 (Δ = 0.3 mDa; 1.5 ppm). FT-IR (neat) ν 3194 (NH, w), 2954 (CH, w), 2874 (CH, w), 1642 (C=O, s), 1619 (C=O, m), 1596 (C=O, m), 1454 (m), 1432 (m), 1364 (w), 1305 (m), 1269 (m), 1188 (w), 1155 (m), 1110 (w), 1078 (m), 1062 (w), 1027 (w), 840 (w), 801 (s), 771 (m), 584 (m) cm^{-1} . Melting point: 81.6 – 93.3 °C (MeOH). Crystal structure data for $\text{C}_{24}\text{H}_{33}\text{NO}_9$ (M = 479.51 g/mol): triclinic, space group P-1 (no. 2), a = 8.3185(4) Å, b = 8.5365(4) Å, c = 9.5699(4) Å, α = 73.188(2)°, β = 72.091(2)°, γ = 63.816(2)°, V = 570.82(5) Å³, Z = 1, T = 120 K, $\mu(\text{Mo K}\alpha)$ = 0.107 mm^{-1} , D_{calc} = 1.395 g/cm^3 , 13387 reflections measured ($4.548^\circ \leq 2\theta \leq 69.984^\circ$), 4935 unique (R_{int} = 0.0328, R_{sigma} = 0.0427) which were used in all calculations. The final R_1 was 0.0446 ($I > 2\sigma(I)$) and wR_2 was 0.1249 (all data). Operator reference number: 20srv227.



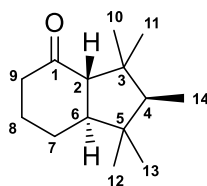
DABCO-Veramoss Complex (129): (25 g, 99% yield; Veramoss recovery: 20 g, 98% yield). ^1H NMR (400 MHz, DMSO- d_6) δ 6.28 (s, 2H), 3.84 (s, 6H), 2.62 (s, 12H), 2.36 (s, 6H), 1.93 (s, 6H). ^{13}C NMR (101 MHz, DMSO- d_6) δ 171.88, 161.71, 160.14, 138.76, 110.58, 108.15, 103.97, 51.98, 46.81, 23.53, 8.04. LC-MS (ESI+) R_t = 2.13 min m/z $[\text{M}+\text{H}]^+$ = 197.4. HR-MS

calculated for $C_{10}H_{13}O_4$ 197.0814, found 197.0814 ($\Delta = 0.0$ mDa; 0.0 ppm). FT-IR (neat) ν 2949 (CH, w), 2879 (CH, w), 1641 (C=O, m), 1432 (m), 1305 (m), 1269 (s), 1192 (m), 1157 (m), 1120 (m), 1057 (w), 1027 (w), 990 (w), 806 (m), 776 (s), 623 (w), 582 (w) cm^{-1} . Melting point: 159.4 – 171.9 °C (MeOH). Crystal structure data for $C_{26}H_{36}N_2O_8$ ($M = 504.57$ g/mol): monoclinic, space group $C2/c$ (no. 15), $a = 19.3807(11)$ Å, $b = 8.9434(5)$ Å, $c = 15.1513(9)$ Å, $\beta = 102.306(2)^\circ$, $V = 2565.8(3)$ Å³, $Z = 4$, $T = 230$ K, $\mu(MoK\alpha) = 0.097$ mm⁻¹, $D_{calc} = 1.306$ g/cm³, 18132 reflections measured ($4.302^\circ \leq 2\Theta \leq 50.03^\circ$), 2256 unique ($R_{int} = 0.0441$, $R_{sigma} = 0.0454$) which were used in all calculations. The final R_1 was 0.0465 ($I > 2\sigma(I)$) and wR_2 was 0.1275 (all data). Operator reference number: 20srv078.

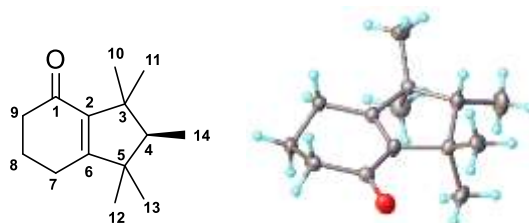


TMEDA-Veramoss Complex (130): (22.6 g, 89% yield; Veramoss recovery: 11 g, 60% yield). ¹H NMR (599 MHz, DMSO-*d*₆) δ 6.28 (s, 2H), 3.84 (s, 6H), 2.36 (s, 6H), 2.29 (s, 4H), 2.12 (s, 12H), 1.94 (s, 6H). ¹³C NMR (151 MHz, DMSO-*d*₆) δ 171.86, 161.70, 160.11, 138.74, 110.57, 108.15, 103.99, 57.02, 51.93, 45.45, 23.48, 8.01. LC-MS (ESI+) $R_t = 2.68$ min m/z $[M+H]^+ = 197.6$. HR-MS calculated for $C_{10}H_{13}O_4$ 197.0814, found 197.0835 ($\Delta = 2.1$ mDa; 10.7 ppm). FT-IR (neat) ν 3395 (OH, w), 2957 (CH, w), 2935 (CH, w), 2885 (CH, w), 2866 (CH, w), 2564 (w), 1635 (C=O, m), 1594 (C=O, m), 1447 (m), 1403 (m), 1305 (s), 1272 (s), 1191 (s), 1160 (s), 1022 (s), 989 (m), 941 (m), 799 (s), 727 (m), 623(m), 576 (m) cm^{-1} . Melting point: 117.5 – 125.4 °C (MeOH). Crystal structure data for $C_{26}H_{40}N_2O_8$ ($M = 508.60$ g/mol): triclinic, space group $P-1$ (no. 2), $a = 8.1679(3)$ Å, $b = 9.0206(4)$ Å, $c = 10.0181(4)$ Å, $\alpha = 99.8117(17)^\circ$, $\beta = 109.5448(17)^\circ$, $\gamma = 96.0334(18)^\circ$, $V = 674.90(5)$ Å³, $Z = 1$, $T = 200$ K, $\mu(Mo K\alpha) = 0.092$ mm⁻¹, $D_{calc} = 1.251$ g/cm³, 10748 reflections measured ($4.422^\circ \leq 2\Theta \leq 56.996^\circ$), 3406 unique ($R_{int} = 0.0250$, $R_{sigma} = 0.0264$) which were used in all calculations. The final R_1 was 0.0499 ($I > 2\sigma(I)$) and wR_2 was 0.1433 (all data). Operator reference number: 20srv218.

4.2. Ambertonic



2,7a-anti-3a,7a-anti-1,1,2,3,3-pentamethyloctahydro-4H-inden-4-one (39): ^1H NMR (600 MHz, Methanol- d_4) δ 2.25 – 2.20 (m, 2H, **9**), 2.18 (dd, $J = 13.9, 1.3$ Hz, 1H, **2**), 2.06 (ddq, $J = 12.7, 6.3, 3.3$ Hz, 1H, **8**), 1.89 – 1.80 (m, 1H, **7**), 1.65 – 1.55 (m, 2H, **8 & 6**), 1.41 (qd, $J = 12.5, 3.8$ Hz, 1H, **7**), 1.25 (d, $J = 7.6$ Hz, 1H, **4**), 1.10 (s, 3H, **10/11**), 0.97 (s, 3H, **12/13**), 0.96 (s, 3H, **10/11**), 0.77 (d, $J = 7.6$ Hz, 3H, **14**), 0.72 (s, 3H, **12/13**). ^{13}C NMR (151 MHz, Methanol- d_4) δ 213.85 (**1**), 64.03 (**2**), 56.09 (**4**), 54.82 (**6**), 43.11 (**9**), 42.67 (**5**), 40.07 (**3**), 28.54 (**10/11**), 27.95 (**12/13**), 26.84 (**8**), 26.79 (**10/11**), 25.88 (**7**), 16.43 (**12/13**), 9.12 (**14**). LC-MS (ESI+) $R_t = 3.79$ min m/z $[\text{M}+\text{H}]^+ = 209.3$. HR-MS calculated for $\text{C}_{14}\text{H}_{25}\text{O}$ 209.1905, found 209.1924 ($\Delta = 1.9$ mDa; 9.1 ppm). FT-IR (neat) ν 2946 (s, CH), 2866 (s), 1697 (s, C=O), 1454 (m), 1385 (w), 1367 (m) cm^{-1} .

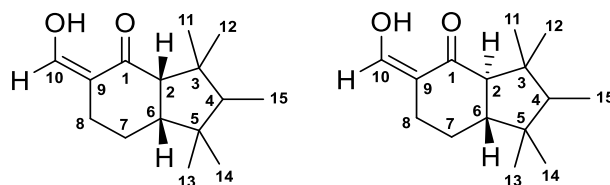


1,1,2,3,3-pentamethyl-1,2,3,5,6,7-hexahydro-4H-inden-4-one (38): ^1H NMR (400 MHz, Chloroform- d) δ 2.40 – 2.15 (m, 5H, **8 & 9**), 1.96 (ddt, $J = 13.3, 7.6, 5.6$ Hz, 2H, **7**), 1.58 (q, $J = 7.4$ Hz, 1H, **4**), 1.20 (s, 3H, **10/11**), 1.03 (s, 3H, **10/11**), 1.00 (s, 3H, **12/13**), 0.91 (s, 3H, **12/13**), 0.86 (d, $J = 7.4$ Hz, 3H, **14**). ^{13}C NMR (101 MHz, Chloroform- d) δ 198.62 (**1**), 170.45 (**6**), 141.84 (**2**), 53.17 (**4**), 47.74 (**5**), 45.44 (**3**), 39.27 (**9**), 27.80 (**10/11**), 26.65 (**12/13**), 23.67 (**7**), 22.95 (**8**), 22.01 (**10/11**), 21.76 (**12/13**), 7.95 (**14**). LC-MS (ESI+) $R_t = 3.58$ min m/z $[\text{M}+\text{H}]^+ = 207.8$. HR-MS calculated for $\text{C}_{14}\text{H}_{23}\text{O}$ 207.1749, found 207.1777 ($\Delta = 2.8$ mDa; 13.5 ppm). FT-IR (neat) ν 2948 (m, CH), 2865 (m, CH), 1646 (s, C=O), 1621 (m, C=C), 1450 (m, CH), 1383 (m, CH), 1361 (m, CH), 1329 (w), 1176 (w), 963 (w), 891 (w, C=C) cm^{-1} . Melting point: 35.2 – 37.5 $^{\circ}\text{C}$. Crystal structure data for $\text{C}_{14}\text{H}_{22}\text{O}$ ($M = 206.31$ g/mol): monoclinic, space group P21/c (no. 14), $a = 13.2412(6)$ \AA , $b = 6.9936(3)$ \AA , $c =$

13.9513(7) Å, $\beta = 104.352(2)^\circ$, $V = 1251.62(10) \text{ \AA}^3$, $Z = 4$, $T = 120 \text{ K}$, $\mu(\text{MoK}\alpha) = 0.066 \text{ mm}^{-1}$, $D_{\text{calc}} = 1.095 \text{ g/cm}^3$, 24924 reflections measured ($6.078^\circ \leq 2\theta \leq 58.262^\circ$), 3366 unique ($R_{\text{int}} = 0.0713$, $R_{\text{sigma}} = 0.0476$) which were used in all calculations. The final $R1$ was 0.0495 ($I > 2\sigma(I)$) and $wR2$ was 0.1304 (all data). Operator reference number: 19srv064.

General procedures for the synthesis of compound 131 using solid alkoxides and other bases

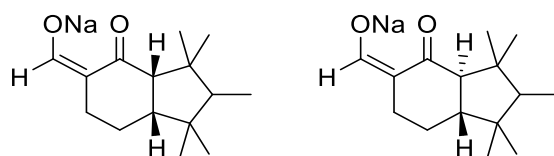
In a three-necked round bottom flask, a mixture of the base (1.2 eq.) in the required volume of dry hexane was prepared under nitrogen. The methyl formate (1.2 – 3 eq.) was then added dropwise at 0 °C to this mixture. After 5 minutes, a solution of **39** (1.0 eq.) in the required volume of dry was added over 30 minutes at the same temperature. After 10 minutes, the ice bath was removed and the reaction was stirred at room temperature overnight. The mixture was then quenched with ice-cooled water and the two phases separated. The aqueous phase then acidified with concentrated hydrochloric acid (38%) and extracted with chloroform ($\times 3$). The combined organic phase was washed with brine, dried over Na_2SO_4 and concentrated *in vacuo* to gain compound **131**. In an alternative work-up performed, the reaction mixture was filtered and the solid washed with small amount of water and hexane until the slurry material becomes a nice powdery solid. The solid was then acidified in the smallest amount of water as possible and extracted with ethyl acetate as above described.



1,1,2,3,3-pentamethyl-4-oxooctahydro-1H-indene-5-carbaldehyde (131): Trans-isomer: ^1H NMR (400 MHz, Chloroform-*d*) δ 14.77 (d, $J = 5.5 \text{ Hz}$, 1H, **OH**), 8.22 – 8.16 (m, 1H, **10**), 2.46 (ddd, $J = 15.2, 5.7, 1.8 \text{ Hz}$, 1H, **8**), 2.40 – 2.29 (m, 1H, **8**), 2.26 (d, $J = 13.4 \text{ Hz}$, 1H, **2**), 1.85 – 1.77 (m, 1H, **7**), 1.53 – 1.44 (m, 1H, **6**), 1.34 (q, $J = 7.5 \text{ Hz}$, 1H, **4**), 1.30 – 1.17 (m, 1H, **7**), 1.12 (s, 3H, **11/12**), 1.00 (s, 3H, **13/14**), 0.94 (s, 3H, **13/14**), 0.77 (dd, $J = 7.5, 1.1 \text{ Hz}$, 3H, **15**), 0.63 (s, 3H, **11/12**). ^{13}C NMR (101 MHz, Chloroform-*d*) δ 194.39 (**10**), 180.48 (**1**), 109.60 (**9**), 57.98 (**2**), 55.47 (**4**), 49.08 (**6**), 41.10 (**5**), 39.61 (**3**), 27.64 (**12/13**), 27.39 (**11/12**), 27.13 (**11/12**), 25.11 (**8**), 22.86 (**7**), 15.94 (**12/13**), 9.10 (**15**). LC-MS (ESI-) $R_t = 3.89 \text{ min}$ m/z [$\text{M-H}]^- = 235.1$. HR-MS calculated for $\text{C}_{15}\text{H}_{23}\text{O}_2$ 235.1698, found 235.1708 ($\Delta = 1.0 \text{ mDa}$; 4.3

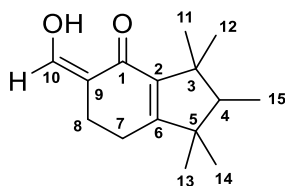
ppm). FT-IR (neat) ν 2947 (s, O-H), 2868 (s), 1713 (s, C=O), 1633 (s), 1584 (s), 1382 (s), 1342 (s), 1142 (s), 1010 (s), 907 (m), 827 (m), 595 (m) cm^{-1} .

Cis-isomer: ^1H NMR (700 MHz, Chloroform-*d*) δ 8.75 (s, 1H, **10**), 2.54 (d, $J = 9.9$ Hz, 1H, **2**), 2.37 (ddd, $J = 14.7, 4.3, 3.8$ Hz, 1H, **8**), 2.19 – 2.13 (m, 1H, **8**), 1.89 (ddd, $J = 13.1, 9.9, 5.1$ Hz, 1H, **6**), 1.77 (ddt, $J = 13.1, 5.1, 3.8$ Hz, 1H, **7**), 1.44 (q, $J = 7.3$ Hz, 1H, **4**), 1.37 – 1.30 (m, 1H, **7**), 1.22 (s, 3H, **11/12**), 1.02 (s, 3H, **13/14**), 0.86 (s, 3H, **13/14**), 0.80 – 0.77 (m, 6H, **11/12** & **15**). ^{13}C NMR (176 MHz, Chloroform-*d*) δ 188.35 (**10**), 185.99 (**1**), 110.20 (**9**), 55.61 (**4**), 53.31 (**2**), 48.03 (**6**), 46.50 (**3**), 41.34 (**5**), 34.20 (**13/14**), 30.92 (**11/12**), 24.40 (**7**), 23.89 (**8**), 20.79 (**13/14**), 18.50 (**11/12**), 8.51 (**15**). LC-MS (ESI-) $R_t = 3.89$ min m/z $[\text{M-H}]^- = 235.1$. HR-MS calculated for $\text{C}_{15}\text{H}_{23}\text{O}_2$ 235.1698, found 235.1683 ($\Delta = -1.5$ mDa; -6.4 ppm). FT-IR (neat) ν 2947 (s, O-H), 2868 (s), 1713 (s, C=O), 1633 (s), 1584 (s), 1382 (s), 1342 (s), 1142 (s), 1010 (s), 907 (m), 827 (m), 595 (m) cm^{-1} .



Sodium (Z)-(1,1,2,3,3-pentamethyl-4-oxohexahydro-1H-inden-5(6H)-ylidene)methanolate (Na-131): A small portion of pink solid was taken before quenching with hydrochloric acid. The solid was a 70%_{w/w} in **39**, and a mixture of *cis* and *trans* isomers (*cis:trans*: 3:7). The peaks reported are the ones which are not overlapping.

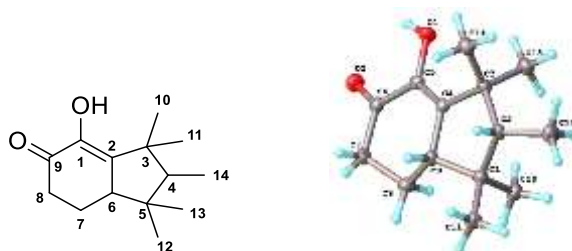
Trans-isomer: ^1H NMR (400 MHz, Methanol-*d*₄) δ 9.09 (s, 1H), 2.65 – 2.57 (m, 1H), 2.19 – 2.07 (m, 1H), 2.05 (d, $J = 13.3$ Hz, 1H), 1.81 (dd, $J = 12.0, 6.1$ Hz, 0H), 1.52 (ddd, $J = 13.3, 12.1, 2.3$ Hz, 1H), 1.31 (q, $J = 7.8$ Hz, 1H), 1.22 – 1.12 (m, 1H), 1.22 – 1.12 (m, 1H), 1.12 (s, 4H), 1.00 (s, 3H), 0.96 (s, 3H), 0.80 (d, $J = 7.5$ Hz, 3H), 0.66 (s, 3H). ^{13}C NMR (101 MHz, Methanol-*d*₄) δ 200.14, 177.90, 111.73, 60.17, 55.44, 50.36, 40.34, 39.15, 26.82, 26.53, 26.49, 23.29, 22.79, 15.00, 7.99. *Cis*-isomer: ^1H NMR (400 MHz, Methanol-*d*₄) δ 9.21 (s, 1H), 2.35 (d, $J = 9.8$ Hz, 1H), 1.99 – 1.90 (m, 1H), 1.04 (s, 3H), 0.91 (d, $J = 0.9$ Hz, 4H), 0.73 (s, 3H).



(*Z*)-5-(hydroxymethylene)-1,1,2,3,3-pentamethyl-2,3,6,7-tetrahydro-1*H*-inden-4(5*H*)-one (**152**): ¹H NMR (700 MHz, Chloroform-*d*) δ 7.33 (d, *J* = 1.1 Hz, 1H, **10**), 2.46 – 2.33 (m, 2H, **8**), 2.32 – 2.26 (m, 1H, **7**), 2.23 – 2.15 (m, 1H, **7**), 1.65 (q, *J* = 7.4 Hz, 1H, **4**), 1.26 (s, 3H, **11/12**), 1.10 (s, 3H, **11/12**), 1.06 (s, 3H, **13/14**), 0.91 (s, 3H, **13/14**), 0.89 (d, *J* = 7.4 Hz, 3H, **15**). ¹³C NMR (176 MHz, Chloroform-*d*) δ 190.65 (**1**), 169.13 (**6**), 163.09 (**10**), 141.78 (**2**), 109.13 (**9**), 53.46 (**4**), 47.94 (**5**), 45.67 (**3**), 27.79 (**11/12**), 26.97 (**13/14**), 24.06 (**8**), 22.24 (**7**), 22.09 (**11/12**), 21.61 (**13/14**), 7.91 (**15**). LC-MS (ESI-) *R*_t = 3.82 min *m/z* [M-H]⁻ = 233.3. HR-MS calculated for C₁₅H₂₁O₂ 233.1542, found 233.1541 (Δ = -0.1 mDa; -0.4 ppm). FT-IR (neat) ν 2955 (m, CH), 2871 (m, CH), 1631 (s, C=O), 1414 (m), 1363 (m), 1327 (m), 1225 (m), 1187 (m), 1178 (m), 1156 (m), 950 (s), 872 (m), 837 (w), 555 (m) cm⁻¹.

Procedure for the synthesis of compound 131 using formate ester 137 as the solvent

In a round bottom flask, a solution of compound **39** (2.08 g, 10 mmol, 1.0 eq.) in methyl formate (**137**) (10 mL) was prepared. A 5 M solution of MeONa in MeOH (2.4 mL, 12 mmol, 1.2 eq.) was added dropwise to the reaction mixture at 0 °C. The reaction was stirred for 2 hours and the resulting solid filtered. The solid was dried under vacuum and revealed to be a mixture of *trans*-**Na-131:138** (1:1, 800 mg). The filtrate was quenched with a concentrated hydrochloric acid (38%) at 0 °C and extracted with AcOEt (2 × 50 mL). The organic phase was washed with brine (20 mL), dried over Na₂SO₄ and concentrated under vacuum to yield **131** as 3:1 mixture with **39** (401 mg, 17% yield).

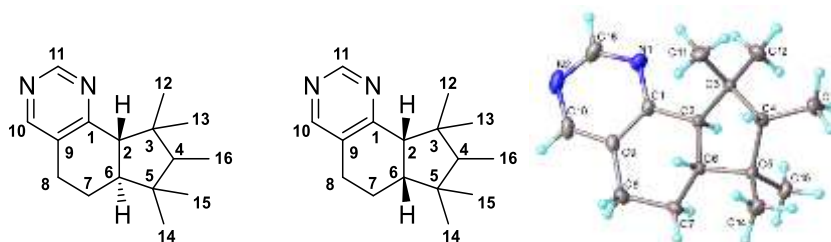


(*2R,7aS*)-4-hydroxy-1,1,2,3,3-pentamethyl-2,3,7,7*a*-tetrahydro-1*H*-inden-5(6*H*)-one (**138**): Crystallized from a 1:1 MeOH:water mixture (356 mg, 16% yield). ¹H NMR (600 MHz, Chloroform-*d*) δ 5.98 (s, 1H, **OH**), 2.63 (ddd, *J* = 17.0, 4.2, 2.4 Hz, 1H, **8**), 2.50 – 2.45 (m, 1H, **6**), 2.35 (dddd, *J* = 17.0, 14.8, 5.0, 0.7 Hz, 1H, **8**), 1.92 (dddd, *J* = 12.6, 5.0, 4.2, 2.4 Hz, 1H, **7**), 1.64 (dddd, *J* = 14.8, 12.6, 11.8, 4.2 Hz, 1H, **7**), 1.53 (q, *J* = 7.3 Hz, 1H, **4**), 1.21 (s, 3H, **10/11**), 1.20 (s, 3H, **10/11**), 0.99 (s, 3H, **12/13**), 0.86 (d, *J* = 7.3 Hz, 3H, **14**), 0.68 (s, 3H, **12/13**). ¹³C NMR (151 MHz, Chloroform-*d*) δ 195.73 (**9**), 149.16 (**2**), 141.96 (**1**), 54.66 (**4**), 52.13 (**6**),

43.10 (**5**), 42.81 (**3**), 35.96 (**8**), 27.71 (**10/11**), 27.11 (**12/13**), 23.42 (**7**), 20.85 (**10/11**), 17.29 (**12/13**), 7.98 (**14**). LC-MS (ESI+) $R_t = 3.67$ min m/z $[M+H]^+ = 223.7$. HR-MS calculated for $C_{14}H_{23}O_2$ 223.1698, found 223.1693 ($\Delta = -0.5$ mDa; -2.2 ppm). FT-IR (neat) ν 3391 (s, OH), 2953 (m, CH), 2871 (m, CH), 1705 (m), 1665 (s, C=O), 1641 (s, C=O), 1454 (m), 1389 (m), 1351 (s), 1327 (s), 1141 (s), 879 (w), 650 (s), 637 (s) cm^{-1} . Melting point: decomposition at 113.8 °C (MeOH). Crystal structure data for $C_{14}H_{22}O_2$ ($M = 222.31$ g/mol): triclinic, space group P-1, $a = 6.4281(4)$ Å, $b = 7.8823(8)$ Å, $c = 13.5995(14)$ Å, $\alpha = 82.685(9)^\circ$, $\beta = 85.889(8)^\circ$, $\gamma = 66.813(11)^\circ$, $V = 628.07(11)$ Å³, $Z = 2$, $T = 120$ K, $\mu(CuK\alpha) = 0.076$ mm⁻¹, $D_{calc} = 1.176$ g/cm³, 7925 reflections measured ($6.042^\circ \leq 2\theta \leq 58.998^\circ$), 3483 unique ($R_{int} = 0.0469$, $R_{sigma} = 0.0654$) which were used in all calculations. The final R_1 was 0.0530 ($I > 2\sigma(I)$) and wR_2 was 0.1366 (all data). Operator reference number: 19srv121.

Procedure for the synthesis of Ambertonic™ from 131

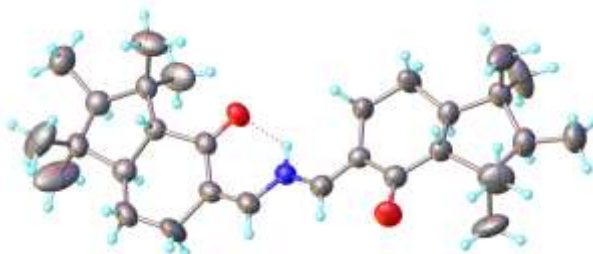
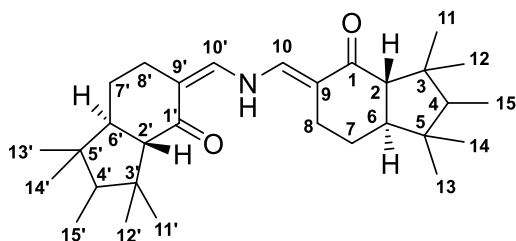
In a 50 mL round bottom flask, compound **131** (2.36 g, 10 mmol, 1.0 eq.), sodium sulfate (1.46 g, 10 mmol, 1 eq.) and formamide (5 mL) were placed. The mixture was heated at 210 °C and stirred for 1 hour. The reaction was then allowed to cool to room temperature and water (40 mL) was added. The aqueous phase was removed and the remained brown sticky oil was dissolved in chloroform (20 mL) and washed first with brine (2×10 mL) and then with water (10 mL). The organic phase was washed again with brine (10 mL), dried over Na_2SO_4 and concentrated under vacuum.



7,7,8,9,9-pentamethyl-6,6a,7,8,9,9a-hexahydro-5H-cyclopenta[h]quinazoline (37): Purified via flash chromatography (Eluent: toluene:MeCN 97.5:2.5). *Trans*-isomer: White crystal ($R_f = 0.25$, toluene:MeCN 97.5:2.5). ¹H NMR (600 MHz, Chloroform-*d*) δ 8.93 (s, 1H, **11**), 8.38 (s, 1H, **10**), 2.92 – 2.86 (m, 1H, **8**), 2.85 – 2.77 (m, 1H, **8**), 2.66 (dd, $J = 13.2, 1.9$ Hz, 1H, **2**), 1.97 (ddt, $J = 12.4, 6.1, 1.9$ Hz, 1H, **7**), 1.59 (td, $J = 13.2, 2.3$ Hz, 1H, **6**), 1.46 – 1.39 (m, 2H, **7** & **4**), 1.31 (s, 3H, **12/13**), 0.99 (s, 3H, **14/15**), 0.95 (s, 3H, **12/13**), 0.84 (d, $J = 7.5$ Hz, 3H, **16**), 0.70 (s, 3H, **14/15**). ¹³C NMR (151 MHz, Chloroform-*d*) δ 169.65 (**1**), 155.62 (**10**), 155.11

(**11**), 131.03 (**9**), 55.98 (**4**), 55.40 (**2**), 49.77 (**6**), 41.17 (**5**), 40.17 (**3**), 27.52 (**14/15**), 27.47 (**12/13**), 27.45 (**8**), 27.24 (**12/13**), 22.25 (**7**), 16.23 (**14/15**), 9.29 (**16**). FT-IR (neat) ν 2956 (s), 2871 (s), 1574 (s), 1537 (s), 1449 (s), 1396 (s), 1382 (m), 1366 (s), 1280 (w), 1265 (w), 1228 (w), 1216 (w), 1164 (w), 1081 (w), 928 (m), 849 (w), 803 (m) cm^{-1} . LC-MS (ESI+) $R_t = 3.49$ min m/z $[M+H]^+ = 245.9$ HR-MS calculated for $\text{C}_{16}\text{H}_{25}\text{N}_2$ 245.2018, found 245.2030 ($\Delta = 1.2$ mDa; 4.9 ppm). Melting point: 45.0 – 54.1 °C (toluene). Crystal structure data for $\text{C}_{16}\text{H}_{24}\text{N}_2$ ($M = 244.37$ g/mol): monoclinic, space group P21/n (no. 14), $a = 7.9439(6)$ Å, $b = 14.7710(11)$ Å, $c = 12.0646(9)$ Å, $\beta = 99.752(3)^\circ$, $V = 1395.20(18)$ Å³, $Z = 4$, $T = 120$ K, $\mu(\text{MoK}\alpha) = 0.068$ mm^{-1} , $D_{\text{calc}} = 1.163$ g/cm^3 , 30363 reflections measured ($4.398^\circ \leq 2\theta \leq 59.998^\circ$), 4063 unique ($R_{\text{int}} = 0.0503$, $R_{\text{sigma}} = 0.0350$) which were used in all calculations. The final R_1 was 0.0547 ($I > 2\sigma(I)$) and wR_2 was 0.1515 (all data). Operator reference number: 13srv003.

Cis-isomer: Colourless oil ($R_f = 0.17$, toluene:MeCN 97.5:2.5). ^1H NMR (400 MHz, Chloroform-*d*) δ 8.98 (s, 1H, **11**), 8.39 (s, 1H, **10**), 3.00 (d, $J = 9.7$ Hz, 1H, **2**), 2.76 (dt, $J = 16.2, 4.2$ Hz, 1H, **8**), 2.56 (dddd, $J = 16.2, 12.0, 4.2, 1.1$ Hz, 1H, **8**), 2.12 (ddd, $J = 12.7, 9.7, 5.2$ Hz, 1H, **6**), 1.89 (dtd, $J = 13.3, 4.9, 3.6$ Hz, 1H, **7**), 1.64 – 1.43 (m, 2H, **7** & **4**), 1.41 (s, 3H, **12/13**), 1.09 (s, 3H, **14/15**), 0.91 (s, 3H, **14/15**), 0.82 (d, $J = 7.3$ Hz, 3H, **16**), 0.53 (s, 3H, **12/13**). ^{13}C NMR (101 MHz, Chloroform-*d*) δ 168.43 (**1**), 155.80 (**10**), 155.39 (**11**), 131.34 (**9**), 55.68 (**4**), 52.75 (**2**), 48.68 (**6**), 47.31 (**3**), 41.29 (**5**), 34.39 (**14/15**), 31.31 (**12/13**), 26.68 (**7**), 23.04 (**8**), 20.90 (**14/15**), 19.04 (**12/13**), 8.90 (**16**). LC-MS (ESI+) $R_t = 3.35$ min m/z $[M+H]^+ = 245.0$ HR-MS calculated for $\text{C}_{16}\text{H}_{25}\text{N}_2$ 245.2018, found 245.2030 ($\Delta = 1.2$ mDa; 4.9 ppm). FT-IR (neat) ν 2945 (s), 2866 (s), 1663 (m, C=N), 1576 (s, C=C), 1539 (s), 1449 (s), 1396 (s), 1366 (s), 806 (m), 721 (m) cm^{-1} .

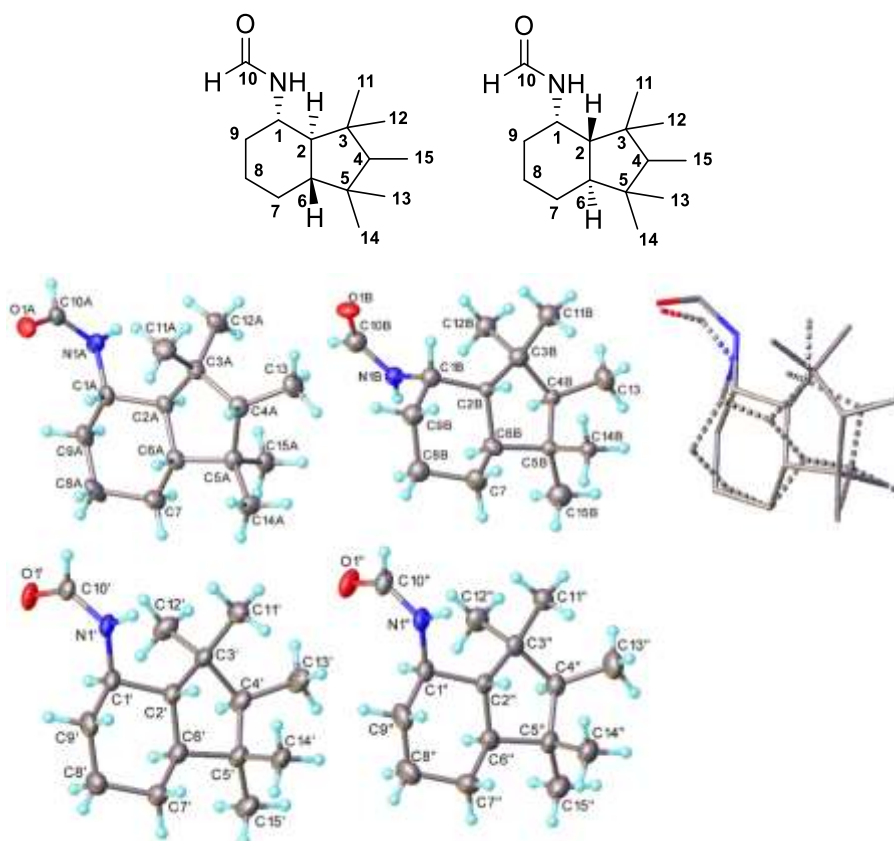


(*5Z,5'E*)-5,5'-(azanediylbis(methanylylidene))bis(1,1,2,3,3-pentamethylhexahydro-1*H*-inden-4(2*H*)-one) (*trans*-**143**): ^1H NMR (700 MHz, Chloroform-*d*) δ 11.26 (q, $J = 11.8$ Hz, 1H, **NH**), 7.37 (d, $J = 13.0$ Hz, 1H, **10**), 6.64 (dd, $J = 10.9, 1.4$ Hz, 1H, **10'**), 2.66 – 2.57 (m, 1H, **8**), 2.51

– 2.43 (m, 2H, **8'**), 2.37 – 2.25 (m, 1H, **8**), 2.09 (d, $J = 13.8$ Hz, 1H, **2'**), 2.01 (dd, $J = 13.7, 1.5$ Hz, 1H, **2**), 1.96 – 1.92 (m, 1H, **7**), 1.84 – 1.78 (m, 1H, **7'**), 1.61 – 1.52 (m, 2H, **6 & 6'**), 1.33 – 1.24 (m, 4H, **4 & 4'**, **7 & 7'**), 1.11 (s, 3H, **11'/12'**), 1.08 (s, 3H, **11/12**), 1.00 (s, 3H, **11'/12'**), 0.97 (s, 3H, **11/12**), 0.94 (s, 3H, **13'/14'**), 0.93 (s, 3H, **13/14**), 0.80 – 0.72 (m, 6H, **15 & 15'**), 0.64 (s, 3H, **13/14**), 0.62 (s, 3H, **13'/14'**). ^{13}C NMR (176 MHz, Chloroform-*d*) δ 203.68 (**1'**), 200.30 (**1**), 142.79 (**10'**), 138.14 (**10**), 114.04 (**9**), 110.56 (**9'**), 62.68 (**2'**), 62.30 (**2**), 55.05 (**4'**), 54.95 (**4**), 49.58 (**6/6'**), 49.57 (**6/6'**), 41.19 (**5**), 41.03 (**5'**), 39.54 (**3**), 39.45 (**3'**), 29.20 (**8'**), 27.68 (**11'/12'**), 27.66 (**11/12**), 27.25 (**13'/14'**), 27.22 (**13/14**), 27.02 (**11'/12'**), 27.00 (**11/12**), 24.67 (**8**), 23.61 (**7'**), 22.48 (**7**), 15.89 (**13/14**), 15.78 (**13'/14'**), 8.81 (**15 & 15'**). FT-IR (neat) ν 3659 (NH, br), 2981 (CH, s), 2975 (s), 2972 (s), 1667 (C=O, s), 1649 (m), 1561 (s), 1445 (m), 1419 (m), 1382 (s), 1370 (m), 1365 (m), 1336 (w), 1268 (w), 1239 (w), 1158 (s), 1125 (w), 1108 (m), 1090 (s), 1077 (s), 927 (w), 813 (m) cm^{-1} . LC-MS (ESI+) $R_t = 4.49$ min m/z $[\text{M}+\text{H}]^+ = 454.3$. HR-MS calculated for $\text{C}_{30}\text{H}_{48}\text{NO}_2$ 454.3685, found 454.3692 ($\Delta = 0.7$ mDa; 1.5 ppm). Melting point: decomposition at 162.6 °C (1,4-dioxane). Crystal structure data for $\text{C}_{30}\text{H}_{47}\text{NO}_2$ ($M = 453.68$ g/mol): monoclinic, space group I2/a (no. 15), $a = 28.950(5)$ Å, $b = 6.4490(12)$ Å, $c = 29.056(8)$ Å, $\beta = 91.888(7)^\circ$, $V = 5422(2)$ Å³, $Z = 8$, $T = 120$ K, $\mu(\text{CuK}\alpha) = 0.518$ mm⁻¹, $D_{\text{calc}} = 1.112$ g/cm³, 18282 reflections measured ($6.086^\circ \leq 2\theta \leq 115.79^\circ$), 3700 unique ($R_{\text{int}} = 0.2689$, $R_{\text{sigma}} = 0.1938$) which were used in all calculations. The final R_1 was 0.0979 ($I > 2\sigma(I)$) and wR_2 was 0.2930 (all data). Operator reference number: 18srv303.

General procedure for the synthesis of compound 147 from compound 39

To a heterogeneous mixture of compound **39** (2.08 g, 10 mmol, 1.0 eq.) in formamide (10 mL), was added sodium sulfate (1.5 g). The mixture was heated and stirred at 210 °C for 4 hours. The reaction was then allowed to cool to room temperature and partitioned between brine (20 mL) and chloroform (20 mL). The organic phase was washed with water (20 mL) and again with brine (20 mL). The brown solution was then dried over Na_2SO_4 and concentrated *in vacuo*. The residue was purified via flash chromatography (Eluent: hexane:AcOEt 7:3) to gain compound **147** (1.35 g, 57% yield) and **37** (195 mg, 8% yield).

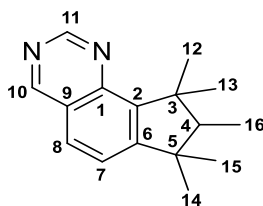


N-(1,1,2,3,3-pentamethyloctahydro-1*H*-inden-4-yl)formamide (**147**): Yellowish crystals (Rf = 0.33, hexane:AcOEt 7:3). Isolated as a mixture 6:4 of two diastereoisomers. *Major isomer* (1,2-*anti*-2,6-*anti*): In the NOESY experiment the signal at δ 1.24 (**2**) shows a strong correlation with the signal at δ 3.81 (**1**). ^1H NMR (600 MHz, Acetonitrile- d_3) δ 8.01 (**10**), 3.81 (**1**), 1.85 (**9**), 1.75 (**8**), 1.63 (**7**), 1.26 (**8**), 1.24 (**2**), 1.19 (**4**), 1.08 (**6** & **9**), 0.96 (**7**), 0.94 (**11/12**), 0.88 (**13/14**), 0.84 (**11/12**), 0.76 (**15**), 0.65 (**13/14**). ^{13}C NMR (151 MHz, Acetonitrile- d_3) δ 159.94 (**10**), 55.29 (**2** & **4**), 52.43 (**6**), 48.49 (**1**), 41.36 (**5**), 39.15 (**3**), 35.01 (**9**), 27.03 (**11/12**), 26.64 (**13/14**), 25.78 (**11/12**), 25.03 (**7**), 24.89 (**8**), 15.68 (**13/14**), 8.23 (**15**). *Minor isomer* (1,2-*syn*-2,6-*anti*): In the NOESY experiment the signal at δ 1.38 (**2**) shows no correlation with the signal at δ 4.41 (**1**). ^1H NMR (600 MHz, Acetonitrile- d_3) 8.00 (**10**), 4.41 (**1**), 1.72 (**8**), 1.65 (**7**), 1.61 (**9**), 1.39 (**9**), 1.38 (**2**), 1.37 (**7**), 1.35 (**6**), 1.19 (**4**), 1.06 (**8**), 0.91 (**13/14**), 0.87 (**11/12**), 0.85 (**11/12**), 0.77 (**15**), 0.63 (**13/14**). ^{13}C NMR (151 MHz, Acetonitrile- d_3) 160.18 (**10**), 54.89 (**4**), 53.90 (**2**), 47.92 (**6**) 43.66 (**1**), 41.31 (**5**), 39.57 (**3**), 33.41 (**7**), 26.93 (**11/12**), 26.86 (**13/14**), 26.56 (**11/12**), 26.12 (**8**), 20.46 (**9**), 15.50 (**13/14**), 7.83 (**15**). FT-IR (neat) ν 3287 (br, N-H), 2928 (m, C-H), 2867 (m, C-H), 1655 (s, C=O), 1532 (m), 1459 (m), 1380 (m), 1372 (m), 1366 (m), 1214 (w) cm^{-1} . LC-MS (ESI+) Rt = 2.92 min m/z $[\text{M}+\text{H}]^+ = 238.3$ HR-MS calculated for $\text{C}_{15}\text{H}_{28}\text{NO}$ 238.2171, found 238.2176 ($\Delta = 0.5$ mDa; 2.1 ppm). Melting point: 62.5 – 77.7 $^\circ\text{C}$.

Crystal structure data for C₁₅H₂₇NO (*M* = 237.37 g/mol): triclinic, space group P-1 (no. 2), *a* = 13.0853(12) Å, *b* = 13.2624(12) Å, *c* = 15.6921(18) Å, α = 77.213(5)°, β = 65.399(3)°, γ = 62.276(3)°, *V* = 2190.5(4) Å³, *Z* = 6, *T* = 120 K, $\mu(\text{MoK}\alpha)$ = 0.066 mm⁻¹, *D*_{calc} = 1.080 g/cm³, 34010 reflections measured (4.42° ≤ 2 Θ ≤ 50.054°), 7732 unique (*R*_{int} = 0.0530, *R*_{sigma} = 0.0573) which were used in all calculations. The final *R*₁ was 0.0668 (*I* > 2 σ (*I*)) and *wR*₂ was 0.1879 (all data). Operator reference number: 18srv509.

General procedure for the synthesis of the compound 151 from Ambertonic™ (37)

A mixture of *trans*-Ambertonic **37** (50 mg, 0.2 mmol), formamide (200 μL) and calcium chloride (50 mg) was heated at 180 °C for 4 hours. The mixture was cooled to room temperature and extracted with toluene (10 mL) and brine (2 mL). The organic phase was dried over Na₂SO₄ and concentrated *in vacuo* to gain **151** (Conversion: 77%). Characterisation was performed on the crude mixture.

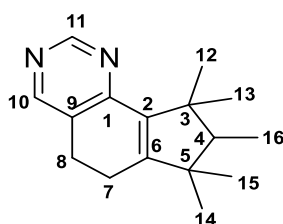


7,7,8,9,9-pentamethyl-8,9-dihydro-7H-cyclopenta[h]quinazoline (**151**): ¹H NMR (700 MHz, Chloroform-*d*) δ 9.31 (s, 1H, **10**), 9.27 (s, 1H, **11**), 7.77 (d, *J* = 8.2 Hz, 1H, **8**), 7.49 (d, *J* = 8.2 Hz, 1H, **7**), 2.03 (q, *J* = 7.4 Hz, 1H, **4**), 1.73 (s, 3H, **12/13**), 1.39 (s, 3H, **12/13**), 1.37 (s, 3H, **14/15**), 1.11 (s, 3H, **14/15**), 1.07 (d, *J* = 7.4 Hz, 3H, **16**). ¹³C NMR (176 MHz, Chloroform-*d*) δ 160.29 (**10**), 157.66 (**6**), 154.19 (**11**), 147.81 (**1**), 145.52 (**2**), 126.91 (**8**), 125.08 (**9**), 123.64 (**7**), 54.88 (**4**), 46.72 (**3**), 45.94 (**5**), 28.97 (**12/13**), 28.76 (**14/15**), 25.63 (**14/15**), 23.40 (**12/13**), 8.30 (**16**). GC-MS polar compounds (EI) *R*_t = 5.17 min *m/z* [*M*]⁺ = 240.2.

General procedure for the one-pot synthesis of Ambertonic™ (37) and Sinfonide (153)

In a three-necked round bottom flask, a suspension of MeONa (1.3 g, 24 mmol, 1.2 eq.) in dry hexane (10 mL) was prepared under nitrogen and cooled to 0 °C. To this mixture was added dropwise methyl formate (**137**) (1.5 mL, 24 mmol, 1.2 eq.). After 5 minutes, a solution of compound **38** (4.13 g, 20 mmol, 1 eq., for Sinfonide) or a solution of compound **39** (4.16 g, 20 mmol, 1 eq., for Ambertonic) in dry hexane (10 mL) was added over 30 minutes at the same

temperature. After 10 minutes, the ice bath was removed and the reaction was stirred at room temperature overnight. Formamide (**139**) (20 mL) was added to the reaction mixture and PPA (2.0 g, 24 mmol, 1.2 eq.) at 0 °C. The hexane was removed by distillation (addition of a vacuum pump when needed). Once >90% of the hexane was removed, calcium chloride (6 g) was added in one portion and the mixture was heated to 180 °C and stirred for 4 hours. The reaction was then allowed to cool to room temperature. The mixture was extracted with toluene (200 mL) and brine (10 mL). The organic phase was dried over Na₂SO₄ and concentrated *in vacuo*. The mixture was distilled under vacuum and at 180 °C & 10 mbar to yield Ambertonic™ (**37**) in 95% purity (3.0 g, 58% yield) or Sinfonide (**153**) in 95% purity (2.6 g, 51% yield).



7,7,8,9,9-pentamethyl-6,7,8,9-tetrahydro-5H-cyclopenta[h]quinazoline (153): ¹H NMR (599 MHz, Chloroform-*d*) δ 8.91 (s, 1H, **11**), 8.31 (d, *J* = 0.9 Hz, 1H, **10**), 2.84 – 2.74 (m, 2H, **8**), 2.37 (ddd, *J* = 17.0, 7.2, 5.1 Hz, 1H, **7**), 2.26 (ddd, *J* = 17.0, 12.5, 8.1 Hz, 1H, **7**), 1.73 (q, *J* = 7.4 Hz, 1H, **4**), 1.37 (s, 3H, **12/13**), 1.23 (s, 3H, **12/13**), 1.10 (s, 3H, **14/15**), 0.94 (d, *J* = 7.4 Hz, 3H, **16**), 0.92 (s, 3H, **14/15**). ¹³C NMR (151 MHz, Chloroform-*d*) δ 160.20 (**1**), 158.95 (**6**), 156.99 (**11**), 153.23 (**10**), 139.64 (**2**), 127.93 (**9**), 54.09 (**4**), 47.29 (**5**), 46.35 (**3**), 27.74 (**12/13**), 27.60 (**14/15**), 24.80 (**8**), 21.90 (**12/13**), 21.55 (**14/15**), 20.19 (**7**), 8.07 (**16**). LC-MS (ESI+) Rt = 3.63 min *m/z* [M+H]⁺ = 243.8. HR-MS calculated for C₁₆H₂₃N₂ 243.1861, found 243.1855 (Δ = -0.6 mDa: -2.5 ppm). FT-IR (neat) ν 2972 (s, CH), 2885 (m, CH), 1629 (w, CN), 1576 (m), 1534 (w), 1451 (s), 1402 (s), 800 (s), 671 (m) cm⁻¹. Melting point: 78.3 – 80.4 °C.

General procedure for the synthesis of compounds 155a

Basic condition.²⁶⁹ In a 100 mL round bottom flask compound **131** (1.18 g, 5 mmol, 1 eq.), guanidine hydrochloride (**157a**) (1.91 g, 20 mmol, 4 eq.) and sodium hydroxide (1.4 g, 35 mmol, 7 eq.) were dissolved in EtOH (50 mL). The pale orange mixture was heated under reflux for 3 hours. After cooling to room temperature, the crude orange mixture was concentrated *in vacuo* and partitioned between water (10 mL) and AcOEt (10 mL). The phases were separated and the aqueous phase was again extracted with AcOEt (2 × 10 mL). The

combined organic phase was washed with brine (10 mL), dried over Na₂SO₄ and concentrated to gain a yellow solid which was analyzed by GC-MS polar compounds (EI) and ¹H-NMR spectra. The results are depicted in *Scheme 58*.

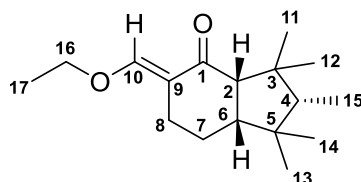
General procedure for the synthesis of compounds 155b

*Basic condition:*²⁶⁹ In a 100 mL round bottom flask compound **131** (1.18 g, 5 mmol, 1 eq.), urea (**157b**) (1.20 g, 20 mmol, 4 eq.) and sodium hydroxide (600 mg, 15 mmol, 3 eq.) were dissolved in EtOH (50 mL). The pale orange mixture was heated under reflux for 3 hours. After cooling to room temperature, the crude orange mixture was concentrated *in vacuo* and partitioned between water (10 mL) and AcOEt (10 mL). The phases were separated and the aqueous phase was again extracted with AcOEt (2 × 10 mL). The combined organic phase was washed with brine (10 mL), dried over Na₂SO₄ and concentrated to gain a yellow solid which was analyzed by GC-MS polar compounds (EI) and ¹H-NMR spectra. The results are depicted in *Scheme 58*.

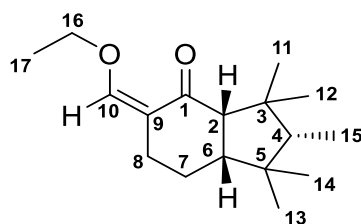
General procedure for the synthesis of compounds 155c

*Basic condition:*²⁶⁹ In a 100 mL round bottom flask compound **131** (1.18 g, 5 mmol, 1 eq.), thiourea (**157c**) (1.52 g, 20 mmol, 4 eq.) and sodium hydroxide (600 mg, 15 mmol, 3 eq.) were dissolved in EtOH (50 mL). The pale orange mixture was heated under reflux for 3 hours. After cooling to room temperature, the crude orange mixture was concentrated *in vacuo* and partitioned between water (10 mL) and AcOEt (10 mL). The phases were separated and the aqueous phase was again extracted with AcOEt (2 × 10 mL). The combined organic phase was washed with brine (10 mL), dried over Na₂SO₄ and concentrated to gain a yellow solid which was analyzed by GC-MS polar compounds (EI) and ¹H-NMR spectra. The results are depicted in *Scheme 58*.

Neutral condition: To a solution of compound **131** (2.36 g, 10 mmol, 1.0 eq.) in EtOH (10 mL), thiourea (**157c**) (3.04 g, 40 mmol, 4.0 eq.) was added. The reaction was heated under reflux and then stirred for 5 days. After cooling to room temperature, the solids were filtered and the orange solution was concentrated under vacuum. The residue was purified via flash chromatography (Eluent: DCM:MeOH 99:1) to gain *E-cis-159* (139 mg, 15% yield), *Z-cis-159* (215 mg, 8% yield), and *trans-158* (353 mg, 12% yield). The results are depicted in *Table 25 (Entry 1)*.

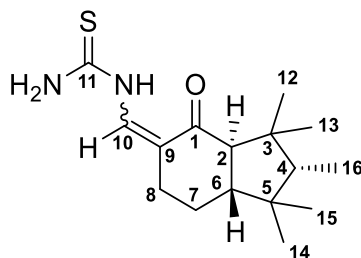


(2,3-anti,2,7-syn,E)-5-(ethoxymethylene)-1,1,2,3,3-pentamethyloctahydro-4H-inden-4-one (*E-cis-159*): Yellow oil ($R_f = 0.89$, DCM:MeOH 99:1). In the NOESY experiment the signals at δ 2.61 and 2.05 (**8**) shows correlation with the signal at δ 7.23 (**10**). ^1H NMR (700 MHz, DMSO- d_6) δ 7.23 (dd, $J = 2.8, 1.6$ Hz, 1H, **10**), 4.11 – 3.98 (m, 2H, **16**), 2.60 (ddt, $J = 16.3, 5.6, 1.6$ Hz, 1H, **8**), 2.05 (dddd, $J = 16.3, 12.9, 6.4, 2.8$ Hz, 1H, **8**), 1.90 (d, $J = 13.8$ Hz, 1H, **2**), 1.75 (ddt, $J = 10.9, 6.4, 2.6$ Hz, 1H, **7**), 1.50 (ddd, $J = 13.8, 12.1, 2.6$ Hz, 1H, **6**), 1.22 – 1.16 (m, 4H, **4** & **17**), 0.96 (s, 3H, **11**), 0.89 (s, 3H, **11/12**), 0.88 (s, 3H, **13/14**), 0.69 (d, $J = 7.5$ Hz, 3H, **15**), 0.57 (s, 3H, **13/14**). ^{13}C NMR (176 MHz, DMSO- d_6) δ 200.08 (**1**), 156.01 (**10**), 115.42 (**9**), 70.10 (**16**), 62.23 (**2**), 54.75 (**4**), 49.50 (**6**), 41.24 (**5**), 39.37 (**3**), 27.96 (**11/12**), 27.52 (**13/14**), 27.21 (**11/12**), 23.66 (**8**), 22.65 (**7**), 16.23 (**13/14**), 15.80 (**17**), 9.18 (**15**). LC-MS (ESI+) $R_t = 4.08$ min m/z [M-H] $^- = 265.1$. HR-MS calculated for $\text{C}_{17}\text{H}_{29}\text{O}_2$ 265.2168, found 265.2196 ($\Delta = 2.8$ mDa; 10.6 ppm).



(2,3-anti,2,7-syn,Z)-5-(ethoxymethylene)-1,1,2,3,3-pentamethyloctahydro-4H-inden-4-one (*Z-cis-159*): Yellow oil ($R_f = 0.82$, DCM:MeOH 99:1). In the NOESY experiment the signals at δ 2.60 and 1.96 – 1.89 (**8**) shows correlation with the signal at δ 7.26 (**10**). ^1H NMR (700 MHz, DMSO- d_6) δ 7.26 (dd, $J = 2.5, 1.1$ Hz, 1H, **10**), 4.11 – 4.03 (m, 2H, **16**), 2.60 (dtd, $J = 15.6, 3.8, 1.1$ Hz, 1H, **8**), 2.35 (d, $J = 10.3$ Hz, 1H, **2**), 2.01 (ddd, $J = 13.4, 10.3, 5.0$ Hz, 1H, **6**), 1.96 – 1.89 (m, 1H, **8**), 1.73 (dq, $J = 13.4, 3.8$ Hz, 1H, **7**), 1.29 (q, $J = 7.3$ Hz, 1H, **4**), 1.19 (m, 4H, **7** & **17**), 1.11 (s, 3H, **11/12**), 0.97 (d, $J = 4.2$ Hz, 3H, **13/14**), 0.79 (s, 3H, **13/14**), 0.70 (d, $J = 7.3$ Hz, 3H, **15**), 0.66 (s, 3H, **11/12**). ^{13}C NMR (176 MHz, DMSO- d_6) δ 201.13 (**1**), 155.53 (**10**), 116.07 (**9**), 70.17 (**16**), 58.69 (**2**), 54.99 (**4**), 49.38 (**6**), 46.70 (**3**), 41.63 (**5**), 34.21 (**13/14**), 31.27 (**11/12**), 24.65 (**7**), 23.17 (**8**), 21.04 (**13/14**), 18.90 (**11/12**), 15.75 (**17**), 8.64 (**15**). LC-MS

(ESI+) Rt = 3.67 min m/z [M+H]⁺ = 265.1. HR-MS calculated for C₁₇H₂₉O₂ 265.2168, found 265.2188 (Δ = 2.0 mDa; 7.5 ppm).



1-((1,1,2,3,3-pentamethyl-4-oxohexahydro-1H-inden-5(6H)-ylidene)methyl)thiourea (trans-158): Yellow oil (Rf = 0.21, DCM:MeOH 99:1). Isolated as a mixture 7:3 *E*:*Z*. ASAP (MeCN) m/z [M+H]⁺ = 295.2. HR-MS calculated for C₁₆H₂₇N₂OS 295.1844, found 295.1840 (Δ = -0.4 mDa; -1.4 ppm). *E*-isomer: ¹H NMR (700 MHz, DMSO-*d*₆) δ 9.51 (d, *J* = 11.7 Hz, 1H, **NH**), 8.54 (s, 2H, **NH**), 8.16 (dd, *J* = 11.7, 2.3 Hz, 1H, **10**), 2.54 (ddt, *J* = 16.1, 5.7, 1.7 Hz, 1H, **8**), 2.19 (dddd, *J* = 16.1, 12.6, 6.4, 2.3 Hz, 1H, **8**), 1.93 (d, *J* = 13.8 Hz, 1H, **2**), 1.86 – 1.79 (m, 1H, **7**), 1.58 – 1.47 (m, 1H, **6**), 1.27 – 1.18 (m, 2H, **4** & **7**), 0.98 (s, 3H, **12/13**), 0.89 (s, 3H, **14/15**), 0.88 (s, 3H, **12/13**), 0.69 (d, *J* = 7.5 Hz, 3H, **16**), 0.58 (s, 3H, **14/15**). ¹³C NMR (176 MHz, DMSO-*d*₆) δ 199.03 (**1**), 182.17 (**11**), 134.97 (**10**), 114.75 (**9**), 61.76 (**2**), 54.34 (**4**), 48.71 (**6**), 40.82 (**5**), 39.03 (**3**), 27.54 (**14/15**), 27.10 (**12/13**), 26.71 (**12/13**), 24.79 (**8**), 22.11 (**7**), 15.80 (**14/15**), 8.75 (**16**). *Z*-isomer: ¹H NMR (700 MHz, DMSO-*d*₆) δ 9.73 (d, *J* = 11.8 Hz, 1H, **NH**), 8.67 (s, 2H, **NH**), 8.21 – 8.17 (m, 1H, **10**), 2.54 – 2.51 (m, 1H, **8**), 2.47 – 2.43 (m, 1H, **8**), 2.10 (d, *J* = 13.9 Hz, 1H, **2**), 1.82 – 1.73 (m, 1H, **7**), 1.63 – 1.59 (m, 1H, **6**), 1.31 – 1.24 (m, 2H, **4** & **7**), 1.04 – 1.03 (m, 3H, **12/13**), 0.97 (s, 3H, **12/13**), 0.92 – 0.91 (m, 3H, **14/15**), 0.72 – 0.68 (m, 3H, **16**), 0.60 (s, 3H, **14/15**). ¹³C NMR (176 MHz, DMSO-*d*₆) δ 203.18 (**1**), 182.10 (**11**), 135.02 (**10**), 111.14 (**9**), 62.19 (**2**), 54.45 (**4**), 48.97 (**6**), 40.65 (**5**), 38.81 (**3**), 29.18 (**8**), 27.51 (**12/13**), 27.03 (**14/15**), 26.59 (**12/13**), 23.25 (**7**), 15.65 (**14/15**), 7.99 (**16**).

Acidic condition: To a solution of compound **131** (2.36 g, 10 mmol, 1.0 eq.) in EtOH (10 mL), was added thiourea (**157c**) (3.04 g, 40 mmol, 4 eq.) and sulfuric acid (53 μ L, 1 mmol, 0.1 eq.). The reaction mixture was heated at reflux with stirring for 1 hour. After cooling to room temperature, the solids were filtered and the orange solution was concentrated *in vacuo* to gain an orange residue, which was analyzed by GC-MS polar compounds (EI). The results are depicted in *Table 25 (Entry 2)*.

Acidic conditions in SFC: To compound **131** (2.36 g, 10 mmol, 1.0 eq.), was added thiourea (**157c**) (761 mg, 10 mmol, 1 eq.) and sulfuric acid (53 μ L, 1 mmol, 0.1 eq.) and the reaction was heated at 150 °C for 1 hour. The reaction mixture was allowed to cool to room temperature before being partitioned between chloroform (10 mL) and water (10 mL). The organic phase was washed with water (10 mL), brine (10 mL), dried over Na₂SO₄ and concentrated under vacuum. The orange residue was then analyzed by GC-MS polar compounds (EI). The results are depicted in *Table 25 (Entry 3)*.

Neutral condition using microwave irradiation: Thiourea (**157c**) (3.04 g, 40 mmol, 4 eq.) was added in one portion to a solution of compound **70** (2.36 g, 10 mmol, 1.0 eq.) in 1,4-dioxane (10 mL). The 20 mL microwave vial was sealed and heated under microwave irradiation for 1 hour (Biotage synthesizer) (Two individual experiments were performed at different temperatures: 160 °C or 181 °C). The reaction mixture was allowed to cool to room temperature and was concentrated under vacuum. The reaction was analysed via GC-MS polar compound (EI). The results are depicted in *Table 25 (Entries 4&5)*.

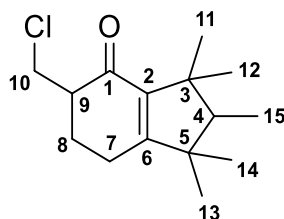
General procedure for the synthesis of compounds 155d

*Basic condition.*²⁶⁹ In a 100 mL round bottom flask compound **131** (1.18 g, 5 mmol, 1 eq.), aminoguanidine bicarbonate (**157d**) (2.72 g, 20 mmol, 4 eq.) and sodium hydroxide (1.4 g, 35 mmol, 7 eq.) were dissolved in EtOH (50 mL). The pale orange mixture was heated under reflux for 3 hours. After cooling to room temperature, the crude orange mixture was concentrated *in vacuo* and partitioned between water (10 mL) and AcOEt (10 mL). The organic phase was removed and the aqueous phase was further extracted with AcOEt (2 \times 10 mL). The combined organic phase was washed with brine (10 mL), dried over Na₂SO₄ and concentrated to gain a yellow residue which was analyzed by GC-MS polar compounds (EI) and ¹H-NMR spectra. The results are depicted in *Scheme 58*.

General procedure used to attempt the synthesis of compound 164

To a solution of compound **131** (1.18 g, 5 mmol, 1.0 eq.) in the required solvent (toluene 1 M, tetrahydrofuran 0.5 M), was slowly added thionyl chloride or chloroacetyl chloride (1.2 eq. or 0.8 eq. respectively), then DMF (10 μ L). The resultant yellow solution was stirred for 3 hours at either room temperature (thionyl chloride) or at 0 °C (chloroacetyl chloride). The solvent

was removed under reduced pressure and the residue was purified via flash chromatography (Eluent: toluene:MeCN 99:1) to gain **165** (888 mg, 70% yield).



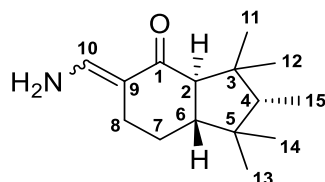
5-(chloromethyl)-1,1,2,3,3-pentamethyl-2,3,6,7-tetrahydro-1H-inden-4(5H)-one (**165**): Orange oil (R_f = 0.45, toluene:MeCN 99:1). Isolated as a 1:1 mixture of isomers. ASAP m/z [M+H]⁺ = 255.1 (100%)/ 257.1 (30%). HR-MS calculated for C₁₅H₂₄OCl 255.1516, found 255.1500 (Δ = -1.6 mDa; -6.3 ppm).

Isomer A: ¹H NMR (700 MHz, Chloroform-*d*) δ 3.94 (dd, J = 11.0, 3.7 Hz, 1H, **10**), 3.71 (dd, J = 11.0, 7.8 Hz, 1H, **10**), 2.53 (ddt, J = 12.0, 8.0, 4.1 Hz, 1H, **9**), 2.45 – 2.23 (m, 3H, **7 & 8**), 1.95 – 1.88 (m, 1H, **8**), 1.65 – 1.56 (m, 1H, **4**), 1.22 (s, 3H, **11/12**), 1.07 (s, 3H, **13/14**), 0.99 (s, 3H, **11/12**), 0.93 (s, 3H, **13/14**), 0.87 (dd, J = 7.4, 1.2 Hz, 3H, **15**). ¹³C NMR (176 MHz, Chloroform-*d*) δ 195.96 (**1**), 170.63 (**6**), 141.43 (**2**), 53.30 (**4**), 48.91 (**9**), 47.46 (**5**), 45.43 (**3**), 44.47 (**10**), 28.07 (**11/12**), 26.55 (**13/14**), 26.20 (**8**), 21.94 (**13/14**), 21.57 (**7**), 21.41 (**11/12**), 7.75 (**15**).

Isomer B: ¹H NMR (700 MHz, Chloroform-*d*) δ 3.98 (dd, J = 11.2, 3.7 Hz, 1H, **10**), 3.62 (dd, J = 11.2, 8.0 Hz, 1H, **10**), 2.66 – 2.59 (m, 1H, **9**), 2.45 – 2.22 (m, 2H, **7 & 8**), 1.85 (tdd, J = 12.7, 9.6, 6.5 Hz, 1H, **8**), 1.65 – 1.55 (m, 1H, **4**), 1.19 (s, 3H, **11/12**), 1.03 (s, 3H, **13/14**), 1.01 (s, 3H, **11/12**), 0.94 (s, 3H, **13/14**), 0.87 (dd, J = 7.4, 1.2 Hz, 3H, **15**). ¹³C NMR (176 MHz, Chloroform-*d*) δ 196.43 (**1**), 170.47 (**6**), 141.60 (**2**), 53.30 (**4**), 48.91 (**9**), 47.46 (**5**), 45.43 (**3**), 44.47 (**10**), 27.65 (**8**), 27.11 (**11/12**), 26.38 (**13/14**), 22.32 (**7**), 22.21 (**11/12**), 21.30 (**13/14**), 7.84 (**15**).

Procedure for the Synthesis of compound 146

To a 0.5 M solution of ammonia in 1,4-dioxane (40 mL, 20 mmol, 2 eq.), was added in one portion compound **131** (2.36 g, 10 mmol, 1 eq.) and the reaction was stirred for 3 hours at room temperature. The solvent was removed *in vacuo* and the residue was purified via flash chromatography (Eluent: toluene:MeCN 95:5) to gain **146** (1.32 g, 56% yield).



5-(aminomethylene)-1,1,2,3,3-pentamethylhexahydro-1H-inden-4(2H)-one (146): Yellow powder ($R_f = 0.42$, toluene:MeCN 95:5). Isolated as a mixture 1:1 *E:Z*. FT-IR (neat) ν 3439 (NH), 3333 (NH), 3289 (NH), 3223 (NH), 2945 (CH, s), 2934 (CH, s), 2927 (CH, s), 2872 (CH, s), 1653 (C=O, s), 1631 (C=O, s), 1618 (C=C, s), 1551 (s), 1534 (m), 1509 (s), 1484 (m), 1458 (s), 1443 (m), 1379 (s), 1364 (m), 1306 (m), 1293 (s), 1190 (s), 973 (C=C, s), 694 (C=C, s) cm^{-1} . LC-MS (ESI+) $R_t = 2.88$ min m/z $[M+H]^+ = 236.2$. HR-MS calculated for $\text{C}_{15}\text{H}_{26}\text{NO}$ 236.2014, found 236.1998 ($\Delta = -1.6$ mDa; -6.8 ppm).

Z-isomer: In the NOESY experiment the signals at δ 2.38 – 2.34 (**8**) shows correlation with the signal at δ 6.70 (**10**). ^1H NMR (599 MHz, Acetonitrile- d_3) δ 6.70 (tt, $J = 10.7, 1.0$ Hz, 1H, **10**), 2.38 – 2.34 (m, 2H, **8**), 2.04 (d, $J = 13.7$ Hz, 1H, **2**), 1.76 (ddq, $J = 12.3, 4.8, 2.4$ Hz, 1H, **7**), 1.57 – 1.51 (m, 1H, **6**), 1.30 – 1.22 (m, 2H, **4** & **7**), 1.08 (s, 3H, **11/12**), 0.95 (s, 3H, **11/12**), 0.93 (s, 3H, **13/14**), 0.77 (d, $J = 7.5$ Hz, 3H, **15**), 0.63 (s, 3H, **13/14**). ^{13}C NMR (151 MHz, Acetonitrile- d_3) δ 201.97 (**1**), 149.51 (**10**), 104.01 (**9**), 62.27 (**2**), 56.13 (**4**), 50.76 (**6**), 41.63 (**5**), 40.02 (**3**), 29.70 (**8**), 28.08 (**1**), 27.69 (**13/14**), 27.56 (**11/12**), 24.92 (**7**), 16.25 (**13/14**), 9.32 (**15**).

E-isomer: In the NOESY experiment the signals at δ 2.37 – 2.34 (**8**) shows no correlation with the signal at δ 7.40 (**10**). ^1H NMR (599 MHz, Acetonitrile- d_3) δ 7.40 (tt, $J = 11.2, 1.9$ Hz, 1H, **10**), 2.37 – 2.34 (m, 1H, **8**), 2.12 – 2.05 (m, 1H, **8**), 1.94 – 1.90 (m, 1H, **2**), 1.90 – 1.85 (m, 1H, **7**), 1.57 – 1.51 (m, 1H, **6**), 1.31 – 1.22 (m, 2H, **4** & **7**), 1.05 (s, 3H, **11/12**), 0.94 (s, 3H, **13/14**), 0.92 (s, 3H, **11/12**), 0.77 (d, $J = 7.5$ Hz, 3H, **15**), 0.64 (s, 3H, **13/14**). ^{13}C NMR (151 MHz, Acetonitrile- d_3) δ 198.92 (**1**), 143.00 (**10**), 107.85 (**9**), 61.99 (**2**), 55.94 (**4**), 50.54 (**6**), 41.73 (**5**), 40.09 (**3**), 28.02 (**11/12**), 27.58 (**13/14**), 27.50 (**11/12**), 24.34 (**8**), 23.47 (**7**), 16.29 (**13/14**), 9.23 (**15**).

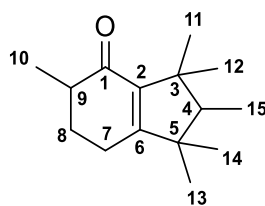
Attempt for the synthesis of compound 155c from compound 146

Potassium thiocyanate (360 mg, 1.53 mmol, 1 eq.) and ammonium chloride (82 mg, 1.53 mmol, 1 eq.) were added to a solution of compound **131** (360 mg, 1.53 mmol, 1 eq.) in the required

solvent (1.5 mL, 1 M). The reaction mixture was stirred under reflux for 6 hours. The mixture was allowed to cool to room temperature and then concentrated under vacuum. The mixture was analysed by LC-MS (ESI) and ¹H-NMR. The results are depicted in *Scheme 61*.

General procedure for the attempted synthesis of compound 166

In a round bottom flask was prepared a solution of compound **39** (2.08 g, 10 mmol, 1.0 eq.) in THF (10 – 100 mL). To the solution was added, in order, paraformaldehyde (600 mg, 20 mmol, 2 eq.), the required base (diisopropylamine, pyrrolidine, or *N,N*-diethylethylenediamine, 10 mmol, 1.0 eq.) and trifluoroacetic acid (839 μL, 11 mmol, 1.1 eq.). The reaction was stirred under reflux for 4 hours and then a further portion of paraformaldehyde (600 mg, 20 mmol, 2 eq.) was added to the reaction mixture and the heating continued. After 24 hours the reaction was allowed to cool to room temperature and the reaction analysed via GC-MS polar compounds (EI) and ¹H-NMR spectra. The results are depicted in *Scheme 63*. The reaction using diisopropylamine as the base was purified via flash chromatography (Toluene: DCM 97.5:2.5) to gain compound **168** (1.10 g, 50% yield).



1,1,2,3,3,5-hexamethyl-1,2,3,5,6,7-hexahydro-4H-inden-4-one (168): Pale yellow oil (*R*_f = 0.35, Toluene: DCM 97.5:2.5) Isolated as a mixture of isomers. *Isomer A*: ¹H NMR (599 MHz, Chloroform-*d*) δ 2.39 – 2.17 (m, 2H, **7** & **9**), 2.11 – 2.00 (m, 1H, **8**), 1.72 – 1.63 (m, 1H, **8**), 1.61 – 1.56 1.58 (m, 1H, **4**), 1.18 (s, 3H, **11/12**), 1.09 (d, *J* = 6.8 Hz, 3H, **10**), 1.02 (s, 3H, **13/14**), 1.01 (s, 3H, **11/12**), 0.92 (s, 3H, **13/14**), 0.86 (d, *J* = 7.5 Hz, 3H, **15**) ¹³C NMR (151 MHz, Chloroform-*d*) δ 201.06 (**1**), 169.13 (**6**), 141.49 (**2**), 53.45 (**4**), 47.44 (**5**), 45.49 (**3**), 42.16 (**9**), 32.36 (**8**), 27.41(**11/12**), 26.63 (**13/14**), 22.61 (**7**), 22.36 (**11/12**), 21.53 (**13/14**), 15.04 (**10**), 8.04 (**15**). LC-MS (ESI+) *R*_t = 3.60 min *m/z* [*M*+*H*]⁺ = 221.3 HR-MS calculated for C₁₅H₂₅O 221.1905, found 221.1917 (Δ = 1.2 mDa; 5.4 ppm). Under the stated LC-MS conditions, the two isomers could not be resolved, thus the HR-MS was acquired on the mixture.

Isomer B: ¹H NMR (599 MHz, Chloroform-*d*) δ 2.38 – 2.17 (m, 3H, **7** & **9**), 2.11 – 2.01 (m, 1H, **8**), 1.73 – 1.63 (m, 1H, **8**), 1.61 – 1.56 1.58 (m, 1H, **4**), 1.22 (s, 3H, **11/12**), 1.12 (d, *J* = 6.9

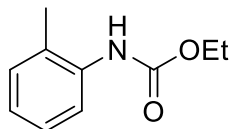
Hz, 3H, **10**), 1.05 (s, 3H, **13/14**), 0.99 (s, 3H, **11/12**), 0.91 (s, 3H, , **13/14**), 0.86 (d, $J = 7.5$ Hz, 3H, **15**). ^{13}C NMR (151 MHz, Chloroform- d) δ 200.99 (**1**), 169.26 (**6**), 141.07 (**2**), 53.29 (**4**), 47.57 (**5**), 45.39 (**3**), 42.44 (**9**), 31.08 (**8**), 28.30 (**11/12**), 26.81 (**13/14**), 22.05 (**11/12**), 21.82 (**13/14**), 21.69 (**7**), 15.38 (**10**), 7.98 (**15**). ^1H - ^{13}C HMBC experiment shows correlation between the carbonyl peaks at 200 ppm with the methyl peaks at 1.12 and 1.09 ppm. ^1H - ^{13}C HSBC experiment also shows correlation between the quaternary carbons at 141 and 170 ppm with the signals in the 1.25 – 0.85 ppm range (not with signals at 1.09 and 1.12 ppm).

General procedure for the synthesis of compound 37 via Hetero-Diels-Alder reaction

To a round bottom flask, was added compound **39** (416 mg, 2 mmol, 2.0 eq.) in DMSO (2.5 mL). To the solution was added 1,3,5-triazine (81.1 mg, 1 mmol, 1.0 eq.) and the desired base (prolinamide, pyrrolidine, morpholine, benzylamine, 0.2 mmol, 0.2 eq.). The reaction mixture was heated to 90 °C for 24 hours. The mixture was allowed to cool to room temperature and was partitioned between chloroform (10 mL) and brine (2 mL). The aqueous phase was extracted with chloroform (2 \times 10 mL) and the combined organic phase dried over Na_2SO_4 and concentrated under vacuum. The crude residue was analysed via ^1H -NMR and GC-MS polar compounds (EI). The results are depicted in *Table 26*.

General procedure for the synthesis of compound 175

To an ice-cooled solution of ethyl chloroformate (8.05 mL, 100 mmol, 0.5 eq.) in DCM (8 mL), was added a solution of *o*-toluidine (21.2 mL, 200 mmol, 1.0 eq.) in DCM (20 mL) over 30 minutes and keeping the temperature around 10 – 15 °C. The mixture was then stirred at room temperature for 3 hours. The mixture was then washed with water (10 mL), brine (10 mL), dried over Na_2SO_4 and concentrated *in vacuo* to yield **175** (15.0 g, 85% yield).



Ethyl o-tolylcarbamate (175).³⁴⁰ Pinkish solid. ^1H NMR (400 MHz, Chloroform- d) δ 7.79 (s, 1H), 7.24 – 7.12 (m, 2H), 7.02 (t, $J = 7.5$ Hz, 1H), 6.37 (s, 1H), 4.23 (qd, $J = 7.2, 1.1$ Hz, 2H), 2.26 (s, 3H), 1.32 (td, $J = 7.1, 1.1$ Hz, 3H). ^{13}C NMR (101 MHz, Chloroform- d) δ 154.03, 136.06, 130.50 (2C), 127.01, 124.14, 121.00, 61.41, 17.81, 14.70. FT-IR (neat) ν 3296 (s), 2983 (w), 2927 (w), 1692 (s), 1590 (s), 1527 (s), 1491 (s), 1484 (s), 1471 (s), 1456 (s), 1389

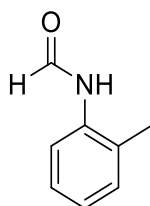
(m), 1289 (s), 1237 (s), 1197 (w), 1191 (w), 1121 (w), 1068 (s), 941 (m), 845 (m), 772 (s), 753 (s) cm^{-1} . LC-MS (ESI+) $R_t = 2.50$ min m/z $[M+H]^+ = 180.6$ HR-MS calculated for $\text{C}_{10}\text{H}_{14}\text{NO}_2$ 180.1025, found 180.1030 ($\Delta = 0.5$ mDa; 2.8 ppm). Melting point: 39.3 – 40.2 °C (DCM), literature: 44 – 45 °C.³⁴¹

General procedure for the attempted synthesis of 174 from 172

In a 50 mL round bottom flask, *o*-toluidine (**172**) (535 mg, 10 mmol, 1 eq.), calcium chloride (1.46 g) and formamide (10 mL) were placed. The mixture was heated at 180 °C and stirred for 4 hours. The reaction was then allowed to cool to room temperature and water (40 mL) was added. The aqueous phase was separated and the remained brown sticky oil was dissolved in chloroform (20 mL) and washed first with brine (2×10 mL) and then with water (10 mL). The organic phase was washed again with brine (10 mL), dried over Na_2SO_4 and concentrated under vacuum. The residue was then analysed through ^1H -NMR spectra. The results are depicted in *Scheme 65*.

*General procedure for the synthesis of compound 173*³⁴²

The reagents *o*-toluidine (**172**) (1.07 g, 20 mmol, 1 eq.) and ethyl formate (14.4 mL, 180 mmol, 9.0 eq.) were introduced to a 25 mL round bottom flask and heated at 90 °C for 3 days. The reaction was allowed to cool to room temperature and partitioned between chloroform (10 mL) and a 1 M aqueous solution of HCl (10 mL). The organic phase was collected, washed with brine (10 mL), dried over Na_2SO_4 and concentrated *in vacuo* to obtain compound **173** as a black solid (20.6 g, 85% yield).

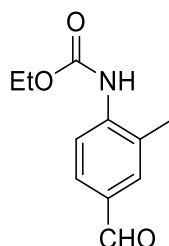


N-*o*-tolylformamide (**173**):³⁴² Black solid. ^1H NMR (600 MHz, Chloroform-*d*) δ 8.56 – 8.39 (m, 1H), 7.91 – 7.73 (m, 1H), 7.24 – 7.05 (m, 4H), 2.28 (d, $J = 12.0$ Hz, 3H). ^{13}C NMR (151 MHz, Chloroform-*d*) δ 163.33, 159.17, 135.09, 134.74, 131.39, 130.70, 129.73, 128.58, 127.29, 127.02, 126.19, 125.65, 123.12, 120.75, 17.83. The complexity of the NMR spectra is due to isomerism on the amide bond as described in literature.³⁴² FT-IR (neat) ν 3194 (br, N-

H), 3100 (br, N-H), 3045 (w), 2962 (w, C-H), 2880 (w), 1666 (s, C=O), 1586 (s), 1541 (s), 1514 (m), 1506 (s), 1475 (m), 1455 (s), 1398 (s), 1301 (s), 1283 (s), 1274 (s), 1105 (w), 1042 (m), 996 (w), 873 (w), 815 (w), 790 (w) cm^{-1} . LC-MS (ESI+) $R_t = 1.35$ min m/z $[\text{M}+\text{H}]^+ = 136.4$. HR-MS calculated for $\text{C}_8\text{H}_{10}\text{NO}$ 136.0762, found 136.0763 ($\Delta = 0.1$ mDa; 0.7 ppm). Melting point: 53.4 – 58.2 $^\circ\text{C}$ (CHCl_3), literature: 53 $^\circ\text{C}$.³⁴²

General procedure for the synthesis of quinazoline compound 174 in flow

A solution of compound **175** (358 mg, 2 mmol, 1.0 eq.) and HMTA (**177**) (280 mg, 2 mmol, 1.0 eq.) in TFA (6.7 mL) was charged to a 10 mL sample loop (Vapourtec R2/R4 unit) and pumped at 2 mL min^{-1} into a 20 mL PTFE reactor coil at 110 $^\circ\text{C}$. The collected reaction mixture was concentrated under vacuum and analysed with ^1H -NMR and LC-MS. The crude reaction mixture prepared using compound **175** was purified via flash chromatography (Eluent: Hexane:AcOEt 8:2) to obtain compound **181** (104 mg, 25% yield).

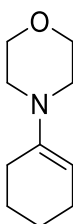


Ethyl (4-formyl-2-methylphenyl)carbamate (181):³⁴³ Yellow solid ($R_f = 0.44$, Hexane:AcOEt 8:2). ^1H NMR (700 MHz, Chloroform-*d*) δ 9.86 (s, 1H), 8.19 (d, $J = 8.4$ Hz, 1H), 7.74 – 7.68 (m, 1H), 7.67 (dd, $J = 1.9, 1.0$ Hz, 1H), 6.70 (s, 1H), 4.25 (q, $J = 7.1$ Hz, 2H), 2.30 (s, 3H), 1.32 (t, $J = 7.1$ Hz, 3H). ^{13}C NMR (176 MHz, Chloroform-*d*) δ 191.38, 153.21, 142.16, 131.53, 131.36, 130.11, 125.91, 118.86, 61.90, 17.63, 14.58. FT-IR (neat) ν 3293 (w, N-H), 2985 (w, C-H), 1729 (s, C=O), 1674 (s, C=O), 1578 (s), 1524 (s), 1496 (m), 1441 (s), 1379 (m), 1315 (m), 1274 (m), 1206 (s), 1166 (s), 941 (m), 842 (m), 778 (m) cm^{-1} . LC-MS (ESI+) $R_t = 1.93$ min m/z $[\text{M}+\text{H}]^+ = 208.7$. HR-MS calculated for $\text{C}_{11}\text{H}_{14}\text{NO}_3$ 208.0974, found 208.0990 ($\Delta = 1.6$ mDa; 7.7 ppm).

4.3. Galbascone

General procedure for the synthesis of compound 197

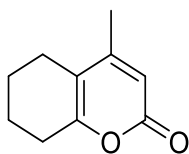
A solution of cyclohexanone (**195**) (25.8 mL, 250 mmol, 1 eq.) and morpholine (**196**) (31 mL, 360 mmol, 1.44 eq.) in cyclohexane (30 mL) was heated at reflux in a Dean-Stark apparatus for 4 days until disappearance of the starting material by GC-MS nonpolar compounds (EI) (Rt of **195** = 2.89 min, Rt of **197** = 4.27 min). The red solution was then allowed to cool to room temperature and concentrated under vacuum to gain compound **197** in 92% purity (46.7 g, 88% yield).



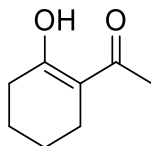
4-(cyclohex-1-en-1-yl)morpholine (187):³⁴⁴ Red oil. ¹H NMR (400 MHz, Chloroform-*d*) δ 4.66 (tt, $J = 3.8, 1.1$ Hz, 1H), 3.75 – 3.69 (m, 4H), 2.80 – 2.71 (m, 4H), 2.13 – 1.99 (m, 4H), 1.74 – 1.61 (m, 2H), 1.59 – 1.48 (m, 2H). ¹³C NMR (101 MHz, Chloroform-*d*) δ 145.53, 100.57, 67.13, 48.54, 26.97, 24.52, 23.32, 22.87. FT-IR (neat) ν 2932 (CH, m), 2854 (CH, m), 1708 (CH, s), 1646 (C=C, w), 1449 (m), 1265 (w), 1203 (w), 1117 (CO, s), 1097 (CO, s), 898 (w), 788 (w) cm^{-1} . LC-MS (ESI+) Rt = 0.96 min m/z $[M+H]^+ = 168.3$. HR-MS calculated for $\text{C}_{10}\text{H}_{18}\text{NO}$ 168.1388, found 168.1396 ($\Delta = 0.8$ mDa; 4.8 ppm).

General procedure for the attempt of the synthesis of compound 198

To a solution of compound **197** (10.0 g, 60 mmol, 1.0 eq.) and triethylamine (TEA) (12.5 mL, 90 mmol, 1.5 eq.) in dry DCM (30 mL), a solution of acetyl chloride (5.5 mL, 78 mmol, 1.3 eq.) in dry DCM (20 mL) was slowly added at 35 – 40 °C. After stirring overnight, the reaction mixture was cooled and concentrated *in vacuo*. The residues were taken up in diethyl ether and the triethylamine hydrochloride was filtered off and the yellow solution was concentrated under vacuum. The residue (11.7 g) was split into 3.2-grams aliquots where attempts of purifications via vacuum distillation (section 2.3.1), and chromatography (Eluent: hexane:AcOEt 9:1 & 3% TEA) were performed. Through flash chromatography, the compounds **202** (180 mg) and **204** (360 mg) were isolated.



4-methyl-5,6,7,8-tetrahydro-2H-chromen-2-one (202): White solid ($R_f = 0.3$, hexane:AcOEt 9:1 & 3% TEA). ^1H NMR (400 MHz, Chloroform-*d*) δ 6.04 (d, $J = 0.8$ Hz, 1H), 2.51 (tt, $J = 6.4, 1.7$ Hz, 2H), 2.42 (tt, $J = 6.2, 1.8$ Hz, 2H), 2.21 (d, $J = 0.8$ Hz, 3H), 1.86 – 1.74 (m, 2H), 1.74 – 1.64 (m, 2H). ^{13}C NMR (101 MHz, Chloroform-*d*) δ 179.80, 164.56, 163.40, 121.74, 112.88, 27.46, 21.98, 21.61, 20.72, 19.91. FT-IR (neat) ν 3065 (w), 2939 (CH, m), 2926 (CH, m), 2883 (CH, w), 1664 (C=O, s), 1595 (C=O, s), 1416 (s), 1355 (m), 1201 (w), 1181 (m), 1130 (m), 1046 (m), 976 (s), 874 (s), 753 (w), 721 (m), 598 (m), 578 (w), 505 (w) cm^{-1} . LC-MS (ESI+) $R_t = 2.17$ min m/z $[\text{M}+\text{H}]^+ = 165.6$. HR-MS calculated for $\text{C}_{10}\text{H}_{13}\text{O}_2$ 165.0916, found 165.0913 ($\Delta = -0.3$ mDa; -1.8 ppm).



1-(2-hydroxycyclohex-1-en-1-yl)ethan-1-one (204):³⁴⁵ Yellow oil ($R_f = 0.25$, hexane:AcOEt 95:5). ^1H NMR (400 MHz, Chloroform-*d*) δ 15.92 (s, 1H), 2.36 – 2.27 (m, 4H), 2.12 (s, 3H), 1.68 (qd, $J = 3.9, 1.6$ Hz, 4H). ^{13}C NMR (101 MHz, Chloroform-*d*) δ 199.34, 182.03, 107.20, 31.19, 25.16, 24.40, 22.92, 21.76. FT-IR (neat) ν 2936 (CH, m), 2862 (CH, m), 1593 (C=O, s), 1412 (s), 1363 (s), 1308 (s), 1237 (s), 1174 (m), 953 (s), 879 (m), 824 (w), 679 (w) cm^{-1} . LC-MS (ESI+) $R_t = 2.09$ min m/z $[\text{M}+\text{H}]^+ = 141.4$. HR-MS calculated for $\text{C}_8\text{H}_{13}\text{O}_2$ 141.0916, found 141.0910 ($\Delta = -0.6$ mDa; -4.3 ppm).

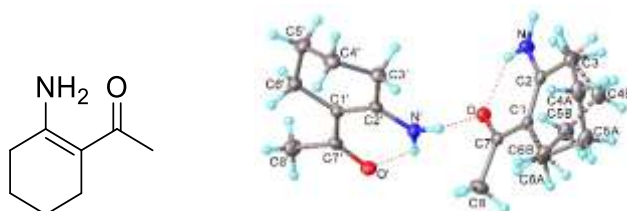
General procedure for the synthesis of compound 204

To a solution of compound **197** (20.0 g, 110 mmol, 1.0 eq.) and triethylamine (18.4 mL, 132 mmol, 1.2 eq.) in dry DCM (143 mL) maintained at 35 – 40 °C was added slowly a solution of acetyl chloride (8.6 mL, 121 mmol, 1.1 eq.) in DCM (60 mL). After stirring overnight, a 6 M aqueous solution of hydrochloric acid (55 mL) was added to the mixture and the solution heated to reflux for 2 hours. After cooling to room temperature, the pH was adjusted to 5 – 6 with a 2 M aqueous solution of NaOH (~100 mL) and the aqueous phase was extracted with DCM (3 \times 50 mL). The combined organic phase was washed with brine (100 mL), dried over Na_2SO_4 ,

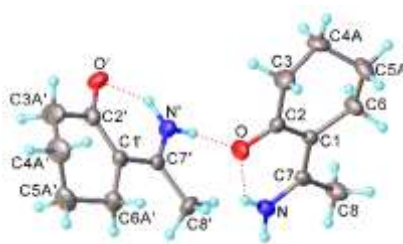
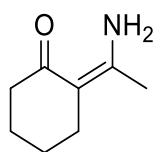
and concentrated under vacuum. The residue was purified by column chromatography (hexane:AcOEt 95:5) to gain compound **204** (10.3 g, 67% yield). The analysis data was identical to the previously prepared material.

General procedure for the synthesis of compounds 24 and 25

To a solution of compound **204** (338 mg, 2.41 mmol, 1.0 eq.) in MeOH (5 mL), was added a solution of NH₃ (7 M in MeOH, 1.4 mL, 2.41 mmol, 4 eq.). The mixture was stirred overnight and then concentrated under vacuum. The residue was purified via flash chromatography (Eluent: gradient: hexane:AcOEt, 85:15 to 1:1) to obtain compounds **207** (212 mg, 60% yield) and **208** (71 mg, 20% yield).



1-(2-aminocyclohex-1-en-1-yl)ethan-1-one (207): White solid ($R_f = 0.35$, hexane:AcOEt, 85:15). ¹H NMR (400 MHz, Chloroform-*d*) δ 9.82 (s, 1H), 4.72 (s, 1H), 2.36 – 2.28 (m, 2H), 2.27 – 2.21 (m, 2H), 2.10 (s, 3H), 1.71 – 1.55 (m, 4H). ¹³C NMR (101 MHz, Chloroform-*d*) δ 198.84, 158.22, 101.93, 31.02, 28.04, 25.69, 23.62, 21.90. FT-IR (neat) ν 3290 (NH, br), 3149 (NH, br), 2928 (CH, m), 1602 (C=O, s), 1489 (s), 1367 (m), 1253 (s), 1228 (s), 1174 (s), 1056 (m), 1014 (m), 951 (m), 824 (w) cm⁻¹. LC-MS (ESI+) $R_t = 1.50$ min m/z [M+H]⁺ = 140.4. HR-MS calculated for C₈H₁₄O 140.1075, found 140.1062 ($\Delta = -1.3$ mDa; -9.3 ppm). Melting point: 95.5 – 105.6 °C (EtOAc). Crystal structure data for C₈H₁₃NO ($M = 139.19$ g/mol): monoclinic, space group P2₁/n (no. 14), $a = 10.1126(4)$ Å, $b = 12.3037(4)$ Å, $c = 13.0794(5)$ Å, $\beta = 108.3649(14)^\circ$, $V = 1544.49(10)$ Å³, $Z = 8$, $T = 120$ K, $\mu(\text{Mo K}\alpha) = 0.079$ mm⁻¹, $D_{\text{calc}} = 1.197$ g/cm³, 23509 reflections measured ($4.472^\circ \leq 2\theta \leq 55.992^\circ$), 3730 unique ($R_{\text{int}} = 0.0507$, $R_{\text{sigma}} = 0.0359$) which were used in all calculations. The final R_1 was 0.0498 ($I > 2\sigma(I)$) and wR_2 was 0.1174 (all data). Operator reference number: 20srv294.



(*Z*)-2-(1-aminoethylidene)cyclohexan-1-one (**208**): White solid ($R_f = 0.33$, hexane:AcOEt, 7:3). ^1H NMR (400 MHz, Chloroform-*d*) δ 10.84 (s, 1H), 5.12 (s, 1H), 2.31 (q, $J = 5.8$ Hz, 4H), 1.93 (s, 3H), 1.69 (qp, $J = 7.0, 2.7$ Hz, 4H). ^{13}C NMR (101 MHz, Chloroform-*d*) δ 197.18, 160.96, 101.41, 38.49, 26.22, 24.00, 23.13, 21.31. FT-IR (neat) ν 3236 (NH, br), 3089 (NH, br), 2934 (CH, w), 2856 (CH, w), 1594 (C=O, s), 1482 (CH, s), 1440 (s), 1370 (s), 1290 (s), 1264 (s), 1200 (s), 1159 (s), 1083 (m), 1030 (m), 963 (m), 817 (w), 678 (s), 639 (s) cm^{-1} . LC-MS (ESI+) $R_t = 1.69$ min m/z $[\text{M}+\text{H}]^+ = 140.5$. HR-MS calculated for $\text{C}_8\text{H}_{14}\text{O}$ 140.1075, found 140.1059 ($\Delta = -1.6$ mDa; -11.4 ppm). Melting point: 109.6 – 114.3 °C (EtOAc). Crystal structure data for $\text{C}_8\text{H}_{13}\text{NO}$ ($M = 139.19$ g/mol): monoclinic, space group $\text{P}2_1/\text{n}$ (no. 14), $a = 11.4750(4)$ Å, $b = 8.4528(3)$ Å, $c = 17.0975(6)$ Å, $\beta = 105.0287(14)^\circ$, $V = 1601.66(10)$ Å³, $Z = 8$, $T = 120$ K, $\mu(\text{Mo K}\alpha) = 0.076$ mm^{-1} , $D_{\text{calc}} = 1.154$ g/cm^3 , 19884 reflections measured ($3.858^\circ \leq 2\Theta \leq 54.998^\circ$), 3669 unique ($R_{\text{int}} = 0.0449$, $R_{\text{sigma}} = 0.0359$) which were used in all calculations. The final R_1 was 0.0563 ($I > 2\sigma(I)$) and wR_2 was 0.1249 (all data). Operator reference number: 20srv295.

General procedure for the reduction of **204** employing sodium borohydride

To an ice-cooled solution of compound **204** (1.4 g, 10 mmol, 1.0 eq.) in MeOH (50 mL) was added portion-wise sodium borohydride (454 mg, 12 mmol, 1.2 eq.). After the addition, the mixture was allowed to warm to room temperature with stirring. The mixture was sampled after 1, 4, and 24 hours and monitored via LC-MS (ESI). Additional sodium borohydride (378 mg, 10 mmol, 1.0 eq.) was added after 30 hours of stirring and a further sample was taken for monitoring. The mixture was cooled to 0 °C and quenched with a 1 M solution of hydrochloric acid (30 mL). The organic solvent was removed *in vacuo* and the remaining aqueous layer extracted with EtOAc (3×15 mL). The combined organic phase was washed with water, brine, dried over Na_2SO_4 , and concentrated to yield a pale yellow oil which was analysed via LC-MS (ESI) and NMR spectroscopy. The results are depicted in *Scheme 78* and *Figure 43*.

General procedure for the reduction of compound **204** employing baker's yeast

Dry baker's yeast (8 g), water (152 mL), glucose (8 g), and allyl alcohol (4.1 mL, 60 mmol, 30 eq.) were mixed and warmed at 50 °C for 30 minutes. The mixture was cooled to 30 °C and a solution of compound **204** (280 mg, 2 mmol, 1.0 eq.) in Et₂O:hexane (1:1, 2 mL) was added. The reaction was monitored via LC-MS (ESI). The results are depicted in *Scheme 78*.

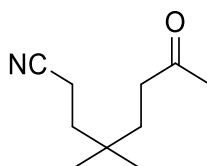
General procedure for the hydrogenation of 207

Flow mode (Thales Nano H-Cube)[®]: A solution of compound **207** (18.8 mg, 0.135 mmol, 1 eq.) in MeOH (1.5 mL) was pumped at a flow rate of 0.5 to 1 mL min⁻¹ through a H-Cube[®] apparatus containing a Pd/C (or PtO₂) cartridge. Four different experiments were performed changing the flowrate, temperature, and hydrogen pressure. Two experiments were run at r.t. and 1 bar of hydrogen varying the flowrate between 0.5 and 1 mL min⁻¹, and two at 50 °C under a pressure of 10 bar of hydrogen varying the flowrate between 0.5 and 1 mL min⁻¹. The mixtures were collected and analysed by TLC (Eluent: hexane:EtOAc 85:15, R_f of **207** = 0.35). The results are depicted in *Scheme 79*.

Batch mode: To a solution of compound **207** (18.8 mg, 0.135 mmol, 1 eq.) in MeOH (1.5 mL), was added in one portion PtO₂ (1 mg, 0.004 mmol, 0.03 eq.) or 5% Pd/C (3 mg, 0.00135 mmol, 0.01 eq.). A balloon filled with hydrogen was used to purge the sealed round bottom flask. Once purged, the vent needle was removed, a second filled hydrogen balloon was added and the mixture was stirred for 3 days at room temperature. The mixture was heated at reflux for a further 2 days and monitored via TLC (Eluent: hexane:EtOAc 85:15, R_f of **207** = 0.35).

General procedure for the synthesis of 189

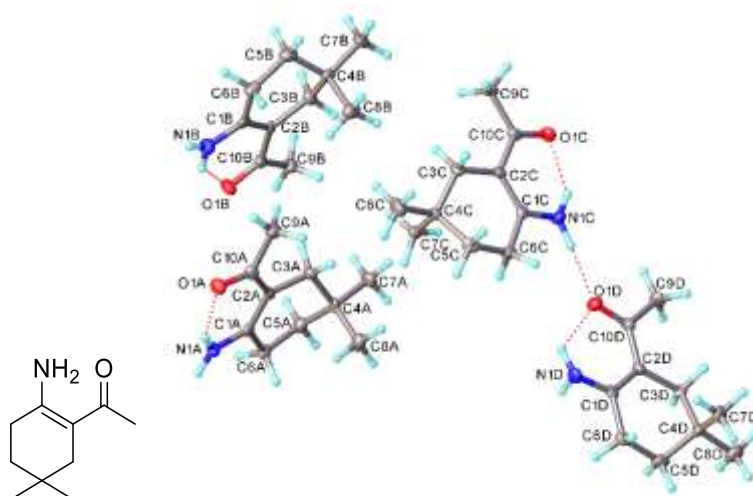
A solution of acrylonitrile (**185**) (2.62 mL, 40 mmol, 1 eq.), 5-methyl-hexan-2-one (**184**) (56 mL, 400 mol, 10 eq.), and TBADT (**210**) (2.66 g, 0.8 mmol, 0.02 eq.) in acetonitrile (39 mL) was prepared and pumped at a flow rate of 208 μL min⁻¹ through a 10 mL PFA coil reactor cooled to 20 °C (Run through a Vapourtec easy-photochem E-series equipped with a 365 nm 16 W Gen-2 LED). The collected mixture was concentrated under vacuum and the residue was purified via column chromatography (Eluent: hexane:AcOEt 85:15) to yield compound **189** as a 95:5 mixture with **211** (4.44 g, 63% yield).



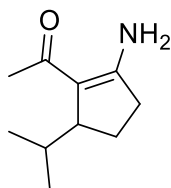
4,4-Dimethyl-7-oxooctanenitrile (189):³⁰¹ Colourless oil ($R_f = 0.32$, hexane:AcOEt 85:15). ^1H NMR (400 MHz, Chloroform-*d*) δ 2.42 – 2.35 (m, 2H), 2.31 – 2.24 (m, 2H), 2.16 (s, 3H), 1.64 – 1.56 (m, 2H), 1.53 – 1.45 (m, 2H), 0.89 (s, 6H). ^{13}C NMR (101 MHz, Chloroform-*d*) δ 208.63, 120.44, 38.52, 37.30, 34.44, 32.41, 30.22, 26.21, 12.47. FT-IR (neat) ν 2962 (CH, m), 2936 (CH, w), 2874 (CH, w), 2246 (CN, w), 1712 (C=O, s), 1472 (w), 1423 (w), 1369 (m), 1356 (m), 1163 (m), 755 (w) cm^{-1} . LC-MS (ESI+) $R_t = 1.81$ min m/z $[\text{M}+\text{H}]^+ = 168.6$. HR-MS calculated for $\text{C}_{10}\text{H}_{18}\text{NO}$ 168.1388, found 168.1413 ($\Delta = 2.5$ mDa; 14.9 ppm).

*Procedure A for the attempted synthesis of compound 190 employing potassium hydroxide*³¹⁸

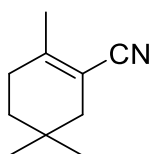
To a solution of compound **189** (1.0 g, 6 mmol, 1.0 eq.) in ethanol (12 mL), was added in one portion potassium hydroxide (337 mg, 6 mmol, 1.0 eq.) and the mixture was heated at reflux. After 18 hours at reflux, the reaction was allowed to cool to room temperature. The mixture was concentrated under vacuum and partitioned between water (15 mL) and Et_2O (15 mL). The aqueous phase was extracted with Et_2O (2×15 mL) and the combined organic layers were washed with brine, and dried over Na_2SO_4 , and concentrated *in vacuo*. The residue was purified by column chromatography (Eluent: gradient: Toluene:MeCN 9:1 to 7:3) to isolate the compounds **190** (20.1 mg, 2% yield), **212** (20.1 mg, 40% yield), **213** (510 mg, 57% yield), **214-A** (44.5 mg, 4% yield), **214-B** (55.6 mg, 5% yield).



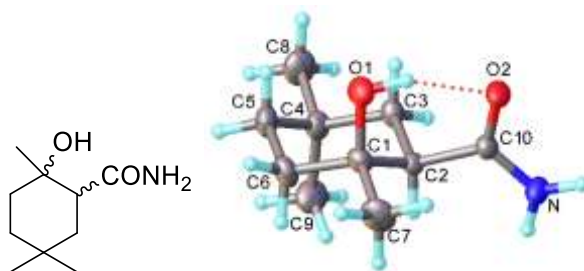
1-(2-amino-5,5-dimethylcyclohex-1-en-1-yl)ethan-1-one (190): White crystal ($R_f = 0.45$, Toluene:MeCN 9:1). $^1\text{H NMR}$ (400 MHz, Chloroform-*d*) δ 2.26 (tt, $J = 6.7, 1.0$ Hz, 2H), 2.10 (s, 5H), 1.39 (t, $J = 6.8$ Hz, 2H), 0.96 (s, 6H). $^{13}\text{C NMR}$ (101 MHz, Chloroform-*d*) δ 198.97, 157.22, 101.04, 39.77, 34.27, 29.81, 28.26, 28.24, 28.14. FT-IR (neat) ν 3285 (NH, m), 3137 (NH, m), 2950 (CH, m), 2918 (CH, m), 2866 (CH, w), 1603 (C=O, s), 1493 (s), 1420 (m), 1384 (m), 1360 (m), 1224 (m), 1215 (s), 1040 (m), 1063 (m), 988 (w), 928 (w), 623 (s), 580 (s) cm^{-1} . LC-MS (ESI+) $R_t = 2.09$ min m/z $[\text{M}+\text{H}]^+ = 168.6$. HR-MS calculated for $\text{C}_{10}\text{H}_{18}\text{NO}$ 168.1388, found 168.1408 ($\Delta = 2.0$ mDa; 11.9 ppm). Melting point: 85.6 – 92.1 °C (AcOEt). Crystal structure data for $\text{C}_{10}\text{H}_{17}\text{NO}$ ($M = 167.24$ g/mol): triclinic, space group P-1 (no. 2), $a = 9.5895(6)$ Å, $b = 9.6078(6)$ Å, $c = 22.7528(13)$ Å, $\alpha = 93.765(2)^\circ$, $\beta = 93.596(2)^\circ$, $\gamma = 103.257(2)^\circ$, $V = 2029.5(2)$ Å³, $Z = 8$, $T = 120$ K, $\mu(\text{Mo K}\alpha) = 0.070$ mm⁻¹, $D_{\text{calc}} = 1.095$ g/cm³, 21990 reflections measured ($4.37^\circ \leq 2\Theta \leq 50.054^\circ$), 7175 unique ($R_{\text{int}} = 0.0483$, $R_{\text{sigma}} = 0.0622$) which were used in all calculations. The final R_1 was 0.0643 ($I > 2\sigma(I)$) and wR_2 was 0.1475 (all data). Operator reference number: 21srv023.



1-(2-amino-5-isopropylcyclopent-1-en-1-yl)ethan-1-one (212): Yellow oil ($R_f = 0.35$, Toluene:MeCN 9:1). $^1\text{H NMR}$ (600 MHz, Chloroform-*d*) δ 8.63 (brs, 1H), 4.71 (brs, 1H), 2.87 (dddd, $J = 8.9, 3.6, 1.7, 0.9$ Hz, 1H), 2.58 – 2.50 (m, 1H), 2.35 – 2.24 (m, 1H), 2.08 (s, 3H), 1.92 – 1.85 (m, 1H), 1.85 – 1.78 (m, 1H), 1.70 (ddt, $J = 13.0, 8.8, 1.9$ Hz, 1H), 0.94 (d, $J = 6.8$ Hz, 3H), 0.73 (d, $J = 6.8$ Hz, 3H). $^{13}\text{C NMR}$ (151 MHz, Chloroform-*d*) δ 195.78, 164.75, 110.07, 49.18, 34.42, 32.36, 27.76, 22.23, 21.70, 16.53. LC-MS (ESI+) $R_t = 2.09$ min m/z $[\text{M}+\text{H}]^+ = 168.4$. HR-MS calculated for $\text{C}_{10}\text{H}_{18}\text{NO}$ 168.1388, found 168.1391 ($\Delta = 0.3$ mDa; 1.8 ppm).



2,5,5-trimethylcyclohex-1-ene-1-carbonitrile (213): Yellow oil ($R_f = 0.72$, Toluene:MeCN 9:1). ^1H NMR (400 MHz, Chloroform-*d*) δ 2.13 (ddt, $J = 6.6, 5.5, 1.1$ Hz, 2H), 1.99 (s, 5H), 1.38 (t, $J = 6.4$ Hz, 2H), 0.92 (s, 6H). ^{13}C NMR (101 MHz, Chloroform-*d*) δ 152.43, 119.60, 105.46, 40.59, 34.53, 29.45, 28.61, 27.73, 22.62. FT-IR (neat) ν 2954 (CH, s), 2917 (CH, s), 2870 (CH, s), 2214 (CN, m), 1647 (m), 1447 (s), 1447 (m), 1424 (m), 1387 (m), 1367 (m), 1229 (w), 1162 (w), 943 (w), 839 (w) cm^{-1} . LC-MS (ESI+) $R_t = 2.97$ min m/z $[\text{M}+\text{H}]^+ = 150.3$. HR-MS calculated for $\text{C}_{10}\text{H}_{16}\text{N}$ 150.1283, found 150.1312 ($\Delta = 2.9$ mDa; 19.3 ppm).



2-hydroxy-2,5,5-trimethylcyclohexane-1-carboxamide (214): Two isomers isolated. Isomer A: White crystal ($R_f = 0.20$, Toluene:MeCN 8:2). ^1H NMR (400 MHz, CD_3CN) δ 6.52 (s, 1H), 5.88 (s, 1H), 4.66 (s, 1H), 2.29 (ddd, $J = 13.3, 3.8, 0.9$ Hz, 1H), 2.23 (s, 1H), 1.69 (t, $J = 13.1$ Hz, 1H), 1.61 (ddd, $J = 12.9, 11.1, 7.3$ Hz, 1H), 1.43 (d, $J = 3.3$ Hz, 1H), 1.40 (t, $J = 3.4$ Hz, 1H), 1.24 (ddd, $J = 12.9, 3.8, 2.5$ Hz, 1H), 1.13 (s, 2H), 0.92 (s, 3H), 0.91 (s, 3H). ^{13}C NMR (101 MHz, CD_3CN) δ 180.54, 69.18, 47.74, 39.87, 35.41, 34.69, 32.90, 30.44, 29.50, 24.20. FT-IR (neat) ν 3299 (OH, w), 3166 (NH, w), 2963 (CH, m), 2902 (CH, m), 1655 (C=O, m), 1409 (s), 1375 (s), 1294 (s), 1265 (s), 1146 (s), 1083 (m), 981 (m), 705 (m), 673 (m) cm^{-1} . LC-MS (ESI+) $R_t = 1.81$ min m/z $[\text{M}+\text{H}]^+ = 168.9$. HR-MS calculated for $\text{C}_{10}\text{H}_{18}\text{NO}$ 168.1388, found 168.1414 ($\Delta = 2.6$ mDa; 15.5 ppm). Crystal structure data for $\text{C}_{10}\text{H}_{19}\text{NO}_2$ ($M = 185.26$ g/mol): monoclinic, space group P21/c (no. 14), $a = 8.5511(2)$ Å, $b = 11.7165(3)$ Å, $c = 11.6031(3)$ Å, $\beta = 106.1754(9)^\circ$, $V = 1116.48(5)$ Å³, $Z = 4$, $T = 200$ K, $\mu(\text{Mo K}\alpha) = 0.076$ mm⁻¹, $D_{\text{calc}} = 1.102$ g/cm³, 19399 reflections measured ($5.044^\circ \leq 2\theta \leq 63.996^\circ$), 3868 unique ($R_{\text{int}} = 0.0349$, $R_{\text{sigma}} = 0.0276$) which were used in all calculations. The final R_1 was 0.0466 ($I > 2\sigma(I)$) and wR_2 was 0.1257 (all data). Operator reference number: 20srv238.

Isomer B: White solid ($R_f = 0.32$, Toluene:MeCN 8:2). ^1H NMR (600 MHz, Chloroform-*d*) δ 9.40 (s, 1H), 3.36 (s, 1H), 2.50 (s, 1H), 2.40 (s, 3H), 1.74 (t, $J = 13.1$ Hz, 1H), 1.65 (td, $J = 13.6, 4.4$ Hz, 1H), 1.57 – 1.44 (m, 2H), 1.38 (ddd, $J = 12.9, 3.5, 2.3$ Hz, 1H), 1.26 (s, 3H), 1.18 (ddd, $J = 13.4, 4.1, 2.3$ Hz, 1H), 0.96 (s, 3H), 0.93 (s, 3H). ^{13}C NMR (151 MHz, Chloroform-

d) δ 173.02, 69.17, 38.86, 35.60, 33.85, 32.50, 30.14, 29.08, 25.61, 23.98. FT-IR (neat) ν 3482 (OH, w), 3246 (NH, w), 3161 (NH, w), 2965 (CH, m), 2936 (CH, m), 2869 (CH, w), 1732 (C=O, s), 1675 (m), 1510 (s), 1390 (s), 1204 (m), 1197 (s), 1182 (s), 981 (w), 914 (w), 546 (w) cm^{-1} . LC-MS (ESI+) $R_t = 1.81$ min m/z $[M+H]^+ = 168.9$. HR-MS calculated for $\text{C}_{10}\text{H}_{18}\text{NO}$ 168.1388, found 168.1414 ($\Delta = 2.6$ mDa; 15.5 ppm).

Procedure B for the attempted synthesis of compound 190

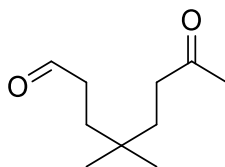
To a solution of compound **189** (1.34 g, 8.02 mmol, 1.0 eq.) in dry toluene (4 mL) under a nitrogen atmosphere was slowly added potassium *t*-butoxide (1.08 g, 9.62 mmol, 1.2 eq.). The reaction was heated at reflux for 3 hours and then allowed to cool to room temperature. The mixture was quenched with saturated aqueous solution of ammonium chloride (15 mL) and the aqueous phase extracted with toluene (2×15 mL). The combined organic layers were washed with water (30 mL), brine (30 mL), and dried over Na_2SO_4 . The residue was purified by column chromatography (Eluent: Hexane:AcOEt 9:1, $R_f = 0.42$) to yield **213** (658 mg, 55% yield).

*Procedure C for the attempted synthesis of compound 190*³¹⁰

A solution of copper(I) iodide (69 mg, 0.36 mmol, 0.2 eq.) and 2,2'-bipyridine (62.5 mg, 0.4 mmol, 0.22 eq.) in dry DMF (3.6 mL) was stirred for 10 minutes before slowly adding compound **189** (300 mg, 1.8 mmol, 1.0 eq.) and sodium *t*-butoxide (808 mg, 7.2 mmol, 4.0 eq.) at room temperature. The mixture was then heated at 80 °C for 15 hours. After cooling to room temperature the reaction was quenched with a saturated solution of ammonium chloride (15 mL). The aqueous solution was extracted with AcOEt (3×15 mL) and the combined organic layer was washed with water (20 mL), brine (20 mL), and dried over Na_2SO_4 . The residue was analysed via $^1\text{H-NMR}$ spectra.

General procedure for the synthesis of compound 193

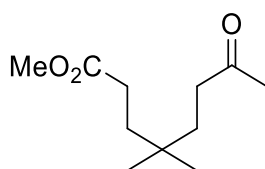
A solution of acrolein (**215**) (371 μL , 5 mmol, 1 eq.), 5-methyl-hexan-2-one (**184**) (7.04 mL, 50 mol, 10 eq.), and TBADT (**210**) (332 g, 0.1 mmol, 0.02 eq.) in acetonitrile (50 mL) was prepared and pumped at a flow rate of 208 $\mu\text{L min}^{-1}$ through a 10 mL PTFE coil reactor maintained at 20 °C. The collected reaction mixture was concentrated under reduced pressure and the residue was purified via column chromatography (Eluent: hexane:AcOEt 85:15) to yield compound **193** (213 mg, 25% yield).



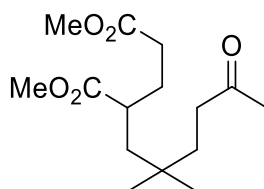
4,4-dimethyl-7-oxooctanal (193):³⁴⁶ Colourless oil (R_f = 0.35, hexane:AcOEt 85:15). ¹H NMR (400 MHz, Chloroform-*d*) δ 9.76 (t, *J* = 1.7 Hz, 1H), 2.43 – 2.32 (m, 4H), 2.16 – 2.11 (m, 3H), 1.53 – 1.42 (m, 4H), 0.84 (s, 6H). ¹³C NMR (101 MHz, Chloroform-*d*) δ 209.18, 202.71, 39.32, 38.76, 34.92, 33.20, 31.95, 30.13, 26.64. FT-IR (neat) ν 2958 (CH, m), 2933 (CH, m), 2870 (CH, m), 1705 (C=O, s), 1367 (w), 1296 (w), 1163 (w), 1128 (w), 913 (w) cm⁻¹. LC-MS (ESI+) Rt = 1.78 min m/z [M+H]⁺ = 171.1. HR-MS calculated for C₁₀H₁₉O₂ 171.1385, found 171.1390 (Δ = 0.5 mDa; 2.9 ppm).

General procedure for the synthesis of compound 221

A solution of methyl acrylate (**220**) (1.72 mL, 20 mmol, 1.0 eq.), 5-methyl-hexan-2-one (**184**) (28.18 mL, 200 mol, 10.0 eq.), and TBADT (**210**) (1.33 g, 0.4 mmol, 0.02 eq.) in acetonitrile (50 mL) was prepared and pumped at a flow rate of 208 μL min⁻¹ through a 10 mL PTFE coil reactor maintained at 20 °C. The collected mixture was concentrated under reduced pressure and the residue was purified via column chromatography (Eluent: hexane:AcOEt 9:1) to yield **221** (2.28g, 57% yield) and isolate **222** (1.43 g, 50% yield).



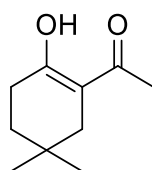
methyl 4,4-dimethyl-7-oxooctanoate (221): Colourless oil (R_f = 0.45, hexane:AcOEt 9:1). ¹H NMR (400 MHz, Chloroform-*d*) δ 3.66 (d, *J* = 1.2 Hz, 3H), 2.44 – 2.33 (m, 2H), 2.32 – 2.20 (m, 2H), 2.15 (dt, *J* = 1.1, 0.6 Hz, 3H), 1.57 – 1.50 (m, 2H), 1.50 – 1.43 (m, 2H), 0.85 (d, *J* = 1.2 Hz, 6H). ¹³C NMR (101 MHz, Chloroform-*d*) δ 209.37, 174.79, 51.78, 38.83, 36.29, 34.92, 32.08, 30.16, 29.41, 26.62. FT-IR (neat) ν 2956 (CH, m), 2874 (CH, m), 1735 (C=O, s), 1714 (C=O, s), 1437 (m), 1367 (m), 1296 (m), 1200 (m), 1163 (s), 1129 (m), 993 (w) cm⁻¹. LC-MS (ESI+) Rt = 2.14 min m/z [M+H]⁺ = 201.4. HR-MS calculated for C₁₁H₂₁O₃ 201.1491, found 201.1499 (Δ = 0.8 mDa; 4.0 ppm).



dimethyl 2-(2,2-dimethyl-5-oxohexyl)pentanedioate (222): Yellow oil ($R_f = 0.25$, hexane:AcOEt 9:1). $^1\text{H NMR}$ (600 MHz, Chloroform-*d*) δ 3.66 (s, 3H), 3.65 (d, $J = 0.7$ Hz, 3H), 2.45 (tdd, $J = 9.4, 5.4, 2.4$ Hz, 1H), 2.36 (ddd, $J = 8.5, 6.8, 4.8$ Hz, 2H), 2.28 (t, $J = 7.6$ Hz, 2H), 2.14 (s, 3H), 1.90 – 1.74 (m, 3H), 1.44 (ddd, $J = 10.1, 6.7, 2.1$ Hz, 2H), 1.19 (dd, $J = 14.3, 2.4$ Hz, 1H), 0.83 (s, 3H), 0.82 (s, 3H). $^{13}\text{C NMR}$ (151 MHz, Chloroform-*d*) δ 209.23, 177.08, 173.35, 51.82, 51.79, 43.94, 40.69, 38.85, 35.34, 32.81, 31.71, 30.11, 29.97, 26.86, 26.72. FT-IR (neat) ν 2954 (CH, m), 2872 (CH, m), 1732 (C=O, s), 1715 (C=O, s), 1436 (m), 1367 (m), 1195 (m), 1158 (s), 1053 (w) cm^{-1} . LC-MS (ESI+) $R_t = 2.32$ min m/z $[\text{M}+\text{H}]^+ = 287.6$. HR-MS calculated for $\text{C}_{15}\text{H}_{27}\text{O}_5$ 287.1858, found 287.1858 ($\Delta = -0.2$ mDa; -0.7 ppm).

General procedure for the synthesis of compound 223 from compound 221

To an ice-cooled solution of compound **221** (1.5 g, 7.5 mmol, 1 eq.) in dry THF (15 mL) under a nitrogen atmosphere was added portion-wise potassium *t*-butoxide (1.3 g, 11.25 mmol, 1.5 eq.). The reaction was stirred at room temperature for 12 hours. The reaction was quenched with a 1 M solution of HCl (15 mL) and the THF was removed under reduced pressure. The aqueous phase was extracted with AcOEt (3×20 mL), and the combined organic phase was washed with water (20 mL), brine (20 mL), dried over Na_2SO_4 and concentrated under reduced pressure. The residue was purified by column chromatography (Eluent: Hexane:AcOEt 95:5) to yield **223** (1.26 g, quant. yield).



1-(2-hydroxy-5,5-dimethylcyclohex-1-en-1-yl)ethan-1-one (223):³⁴⁷ Yellow oil ($R_f = 0.35$, hexane:AcOEt 95:5). $^1\text{H NMR}$ (700 MHz, Chloroform-*d*) δ 2.35 (tt, $J = 6.8, 1.1$ Hz, 2H), 2.11 (s, 3H), 2.09 (d, $J = 1.1$ Hz, 2H), 1.46 (t, $J = 6.8$ Hz, 2H), 0.98 (s, 6H). $^{13}\text{C NMR}$ (176 MHz, Chloroform-*d*) δ 199.44, 181.27, 106.03, 38.44, 34.24, 29.59, 28.45, 25.15. FT-IR (neat) ν 2953 (CH, m), 2927 (CH, m), 2867 (CH, m), 1594 (C=O, s), 1447 (m), 1417 (s), 1363 (s), 1300 (s),

1289 (m), 1244 (s), 1209 (s), 949 (m), 931 (w) cm^{-1} . LC-MS (ESI+) $R_t = 2.64$ min m/z $[\text{M}+\text{H}]^+ = 169.3$. HR-MS calculated for $\text{C}_{10}\text{H}_{17}\text{O}_2$ 169.1229, found 169.1231 ($\Delta = 0.2$ mDa; 1.2 ppm).

*General procedure for the synthesis of compound **190** from compound **223***

A 7 M solution of ammonia in methanol (4 mL, 28 mmol, 4.0 eq.) was slowly added to a solution of compound **223** (1.18 g, 7 mmol, 1.0 eq.) in methanol (10 mL). The reaction mixture was stirred overnight and then concentrated under reduced pressure. The residue was purified by column chromatography (Eluent: hexane:AcOEt 8:2) to yield compound **190** ($R_f = 0.35$, 715 mg, 57% yield).

*General procedures for the hydrogenation of **190***

Flow mode (Thales Nano H-Cube®): A solution of compound **190** (22.6 mg, 0.135 mmol) in MeOH (1.5 mL) was pumped at a flow rate of 0.5 to 1 mL min^{-1} through the H-Cube® apparatus containing a Pd/C (or PtO_2) cartridge. Four different experiments were performed changing the flowrate, temperature, and hydrogen pressure. Two experiments were run at r.t. and 1 bar of hydrogen varying the flowrate between 0.5 and 1 mL min^{-1} , and two at 50 °C under a pressure of 10 bar of hydrogen varying the flowrate between 0.5 and 1 mL min^{-1} . The mixtures were collected and analysed by TLC (Eluent: hexane:EtOAc 8:2, R_f of **190** = 0.40).

Batch mode: To a solution of compound **190** (22.6 mg, 0.135 mmol, 1 eq.) in MeOH (1.5 mL), was added in one portion PtO_2 (1 mg, 0.004 mmol, 0.03 eq.) or 5% Pd/C (3 mg, 0.00135 mmol, 0.01 eq.). A balloon filled with hydrogen was used to purge the sealed round bottom flask. Once purged, the vent needle was removed and a second filled balloon of hydrogen was added and the mixture was stirred for 3 days at room temperature. The mixture was heated at reflux for a further 2 days and monitored via TLC (Eluent: hexane:EtOAc 8:2, R_f of **190** = 0.40).

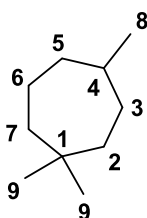
*General procedure for the reduction of compound **190** employing sodium borohydride and acetic acid*

To a suspension of sodium borohydride (974 mg, 25.76 mmol, 4.0 eq.) in dry THF (19 mL) cooled to -10 °C, was added slowly over 10 minutes acetic acid (18.8 mL, 328 mmol, 51.0 eq.). The mixture was stirred for 30 minutes at room temperature and then compound **190** (1.08 g, 6.44 mmol, 1 eq.) was slowly added over 1 hour. The mixture was stirred at room temperature

for 48 hour and then monitored through LC-MR (ESI) and NMR spectra. The results are depicted in *Scheme 87*.

*General procedure for the hydrogenation of compound 186 to compound 191*³²²

To a solution of 3-carene (**186**) (19.6g, 129 mmol, 1 eq.) in propionic acid (200 mL) was added 20% Pd/C (2 g, 0.03 eq.). The reaction was heated to 100 °C for 4 days under hydrogen. The reaction mixture was cooled with an ice bath and a 6 M NaOH solution was slowly added until a pH 14. The aqueous phase was extracted with DCM (3 × 25 mL), and the combined organic phase was washed with brine (50 mL), dried over Na₂SO₄, and concentrated under vacuum to yield the product **191** in 90% purity (13.1 g, 65% yield).



1,1,4-trimethylcycloheptane (191):^{322,348} Colourless oil. ¹H NMR (600 MHz, Chloroform-*d*) δ 1.79 – 1.73 (m, 1H), 1.52 – 1.37 (m, 3H), 1.37 – 1.21 (m, 5H), 1.18 – 1.11 (m, 1H), 0.97 (dtd, *J* = 13.8, 10.9, 2.9 Hz, 1H), 0.88 (d, *J* = 6.7 Hz, 3H), 0.87 (s, 3H), 0.87 (s, 3H). ¹³C NMR (151 MHz, Chloroform-*d*) δ 42.43 (2), 40.41 (5), 39.89 (6), 36.86 (4), 33.39 (1), 31.69 (3), 31.19 (9), 30.62 (9), 24.07 (8), 22.31 (7). ¹³C NMR assignment based on literature data.³⁴⁸ GC-MS nonpolar compounds (EI) Rt = 2.58 min *m/z* [M+H]⁺ = 140.2. FT-IR (neat) ν 2950 (CH, s), 2911 (CH, s), 2855 (CH, m), 1464 (m), 1364 (w), 1185 (w), 953 (w) cm⁻¹.

*Procedure A&B for the attempted synthesis of compound 229*³²⁴

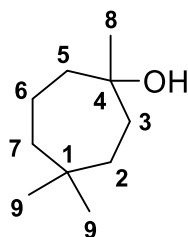
To a solution of **191** (1.4 g, 8.9 mmol, 1.0 eq.) in a mixture MeCN:H₂O (10:1, 100 mL) at 8 - 10 °C, was added six portions of sodium bicarbonate (1.68 g, 20 mmol, 2.0 eq.), oxone (3.07 g, 10 mmol, 1.0 eq.), and 1,1,1-trifluoroacetone (3 mL, 33 mmol, 3.0 eq.) or acetone (1.55 mL, 33 mmol, 3.0 eq.) were added every hour over a period of 6 hours. The reaction was then warmed to room temperature, diluted with water (50 mL) and extracted with DCM (3 × 25 mL). The combined organic phase was washed with brine (25 mL), dried over Na₂SO₄, and concentrated under vacuum. The residue was purified via chromatography (Eluent: hexane:AcOEt 9:1) to gain **229** in (505 mg, 36% yield, when TFA was employed).

Procedure C for the attempted synthesis of compound 229

To a solution of compound **191** (1.40 g, 10 mmol) in *t*BuOMe (62.5 mL) at -78 °C, was bubbled ozone for a period of 1 hours. The blue solution was sampled and analysed by LC-MS (ESI). The results are depicted in *Table 29*.

Procedure D for the attempted synthesis of compound 229

To a solution of compound **191** (1.4 g, 8.9 mmol, 1.0 eq.) in chloroform (22 mL) was added *m*-CPBA (3.45 g, 1.0 eq.). The mixture was heated at reflux for 18 hours or until disappearance of compound **191** as determined by GC-MS nonpolar compounds (EI). The mixture was then quenched with a 10% aqueous solution of Na₂S₂O₃ (20 mL), and washed with a 1 M solution of NaOH (20 mL). The organic layer was washed with water (20 mL), brine (20 mL), dried over Na₂SO₄, and concentrated under reduced pressure. The residue was purified via chromatography (Eluent: hexane:AcOEt 9:1) to obtain compound **229** (393 mg, 28% yield).



1,4,4-trimethylcycloheptan-1-ol (229).³⁴⁸ Colourless oil (*R*_f = 0.45, hexane:AcOEt 9:1). ¹H NMR (600 MHz, Chloroform-*d*) δ 1.65 (dd, *J* = 12.9, 8.0 Hz, 1H), 1.60 – 1.45 (m, 6H), 1.41 (dd, *J* = 14.0, 9.0 Hz, 1H), 1.33 – 1.23 (m, 2H), 1.22 (d, *J* = 1.3 Hz, 3H), 1.20 – 1.12 (m, 1H), 0.90 (d, *J* = 1.3 Hz, 3H), 0.88 (d, *J* = 1.3 Hz, 3H). ¹³C NMR (151 MHz, Chloroform-*d*) δ 73.34 (4), 45.16 (5), 43.36 (7), 36.56 (3), 34.79 (2), 33.04 (1), 31.67 (8), 30.66 (9), 30.53 (9), 19.32 (6). ¹³C NMR assignment based on literature data.³⁴⁸ GC-MS nonpolar compounds (EI) *R*_t = 3.17 min *m/z* [M+H]⁺ = 156.2. FT-IR (neat) ν 3355 (OH, br), 2951 (CH, m), 2922 (CH, m), 2865 (CH, w), 1467 (w), 1364 (w), 1275 (w), 1166 (C-O, s), 1111 (C-O, s) cm⁻¹.

General Procedure for the Amine-Catalysed Irregular Nitro-Aldol reaction to 38

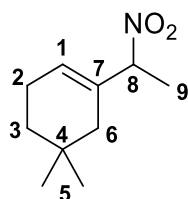
A mixture of 3,3-dimethylcyclohexanone (**68**) (40.0 g, 0.305 mol, 1.0 eq.), *N,N*-diethylethylenediamine (**75**) (4.3 mL, 10 mol%), EtOAc (30 mL) and nitroethane (214 mL, 10 eq.) was heated in a Dean-Stark apparatus (pre-filled with EtOAc). After 3 hours, a second

portion of *N,N*-diethylethylenediamine (**75**) (4.3 mL, 10 mol%) was added and a third portion (4.3 mL, 10 mol%) was added after a further 3 hours. After a total of 22 hours the reaction was cooled to room temperature and the nitroethane and EtOAc were removed under reduced pressure. EtOAc (100 mL) was added and the amine residues were extracted by washing with a 1 M solution of HCl (2×100 mL). The organic solution was concentrated *in vacuo* to give the crude product which was purified according to the methods indicated below.

For monitoring: a 40 μ L sample of the reaction mixture was diluted into a 50 mL volumetric flask and made up to volume with chloroform. The sample was analysed using calibrated GC-MS polar compounds (EI).

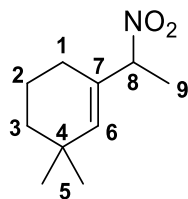
General Procedure for the continuous-flow Amine-Catalysed Irregular Nitro-Aldol reaction to compound 77

A stock solution of compound **68** (0.2 M) and nitroethane (0.25 – 2 M) in AcOEt was pumped via an HPLC pump through a series of two sequential Omnifit glass columns (150 mm x 25 mm) each filled with 13 g of a mixture (2:3) ethylenediamine-functionalised silica gel (**247**) and molecular sieves 3Å. A 3-way valve mixer was employed to dose the amount of solution employed for the investigation. For each screening the mixer was used to pump the solution for 240 min (Total volume 15.36 mL) and then was switched to a solvent stream. The reaction stream was collected for over 12 hours after the solvent switch. The solution was concentrated *in vacuo* and analysed via GC-MS polar compounds (EI) and $^1\text{H-NMR}$ spectra. The results are depicted in *Table 31*.



5,5-Dimethyl-1-(1-nitroethyl)cyclohex-1-ene (77):¹⁴¹ Obtained by reaction of nitroethane with 3,3-dimethyl cyclohexanone (**68**) as a pale yellow liquid (0.305 mol scale, 43.3 g, 78% yield, **77**:**76** = 5.4:1), isolated by vacuum distillation as a mixture of the two isomers (b.p. 105-110 °C & 10 mbar). $^1\text{H NMR}$ (400 MHz, Chloroform-*d*) δ 5.90 (m, 1H, **1**), 5.00 (q, $J = 7.6$ Hz, 1H, **8**), 2.14 (m, 2H, **6**), 1.88 – 1.71 (qq, $J = 18.9, 2.0$ Hz, 2H, **2**), 1.62 (d, $J = 6.8$ Hz, 3H, **9**), 1.39

– 1.33 (m, 2H, **3**), 0.93 (s, 3H, **5**), 0.91 (s, 3H, **5**) ppm; ^{13}C NMR (101 MHz, Chloroform-*d*) δ 132.0 (**7**), 128.4 (**1**), 88.3 (**8**), 37.8 (**2**), 34.4 (**3**), 28.8 (**4**), 28.3 (**5**), 27.4 (**5**), 23.2 (**6**), 16.9 (**9**) ppm; FT-IR (neat) ν 2918 (w) 2918 (w), 1545 (s), 1449 (w), 1384 (m), 1364 (w), 860 (w), 663 (w) cm^{-1} . GC-MS polar compounds (EI) R_t 3.71 min, m/z 137 $[\text{M}-\text{NO}_2]^+$; LC-MS (ESI+) R_t = 3.04 min m/z $[\text{M}+\text{H}]^+$ = 184.3. HR-MS calculated for $\text{C}_{10}\text{H}_{18}\text{NO}_2$ 184.1338, found 184.1366 (Δ = 2.8 mDa; 15.2 ppm). Under the stated LC-MS conditions, the two isomers could not be resolved, thus the HR-MS was acquired on the mixture.



3,3-Dimethyl-1-(1-nitroethyl)cyclohex-1-ene (76):¹⁴¹ Obtained by reaction of nitroethane with 3,3-dimethyl cyclohexanone (**68**) as a pale yellow liquid (0.305 mol scale, 43.3 g, 78% yield, **77**:**76** = 5.4:1), isolated by vacuum distillation as a mixture of the two isomers (b.p. 105 – 110 °C & 10 mbar). ^1H NMR (600 MHz, Chloroform-*d*) δ 5.59 (s, 1H, **6**), 4.92 (q, J = 7.0 Hz, 1H, **8**), 2.02 – 1.87 (m, 2H, **1**), 1.67 – 1.62 (m, 2H, **2**), 1.62 (d, J = 6.8 Hz, 3H, **9**), 1.45 – 1.35 (m, 2H, **3**), 0.98 (s, 3H, **5**), 0.97 (s, 3H, **5**) ppm; ^{13}C NMR (151 MHz, Chloroform-*d*) δ 139.5 (**6**), 130.8 (**7**), 88.3 (**8**), 36.5 (**3**), 32.0 (**4**), 29.6 (**5**), 29.2 (**5**), 24.3 (**1**), 19.4 (**2**), 17.0 (**9**) ppm; FT-IR (neat) ν 2918 (w), 1545 (s), 1449 (w), 1384 (m), 1364 (w), 860 (w), 663 (w) cm^{-1} . GC-MS R_t 3.61 min, m/z 137 $[\text{M}-\text{NO}_2]^+$.

5. References

- (1) Vinevida. Bulk Organic Eucalyptus Essential Oil Gallon in Aluminium Bottle - 100% Pure & Undiluted Essential Oil for DIY Soaps, Candles and Blends https://www.etsy.com/uk/listing/904714198/bulk-organic-eucalyptus-essential-oil?ref=shop_home_recs_87 (accessed Nov 30, 2021).
- (2) Vinevida. Bulk Lavender Essential Oil Gallon (8 Pounds) in Aluminum Bottle - 100% Pure & Undiluted Essential Oil for DIY Soaps, Candles and Blends

- https://www.etsy.com/uk/listing/904104402/bulk-lavender-essential-oil-gallon-8?ref=shop_home_recs_73 (accessed Nov 30, 2021).
- (3) Vinevida. Bulk Jasmine Absolute Oil Gallon (8 Lbs) in Aluminium Bottle - 100% Pure & Undiluted Essential Oil for DIY Soaps, Candles and Blends https://www.etsy.com/uk/listing/918545857/bulk-jasmine-absolute-oil-gallon-8-lbs?ref=sim_items_sameshopitems-1 (accessed Nov 30, 2021).
 - (4) Trades, I. F. of E. O. and A. Jasmine: An Overview of its Essential Oils & Sources <https://www.perfumerflavorist.com/fragrance/ingredients/article/21856925/jasmine-an-overview-of-its-essential-oils-sources> (accessed Nov 30, 2021).
 - (5) Perkin, W. H. VI.—On the Artificial Production of Coumarin and Formation of Its Homologues. *J. Chem. Soc.* **1868**, 21, 53–63. <https://doi.org/10.1039/JS8682100053>.
 - (6) Tiemann, F.; Haarmann, W. Ueber Das Coniferin Und Seine Umwandlung in Das Aromatische Princip Der Vanille. *Berichte der Dtsch. Chem. Gesellschaft* **1874**, 7 (1), 608–623. <https://doi.org/10.1002/cber.187400701193>.
 - (7) Tiemann, F.; Krüger, P. Ueber Veilchenaroma. *Berichte der Dtsch. Chem. Gesellschaft* **1893**, 26 (3), 2675–2708. <https://doi.org/10.1002/cber.18930260373>.
 - (8) Sell, C. *The Chemistry of Fragrances: From Perfumer to Consumer*, 2nd ed.; Royal Society of Chemistry, Ed.; Royal Society of Chemistry: Cambridge, UK, 2006.
 - (9) Gradeff, P. Process for Preparation of Methyl Ionones. US3840601A, 1974.
 - (10) Mottern, H. O. A New Vanillin Synthesis. *J. Am. Chem. Soc.* **1934**, 56 (10), 2107–2108. <https://doi.org/10.1021/ja01325a033>.
 - (11) Knorr, A. . A.; Weissenborn, A. Manufacture of Para-Isopropyl-Alpha-Methyl Hydrocinnamic Aldehyde. US1844013A, 1932.
 - (12) Anselmi, C.; Centini, M.; Mariani, M.; Sega, A.; Pelosi, P. Influence of the Regio- and Stereochemistry on the Floral Odor of THP and THF Ethers. *J. Agric. Food Chem.* **1993**, 41 (5), 781–784. <https://doi.org/10.1021/jf00029a020>.

- (13) Carpenter, M. S.; Easter, J. W. M. 4-Tert.-Butyl Alpha-Methyl Hydrocinnamic Aldehyde. US2875131A, 1959.
- (14) Bauer, K.; Garbe, D.; Surburg, H. *Common Fragrance and Flavor Materials Preparation, Properties and Uses.*, 4th ed.; Wiley: Holzminden, Germany, 2001. <https://doi.org/10.1002/3527608214>.
- (15) About the IFRA Transparency List <https://ifrafragrance.org/initiatives/transparency/ifra-transparency-list> (accessed Nov 18, 2021).
- (16) Malnic, B.; Hirono, J.; Sato, T.; Buck, L. B. Combinatorial Receptor Codes for Odors. *Cell* **1999**, *96* (5), 713–723. [https://doi.org/10.1016/S0092-8674\(00\)80581-4](https://doi.org/10.1016/S0092-8674(00)80581-4).
- (17) Buck, L.; Axel, R. A Novel Multigene Family May Encode Odorant Receptors: A Molecular Basis for Odor Recognition. *Cell* **1991**, *65* (1), 175–187. [https://doi.org/10.1016/0092-8674\(91\)90418-X](https://doi.org/10.1016/0092-8674(91)90418-X).
- (18) Saito, H.; Kubota, M.; Roberts, R. W.; Chi, Q.; Matsunami, H. RTP Family Members Induce Functional Expression of Mammalian Odorant Receptors. *Cell* **2004**, *119* (5), 679–691. <https://doi.org/10.1016/j.cell.2004.11.021>.
- (19) Kraft, P.; Di Cristofaro, V.; Jordi, S. From Cassyrane to Cashmeran - The Molecular Parameters of Odorants. *Chem. Biodivers.* **2014**, *11* (10), 1567–1596. <https://doi.org/10.1002/cbdv.201400071>.
- (20) Armanino, N.; Charpentier, J.; Flachsmann, F.; Goeke, A.; Liniger, M.; Kraft, P. What's Hot, What's Not: The Trends of the Past 20 Years in the Chemistry of Odorants. *Angew. Chemie Int. Ed.* **2020**, *59* (38), 16310–16344. <https://doi.org/10.1002/anie.202005719>.
- (21) Kraft, P.; Bajgrowicz, J. A.; Denis, C.; Fráter, G. Odds and Trends: Recent Developments in the Chemistry of Odorants. *Angew. Chemie - Int. Ed.* **2000**, *39* (17), 2980–3010. [https://doi.org/10.1002/1521-3773\(20000901\)39:17<2980::aid-anie2980>3.0.co;2-#](https://doi.org/10.1002/1521-3773(20000901)39:17<2980::aid-anie2980>3.0.co;2-#).
- (22) Natsch, A.; Laue, H.; Haupt, T.; von Niederhäusern, V.; Sanders, G. Accurate Prediction of Acute Fish Toxicity of Fragrance Chemicals with the RTgill-W1 Cell Assay. *Environ.*

- Toxicol. Chem.* **2018**, *37* (3), 931–941. <https://doi.org/10.1002/etc.4027>.
- (23) Laue, H.; Hostettler, L.; Sanders, G.; Kreutzer, G.; Natsch, A. PeBiToSens™: A Platform for PBT Screening of Fragrance Ingredients Without Animal Testing. *Chim. Int. J. Chem.* **2020**, *74* (3), 168–175. <https://doi.org/10.2533/chimia.2020.168>.
- (24) *Test No. 442D: In Vitro Skin Sensitisation*; OECD Guidelines for the Testing of Chemicals, Section 4; OECD, 2018. <https://doi.org/10.1787/9789264229822-en>.
- (25) Zarzo, M.; Stanton, D. T. Understanding the Underlying Dimensions in Perfumers' Odor Perception Space as a Basis for Developing Meaningful Odor Maps. *Atten. Percept. Psychophys.* **2009**, *71*, 225–247. <https://doi.org/10.3758/APP.71.2.225>.
- (26) Gambacorta, G.; Sharley, J. S.; Baxendale, I. R. A Comprehensive Review of Flow Chemistry Techniques Tailored to the Flavours and Fragrances Industries. *Beilstein J. Org. Chem.* **2021**, *17*, 1181–1312. <https://doi.org/10.3762/bjoc.17.90>.
- (27) Flavors and Fragrances Market Size, Share & Industry Analysis, By Type (Flavors {Natural and Synthetic} and Fragrances {Natural and Synthetic}) By Application (Food & Beverage, Cosmetics & Personal Care, Pharmaceutical, Home & Floor Care, Fine Fragrances, <https://www.fortunebusinessinsights.com/flavors-and-fragrances-market-102329> (accessed Jan 4, 2021).
- (28) Global Pharmaceuticals Market Report 2021: Market is Expected to Grow from \$1228.45 Billion in 2020 to \$1250.24 Billion in 2021 - Long-term Forecast to 2025 & 2030 <https://www.globenewswire.com/en/news-release/2021/03/31/2202135/28124/en/Global-Pharmaceuticals-Market-Report-2021-Market-is-Expected-to-Grow-from-1228-45-Billion-in-2020-to-1250-24-Billion-in-2021-Long-term-Forecast-to-2025-2030.html> (accessed Dec 5, 2021).
- (29) Agrochemicals Market by Pesticide Type (Herbicides, Insecticides, Fungicides), Fertilizer Type (Nitrogenous, Phosphatic, and Potassic), Crop Application (Cereals & Grains, Oilseeds, Fruits & Vegetables), and Region - Global Forecast to 2025 <https://www.marketsandmarkets.com/Market-Reports/global-agro-chemicals-market-report-132.html> (accessed Dec 5, 2021).

- (30) Sell, C. Appendix I: Some of the More Important Natural Fragrance Materials. In *The Chemistry of Fragrances: From Perfumer to Consumer 2nd Edition*; The Royal Society of Chemistry: Cambridge, UK, 2006; p 348.
- (31) Salvito, D.; Lapczynski, A.; Sachse-Vasquez, C.; McIntosh, C.; Calow, P.; Greim, H.; Escher, B. Macrocyclic Fragrance Materials-A Screening-Level Environmental Assessment Using Chemical Categorization. *Ecotoxicol. Environ. Saf.* **2011**, *74*, 1619–1629. <https://doi.org/10.1016/j.ecoenv.2011.05.002>.
- (32) Ohloff, G.; Pickenhagen, W.; Kraft, P. *Scent and Chemistry. The Molecular World of Odors*; Verlag Helvetica Chimica Acta and Wiley-VCH: Zurich, Switzerland, 2011.
- (33) ECOSCENT COMPASSTM - A breakthrough in fragrance transparency <https://www.firmenich.com/fragrance/purpose/ecoscent-compass> (accessed Dec 5, 2021).
- (34) Sustainability report 2018 - Toward a circular future <https://www.iff.com/sites/iff-corp/files/2020-12/iff-sustainability-report-2018.pdf> (accessed Dec 5, 2021).
- (35) Phan, T. V. T.; Gallardo, C.; Mane, J. GREEN MOTION : A New and Easy to Use Green Chemistry Metric from Laboratories to Industry. *Green Chem.* **2015**, *17*, 2846–2852. <https://doi.org/10.1039/c4gc02169j>.
- (36) Our approach to sustainability <https://www.symrise.com/sustainability/our-approach/#introduction> (accessed Dec 5, 2021).
- (37) Givaudan Fragrances launches its FiveCarbon Path <https://www.givaudan.com/media/media-releases/2019/givaudan-fragrances-launches-its-fivecarbon-pathtm> (accessed Dec 5, 2021).
- (38) Deguerry, F.; Schalk, M. Sesquiterpene Synthases from Patchouli. EP1697519B1, 2009.
- (39) van Beek, T. A.; Joulain, D. The Essential Oil of Patchouli, Pogostemon Cablin : A Review. *Flavour Fragr. J.* **2018**, *33* (1), 6–51. <https://doi.org/10.1002/ffj.3418>.
- (40) Schalk, M.; Pastore, L.; Mirata, M. A.; Khim, S.; Schouwey, M.; Deguerry, F.; Pineda, V.; Rocci, L.; Daviet, L. Toward a Biosynthetic Route to Sclareol and Amber Odorants.

- J. Am. Chem. Soc.* **2012**, *134* (46), 18900–18903. <https://doi.org/10.1021/ja307404u>.
- (41) Schalk, M.; Rocci, L. Production of Manool. WO2017001641A1, 2017.
- (42) Snowden, R. L. Cetalox® and Analogues: Synthesis via Acid-Mediated Polyene Cyclizations. *Chem. Biodivers.* **2008**, *5* (6), 958–969. <https://doi.org/10.1002/cbdv.200890107>.
- (43) Palmer, E. Vertex, J&J, GSK, Novartis all working on continuous manufacturing facilities <http://www.fiercepharma.com/supply-chain/vertex-j-j-gsk-novartis-all-working-on-continuous-manufacturing-facilities> (accessed Jul 10, 2017).
- (44) Rogers, L.; Jensen, K. F. Continuous Manufacturing-the Green Chemistry Promise? *Green Chem.* **2019**, *21*, 3481–3498. <https://doi.org/10.1039/c9gc00773c>.
- (45) Hughes, D. L. Asymmetric Organocatalysis in Drug Development - Highlights of Recent Patent Literature. *Org. Process Res. Dev.* **2018**, *22* (5), 574–584. <https://doi.org/10.1021/acs.oprd.8b00096>.
- (46) Testa, C. J.; Hu, C.; Shvedova, K.; Wu, W.; Sayin, R.; Casati, F.; Halkude, B. S.; Hermant, P.; Shen, D. E.; Ramnath, A.; Su, Q.; Born, S. C.; Takizawa, B.; Chattopadhyay, S.; O'Connor, T. F.; Yang, X.; Ramanujam, S.; Mascia, S. Design and Commercialization of an End-to-End Continuous Pharmaceutical Production Process: A Pilot Plant Case Study. *Org. Process Res. Dev.* **2020**, *24*, 2874–2889. <https://doi.org/10.1021/acs.oprd.0c00383>.
- (47) Kamble, S. S.; Gunasekaran, A.; Gawankar, S. A. Sustainable Industry 4.0 Framework: A Systematic Literature Review Identifying the Current Trends and Future Perspectives. *Process Saf. Environ. Prot.* **2018**, *117*, 408–425. <https://doi.org/10.1016/j.psep.2018.05.009>.
- (48) Mittal, S.; Khan, M. A.; Romero, D.; Wuest, T. Smart Manufacturing: Characteristics, Technologies and Enabling Factors. *Proc. Inst. Mech. Eng. Part B J. Eng. Manuf.* **2019**, *233* (5), 1342–1361. <https://doi.org/10.1177/0954405417736547>.
- (49) Mattern, F.; Floerkemeier, C. From the Internet of Computers to the Internet of Things; 2010; pp 242–259. https://doi.org/10.1007/978-3-642-17226-7_15.

- (50) Anastas, P.; Warner, J. *Green Chemistry: Theory and Practice*; Oxford University Press: Oxford, UK, 1998.
- (51) Anastas, P. T.; Zimmerman, J. B. Peer Reviewed: Design Through the 12 Principles of Green Engineering. *Environ. Sci. Technol.* **2003**, *37*, 94A-101A. <https://doi.org/10.1021/es032373g>.
- (52) Harmsen, J. Process Intensification in the Petrochemicals Industry: Drivers and Hurdles for Commercial Implementation. *Chem. Eng. Process. Process Intensif.* **2010**, *49* (1), 70–73. <https://doi.org/10.1016/j.cep.2009.11.009>.
- (53) Fukuyama, T.; Rahman, M.; Sato, M.; Ryu, I. Adventures in Inner Space: Microflow Systems for Practical Organic Synthesis. *Synlett* **2008**, *2008*, 151–163. <https://doi.org/10.1055/s-2007-1000884>.
- (54) Baxendale, I. R.; Brocken, L.; Mallia, C. J. Flow Chemistry Approaches Directed at Improving Chemical Synthesis. *Green Process. Synth.* **2013**, *2*, 211–230. <https://doi.org/10.1515/gps-2013-0029>.
- (55) Ley, S. V.; Baxendale, I. R. New Tools and Concepts for Modern Organic Synthesis. *Nat. Rev. Drug Discov.* **2002**, *1*, 573–586. <https://doi.org/10.1038/nrd871>.
- (56) Baxendale, I. R. The Integration of Flow Reactors into Synthetic Organic Chemistry. *J. Chem. Technol. Biotechnol.* **2013**, *88* (4), 519–552. <https://doi.org/10.1002/jctb.4012>.
- (57) Jas, G.; Kirschning, A. Continuous Flow Techniques in Organic Synthesis. *Chem. - A Eur. J.* **2003**, *9*, 5708–5723. <https://doi.org/10.1002/chem.200305212>.
- (58) Mason, B. P.; Price, K. E.; Steinbacher, J. L.; Bogdan, A. R.; McQuade, D. T. Greener Approaches to Organic Synthesis Using Microreactor Technology. *Chem. Rev.* **2007**, *107*, 2300–2318. <https://doi.org/10.1021/cr050944c>.
- (59) Lee, C.-Y.; Chang, C.-L.; Wang, Y.-N.; Fu, L.-M. Microfluidic Mixing: A Review. *Int. J. Mol. Sci.* **2011**, *12*, 3263–3287. <https://doi.org/10.3390/ijms12053263>.
- (60) Kappe, C. O. High-Speed Combinatorial Synthesis Utilizing Microwave Irradiation. *Curr. Opin. Chem. Biol.* **2002**, *6*, 314–320. <https://doi.org/10.1016/S1367->

5931(02)00306-X.

- (61) Watts, P. The Application of Microreactors in Combinatorial Chemistry. *QSAR Comb. Sci.* **2005**, *24*, 701–711. <https://doi.org/10.1002/qsar.200540004>.
- (62) Wiles, C.; Watts, P.; Haswell, S. J. The Use of Solid-Supported Reagents for the Multi-Step Synthesis of Analytically Pure α,β -Unsaturated Compounds in Miniaturized Flow Reactors. *Lab Chip* **2007**, *7* (3), 322–330. <https://doi.org/10.1039/B615069A>.
- (63) Baxendale, I.; Ley, S. Synthesis of Alkaloid Natural Products Using Solid-Supported Reagents and Scavengers. *Curr. Org. Chem.* **2005**, *9*, 1521–1534. <https://doi.org/10.2174/138527205774370513>.
- (64) Pastre, J. C.; Browne, D. L.; Ley, S. V. Flow Chemistry Syntheses of Natural Products. *Chem. Soc. Rev.* **2013**, *42*, 8849–8869. <https://doi.org/10.1039/c3cs60246j>.
- (65) Liang-Hsuan Lu; Kee Suk Ryu; Chang Liu. A Magnetic Microstirrer and Array for Microfluidic Mixing. *J. Microelectromechanical Syst.* **2002**, *11* (5), 462–469. <https://doi.org/10.1109/JMEMS.2002.802899>.
- (66) Frommelt, T.; Kostur, M.; Wenzel-Schäfer, M.; Talkner, P.; Hänggi, P.; Wixforth, A. Microfluidic Mixing via Acoustically Driven Chaotic Advection. *Phys. Rev. Lett.* **2008**, *100* (3), 034502. <https://doi.org/10.1103/PhysRevLett.100.034502>.
- (67) Glasgow, I.; Aubry, N. Enhancement of Microfluidic Mixing Using Time Pulsing. *Lab Chip* **2003**, *3* (2), 114–120. <https://doi.org/10.1039/B302569A>.
- (68) Ghanem, A.; Lemenand, T.; Della Valle, D.; Peerhossaini, H. Static Mixers: Mechanisms, Applications, and Characterization Methods - A Review. *Chem. Eng. Res. Des.* **2014**, *92* (2), 205–228. <https://doi.org/10.1016/j.cherd.2013.07.013>.
- (69) Hessel, V.; Löwe, H.; Schönfeld, F. Micromixers - A Review on Passive and Active Mixing Principles. *Chem. Eng. Sci.* **2005**, *60* (8-9 SPEC. ISS.), 2479–2501. <https://doi.org/10.1016/j.ces.2004.11.033>.
- (70) Ward, K.; Fan, Z. H. Mixing in Microfluidic Devices and Enhancement Methods. *J. Micromechanics Microengineering* **2015**, *25* (9), 094001. [237](https://doi.org/10.1088/0960-</p></div><div data-bbox=)

1317/25/9/094001.

- (71) Palde, P. B.; Jamison, T. F. Safe and Efficient Tetrazole Synthesis in a Continuous-Flow Microreactor. *Angew. Chemie - Int. Ed.* **2011**, *50* (15), 3525–3528. <https://doi.org/10.1002/anie.201006272>.
- (72) Singh, S.; Michael Köhler, J.; Schober, A.; Alexander Groß, G. The Eschenmoser Coupling Reaction under Continuous-Flow Conditions. *Beilstein J. Org. Chem.* **2011**, *7*, 1164–1172. <https://doi.org/10.3762/bjoc.7.135>.
- (73) Buba, A. E.; Koch, S.; Kunz, H.; Löwe, H. Fluorenylmethoxycarbonyl-N-Methylamino Acids Synthesized in a Flow Tube-in-Tube Reactor with a Liquid-Liquid Semipermeable Membrane. *European J. Org. Chem.* **2013**, No. 21, 4509–4513. <https://doi.org/10.1002/ejoc.201300705>.
- (74) Adeyemi, A.; Bergman, J.; Brånalt, J.; Sävmarker, J.; Larhed, M. Continuous Flow Synthesis under High-Temperature/High-Pressure Conditions Using a Resistively Heated Flow Reactor. *Org. Process Res. Dev.* **2017**, *21* (7), 947–955. <https://doi.org/10.1021/acs.oprd.7b00063>.
- (75) Razzaq, T.; Kappe, C. O. Continuous Flow Organic Synthesis under High-Temperature/Pressure Conditions. *Chem. - An Asian J.* **2010**, NA-NA. <https://doi.org/10.1002/asia.201000010>.
- (76) Colella, M.; Carlucci, C.; Luisi, R. *Supported Catalysts for Continuous Flow Synthesis*; Springer International Publishing, 2018; Vol. 376. <https://doi.org/10.1007/s41061-018-0225-0>.
- (77) Tanimu, A.; Jaenicke, S.; Alhooshani, K. Heterogeneous Catalysis in Continuous Flow Microreactors: A Review of Methods and Applications. *Chem. Eng. J.* **2017**, *327*, 792–821. <https://doi.org/10.1016/j.cej.2017.06.161>.
- (78) Ciriminna, R.; Pagliaro, M.; Luque, R. Heterogeneous Catalysis under Flow for the 21st Century Fine Chemical Industry. *Green Energy Environ.* **2021**, *6* (2), 161–166. <https://doi.org/10.1016/j.gee.2020.09.013>.
- (79) Yu, T.; Jiao, J.; Song, P.; Nie, W.; Yi, C.; Zhang, Q.; Li, P. Recent Progress in

- Continuous-Flow Hydrogenation. *ChemSusChem* **2020**, *13* (11), 2876–2893. <https://doi.org/10.1002/cssc.202000778>.
- (80) Buglioni, L.; Raymenants, F.; Slattery, A.; Zondag, S. D. A. A.; Noël, T. Technological Innovations in Photochemistry for Organic Synthesis: Flow Chemistry, High-Throughput Experimentation, Scale-up, and Photoelectrochemistry. *Chem. Rev.* **2021**. <https://doi.org/10.1021/acs.chemrev.1c00332>.
- (81) Martina, K.; Cravotto, G.; Varma, R. S. Impact of Microwaves on Organic Synthesis and Strategies toward Flow Processes and Scaling Up. *J. Org. Chem.* **2021**, *86* (20), 13857–13872. <https://doi.org/10.1021/acs.joc.1c00865>.
- (82) Noël, T.; Cao, Y.; Laudadio, G. The Fundamentals behind the Use of Flow Reactors in Electrochemistry. *Acc. Chem. Res.* **2019**, *52* (10), 2858–2869. <https://doi.org/10.1021/acs.accounts.9b00412>.
- (83) Ley, S. V.; Baxendale, I. R.; Bream, R. N.; Jackson, P. S.; Leach, A. G.; Longbottom, D. A.; Nesi, M.; Scott, J. S.; Storer, R. I.; Taylor, S. J. Multi-Step Organic Synthesis Using Solid-Supported Reagents and Scavengers: A New Paradigm in Chemical Library Generation. *J. Chem. Soc. Perkin Trans. 1* **2000**, 3815–4195. <https://doi.org/10.1039/b006588i>.
- (84) Sussman, S. Catalysis by Acid-Regenerated Cation Exchangers. *Ind. Eng. Chem.* **1946**, *38*, 1228–1230. <https://doi.org/10.1021/ie50444a010>.
- (85) Booth, R. J.; Hodges, J. C. Solid-Supported Reagent Strategies for Rapid Purification of Combinatorial Synthesis Products. *Acc. Chem. Res.* **1999**, *32*, 18–26. <https://doi.org/10.1021/ar970311n>.
- (86) Adamo, A.; Heider, P. L.; Weeranoppanant, N.; Jensen, K. F. Membrane-Based, Liquid–Liquid Separator with Integrated Pressure Control. *Ind. Eng. Chem. Res.* **2013**, *52*, 10802–10808. <https://doi.org/10.1021/ie401180t>.
- (87) Kralj, J. G.; Sahoo, H. R.; Jensen, K. F. Integrated Continuous Microfluidic Liquid–Liquid Extraction. *Lab Chip* **2007**, *7*, 256–263. <https://doi.org/10.1039/b610888a>.
- (88) Sahoo, H. R.; Kralj, J. G.; Jensen, K. F. Multistep Continuous-Flow Microchemical

- Synthesis Involving Multiple Reactions and Separations. *Angew. Chemie* **2007**, *119*, 5806–5810. <https://doi.org/10.1002/ange.200701434>.
- (89) Hornung, C. H.; Mackley, M. R.; Baxendale, I. R.; Ley, S. V. A Microcapillary Flow Disc Reactor for Organic Synthesis. *Org. Process Res. Dev.* **2007**, *11*, 399–405. <https://doi.org/10.1021/op700015f>.
- (90) Webb, D.; Jamison, T. F. Continuous Flow Multi-Step Organic Synthesis. *Chem. Sci.* **2010**, *1*, 675–680. <https://doi.org/10.1039/c0sc00381f>.
- (91) Perro, A.; Lebourdon, G.; Henry, S.; Lecomte, S.; Servant, L.; Marre, S. Combining Microfluidics and FT-IR Spectroscopy: Towards Spatially Resolved Information on Chemical Processes. *React. Chem. Eng.* **2016**, *1*, 577–594. <https://doi.org/10.1039/c6re00127k>.
- (92) Poh, J. S.; Browne, D. L.; Ley, S. V. A Multistep Continuous Flow Synthesis Machine for the Preparation of Pyrazoles: Via a Metal-Free Amine-Redox Process. *React. Chem. Eng.* **2016**, *1*, 101–105. <https://doi.org/10.1039/c5re00082c>.
- (93) Glotz, G.; Lebl, R.; Dallinger, D.; Kappe, C. O. Integration of Bromine and Cyanogen Bromide Generators for the Continuous-Flow Synthesis of Cyclic Guanidines. *Angew. Chemie - Int. Ed.* **2017**, *56*, 13786–13789. <https://doi.org/10.1002/anie.201708533>.
- (94) Segal-Rosenheimer, M.; Dubowski, Y. Heterogeneous Ozonolysis of Cypermethrin Using Real-Time Monitoring FTIR Techniques. *J. Phys. Chem. C* **2007**, *111*, 11682–11691. <https://doi.org/10.1021/jp072937t>.
- (95) Thomson, C. G.; Jones, C. M. S.; Rosair, G.; Ellis, D.; Marques-Hueso, J.; Lee, A.-L.; Vilela, F. Continuous-Flow Synthesis and Application of Polymer-Supported BODIPY Photosensitisers for the Generation of Singlet Oxygen; Process Optimised by in-Line NMR Spectroscopy. *J. Flow Chem.* **2020**, *10*, 327–345. <https://doi.org/10.1007/s41981-019-00067-4>.
- (96) Trunina, D.; Liauw, M. A. Inline Spectroscopy-Based Optimization of Chemical Reactions Considering Dynamic Process Conditions. *Chemie-Ingenieur-Technik* **2020**, No. 5, 1–7. <https://doi.org/10.1002/cite.201900145>.

- (97) Breen, C. P.; Nambiar, A. M. K.; Jamison, T. F.; Jensen, K. F. Ready, Set, Flow! Automated Continuous Synthesis and Optimization. *Trends Chem.* **2021**, *3* (5), 373–386. <https://doi.org/10.1016/j.trechm.2021.02.005>.
- (98) Browne, D. L.; Deadman, B. J.; Ashe, R.; Baxendale, I. R.; Ley, S. V. Continuous Flow Processing of Slurries: Evaluation of an Agitated Cell Reactor. *Org. Process Res. Dev.* **2011**, *15*, 693–697. <https://doi.org/10.1021/op2000223>.
- (99) Deadman, B. J.; Browne, D. L.; Baxendale, I. R.; Ley, S. V. Back Pressure Regulation of Slurry-Forming Reactions in Continuous Flow. *Chem. Eng. Technol.* **2015**, *38*, 259–264. <https://doi.org/10.1002/ceat.201400445>.
- (100) Sharma, M. K.; Suru, A.; Joshi, A.; Kulkarni, A. A. A Novel Flow Reactor for Handling Suspensions: Hydrodynamics and Performance Evaluation. *Ind. Eng. Chem. Res.* **2020**, *59*, 16462–16472. <https://doi.org/10.1021/acs.iecr.9b06864>.
- (101) Bianchi, P.; Williams, J. D.; Kappe, C. O. Oscillatory Flow Reactors for Synthetic Chemistry Applications. *J. Flow Chem.* **2020**, *10*, 475–490. <https://doi.org/10.1007/s41981-020-00105-6>.
- (102) Doyle, B. J.; Gutmann, B.; Bittel, M.; Hubler, T.; Macchi, A.; Roberge, D. M. Handling of Solids and Flow Characterization in a Baffleless Oscillatory Flow Coil Reactor. *Ind. Eng. Chem. Res.* **2020**, *59*, 4007–4019. <https://doi.org/10.1021/acs.iecr.9b04496>.
- (103) Brennan, Z. FDA calls on manufacturers to begin switch from batch to continuous production <https://www.outsourcing-pharma.com/Article/2015/05/01/FDA-calls-on-manufacturers-to-begin-switch-from-batch-to-continuous-production> (accessed Jan 5, 2022).
- (104) European Medicines Agency. ICH Guideline Q13 on Continuous Manufacturing of Drug Substances and Drug Products. 2021, p 45.
- (105) Lee, S. L.; O'Connor, T. F.; Yang, X.; Cruz, C. N.; Chatterjee, S.; Madurawe, R. D.; Moore, C. M. V.; Yu, L. X.; Woodcock, J. Modernizing Pharmaceutical Manufacturing: From Batch to Continuous Production. *J. Pharm. Innov.* **2015**, *10* (3), 191–199. <https://doi.org/10.1007/s12247-015-9215-8>.

- (106) Baumann, M.; Moody, T. S.; Smyth, M.; Wharry, S. A Perspective on Continuous Flow Chemistry in the Pharmaceutical Industry. *Org. Process Res. Dev.* **2020**, *24* (10), 1802–1813. <https://doi.org/10.1021/acs.oprd.9b00524>.
- (107) Yue, J. Multiphase Flow Processing in Microreactors Combined with Heterogeneous Catalysis for Efficient and Sustainable Chemical Synthesis. *Catal. Today* **2018**, *308* (September 2017), 3–19. <https://doi.org/10.1016/j.cattod.2017.09.041>.
- (108) Hughes, D. L. Applications of Flow Chemistry in the Pharmaceutical Industry - Highlights of the Recent Patent Literature. *Org. Process Res. Dev.* **2020**, *24* (10), 1850–1860. <https://doi.org/10.1021/acs.oprd.0c00156>.
- (109) Macdonald, G. Janssen working on other continuous processes post US FDA OK for Prezista <https://www.outsourcing-pharma.com/Article/2016/04/13/Janssen-working-on-other-continuous-processes-post-US-FDA-OK-for-Prezista> (accessed Jan 12, 2022).
- (110) Kansteiner, F. End-to-end: Can pharma finally make the dream of continuous manufacturing a reality? <https://www.fiercepharma.com/manufacturing/end-to-end-how-pharma-making-dream-continuous-manufacturing-a-reality> (accessed Jan 12, 2022).
- (111) Mascia, S.; Heider, P. L.; Zhang, H.; Lakerveld, R.; Benyahia, B.; Barton, P. I.; Braatz, R. D.; Cooney, C. L.; Evans, J. M. B.; Jamison, T. F.; Jensen, K. F.; Myerson, A. S.; Trout, B. L. End-to-End Continuous Manufacturing of Pharmaceuticals: Integrated Synthesis, Purification, and Final Dosage Formation. *Angew. Chemie - Int. Ed.* **2013**, *52* (47), 12359–12363. <https://doi.org/10.1002/anie.201305429>.
- (112) Testa, C. J.; Hu, C.; Shvedova, K.; Wu, W.; Sayin, R.; Casati, F.; Halkude, B. S.; Hermant, P.; Shen, D. E.; Ramnath, A.; Su, Q.; Born, S. C.; Takizawa, B.; Chattopadhyay, S.; O'Connor, T. F.; Yang, X.; Ramanujam, S.; Mascia, S. Design and Commercialization of an End-to-End Continuous Pharmaceutical Production Process: A Pilot Plant Case Study. *Org. Process Res. Dev.* **2020**, *24* (12), 2874–2889. <https://doi.org/10.1021/acs.oprd.0c00383>.
- (113) Domokos, A.; Nagy, B.; Gyürkés, M.; Farkas, A.; Tacsí, K.; Pataki, H.; Liu, Y. C.; Balogh, A.; Firth, P.; Szilágyi, B.; Marosi, G.; Nagy, Z. K.; Nagy, Z. K. End-to-End

- Continuous Manufacturing of Conventional Compressed Tablets: From Flow Synthesis to Tableting through Integrated Crystallization and Filtration. *Int. J. Pharm.* **2020**, 581 (March), 119297. <https://doi.org/10.1016/j.ijpharm.2020.119297>.
- (114) IFF: International Flavors & Fragrances Inc. <https://www.iff.com> (accessed Nov 24, 2022).
- (115) Walbaum, H.; Rosenthal, A. Über Das Eichenmoosöl. *Berichte der Dtsch. Chem. Gesellschaft (A B Ser.* **1924**, 57 (5), 770–773. <https://doi.org/10.1002/cber.19240570510>.
- (116) Wikipedia. Fougère <https://en.wikipedia.org/wiki/Fougère> (accessed Sep 1, 2018).
- (117) Wikipedia. Chypre <https://en.wikipedia.org/wiki/Chypre> (accessed Sep 1, 2018).
- (118) IFRA. Standards library <http://www.ifraorg.org/en-us/standards-library/s/oakmoss#.W4wXuUxFzIV> (accessed Sep 1, 2018).
- (119) Ohloff, G.; Pickenhagen, W.; Kraft, P. Oakmoss. In *Scent and Chemistry. The molecular world of odors.*; Wiley, Ed.; 2012; p 350.
- (120) Sonn, A. Eine Neue Synthese Der Orsellinsäure. (5. Mitteilung Über Flechtenstoffe.). *Ber. Dtsch. Chem. Ges.* **1928**, 61 (5), 926–927.
- (121) Sonn, A. Synthese Des Betorcinol-Carbonsäure-Methyl-Esters Und Neue Synthese Der Rhizoninsäure. *Berichte der Dtsch. Chem. Gesellschaft (A B Ser.* **1929**, 62 (11), 3012–3016. <https://doi.org/10.1002/cber.19290621111>.
- (122) Steiner, U.; Willhalm, B. Darstellung von 1,1-Dimethyl-cyclohexanon-(3)-carbonsäureester-(2). *Helv. Chim. Acta* **1952**, 35, 1752.
- (123) McMahon, E. M.; Roper, J. N.; Hasek, R. H.; Harris, R. C.; Utermohlen, W. P.; Brant, J. H. Preparation and Properties of Ethyl Vinyl Ketone and of Methyl Isopropenyl Ketone. *J. Am. Chem. Soc.* **1948**, 70 (9), 2971–2977. <https://doi.org/10.1021/ja01189a042>.
- (124) Grossman, J. D.; De Simone, R. S.; Heeringa, L. G. Process for the Preparation of an

- Alkyl Ring-Substituted Resorcinic Acid or Its Ester. DE1941041A1, 1970.
- (125) Cohen, A. M. Process for the Preparation of 3-Mono-Alkyl and 3,6-Dialkyl-Resorcylic Esters. US3944596A, 1976.
- (126) Kulka, K.; Zazula, T. Alkyl Monomethyl-Ringsubstituted-Diacetoxy-Benzoate Perfume Compositions. US3884843A, 1975.
- (127) Klein, E.; Thomel, F.; Struwe, H. Process for Manufacturing Alkyl-Substituted β -Resorcylic Acid Esters. US4142053A, 1979.
- (128) Thoemel, F.; Hoffmann, W. Preparation of Resorcinol Derivatives. US4426332, 1984.
- (129) Hirsenkorn, R. Process for the Preparation of β -Resorcylic Acid Derivatives. US5171878, 1992.
- (130) Hertweck, C. The Biosynthetic Logic of Polyketide Diversity. *Angew. Chemie - Int. Ed.* **2009**, *48* (26), 4688–4716. <https://doi.org/10.1002/anie.200806121>.
- (131) Barrett, A. G. M.; Morris, T. M.; Barton, D. H. R. Convenient Syntheses of Alkyl β -Resorcylic Acid Derivatives. *J. Chem. Soc., Perkin Trans. 1* **1980**, *0*, 2272.
- (132) Monteleone, Mi. G.; Belko, R. P.; Schiet, F. T.; Jones, P. D.; Levorse, A. T. J. Novel Quinazoline Compounds and Their Use in Perfume Compositions. US2012207697, 2012.
- (133) Baran, P. S.; Shenvi, R. A.; Nguyen, S. A. One-Step Synthesis of 4,5-Disubstituted Pyrimidines Using Commercially Available and Inexpensive Reagents. *Heterocycles* **2006**, *70* (Scheme 1), 581–586. [https://doi.org/10.3987/COM-06-S\(W\)27](https://doi.org/10.3987/COM-06-S(W)27).
- (134) Upare, A.; Sathyanarayana, P.; Kore, R.; Sharma, K.; Bathula, S. R. Catalyst Free Synthesis of Mono- and Disubstituted Pyrimidines from O-Acyl Oximes. *Tetrahedron Lett.* **2018**, *59* (25), 2430–2433. <https://doi.org/10.1016/j.tetlet.2018.05.023>.
- (135) Williams, A. Rose Ketones: Celebrating 30 Years of Success. *Perfumer & Flavorist*. Geneva 2002, pp 18–31.
- (136) Schulte-Elte, K.-H.; Willhalm, B.; Gautchl, F.; Schulte-Elte, K.-H.; Willhalm, B.;

- Gautschi, F. Cyclic C6 Ketones in Perfumes. US4147672A, 1979.
- (137) Morris, A. F.; Näf, F.; Snowden, R. L. Dynascone: The Ultime Captive. *Perfumer&Flavorist*. Palma de Mallorca May 1991, pp 33–35.
- (138) Liu, J.; Zhang, Q.; Li, P.; Qu, Z.; Sun, S.; Ma, Y.; Su, D.; Zong, Y.; Zhang, J. Six-Membered Silacycle Odorants: Synthesis and Olfactory Characterization of Si Analogues of Artemone, β -Dynascone, and Herbac. *Eur. J. Inorg. Chem.* **2014**, No. 21, 3435–3440. <https://doi.org/10.1002/ejic.201402093>.
- (139) Muratore, A.; Chantot, J.-J. Compounds with a Woody Note. US9085516B2, 2015.
- (140) Hongliang, M.; Qilin, W.; Rui, L.; Xingtao, J.; Hanmou, Y.; Qingting, L. Preparation Method of 1-(5,5-Dimethyl-1-Cyclohexen-1-Yl) -4-Penten-1-One. CN104341284A, 2015.
- (141) Espinos Ferri, E.; Collado Perez, A. M. Preparation of Cyclic Allylic Nitro Compounds. WO2018187542A1, 2018.
- (142) Bonrath, W.; Letinois, U.; Schütz, J. Synthesis of Green Ketone Intermediate. US8674143B2, 2014.
- (143) Merkel, D. Die Rupe-Umlagerung von Dehydrolinalool. *Zeitschrift für Chemie* **1969**, 9, 63–64.
- (144) Barton, D. H. R. R.; Motherwell, W. B.; Zard, S. Z. A Simple Construction of the Hydroxy-Ketone Side Chain of Corticosteroids from 17-Oxo-Steroids via Nitro-Olefins. *J. Chem. Soc. Chem. Commun.* **1982**, No. 10, 551. <https://doi.org/10.1039/c39820000551>.
- (145) Tamura, R.; Sato, M.; Oda, D. Facile Synthesis of Allylic Nitro Compounds by N,N-Dimethylethylenediamine-Catalyzed Condensation of Aliphatic and Alicyclic Ketones with Primary Nitroalkanes. *J. Org. Chem.* **1986**, 51 (23), 4368–4375. <https://doi.org/10.1021/jo00373a007>.
- (146) Bode, J. W.; Hachisu, Y.; Matsuura, T.; Suzuki, K. Facile Construction and Divergent Transformation of Polycyclic Isoxazoles: Direct Access to Polyketide Architectures.

- Org. Lett.* **2003**, 5 (4), 391–394. <https://doi.org/10.1021/ol027283f>.
- (147) Toshio Nakamatsu, K.; Yasuhiro Nishida, I.; Norio Kometani, K. PROCESS FOR PRODUCING 2-METHYL-1,3-CYCLOHEXANEDIONE AND 2-METHYLRESORCINOL 75. US5276198, 1994.
- (148) Ruiz, J.; Mallet-Ladeira, S.; Maynadier, M.; Vial, H.; André-Barrès, C. Design, Synthesis and Evaluation of New Tricyclic Endoperoxides as Potential Antiplasmodial Agents. *Org. Biomol. Chem.* **2014**, 12 (28), 5212–5221. <https://doi.org/10.1039/C4OB00787E>.
- (149) Kraem, J. Ben; Amri, H. Concise Synthesis of α -(Hydroxymethyl) Alkyl and Aryl Vinyl Ketones. *Synth. Commun.* **2013**, 43 (1), 110–117. <https://doi.org/10.1080/00397911.2011.592626>.
- (150) Ramachary, D. B.; Kishor, M. Organocatalytic Sequential One-Pot Double Cascade Asymmetric Synthesis of Wieland-Miescher Ketone Analogues from a Knoevenagel/Hydrogenation/Robinson Annulation Sequence: Scope and Applications of Organocatalytic Biomimetic Reductions. *J. Org. Chem.* **2007**, 72 (14), 5056–5068. <https://doi.org/10.1021/jo070277i>.
- (151) Riveira, M. J.; Mischne, M. P. One-Pot Organocatalytic Tandem Aldol/Polycyclization Reactions between 1,3-Dicarbonyl Compounds and $\alpha,\beta,\gamma,\delta$ -Unsaturated Aldehydes for the Straightforward Assembly of Cyclopenta[b]Furan-Type Derivatives: New Insight into the Knoevenagel Reaction. *Chem. - A Eur. J.* **2012**, 18 (8), 2382–2388. <https://doi.org/10.1002/chem.201103080>.
- (152) Yu, J.-J.; Wang, L.-M.; Liu, J.-Q.; Guo, F.-L.; Liu, Y.; Jiao, N. Synthesis of Tetraketones in Water and under Catalyst-Free Conditions. *Green Chem.* **2010**, 12 (2), 216–219. <https://doi.org/10.1039/B913816A>.
- (153) Saimoto, H.; Yoshida, K.; Murakami, T.; Morimoto, M.; Sashiwa, H.; Shigemasa, Y. Effect of Calcium Reagents on Aldol Reactions of Phenolic Enolates with Aldehydes in Alcohol. *J. Org. Chem.* **1996**, 61 (20), 6768–6769. <https://doi.org/10.1021/jo961352k>.
- (154) Sharley, J. S.; Collado Pérez, A. M.; Ferri, E. E.; Miranda, A. F.; Baxendale, I. R. α,β -

- Unsaturated Ketones via Copper(II) Bromide Mediated Oxidation. *Tetrahedron* **2016**, 72 (22), 2947–2954. <https://doi.org/10.1016/j.tet.2016.04.011>.
- (155) Kosower, E. M.; Wu, G. S. Halogenation with Copper(II). II. Unsaturated Ketones. *J. Org. Chem.* **1963**, 28 (3), 633–638. <https://doi.org/10.1021/jo01038a008>.
- (156) Kojima, Y.; Kawaguchi, S. Bromination of Aliphatic Ketones with Copper(II) Bromide in Organic Solvents. I. The Reaction of Acetone with Copper(II) Bromide in Methanol. *Bulletin of the Chemical Society of Japan*. 1972, pp 1293–1299. <https://doi.org/10.1246/bcsj.45.1293>.
- (157) Kosower, E. M.; Cole, W. J.; Wu, G.-S.; Cardy, D. E.; Meisters, G. Halogenation with Copper(II). I. Saturated Ketones and Phenol. *J. Org. Chem.* **1963**, 28 (3), 630–633. <https://doi.org/10.1021/jo01038a007>.
- (158) Nonhebel, D. C.; Russell, J. A. Reactions of Cupric Halides with Organic Compounds-VIII. Reactions of 9-Acylanthracenes. *Tetrahedron* **1970**, 26 (11), 2781–2786. [https://doi.org/10.1016/S0040-4020\(01\)92853-4](https://doi.org/10.1016/S0040-4020(01)92853-4).
- (159) Kochi, J. K. The Reduction of Cupric Chloride by Carbonyl Compounds. *J. Am. Chem. Soc.* **1955**, 77 (20), 5274–5278. <https://doi.org/10.1021/ja01625a016>.
- (160) Li, S.; Cheng, L.; Wu, Q.; Zhang, Q.; Yang, J.; Liu, J. Mechanism of Aerobic Alcohol Oxidation Mediated by Water-Soluble Cu^{II}-TEMPO Catalyst in Water: A Density Functional Theory Study. *ChemistrySelect* **2018**, 3 (4), 1268–1274. <https://doi.org/10.1002/slct.201702755>.
- (161) Kim, S. S.; Jung, H. C. An Efficient Aerobic Oxidation of Alcohols to Aldehydes and Ketones with TEMPO/Ceric Ammonium Nitrate as Catalysts. *Synthesis (Stuttg)*. **2003**, No. 14, 2135–2137. <https://doi.org/10.1055/s-2003-41065>.
- (162) Papadopoulos, E. P.; Jarrar, A.; Issidorides, C. H. Oxidations with Manganese Dioxide. *J. Org. Chem.* **1966**, 31 (2), 615–616. <https://doi.org/10.1021/jo01340a520>.
- (163) Kawashita, Y.; Hayashi, M. Synthesis of Heteroaromatic Compounds by Oxidative Aromatization Using an Activated Carbon/Molecular System Oxygen. *Molecules* **2009**, 14 (8), 3073–3093. <https://doi.org/10.3390/molecules14083073>.

- (164) Sylla, M.; Joseph, D.; Chevallier, E.; Camara, C.; Dumas, F. A Simple and Direct Access to Ethylidene Malonates. *Synthesis (Stuttg)*. **2006**, 1045–1049. <https://doi.org/10.1055/s-2006-926344>.
- (165) Liotta, D.; Saindane, M.; Barnum, C.; Ensley, H.; Balakrishnan, P. Reactions Involving Selenium Metal as an Electrophile. 2. A General Procedure for the Preparation of Unsaturated β -Dicarbonyl Compounds. *Tetrahedron Lett.* **1981**, 22 (32), 3043–3046. [https://doi.org/10.1016/S0040-4039\(01\)81822-0](https://doi.org/10.1016/S0040-4039(01)81822-0).
- (166) Mukherjee, H.; Martinez, C. A. Biocatalytic Route to Chiral Precursors of β -Substituted- γ -Amino Acids. *ACS Catal.* **2011**, 1 (9), 1010–1013. <https://doi.org/10.1021/cs2002466>.
- (167) Ötvös, S. B.; Llanes, P.; Pericàs, M. A.; Kappe, C. O. Telescoped Continuous Flow Synthesis of Optically Active γ -Nitrobutyric Acids as Key Intermediates of Baclofen, Phenibut, and Fluorophenibut. *Org. Lett.* **2020**, 22, 8122–8126. <https://doi.org/10.1021/acs.orglett.0c03100>.
- (168) Ishitani, H.; Kanai, K.; Saito, Y.; Tsubogo, T.; Kobayashi, S. Synthesis of (\pm)-Pregabalin by Utilizing a Three-Step Sequential-Flow System with Heterogeneous Catalysts. *European J. Org. Chem.* **2017**, 2017, 6491–6494. <https://doi.org/10.1002/ejoc.201700998>.
- (169) Tsubogo, T.; Oyamada, H.; Kobayashi, S. Multistep Continuous-Flow Synthesis of (R)- and (S)-Rolipram Using Heterogeneous Catalysts. *Nature* **2015**, 520, 329–332. <https://doi.org/10.1038/nature14343>.
- (170) Thakur, P. B.; Sirisha, K.; Sarma, A. V. S.; Nanubolu, J. B.; Meshram, H. M. Highly Regioselective and Metal-Free γ -Addition of β -Keto Esters to Isatins, Catalyzed by DABCO: Direct Access to Novel Class of Diversely Functionalized 3-Hydroxy-2-Oxindole Scaffolds. *Tetrahedron* **2013**, 69 (31), 6415–6423. <https://doi.org/10.1016/j.tet.2013.05.101>.
- (171) Robl, J. A.; Duncan, L. A.; Pluscec, J.; Karanewsky, D. S.; Gordon, E. M.; Ciosek, C. P.; Rich, L. C.; Dehmel, V. C.; Slusarchyk, D. A. Phosphorus-Containing Inhibitors of HMG-CoA Reductase. 2. Synthesis and Biological Activities of a Series of Substituted

- Pyridines Containing a Hydroxyphosphinyl Moiety. *J. Med. Chem.* **1991**, *34* (9), 2804–2815. <https://doi.org/10.1021/jm00113a019>.
- (172) Burnouf, C.; Berecibar, A.; Navet, M. Novel Substituted Pyrazolo[4,3-e]Diazepines, Pharmaceutical Compositions Containing Them, Use as Medicinal Products and Processes for Preparing Them. WO2001049689A2, 2001.
- (173) Kuhajda, F. P.; Townsend, C. A.; Medghalchi, S. M.; Mcfadden, J. M. Novel Compounds, Pharmaceutical Compositions Containing Same, and Methods of Use for Same. WO2007014247A2, 2007.
- (174) Punk, M.; Merkley, C.; Kennedy, K.; Morgan, J. B. Palladium-Catalyzed, Enantioselective Heine Reaction. *ACS Catal.* **2016**, *6* (7), 4694–4698. <https://doi.org/10.1021/acscatal.6b01400>.
- (175) Barbier, V.; Couty, F.; David, O. R. P. Furan-2,3-Diones as Masked Dipoles: Synthesis of Isotetronic Acids and Mechanistic Considerations. *Tetrahedron* **2016**, *72* (36), 5646–5651. <https://doi.org/10.1016/j.tet.2016.07.072>.
- (176) Gein, V. L.; Gein, L. F.; Bezmaternykh, N.; Voronina, E. V. Synthesis and Antimicrobial Activity of 4-Aroyl-3-Hydroxy-2,5-Dihydrofuran-2-Ones and Their Derivatives. *Pharm. Chem. J.* **2000**, *34* (5), 254–256. <https://doi.org/10.1007/BF02524633>.
- (177) Nield, C. H. The Preparation of α -Bromo- α,β -Unsaturated Ketones and Esters. *J. Am. Chem. Soc.* **1945**, *67* (7), 1145–1148. <https://doi.org/10.1021/ja01223a032>.
- (178) Arai, S.; Nakayama, K.; Hatano, K. I.; Shioiri, T. Stereoselective Synthesis of Cyclopropane Rings under Phase-Transfer-Catalyzed Conditions. *J. Org. Chem.* **1998**, *63* (25), 9572–9575. <https://doi.org/10.1021/jo981409y>.
- (179) Jiménez, R.; Maldonado, L. A.; Salgado-Zamora, H. Synthesis of Demethylated Nidulol via an Intramolecular Michael Reaction. *Nat. Prod. Res.* **2010**, *24* (13), 1274–1281. <https://doi.org/10.1080/14786410903458265>.
- (180) Covarrubias-Zúñiga, A.; Maldonado, L. A.; Ríos-Barrios, E.; González-Lucas, A. Synthesis of Resorcinols via a Michael Addition-Dieckman Cyclization Sequence of

- Dimethyl 1,3-Acetonedicarboxylate Anion with Alkyl Alkynoates. *Synth. Commun.* **1998**, 28 (18), 3461–3469. <https://doi.org/10.1080/00397919808004454>.
- (181) Zhang, J.; Liu, L.; Duan, J.; Gu, L.; Chen, B.; Sun, T.; Gong, Y. Stereoselective One-Pot Sequential Dehydrochlorination/Trans-Hydrofluorination Reaction of β -Chloro- α,β -Unsaturated Aldehydes or Ketones: Facile Access to (Z)- β -Fluoro- β -Arylenals/ β -Fluoro- β -Arylenones. *Adv. Synth. Catal.* **2017**, 359 (24), 4348–4358. <https://doi.org/10.1002/adsc.201700981>.
- (182) Health And Safety Executive. *Safe Handling Of Chlorine From Drums And Cylinders, HSG40*; HSE Books: London, 1999.
- (183) Corey, E. J.; Estreicher, H. An Effective and Mild Method for the Conversion of Oximes to Secondary Nitro Compounds. *Tetrahedron Lett.* **1980**, 21 (12), 1117–1120. [https://doi.org/10.1016/S0040-4039\(01\)83928-9](https://doi.org/10.1016/S0040-4039(01)83928-9).
- (184) Hopkins, C. Y.; Chisholm, M. J. Chlorination by Aqueous Sodium Hypochlorite. *Can. J. Res.* **1946**, 24b (5), 208–210. <https://doi.org/10.1139/cjr46b-027>.
- (185) Unangst, P. C. Hypochlorous Acid. In *Encyclopedia of Reagents for Organic Synthesis*; John Wiley & Sons, Ltd: Chichester, UK, 2001; Vol. 1624, pp 92–92. <https://doi.org/10.1002/047084289X.rh073>.
- (186) Swain, C. G.; Crist, D. R. Mechanisms of Chlorination by Hypochlorous Acid. The Last of Chlorinium Ion, Cl^{+1} . *J. Am. Chem. Soc.* **1972**, 94 (9), 3195–3200. <https://doi.org/10.1021/ja00764a050>.
- (187) Mhasni, O.; Rezgui, F. Efficient α -Chlorination of 2-[(1-Oxocyclohex-2-En-2-Yl)Methyl]-1,3-Dicarbonyl Compounds Using Sodium Hypochlorite. *J. Chem. Res.* **2013**, 37 (2), 122–124. <https://doi.org/10.3184/174751913X13587668947648>.
- (188) Fukuyama, T.; Tokizane, M.; Matsui, A.; Ryu, I. A Greener Process for Flow C-H Chlorination of Cyclic Alkanes Using: In Situ Generation and on-Site Consumption of Chlorine Gas. *React. Chem. Eng.* **2016**, 1 (6), 613–615. <https://doi.org/10.1039/c6re00159a>.
- (189) Mohrig, J. R.; Nienhuis, D. M.; Linck, C. F.; Van Zoeren, C.; Fox, B. G.; Mahaffy, P.

- G. The Design of Laboratory Experiments in the 1980's: A Case Study on the Oxidation of Alcohols with Household Bleach. *J. Chem. Educ.* **1985**, 62 (6), 519–521. <https://doi.org/10.1021/ed062p519>.
- (190) Grossman, J. D.; De Simone, R. S.; Heeringa, L. G. Process for the Preparation of 3,5-Dialkyl Resorcylic Acids and Esters Abstract. US3634491A, 1972.
- (191) Xu, S.; Fang, M. Process for Preparing Perfume 2,5-Dimethylmethyl Resorcyate. CN106631794A, 2016.
- (192) Tilstam, U.; Weinmann, H. Trichloroisocyanuric Acid: A Safe and Efficient Oxidant. *Org. Process Res. Dev.* **2002**, 6 (4), 384–393. <https://doi.org/10.1021/op010103h>.
- (193) Gaspa, S.; Carraro, M.; Pisano, L.; Porcheddu, A.; De Luca, L. Trichloroisocyanuric Acid: A Versatile and Efficient Chlorinating and Oxidizing Reagent. *European J. Org. Chem.* **2019**, 2019 (22), 3544–3552. <https://doi.org/10.1002/ejoc.201900449>.
- (194) Rogers, D. A.; Bensalah, A. T.; Espinosa, A. T.; Hoerr, J. L.; Refai, F. H.; Pitzel, A. K.; Alvarado, J. J.; Lamar, A. A. Amplification of Trichloroisocyanuric Acid (TCCA) Reactivity for Chlorination of Arenes and Heteroarenes via Catalytic Organic Dye Activation. *Org. Lett.* **2019**, 21 (11), 4229–4233. <https://doi.org/10.1021/acs.orglett.9b01414>.
- (195) Motati, D. R.; Uredi, D.; Watkins, E. B. A General Method for the Metal-Free, Regioselective, Remote C-H Halogenation of 8-Substituted Quinolines. *Chem. Sci.* **2018**, 9 (7), 1782–1788. <https://doi.org/10.1039/c7sc04107a>.
- (196) Kovacic, P.; Lowery, M. K.; Field, K. W. Chemistry of N-Bromamines and N-Chloramines. *Chem. Rev.* **1970**, 70 (6), 639–665. <https://doi.org/10.1021/cr60268a002>.
- (197) Stella, L. Homolytic Cyclizations Of N-Chloroalkenylamines. *Angew. Chemie Int. Ed. English* **1983**, 22 (5), 337–350. <https://doi.org/10.1002/anie.198303373>.
- (198) Daoust, B.; Lessard, J. Photolysis of Olefinic N-Chloropyrrolidinones, N-Chlorosuccinimides and N-Chloro-Oxazolidinones: Reactivity of Cyclic Carboxamidyl, Imidyl and Carbamyl Radicals in Intramolecular Reactions. *Tetrahedron* **1999**, 55 (12), 3495–3514. [https://doi.org/10.1016/S0040-4020\(98\)01158-2](https://doi.org/10.1016/S0040-4020(98)01158-2).

- (199) Wille, U. Product Class 4: N-Haloamines. In *Category 5, Compounds with One Saturated Carbon Heteroatom Bond*; Enders, Schaumann, Eds.; Georg Thieme Verlag: Stuttgart, 2009. <https://doi.org/10.1055/sos-SD-040-00600>.
- (200) Veisi, H.; Ghorbani-Vaghei, R.; Zolfigol, M. A. Recent Progress in the Use of N-Halo Compounds in Organic Synthesis. *Org. Prep. Proced. Int.* **2011**, *43* (6), 489–540. <https://doi.org/10.1080/00304948.2011.629553>.
- (201) Hendrick, C. E.; Wang, Q. Synthesis of Ortho -Haloaminoarenes by Aryne Insertion of Nitrogen-Halide Bonds. *J. Org. Chem.* **2015**, *80* (2), 1059–1069. <https://doi.org/10.1021/jo502541t>.
- (202) Hering, T.; König, B. Photocatalytic Activation of N-Chloro Compounds for the Chlorination of Arenes. *Tetrahedron* **2016**, *72* (48), 7821–7825. <https://doi.org/10.1016/j.tet.2016.06.028>.
- (203) Misal, B.; Palay, A.; Ganwir, P.; Chaturbhuji, G. Activator Free, Expeditious and Eco-Friendly Chlorination of Activated Arenes by N-Chloro-N-(Phenylsulfonyl)Benzene Sulfonamide (NCBSI). *Tetrahedron Lett.* **2021**, *63*, 152689. <https://doi.org/10.1016/j.tetlet.2020.152689>.
- (204) Hiegel, G. A.; Pozzi, G. Trichloroisocyanuric Acid. *Encycl. Reagents Org. Synth.* **2008**, *1* (1). <https://doi.org/10.1002/047084289x.rt209.pub2>.
- (205) Guillemin, J.-C.; Denis, J.-M. Vacuum Dynamic Gas-Phase/Solid-Phase Reactions: N-Chlorination of Primary Amines and the α -Elimination of the Resulting Chloramines: Access to Reactive (E)- and (Z)-Aldimines. *Angew. Chemie Int. Ed. English* **1982**, *21* (S9), 1515–1524. <https://doi.org/10.1002/anie.198215150>.
- (206) Back, T. G.; Chau, J. H.-L.; Dyck, B. P.; Gladstone, P. L. The Synthesis of Some Novel N -Chloro- Δ 1 -4-Azasteroids by Efficient N -Chlorination of Azasteroid Lactams with Trichloroisocyanuric Acid . *Can. J. Chem.* **1991**, *69* (9), 1482–1486. <https://doi.org/10.1139/v91-219>.
- (207) Zhao, Z.; Wang, B.; Wang, D.; Cheng, L.; Ding, F.; Cao, H.; Cao, L. Method for Synthesizing Tauroursodeoxycholic Acid under Promotion of Trichloroisocyanuric

- Acid. CN112592380A, 2021.
- (208) Kolvari, E.; Ghorbani-Choghamarani, A.; Salehi, P.; Shirini, F.; Zolfigol, M. A. Application of N-Halo Reagents in Organic Synthesis. *J. Iran. Chem. Soc.* **2007**, *4* (2), 126–174. <https://doi.org/10.1007/BF03245963>.
- (209) Yang, Y.; Shen, A. Method for Synthesizing Mandelic Acid. CN112321410A, 2021.
- (210) Juenge, E. C.; Beal, D. A.; Duncan, W. P. Chlorination of Aromatic Systems with Trichloroisocyanuric Acid under Polar and Free-Radical Conditions. *J. Org. Chem.* **1970**, *35* (3), 719–722. <https://doi.org/10.1021/jo00828a039>.
- (211) Pereira, L.; Freire, O.; Mascarenhas, A.; Boeck, G. Wilhelm Ostwald Para Além Do Antiatomismo. *Quim. Nova* **2020**. <https://doi.org/10.21577/0100-4042.20170645>.
- (212) Mishra, A. K.; Nagarajaiah, H.; Moorthy, J. N. Trihaloisocyanuric Acids as Atom-Economic Reagents for Halogenation of Aromatics and Carbonyl Compounds in the Solid State by Ball Milling. *European J. Org. Chem.* **2015**, *2015* (12), 2733–2738. <https://doi.org/10.1002/ejoc.201403463>.
- (213) Mendonça, G. F.; Senra, M. R.; Esteves, P. M.; De Mattos, M. C. S. Trichloroisocyanuric Acid in 98% Sulfuric Acid: A Superelectrophilic Medium for Chlorination of Deactivated Arenes. *Appl. Catal. A Gen.* **2011**, *401* (1–2), 176–181. <https://doi.org/10.1016/j.apcata.2011.05.017>.
- (214) Mendonça, G. F.; Magalhães, R. R.; De Mattos, M. C. S.; Esteves, P. M. Trichloroisocyanuric Acid in H₂SO₄: An Efficient Superelectrophilic Reagent for Chlorination of Isatin and Benzene Derivatives. *J. Braz. Chem. Soc.* **2005**, *16* (4), 695–698. <https://doi.org/10.1590/S0103-50532005000500003>.
- (215) Sugimoto, O.; Tanji, K. An Improved Method for Chlorination of Nitrogen-Containing π -Deficient Heteroaromatics Using Triphenylphosphine and Trichloroisocyanuric Acid. *Heterocycles* **2005**, *65* (1), 181. <https://doi.org/10.3987/COM-04-10245>.
- (216) Hiegel, G. A.; Ramirez, J.; Barr, R. K. Chlorine Substitution Reactions Using Trichloroisocyanuric Acid with Triphenylphosphine. *Synth. Commun.* **1999**, *29* (8), 1415–1419. <https://doi.org/10.1080/00397919908086119>.

- (217) Hiegel, G. A.; Rubino, M. Conversion of Alcohols into Alkyl Chlorides Using Trichloroisocyanuric Acid with Triphenylphosphine. *Synth. Commun.* **2002**, *32* (17), 2691–2694. <https://doi.org/10.1081/SCC-120006034>.
- (218) Phakhodee, W.; Yamano, D.; Pattarawarapan, M. Ultrasound-Assisted Synthesis of N -Acylcyanamides and N -Acyl-Substituted Imidazolones from Carboxylic Acids by Using Trichloroisocyanuric Acid/Triphenylphosphine. *Synlett* **2020**, *31* (7), 703–707. <https://doi.org/10.1055/s-0039-1691583>.
- (219) Liang, Y.; Zhao, Z.; Taya, A.; Shibata, N. Acyl Fluorides from Carboxylic Acids, Aldehydes, or Alcohols under Oxidative Fluorination. *Org. Lett.* **2021**, *23* (3), 847–852. <https://doi.org/10.1021/acs.orglett.0c04087>.
- (220) Duguta, G.; Kamatala, C. R.; Mukka, S. K.; Muddam, B.; Chityala, Y. N, N'-Dimethyl Formamide (DMF) Mediated Vilsmeier–Haack Adducts with 1,3,5-Triazine Compounds as Efficient Catalysts for the Transesterification of β -Ketoesters. *Synth. Commun.* **2020**, *50* (11), 1641–1655. <https://doi.org/10.1080/00397911.2020.1750033>.
- (221) Hone, C. A.; Boyd, A.; O’Kearney-Mcmullan, A.; Bourne, R. A.; Muller, F. L. Definitive Screening Designs for Multistep Kinetic Models in Flow. *React. Chem. Eng.* **2019**, *4*, 1565–1570. <https://doi.org/10.1039/c9re00180h>.
- (222) Takagaki, K.; Ito, T.; Arai, H.; Obata, Y.; Takayama, K.; Onuki, Y. The Usefulness of Definitive Screening Design for a Quality by Design Approach as Demonstrated by a Pharmaceutical Study of Orally Disintegrating Tablet. *Chem. Pharm. Bull.* **2019**, *67* (10), 1144–1151. <https://doi.org/10.1248/cpb.c19-00553>.
- (223) Jones, B.; Nachtsheim, C. J. A Class of Three-Level Designs for Definitive Screening in the Presence of Second-Order Effects. *J. Qual. Technol.* **2011**, *43* (1), 1–15. <https://doi.org/10.1080/00224065.2011.11917841>.
- (224) Jones, B.; Nachtsheim, C. J. Definitive Screening Designs with Added Two-Level Categorical Factors. *J. Qual. Technol.* **2013**, *45* (2), 121–129. <https://doi.org/10.1080/00224065.2013.11917921>.
- (225) Shainyan, B. A.; Danilevich, Y. S. Reaction of Trifluoromethanesulfonyl Chloride with

- CH Acids. *Russ. J. Org. Chem.* **2009**, *45* (9), 1412–1413.
<https://doi.org/10.1134/S1070428009090176>.
- (226) Zhang, Y.; Feng, J.; Li, C. J. Palladium-Catalyzed Methylation of Aryl C-H Bond by Using Peroxides. *J. Am. Chem. Soc.* **2008**, *130* (10), 2900–2901.
<https://doi.org/10.1021/ja0775063>.
- (227) Zhou, Z. H.; Li, C. K.; Zhou, S. F.; Shoberu, A.; Zou, J. P. Copper-Catalyzed Methylation of 1,3-Diketones with Tert-Butyl Peroxybenzoate. *Tetrahedron* **2017**, *73* (19), 2740–2746. <https://doi.org/10.1016/j.tet.2017.03.058>.
- (228) Payne, G. F.; Sun, W. Q. Tyrosinase Reaction and Subsequent Chitosan Adsorption for Selective Removal of a Contaminant from a Fermentation Recycle Stream. *Appl. Environ. Microbiol.* **1994**, *60* (2), 397–401.
- (229) Ikehata, K.; Nicell, J. A. Color and Toxicity Removal Following Tyrosinase-Catalyzed Oxidation of Phenols. *Biotechnol. Prog.* **2000**, *16* (4), 533–540.
<https://doi.org/10.1021/bp0000510>.
- (230) Ensuncho, L.; Alvarez-Cuenca, M.; Legge, R. L. Removal of Aqueous Phenol Using Immobilized Enzymes in a Bench Scale and Pilot Scale Three-Phase Fluidized Bed Reactor. *Bioprocess Biosyst. Eng.* **2005**, *27* (3), 185–191.
<https://doi.org/10.1007/s00449-005-0400-x>.
- (231) Rouet-Mayer, M. A.; Ralambosoa, J.; Philippon, J. Roles of O-Quinones and Their Polymers in the Enzymic Browning of Apples. *Phytochemistry* **1990**, *29* (2), 435–440.
[https://doi.org/10.1016/0031-9422\(90\)85092-T](https://doi.org/10.1016/0031-9422(90)85092-T).
- (232) Barry, J. E.; Finkelstein, M.; Ross, S. D. Hydrogen-Bonded Complexes. 5. Phenol-Amine Complexes. *J. Org. Chem.* **1984**, *49* (9), 1669–1671.
<https://doi.org/10.1021/jo00183a041>.
- (233) Hanson, A. .; McClulloch, A. .; McInnes, A. . Complexes of Aromatic Hydroxy Compounds with Ammonium Salts and Amines Novel Hydrogen-Bonding Networks. *Tetrahedron Lett.* **1982**, *23* (6), 607–610. [https://doi.org/10.1016/S0040-4039\(00\)86902-6](https://doi.org/10.1016/S0040-4039(00)86902-6).

- (234) Guo, W.; Hou, Y.; Wu, W.; Ren, S.; Tian, S.; Marsh, K. N. Separation of Phenol from Model Oils with Quaternary Ammonium Salts via Forming Deep Eutectic Solvents. *Green Chem.* **2013**, *15* (1), 226–229. <https://doi.org/10.1039/c2gc36602a>.
- (235) Evans, R.; Dal Poggetto, G.; Nilsson, M.; Morris, G. A. Improving the Interpretation of Small Molecule Diffusion Coefficients. *Anal. Chem.* **2018**, *90* (6), 3987–3994. <https://doi.org/10.1021/acs.analchem.7b05032>.
- (236) Lechel, T.; Kumar, R.; Bera, M. K.; Zimmer, R.; Reissig, H. U. The LANCA Three-Component Reaction to Highly Substituted β -Ketoenamides – Versatile Intermediates for the Synthesis of Functionalized Pyridine, Pyrimidine, Oxazole and Quinoxaline Derivatives. *Beilstein J. Org. Chem.* **2019**, *15*, 655–678. <https://doi.org/10.3762/bjoc.15.61>.
- (237) Farooq, S.; Ngaini, Z. One-Pot and Two-Pot Methods for Chalcone Derived Pyrimidines Synthesis and Applications. *J. Heterocycl. Chem.* **2021**, *58* (6), 1209–1224. <https://doi.org/10.1002/jhet.4226>.
- (238) Nagata, T.; Obora, Y. Transition-Metal-Mediated/Catalyzed Synthesis of Pyridines, Pyrimidines, and Triazines by [2+2+2] Cycloaddition Reactions. *Asian J. Org. Chem.* **2020**, *9* (10), 1532–1547. <https://doi.org/10.1002/ajoc.202000240>.
- (239) Jubeen, F.; Iqbal, S. Z.; Shafiq, N.; Khan, M.; Parveen, S.; Iqbal, M.; Nazir, A. Eco-Friendly Synthesis of Pyrimidines and Its Derivatives: A Review on Broad Spectrum Bioactive Moiety with Huge Therapeutic Profile. *Synth. Commun.* **2018**, *48* (6), 601–625. <https://doi.org/10.1080/00397911.2017.1408840>.
- (240) Ibraheem, F.; Saddique, F. A.; Aslam, S.; Mansha, A.; Farooq, T.; Ahmad, M. Recent Synthetic Methodologies for Pyrimidine and Its Derivatives. *Turkish J. Chem.* **2018**, *42* (6), 1421–1458. <https://doi.org/10.3906/kim-1806-8>.
- (241) Su, L.; Sun, K.; Pan, N.; Liu, L.; Sun, M.; Dong, J.; Zhou, Y.; Yin, S.-F. Cyclization of Ketones with Nitriles under Base: A General and Economical Synthesis of Pyrimidines. *Org. Lett.* **2018**, *20* (11), 3399–3402. <https://doi.org/10.1021/acs.orglett.8b01324>.
- (242) Liu, F.; Zhang, X.; Qian, Q.; Yang, C. A Concise and Efficient Approach to 2,6-

- Disubstituted 4-Fluoro-pyrimidines from α -CF₃ Aryl Ketones. *Synthesis (Stuttg)*. **2020**, 52 (02), 273–280. <https://doi.org/10.1055/s-0039-1690248>.
- (243) Romanov, A. R.; Rulev, A. Y.; Popov, A. V.; Kondrashov, E. V.; Zinchenko, S. V. Reaction of Bromoenones with Amidines: A Simple Catalyst-Free Approach to Trifluoromethylated Pyrimidines. *Synthesis (Stuttg)*. **2020**, 52 (10), 1512–1522. <https://doi.org/10.1055/s-0040-1707969>.
- (244) Domínguez, E.; Marigorta, E. M. de; Olivera, R.; SanMartín, R. A Short and Efficient Synthesis of 4,5-Diarylpyrimidines. *Synlett* **1995**, 1995 (09), 955–956. <https://doi.org/10.1055/s-1995-5132>.
- (245) Aboujaoude, E. E.; Collignon, N.; Savignac, P. Dialkyl Formyl-1 Methylphosphonates α -Fonctionnels—II. *Tetrahedron* **1985**, 41 (2), 427–433. [https://doi.org/10.1016/S0040-4020\(01\)96436-1](https://doi.org/10.1016/S0040-4020(01)96436-1).
- (246) Sato, M.; Takayama, K.; Sekiguchi, K.; Abe, Y.; Furuya, T.; Inukai, N.; Kaneko, C. Synthesis of Optically Active Cyclopenta[c]Pyran-4-Carboxylic Acid Derivatives, Building Blocks for Iridoids. An Attractive Alternative to Asymmetric de Mayo Reaction. *Chem. Lett.* **1989**, 18 (11), 1925–1928. <https://doi.org/10.1246/cl.1989.1925>.
- (247) Garvey, D. S.; May, P. D.; Nadzan, A. M. 3,4-Disubstituted γ -Lactam Rings as Conformationally Constrained Mimics of Peptide Derivatives Containing Aspartic Acid or Norleucine. *J. Org. Chem.* **1990**, 55 (3), 936–940. <https://doi.org/10.1021/jo00290a026>.
- (248) Oishi, T.; Ootou, K.; Shibata, H.; Murata, M. Second-Generation Synthesis of Endogenous Sperm-Activating and Attracting Factor (SAAF) Isolated from the Ascidian *Ciona Intestinalis*. *Tetrahedron Lett.* **2010**, 51 (19), 2600–2602. <https://doi.org/10.1016/j.tetlet.2010.03.011>.
- (249) Camerino, B.; Patelli, B.; Sciaky, R. Oxidation of 3-Keto Steroids in Alkaline Medium. *Tetrahedron Lett.* **1961**, 2 (16), 554–559. [https://doi.org/10.1016/S0040-4039\(01\)91646-6](https://doi.org/10.1016/S0040-4039(01)91646-6).
- (250) Tang, S.; Zhao, H. Glymes as Versatile Solvents for Chemical Reactions and Processes:

- From the Laboratory to Industry. *RSC Adv.* **2014**, *4* (22), 11251–11287. <https://doi.org/10.1039/c3ra47191h>.
- (251) Muller, T. J. J. Synthesis by Formylation of Enolates. In *Science of Synthesis, 25: Category 4, Compounds with Two Carbon Heteroatom Bonds*; Brückner, Ed.; Georg Thieme Verlag: Stuttgart, 2007; pp 213–236. <https://doi.org/10.1055/sos-SD-025-00165>.
- (252) Brederbeck, H.; Gompper, R.; Morlock, G. Eine Neue Pyrimidin-Synthese. *Chem. Ber* **1957**, *90* (6), 942–952.
- (253) Alexander, E. R.; Wildman, R. B. Studies on the Mechanism of the Leuckart Reaction. *J. Am. Chem. Soc.* **1948**, *70* (3), 1187–1189. <https://doi.org/10.1021/ja01183a091>.
- (254) Pollard, C. B.; Young, D. C. The Mechanism of the Leuckart Reaction. *J. Org. Chem.* **1951**, *16* (5), 661–672. <https://doi.org/10.1021/jo01145a001>.
- (255) Bipp, H.; Kieczka, H. Formamides. In *Ullmann's Encyclopedia of Industrial Chemistry*; Wiley-VCH Verlag GmbH & Co. KGaA: Weinheim, Germany, 2000; p 12. https://doi.org/10.1002/14356007.a12_001.
- (256) Wuts, P. G. M. *Greene's Protective Groups in Organic Synthesis*, 5th ed.; Wiley-VCH Verlag GmbH & Co. KGaA, 2014; Vol. 111. <https://doi.org/10.1192/bjp.111.479.1009-a>.
- (257) Ondi, L.; Lefebvre, O.; Schlosser, M. Brominated 4-(Trifluoromethyl)Pyrimidines: A Convenient Access to Versatile Intermediates. *European J. Org. Chem.* **2004**, No. 17, 3714–3718. <https://doi.org/10.1002/ejoc.200400209>.
- (258) Barlow, G. B.; Tatlow, J. C. 916. The Reactions of Highly Fluorinated Organic Compounds. Part II. Reactions of Perfluorodicyclohexyl and Perfluoro(Isopropyl-Cyclohexane). *J. Chem. Soc.* **1952**, 4695. <https://doi.org/10.1039/jr9520004695>.
- (259) Xia, R.; Xie, M. S.; Niu, H. Y.; Qu, G. R.; Guo, H. M. Efficient Synthesis of Nebularine and Vidarabine via Dehydrazination of (Hetero)Aromatics Catalyzed by CuSO₄ in Water. *Green Chem.* **2014**, *16* (3), 1077–1081. <https://doi.org/10.1039/c3gc41658e>.

- (260) Grivas, S.; Ronne, E. Facile Desulfurization of Cyclic Thioureas by Hydrogen Peroxide in Acetic Acid. *Acta chemica Scandinavica (Copenhagen, Denmark : 1989)*. 1995, pp 225–229. <https://doi.org/10.3891/acta.chem.scand.49-0225>.
- (261) Röder, L.; Nicholls, A. J.; Baxendale, I. R. Flow Hydrodediazonation of Aromatic Heterocycles. *Molecules* **2019**, *24* (10), 1–18. <https://doi.org/10.3390/molecules24101996>.
- (262) Matsui, M.; Kamiya, K.; Kawamura, S.; Shibata, K.; Muramatsu, H. Ozonization of Thio- and Azauracils. *Bull. Chem. Soc. Jpn.* **1989**, *62* (9), 2939–2941. <https://doi.org/10.1246/bcsj.62.2939>.
- (263) Allen, D. W.; Buckland, D. J.; Hutley, B. G.; Oades, A. C.; Turner, J. B. Photolysis of 5-Iodopyrimidines in Benzene or Heteroarenes; a Convenient Route to 5-Phenyl- and 5-Heteroaryl-Pyrimidines. *J. Chem. Soc. Perkin Trans. 1* **1977**, No. 6, 621. <https://doi.org/10.1039/p19770000621>.
- (264) Katritzky, A. R.; Chermprapai, A.; Bravo, S.; Patel, R. C. Reductive Deamination of Aryl- and Heteroaryl-Amines via Pyridinium Fluorides. *Tetrahedron* **1981**, *37* (21), 3603–3607. [https://doi.org/10.1016/S0040-4020\(01\)98888-X](https://doi.org/10.1016/S0040-4020(01)98888-X).
- (265) Felipe-Blanco, D.; Alonso, F.; Gonzalez-Gomez, J. C. Salicylic Acid-Catalyzed One-Pot Hydrodeamination of Aromatic Amines by Tert-Butyl Nitrite in Tetrahydrofuran. *Adv. Synth. Catal.* **2017**, *359* (16), 2857–2863. <https://doi.org/10.1002/adsc.201700475>.
- (266) Benkovic, S. J.; Sammons, D.; Armarego, W. L. F.; Waring, P.; Inners, R. Tautomeric Nature of Quinonoid 6,7-Dimethyl-7,8-Dihydro-6H-Pterin in Aqueous Solution: A Nitrogen-15 NMR Study. *J. Am. Chem. Soc.* **1985**, *107* (12), 3706–3712. <https://doi.org/10.1021/ja00298a048>.
- (267) Elgemeie, G. H.; Farag, A. B. Design, Synthesis, and in Vitro Anti-Hepatocellular Carcinoma of Novel Thymine Thioglycoside Analogs as New Antimetabolic Agents. *Nucleosides, Nucleotides and Nucleic Acids* **2017**, *36* (5), 328–342. <https://doi.org/10.1080/15257770.2017.1287377>.
- (268) Ali, T. E.; Abdel-Aziz, S. A.; El-Edfawy, S. M.; Mohamed, E. H. A.; Abdel-Kariem, S.

- M. Cleavage of Diethyl Chromonyl α -Aminophosphonate with Nitrogen and Carbon Nucleophiles: A Synthetic Approach and Biological Evaluations of a Series of Novel Azoles, Azines, and Azepines Containing α -Aminophosphonate and Phosphonate Groups. *Synth. Commun.* **2014**, *44* (24), 3610–3629. <https://doi.org/10.1080/00397911.2014.948965>.
- (269) Zhang, C.-J.; Han, W.-Y.; Gao, M.-X.; Xu, F.-F.; Zhang, Z.-T. One-Step Synthesis of 2,4,5-Trisubstituted Pyrimidines. *J. Heterocycl. Chem.* **2011**, *48* (5), 1073–1078. <https://doi.org/10.1002/jhet.606>.
- (270) Gershon, H.; Grefig, A. T.; Scala, A. A. Pyrimidines. 6. 6-Trifluoromethyl Chloropyrimidines and Related Compounds. *J. Heterocycl. Chem.* **1983**, *20* (1), 219–223. <https://doi.org/10.1002/jhet.5570200145>.
- (271) Osisanya, R. A.; Oluwadiya, J. O. Synthesis of N -Heterocycles via Chalcone Epoxides. 1. Amino and Hydrazinopyrimidines. *J. Heterocycl. Chem.* **1989**, *26* (4), 947–948. <https://doi.org/10.1002/jhet.5570260412>.
- (272) Chaudhary, C. L.; Chaudhary, P.; Dahal, S.; Bae, D.; Nam, T. gyu; Kim, J. A.; Jeong, B. S. Inhibition of Colitis by Ring-Modified Analogues of 6-Acetamido-2,4,5-Trimethylpyridin-3-Ol. *Bioorg. Chem.* **2020**, *103* (April), 104130. <https://doi.org/10.1016/j.bioorg.2020.104130>.
- (273) Cui, X.; Ma, J.; Zeng, T.; Xu, J.; Li, Y.; Wang, X. Metal-Free Cascade Synthesis of Unsymmetrical 2-Aminopyrimidines from Imidazolite Enaminones. *RSC Adv.* **2021**, *11* (39), 24247–24253. <https://doi.org/10.1039/d1ra04319f>.
- (274) Santoso, K. T.; Brett, M. W.; Cheung, C.; Cook, G. M.; Stocker, B. L.; Timmer, M. S. M. Synthesis of Functionalised Chromonyl-pyrimidines and Their Potential as Antimycobacterial Agents. *ChemistrySelect* **2020**, *5* (14), 4347–4355. <https://doi.org/10.1002/slct.202000799>.
- (275) Faidallah, H. M.; Rostom, S. A. F. Synthesis, Anti-Inflammatory Activity, and COX-1/2 Inhibition Profile of Some Novel Non-Acidic Polysubstituted Pyrazoles and Pyrano[2,3-c]Pyrazoles. *Arch. Pharm. (Weinheim)*. **2017**, *350* (5), 1–17. <https://doi.org/10.1002/ardp.201700025>.

- (276) Johnson, W. S.; Posvic, H.; Posvic, H. Introduction of the Angular Methyl Group. III. The Alkoxyethylene Blocking Group. *J. Am. Chem. Soc.* **1947**, *69* (6), 1361–1366. <https://doi.org/10.1021/ja01198a036>.
- (277) Mori, K.; Takechi, S. Synthesis of the Natural Enantiomers of Ascochlorin, Ascofuranone and Ascofuranol. *Tetrahedron* **1985**, *41* (15), 3049–3062. [https://doi.org/10.1016/S0040-4020\(01\)96657-8](https://doi.org/10.1016/S0040-4020(01)96657-8).
- (278) Von Angerer, S. Product Class 12: Pyrimidines. *Categ. 2, Heterocycles Relat. Ring Syst.* **2004**, *2*, 2–7. <https://doi.org/10.1055/sos-SD-016-00463>.
- (279) Funabiki, K.; Nakamura, H.; Matsui, M.; Shibata, K. One-Pot Preparation of 2,6-Disubstituted 4-(Trifluoromethyl)Pyrimidines via the Tandem Cyclization, Dehydration, and Oxidation Reaction of α,β -Unsaturated Trifluoromethyl Ketones Using POCl₃-Pyridine-Silica Gel and MnO₂ systems. *Synlett* **1999**, No. 6, 756–758. <https://doi.org/10.1055/s-1999-2741>.
- (280) Bugarin, A.; Jones, K. D.; Connell, B. T. Efficient, Direct α -Methylenation of Carbonyls Mediated by Diisopropylammonium Trifluoroacetate. *Chem. Commun.* **2010**, *46* (10), 1715–1717. <https://doi.org/10.1039/b924577d>.
- (281) Hon, Y. S.; Hsu, T. R.; Chen, C. Y.; Lin, Y. H.; Chang, F. J.; Hsieh, C. H.; Szu, P. H. Dibromomethane as One-Carbon Source in Organic Synthesis: Microwave-Accelerated α -Methylenation of Ketones with Dibromomethane and Diethylamine. *Tetrahedron* **2003**, *59* (9), 1509–1520. [https://doi.org/10.1016/S0040-4020\(03\)00080-2](https://doi.org/10.1016/S0040-4020(03)00080-2).
- (282) Li, Y. M.; Lou, S. J.; Zhou, Q. H.; Zhu, L. W.; Zhu, L. F.; Li, L. Iron-Catalyzed α -Methylenation of Ketones with N,N-Dimethylacetamide: An Approach for α,β -Unsaturated Carbonyl Compounds. *European J. Org. Chem.* **2015**, *2015* (14), 3044–3047. <https://doi.org/10.1002/ejoc.201500189>.
- (283) Erkkilä, A.; Pihko, P. M. Mild Organocatalytic α -Methylenation of Aldehydes. *J. Org. Chem.* **2006**, *71* (6), 2538–2541. <https://doi.org/10.1021/jo052529q>.
- (284) Basu, K.; Richards, J.; Paquette, L. A. Mono- and Bis-Acrolein Derivatives by Reliable and Efficient One-Step Methylenation of Aldehyde Precursors. *Synthesis (Stuttg.)* **2004**,

No. 17, 2841–2844. <https://doi.org/10.1055/s-2004-834866>.

- (285) Boger, D. L.; Schumacher, J.; Mullican, M. D.; Patel, M.; Panek, J. S. Thermal Cycloaddition of 1,3,5-Triazine with Enamines: Regiospecific Pyrimidine Annulation. *J. Org. Chem.* **1982**, *47* (13), 2673–2675. <https://doi.org/10.1021/jo00134a034>.
- (286) Yang, G.; Jia, Q.; Chen, L.; Du, Z.; Wang, J. Direct Access to Pyrimidines through Organocatalytic Inverse-Electron-Demand Diels–Alder Reaction of Ketones with 1,3,5-Triazine. *RSC Adv.* **2015**, *5* (94), 76759–76763. <https://doi.org/10.1039/C5RA16995J>.
- (287) Weber, S. H.; Spoelstra, D. B.; Polak, E. H. New Musk Odorants: The Structure of Tert.Amylated p-Cymene. A New Synthesis of Polyalkylindans. I. *Recl. des Trav. Chim. des Pays-Bas* **2010**, *74* (10), 1179–1196. <https://doi.org/10.1002/recl.19550741001>.
- (288) Spoelstra, D. B.; Weber, S. H.; Kleipool, R. J. C. New Musk Odorants V: A New Synthesis of Polyalkylindanes Starting from Styrenes. *Recl. des Trav. Chim. des Pays-Bas* **2010**, *82* (11), 1100–1106. <https://doi.org/10.1002/recl.19630821114>.
- (289) Chilin, A.; Marzaro, G.; Zanatta, S.; Barbieri, V.; Pastorini, G.; Manzini, P.; Guiotto, A. A New Access to Quinazolines from Simple Anilines. *Tetrahedron* **2006**, *62* (52), 12351–12356. <https://doi.org/10.1016/j.tet.2006.09.103>.
- (290) Chilin, A.; Marzaro, G.; Zanatta, S.; Guiotto, A. A Microwave Improvement in the Synthesis of the Quinazoline Scaffold. *Tetrahedron Lett.* **2007**, *48* (18), 3229–3231. <https://doi.org/10.1016/j.tetlet.2007.03.027>.
- (291) Marzaro, G.; Chilin, A.; Pastorini, G.; Guiotto, A. A Novel Convenient Synthesis of Benzoquinazolines. *Org. Lett.* **2006**, *8* (2), 255–256. <https://doi.org/10.1021/ol052594m>.
- (292) Ferrini, S.; Ponticelli, F.; Taddei, M. Convenient Synthetic Approach to 2,4-Disubstituted Quinazolines. *Org. Lett.* **2007**, *9* (1), 69–72. <https://doi.org/10.1021/ol062540s>.
- (293) Bredereckef, H.; Gompper, R.; Morlock, G. Formamid-Reaktionen, VIII. Eine Neue Pyrimidin-Synthese. *Chem. Ber* **1957**, *90* (6), 942–952.

- (294) Hall, J. B. Indanone Derivatives and Processes for Producing Same. US3773836A, 1973.
- (295) The Data and Calculations Are Propriety Information of IFF Who Has Not Realised the Full Report to Us.
- (296) Gawronski, J. K.; Kwit, M.; Boyd, D. R.; Sharma, N. D.; Malone, J. F.; Drake, A. F. Absolute Configuration, Conformation, and Circular Dichroism of Monocyclic Arene Dihydrodiol Metabolites: It Is All Due to the Heteroatom Substituents. *J. Am. Chem. Soc.* **2005**, *127* (12), 4308–4319. <https://doi.org/10.1021/ja042895b>.
- (297) Snatzke, G. Circular Dichroism and Absolute Conformation: Application of Qualitative MO Theory to Chiroptical Phenomena. *Angew. Chemie Int. Ed. English* **1979**, *18* (5), 363–377. <https://doi.org/10.1002/anie.197903631>.
- (298) Li, X.-C.; Ferreira, D.; Ding, Y. Determination of Absolute Configuration of Natural Products: Theoretical Calculation of Electronic Circular Dichroism as a Tool. *Curr. Org. Chem.* **2010**, *14* (16), 1678–1697. <https://doi.org/10.2174/138527210792927717>.
- (299) Zhang, P.; Li, L.-C. Synthesis of α,β -Unsaturated Ketones via Enamines. *Synth. Commun.* **1986**, *16* (8), 957–965. <https://doi.org/10.1080/00397918608077298>.
- (300) Tülay Yıldız, Nurgül Çanta, A. Y. Tetrahedron : Asymmetry Synthesis of New Chiral Keto Alcohols by Baker ' s Yeast. **2014**, *25*, 340–347. <https://doi.org/10.1016/j.tetasy.2014.01.003>.
- (301) Yamada, K.; Okada, M.; Fukuyama, T.; Ravelli, D.; Fagnoni, M.; Ryu, I. Photocatalyzed Site-Selective C-H to C-C Conversion of Aliphatic Nitriles. *Org. Lett.* **2015**, *17* (5), 1292–1295. <https://doi.org/10.1021/acs.orglett.5b00282>.
- (302) Yamada, K.; Fukuyama, T.; Fujii, S.; Ravelli, D.; Fagnoni, M.; Ryu, I. Cooperative Polar/Steric Strategy in Achieving Site-Selective Photocatalyzed C(Sp³)-H Functionalization. *Chem. - A Eur. J.* **2017**, *23* (36), 8615–8618. <https://doi.org/10.1002/chem.201701865>.
- (303) Capaldo, L.; Ravelli, D. Hydrogen Atom Transfer (HAT): A Versatile Strategy for Substrate Activation in Photocatalyzed Organic Synthesis. *European J. Org. Chem.*

- 2017**, *2017* (15), 2056–2071. <https://doi.org/10.1002/ejoc.201601485>.
- (304) Capaldo, L.; Quadri, L. L.; Ravelli, D. Photocatalytic Hydrogen Atom Transfer: The Philosopher’s Stone for Late-Stage Functionalization? *Green Chem.* **2020**, *22* (11), 3376–3396. <https://doi.org/10.1039/d0gc01035a>.
- (305) Sarkar, S.; Cheung, K. P. S.; Gevorgyan, V. C-H Functionalization Reactions Enabled by Hydrogen Atom Transfer to Carbon-Centered Radicals. *Chem. Sci.* **2020**, *11* (48), 12974–12993. <https://doi.org/10.1039/d0sc04881j>.
- (306) Ravelli, D.; Protti, S.; Fagnoni, M. Decatungstate Anion for Photocatalyzed “Window Ledge” Reactions. *Acc. Chem. Res.* **2016**, *49* (10), 2232–2242. <https://doi.org/10.1021/acs.accounts.6b00339>.
- (307) Sambigiato, C.; Noël, T. Flow Photochemistry: Shine Some Light on Those Tubes! *Trends Chem.* **2020**, *2*, 92–106. <https://doi.org/10.1016/j.trechm.2019.09.003>.
- (308) Knowles, J. P.; Elliott, L. D.; Booker-Milburn, K. I. Flow Photochemistry: Old Light through New Windows. *Beilstein J. Org. Chem.* **2012**, *8*, 2025–2052. <https://doi.org/10.3762/bjoc.8.229>.
- (309) Bonassi, F.; Ravelli, D.; Protti, S.; Fagnoni, M. Decatungstate Photocatalyzed Acylations and Alkylations in Flow via Hydrogen Atom Transfer. *Adv. Synth. Catal.* **2015**, *357* (16–17), 3687–3695. <https://doi.org/10.1002/adsc.201500483>.
- (310) Yu, X.; Wang, L.; Feng, X.; Bao, M.; Yamamoto, Y. Copper-Catalyzed Aldol-Type Addition of Ketones to Aromatic Nitriles: A Simple Approach to Enaminone Synthesis. *Chem. Commun.* **2013**, *49* (28), 2885–2887. <https://doi.org/10.1039/c3cc40466h>.
- (311) Agapiou, K.; Cauble, D. F.; Krische, M. J. Copper-Catalyzed Tandem Conjugate Addition-Electrophilic Trapping: Ketones, Esters, and Nitriles as Terminal Electrophiles. *J. Am. Chem. Soc.* **2004**, *126* (14), 4528–4529. <https://doi.org/10.1021/ja030603l>.
- (312) Croxtall, B.; Hope, E. G.; Stuart, A. M. Separation, Recovery and Recycling of a Fluorous-Tagged Nickel Catalyst Using Fluorous Solid-Phase Extraction. *Chem. Commun.* **2003**, *3* (19), 2430–2431. <https://doi.org/10.1039/b308543k>.

- (313) Veronese, A. C.; Gandolfi, V.; Corain, B.; Basato, M. Malononitrile as an Electrophile in Metal-Catalysed Addition Reactions to β -Dicarbonyls. *J. Mol. Catal.* **1986**, *36* (3), 339–341. [https://doi.org/10.1016/0304-5102\(86\)85089-1](https://doi.org/10.1016/0304-5102(86)85089-1).
- (314) Takaya, H.; Ito, M.; Murahashi, S. I. Rhenium-Catalyzed Addition of Carbonyl Compounds to the Carbon-Nitrogen Triple Bonds of Nitriles: α -C-H Activation of Carbonyl Compounds. *J. Am. Chem. Soc.* **2009**, *131* (31), 10824–10825. <https://doi.org/10.1021/ja9036669>.
- (315) Maggi, R.; Bosica, G.; Gherardi, S.; Oro, C.; Sartori, G. ZrNaY Zeolite Catalysed Reaction of β -Dicarbonyl Compounds with Ethyl Cyanoformate under Solventless Conditions. *Green Chem.* **2005**, *7* (4), 182–184. <https://doi.org/10.1039/b416665e>.
- (316) Basato, M.; Corain, B.; Veronese, A. C.; D'Angeli, F.; Valle, G.; Zanotti, G. Metal-Catalyzed Synthesis of Cyano Enaminodiones from β -Dicarbonyl Compounds and Cyanogen. Identification of Traube's Isomers. *J. Org. Chem.* **1984**, *49* (24), 4696–4700. <https://doi.org/10.1021/jo00198a021>.
- (317) De Risi, C.; Pollini, G. P.; Veronese, A. C.; Bertolasi, V. A New Simple Route for the Synthesis of (\pm)-2-Azetidinones Starting from β -Enaminoketoesters. *Tetrahedron* **2001**, *57* (51), 10155–10161. [https://doi.org/10.1016/S0040-4020\(01\)01036-5](https://doi.org/10.1016/S0040-4020(01)01036-5).
- (318) Tkachev, A. V.; Rukavishnikov, A. V. Enaminones of the 2-Acetylcyclopent-1-En-1-Ylamine Type Derived from the Terpenic Compounds Limonene, 3-Carene and δ -Cadinol. *Mendeleev Commun.* **1992**, *2* (4), 161–162. <https://doi.org/10.1070/MC1992v002n04ABEH000186>.
- (319) West, J. G.; Huang, D.; Sorensen, E. J. Acceptorless Dehydrogenation of Small Molecules through Cooperative Base Metal Catalysis. *Nat. Commun.* **2015**, *6*, 1–7. <https://doi.org/10.1038/ncomms10093>.
- (320) Manfredini, S.; Simoni, D.; Zanirato, V.; Casolari, A. A Convenient Synthesis of λ -Oxo Acrylates. *Tetrahedron Lett.* **1988**, *29* (32), 3997–4000. [https://doi.org/10.1016/S0040-4039\(00\)80403-7](https://doi.org/10.1016/S0040-4039(00)80403-7).
- (321) Haight, A. R.; Stuk, T. L.; Allen, M. S.; Bhagavatula, L.; Fitzgerald, M.; Hannick, S.

- M.; Kerdesky, F. A. J.; Menzia, J. A.; Parekh, S. I.; Robbins, T. A.; Scarpetti, D.; Tien, J. H. J. Reduction of an Enaminone: Synthesis of the Diamino Alcohol Core of Ritonavir. *Org. Process Res. Dev.* **1999**, *3* (2), 94–100. <https://doi.org/10.1021/op9802071>.
- (322) Cocker, W.; Shannon, P. V. R.; Staniland, P. A. The Chemistry of Terpenes. Part I. Hydrogenation of the Pinenes and the Carenes. *J. Chem. Soc. C Org.* **1966**, 41–47.
- (323) Bovicelli, P.; Lupattelli, P.; Mincione, E.; Prencipe, T.; Curci, R. Oxidation of Natural Targets by Dioxiranes. 2. Direct Hydroxylation at the Side-Chain C-25 of Cholestane Derivatives and of Vitamin D3 Windaus-Grundmann Ketone. *J. Org. Chem.* **1992**, *57* (19), 5052–5054. <https://doi.org/10.1021/jo00045a004>.
- (324) Sikervar, V.; Fleet, J. C.; Fuchs, P. L. Fluoride-Mediated Elimination of Allyl Sulfones: Application to the Synthesis of a 2,4-Dimethyl-A-Ring Vitamin D3 Analogue. *J. Org. Chem.* **2012**, *77* (11), 5132–5138. <https://doi.org/10.1021/jo300672a>.
- (325) Murray, R. W. Chemistry of Dioxiranes. 12. Dioxiranes. *Chem. Rev.* **1989**, *89* (5), 1187–1201. <https://doi.org/10.1021/cr00095a013>.
- (326) Varkony, H.; Pass, S.; Mazur, Y. Reactions of Ozone with Saturated Hydrocarbons. Ozone-Hydrocarbon Complexes. *J. Chem. Soc. Chem. Commun.* **1974**, No. 11, 437–438. <https://doi.org/10.1039/C39740000437>.
- (327) Cohen, Z.; Keinan, E.; Mazur, Y.; Varkony, T. H. Dry Ozonation. Method for Stereoselective Hydroxylation of Saturated Compounds on Silica Gel. *J. Org. Chem.* **1975**, *40* (14), 2141–2142. <https://doi.org/10.1021/jo00902a035>.
- (328) Khalitova, L. R.; Grabovskiy, S. A.; Antipin, A. V.; Spirikhin, L. V.; Kabal’Nova, N. N. Products of Ozone Oxidation of Some Saturated Cyclic Hydrocarbons. *Russ. J. Org. Chem.* **2015**, *51* (12), 1710–1716. <https://doi.org/10.1134/S1070428015120076>.
- (329) Schneider, H. J.; Mueller, W. Selective Functionalization of Hydrocarbons. 6. Mechanistic and Preparative Studies on the Regio- and Stereoselective Paraffin Hydroxylation with Peracids. *J. Org. Chem.* **1985**, *50* (23), 4609–4615. <https://doi.org/10.1021/jo00223a036>.

- (330) Author Guidelines - The journal of Organic Chemistry https://publish.acs.org/publish/author_guidelines?coden=joceah (accessed Jun 12, 2022).
- (331) Hu, H.; Harrison, T. J.; Wilson, P. D. A Modular and Concise Total Synthesis of (\pm)-Daurichromenic Acid and Analogues. *J. Org. Chem.* **2004**, *69* (11), 3782–3786. <https://doi.org/10.1021/jo049703f>.
- (332) Wang, X.; Yu, W.; Lou, H. Antifungal Constituents from the Chinese Moss *Homalia Trichomanoides*. *Chem. Biodivers.* **2005**, *2* (1), 139–145. <https://doi.org/10.1002/cbdv.200490165>.
- (333) Ragab, F. A.; Hassan, G. S.; Yossef, H. A.; Hashem, H. A. Synthesis of 6- and 9-Alkylaminomethyl Furoflavones as Gastroprotective Agents. *Eur. J. Med. Chem.* **2007**, *42* (8), 1117–1127. <https://doi.org/10.1016/j.ejmech.2007.01.019>.
- (334) Dyke, H. J.; Elix, J. A.; Marcuccio, S. M.; Whitton, A. A. Oxidation of Alkyl 1,6-Dihydroorsellinates. A New Method for the Synthesis of Methyl Orsellinate and Homologs. *Aust. J. Chem.* **1987**, *00040* (00002), 431–434.
- (335) Lopes, T. I. B.; Coelho, R. G.; Yoshida, N. C.; Honda, N. K. Radical-Scavenging Activity of Orsellinates. *Chem. Pharm. Bull. (Tokyo)*. **2008**, *56* (11), 1551–1554. <https://doi.org/10.1248/cpb.56.1551>.
- (336) Liu, W.; Liu, J.; Ogawa, D.; Nishihara, Y.; Guo, X.; Li, Z. Iron-Catalyzed Oxidation of Tertiary Amines: Synthesis of β -1,3-Dicarbonyl Aldehydes by Three-Component C–C Couplings. *Org. Lett.* **2011**, *13* (23), 6272–6275. <https://doi.org/10.1021/ol202749x>.
- (337) Zhang, Z.; Xie, S.; Cheng, B.; Zhai, H.; Li, Y. Enantioselective Total Synthesis of (+)-Arboridinine. *J. Am. Chem. Soc.* **2019**, *141* (17), 7147–7154. <https://doi.org/10.1021/jacs.9b02362>.
- (338) Asahina, Y.; Simosato, Z.; Sakurai, Y. Lichen Substances. XC. Orcinoldicarboxylic Acid Monomethyl Ethers and the Non-Existence of the so-Called Isosquamatic Acid. *Berichte der Dtsch. Chem. Gesellschaft [Abteilung] B Abhandlungen* **1938**, *71B*, 2561–2668.

- (339) Makrrougras, M.; Coffinier, R.; Oger, S.; Chevalier, A.; Sabot, C.; Franck, X. Total Synthesis and Structural Revision of Chaetoviridins A. *Org. Lett.* **2017**, *19* (15), 4146–4149. <https://doi.org/10.1021/acs.orglett.7b02053>.
- (340) Watanabe, Y.; Tsuji, Y.; Takeuchi, R.; Suzuki, N. The Platinum Complex Catalyzed Reductive N -Carbonylation of Nitroarenes to the Carbamates. *Bull. Chem. Soc. Jpn.* **1983**, *56* (11), 3343–3348. <https://doi.org/10.1246/bcsj.56.3343>.
- (341) IWAKURA, Y.; IZAWA, S. Syntheses of 3, 5-Substituted-2-Oxazolidones by the Reaction between N-Arylurethans and Substituted Phenyl Glycidyl Ethers. *J. Synth. Org. Chem. Japan* **1966**, *24* (1), 60–65. <https://doi.org/10.5059/yukigoseikyokaishi.24.60>.
- (342) Quintanilla-Licea, R.; Colunga-Valladares, J. F.; Caballero-Quintero, A.; Rodríguez-Padilla, C.; Tamez-Guerra, R.; Gómez-Flores, R.; Waksman, N. NMR Detection of Isomers Arising from Restricted Rotation of the C-N Amide Bond of N-Formyl-o-Toluidine and N,N'-Bis-Formyl-o-Tolidine. *Molecules* **2002**, *7* (8), 662–673. <https://doi.org/10.3390/70800662>.
- (343) Riemer, D.; Hirapara, P.; Das, S. Chemoselective Synthesis of Carbamates Using CO₂ as Carbon Source. *ChemSusChem* **2016**, *9* (15), 1916–1920. <https://doi.org/10.1002/cssc.201600521>.
- (344) Erős, G.; Mehdi, H.; Pápai, I.; Rokob, T. A.; Király, P.; Tárkányi, G.; Soós, T. Expanding the Scope of Metal-Free Catalytic Hydrogenation through Frustrated Lewis Pair Design. *Angew. Chemie Int. Ed.* **2010**, *49* (37), 6559–6563. <https://doi.org/10.1002/anie.201001518>.
- (345) Bolvig, S.; Hansen, P. E. Deuterium-Induced Isotope Effects On¹³C Chemical Shifts as a Probe for Tautomerism in Enolic β-Diketones. *Magn. Reson. Chem.* **1996**, *34* (6), 467–478. [https://doi.org/10.1002/\(SICI\)1097-458X\(199606\)34:6<467::AID-OMR906>3.0.CO;2-L](https://doi.org/10.1002/(SICI)1097-458X(199606)34:6<467::AID-OMR906>3.0.CO;2-L).
- (346) Cockerill, G. S.; Kocienski, P.; Treadgold, R. Silicon-Mediated Annulation. Part 2. A Synthesis of β-Alkoxy Cyclo-Octanones via Intramolecular Directed Aldol Reactions. *J. Chem. Soc., Perkin Trans. 1* **1985**, 2101–2108.

<https://doi.org/10.1039/P19850002101>.

- (347) Wang, P.-S.; Zhou, X.-L.; Gong, L.-Z. An Organocatalytic Asymmetric Allylic Alkylation Allows Enantioselective Total Synthesis of Hydroxymetasequirin-A and Metasequirin-B Tetramethyl Ether Diacetates. *Org. Lett.* **2014**, *16* (3), 976–979. <https://doi.org/10.1021/ol4037055>.
- (348) Christl, M.; Roberts, J. D. Carbon-13 Nuclear Magnetic Resonance Spectroscopy. Conformational Analysis of Methyl-Substituted Cycloheptanes, Cycloheptanols, and Cycloheptanones. *J. Org. Chem.* **1972**, *37* (22), 3443–3452. <https://doi.org/10.1021/jo00795a014>.